UNIVERSITÉ DE MONTRÉAL

THE IMPACT OF CONTAMINANT MIGRATION
ON THE STRUCTURE OF COMPACTED KAOLINITE

YASSER M.H. FAHMY

DÉPARTEMENT DES GÉNIES CIVIL,

GÉOLOGIQUE ET DES MINES

ÉCOLE POLYTECHNIQUE DE MONTRÉAL

THÈSE PRÉSENTÉE EN VUE DE L'OBTENTION

DU DIPLÔME DE PHILOSOPHIAE DOCTOR (Ph.D.)

(GÉNIE CIVIL)

JUIN 1999

0-612-46632-9

Canada

UNIVERSITÉ DE MONTRÉAL

ÉCOLE POLYTECHNIQUE DE MONTRÉAL

Cette thèse intitulée:

THE IMPACT OF CONTAMINANT MIGRATION
ON THE STRUCTURE OF COMPACTED KAOLINITE

présentée par: FAHMY Yasser M.H.

en vue de l'obtention du diplôme de: Philosophiae Doctor

a été dûment acceptée par le jury d'examen constitué de:

M. KAHAWITA René, Ph.D., président

M. SILVESTRI Vincent, Ph.D., membre et directeur de recherche

M. MONTÈS Pierre, Ph.D., membre

M. POOROOSHASB Hormoz, Ph.D., membre

DEDICATION

To my wife..

To my parents..

To my professors and friends..

To all those who believe that:

"A journey of a thousand miles starts out with a single step"

Chinese Proverb-

ACKNOWLEDGMENTS

The author would like to express his deepest gratitude and sincere appreciation to his advisor, Dr. V. Silvestri, for his academic as well as financial support (through NSERC and FCAR research grants), valuable advice, and constructive guidance throughout all the stages of this study.

My thanks to all those, at the Department of Civil, Geological and Mining Engineering, Chair, Staff and Faculty members, secretaries, lab operators, and colleagues: F. Behidj, M. Benyamina, and A. Sassi, who helped a great deal in carrying out this dissertation.

Special thanks are expressed to Mr. G. Guérin of the Centre for Microscopic Characterization of Materials (CM)^2 for his technical support during the Scanning Electron Microscopy analyses. It has indeed been my privilege to be associated with the caliber of people who work at (CM)^2. Thanks are also extended to Messrs. D. Bouchard and M. Dugal of the Environmental Engineering laboratory for their assistance in conducting part of the physico-chemical tests of this study.

Last, but not least, I would especially like to thank Dr. P. Montès for his unbounded encouragement and practical advice.

RÉSUMÉ

L'utilisation fréquente des sols argileux compactés en tant que barrières au transport de contaminant exige une meilleure compréhension des relations entre la structure d'argile et le comportement hydraulique. Cette recherche vise à adresser deux problèmes: (1) étudier les effets du contaminant lixiviant et/ou de son exposition sur la structure de l'argile compactée; et (2) mieux comprendre le comportement hydraulique de l'argile compactée à la teneur en eau optimum. La microscopie à balayage électronique, des essais de lixiviation, des essais de trempage, et la méthode d'éléments finis sont employés pour étudier les caractéristiques microscopiques et macroscopiques de deux kaolinites ayant des particules de dimensions différentes.

La kaolinite compactée à la teneur en eau optimum se caractérise par une structure avec domaines relativement préférentiellement-orientés. La matrice se compose de domaines de particules ayant un arrangement face-à-face, alors que les agrégats sont disposés par des groupes de domaines ayant des arrangements tête-à-tête et tête-à-face. La matrice dispersée est responsable de la densité sèche maximum obtenue à la teneur en eau optimum, tandis que l'arrangement en agrégats floculés explique la raison pour laquelle la conductivité hydraulique de l'argile compactée n'atteint pas une valeur minimum.

L'attaque par l'acide organique a confirmé le phénomène de dissolution-précipitation pour les échantillons lixiviés et imbibés. Les dissolvants organiques purs peuvent causer la floculation des particules d'argile en rétrécissant la double couche à cause de leurs constantes diélectriques relativement basses. Cependant, on a observé des changements structurels limités dans les sols contaminés. En outre, les contaminants non polaires et hydrophobes n'ont pas pu remplacer l'eau dans les petits pores, et n'ont ainsi aucun effet sur la structure d'argile comme indiqué par les micrographes du microscope à balayage électronique.

La filtration d'un sel inorganique fortement concentré n'a pas eu comme conséquence un changement substantiel de la perméabilité intrinsèque. L'acide et la base inorganiques ont eu un léger effet sur la structure des argiles, quoique des réactions géochimiques aient été détectées. Les essais de lixiviation, cependant, ont tous mené à une réduction significative de la conductivité hydraulique des kaolinites compactées. D'autres facteurs, concernant les propriétés de la kaolinite et les méthodes d'essai, sont postulés pour avoir masqué l'effet de la structure microscopique de l'argile et ainsi pour avoir influencé les résultats macroscopiques. Les simulations numériques par la méthode d'éléments finis ont confirmé les résultats obtenus à partir du programme expérimental.

ABSTRACT

The extensive use of compacted clayey soils as barriers to contaminant transport requires better understanding of the relations between clay structure and hydraulic behavior. This research is aimed at addressing two problems: (1) to study the effects of contaminant leaching and/or exposure on the structure of compacted clay; and (2) to better understand the hydraulic behavior exhibited by clay compacted at optimum moisture content. Scanning electron microscopy (SEM), leaching tests, soaking tests, and finite element method (FEM) are used to investigate the microscopic and macroscopic features of two different particle-size kaolinites.

Kaolinite compacted at optimum moisture content is characterized by relatively preferentially-oriented domains. The matrix is composed of densely stacked face-to-face domains, while aggregates are constructed by stair-stepped face-to-face and edge-to-face arrangements of domains. The dispersed matrix is responsible for the maximum dry density obtained at optimum moisture content, whereas the flocculated aggregates may explain why hydraulic conductivity of compacted clay does not reach a minimum value simultaneously.

The attack of organic acid confirmed the dissolution-precipitation phenomenon for both leached and soaked samples. Pure organic solvents are able to cause flocculation of clay particles by shrinking the diffuse double layer due to their relatively low permittivities. However, limited structural changes were observed in the contaminated soils. In addition, non-polar and hydrophobic contaminants could not replace water in small pores, and thus had no effect on clay structure as revealed by scanning electron micrographs.

The permeation of a highly concentrated inorganic salt did not result in a substantial change in intrinsic permeability. Inorganic acid and base had a slight effect on the structure of kaolin clays, even though geochemical reactions were detected. Leaching tests, however, all led to significant reduction in hydraulic conductivity of compacted kaolinites. Other factors

relating to kaolinite properties and testing procedures are postulated to have dominated the macroscopic results over clay microfabric. Numerical simulations by finite element method confirmed the results obtained from the experimental program.

CONDENSÉ

1. Définition du problème

Dans les années 40 aux 60, les pays industrialisés du monde ont subi une expansion énorme dans leurs capacités de fabrication des marchandises, traitement du pétrole, et production des nouveaux produits chimiques. Les ingénieurs géotechniques et les scientifiques de la terre ont joué un rôle important dans cette expansion en identifiant les ressources minérales et pétrolières, en caractérisant la stratigraphie et l'état du sol, en concevant les fondations pour les structures complexes et les machines, et en développant des spécifications pour les ouvrages de terre et les travaux de terrassement.

En dépit des avances faites dans le domaine que nous appelons maintenant la géotechnique dans les années 50 et les années 60, il n'y avait pratiquement aucun accent sur les problèmes de l'environnement dans la pratique en matière géotechnique pendant cette période. Pourtant, vers la fin des années 70, la situation ait commencé à changer nettement et irrévocablement. La production des volumes toujours croissants de déchets solides et de matériaux dangereux dans cette période pose un défi sérieux pour les ingénieurs civils, en général, et les ingénieurs géotechniques, en particulier; spécifiquement: *comment traiter ces déchets correctement pour éliminer ou, au moins, pour réduire au minimum leur menace potentielle à la santé publique et à l'environnement*. En dépit de divers techniques chimiques, physiques, et biologiques du traitement de rebut récemment développées, l'enterrement des déchets au sol est toujours une pratique courante partout dans le monde, particulièrement en Amérique du Nord, pour des raisons économiques et technologiques. Des règlements, des normes de rendement, et des directives techniques pour la conception, la construction, et l'exploitation de ces installations de disposition de rebut ont été publiés par les autorités intéressées, notamment l'U.S. Environmental Protection Agency (U.S. EPA, 1985).

Le système de double recouvrement est recommandé pour les sites d'enfouissements des déchets dangereux, avec des couches de collection de lixivia et de détection de fuite situées au-dessus et entre les deux recouvrements. Ces recouvrements peuvent être des recouvrements de membrane flexible (FMLs), des couches de sol compacté, ou un composé de tous les deux. En raison de leurs valeurs extrêmement basses de la conductivité hydraulique après un compactage approprié, les sols fins ont été toujours choisis comme le matériau de construction préféré des barrières hydrauliques pour les remblais et les sites d'enfouissements. Le recouvrement recommandé d'argile compactée a une épaisseur minimum de 0,90 m (3 pi) et une conductivité hydraulique (k) de moins de 1×10^{-9} m/s. Son but est de servir comme barrière finale contre le transfert de lixivia dans l'environnement pendant au moins 30 ans après la fermeture d'un site d'enfouissement, même si le FML s'effondre. L'importance de ces recouvrements d'argile compactées (CCLs) dans l'emprisonnement des matériaux dangereux est évidente.

En tant que paramètre macroscopique mesurant l'intégrité d'un CCL, la conductivité hydraulique a été pour longtemps connue d'être une fonction de teneur en eau de compaction et de l'effort de compactage (Lambe, 1958b). Les valeurs de conductivité hydraulique entre une argile compactée côté sec-de-l'optimum et une compactée côté humide-de-l'optimum peuvent différer par plusieurs ordres de grandeur. Les études précédentes ont indirectement démontré la commande dominante de cette propriété par la structure de l'argile compactée (Lambe, 1958a). Des observations directes et des calculs détaillés, cependant, ont encore à être effectués sur les caractéristiques de tissu et de pore de l'argile compactée.

Le but préliminaire de cette recherche est d'examiner la relation entre la structure et la conductivité hydraulique de la kaolinite compactée à la teneur en eau optimum par observation directe en utilisant la méthode de la microscopie à balayage électronique (SEM). On s'attend à ce que la simulation du transport de contaminant dans les sols par la méthode d'éléments finis (FEM) serve comme passerelle pour évaluer la corrélation entre les propriétés macroscopiques et microscopiques.

La compatibilité chimique du sol compacté a été de souci principal pour les ingénieurs geo-environnementaux et les scientifiques du sol depuis le début des années 80 lorsque des fuites sérieuses des produits chimiques dangereux a été découvertes à travers les sols d'enterrement des déchets dangereux. Des études intensives ont été réalisées sur les interactions de sol-produit chimique et leurs effets sur la conductivité hydraulique du sol. En raison de la complexité du problème, les différentes méthodes employées dans les essais, et la variété des sols et produits chimiques testés, les résultats et les conclusions faits par différents chercheurs sont difficile à comparer et certains sont même contradictoires. Les changements de la conductivité hydraulique dû à la filtration chimique sont habituellement postulés être le résultat des changements microstructurels en vertu d'une chimie différente de fluide de pore. La théorie de double couche est souvent utilisée comme une explication qualitative. Un but principal de cette recherche est d'étudier l'influence de divers polluants sur non seulement la structure mais aussi la conductivité hydraulique de l'argile compactée.

2. **Objectifs de la recherche**

Les objectifs spécifiques de cette recherche sont de:

❑ mieux comprendre la structure des argiles compactées à la densité sèche maximum;

❑ évaluer la compatibilité de l'argile compactée avec différents contaminants et son impact sur la microstructure et la conductivité hydraulique;

❑ explorer les rapports quantitatifs entre les propriétés physiques des contaminants et la conductivité hydraulique des sols compactés, ainsi que entre les caractéristiques de l'argile et la perméabilité intrinsèque;

❑ jeter plus de lumière sur les caractéristiques des pores responsables du comportement hydraulique des argiles compactées;

❑ explorer l'ampleur de la validité de simuler le transfert de contaminant à travers les sols par la méthode d'éléments finis;

❑ adopter la microscopie à balayage électronique pour étudier la structure de l'argile; et

❑ établisser des protocoles pour la caractérisation chimique des sols, la lixiviation des argiles compactées et la préparation des spécimens contaminés pour les observations de SEM.

3. Organisation de la thèse

Le chapitre 2 fournit un bilan des développements précédents dans notre connaissance de la théorie de compaction et des phénomènes de conduction. Également inclus en chapitre 2 est un sommaire des études précédentes de la conductivité hydraulique avec des produits chimiques comme permeants publiées pendant la décennie passée. Une présentation des concepts de base pour décrire le transport de contaminant à travers les matériaux poreux est également couverte en chapitre 2. Le chapitre termine avec le but de l'étude bien défini et spécifié.

Le chapitre 3 décrit les propriétés des matériaux employés dans l'étude. Les avantages et les inconvénients des méthodes adoptées sont également discutés, avec leurs limitations citées. Une attention particulière est prêtée à la méthodologie de la recherche et les approches uniques pour accomplir les objectifs de la recherche. Des procédures pour la caractérisation chimique, la compaction statique, et les mesures de conductivité hydraulique ont été établies et sont discutées. Le matériel des essais et les différents protocoles suivis pour conduire la lixiviation et les essais de trempage sont présentés dans ce chapitre, et les critères d'arrêt pour les tests de compatibilité sont discutés en détail. Des méthodes distinctes sont adoptées pour analyser les divers lixivias selon les propriétés de chaque contaminant. La méthode de la microscopie à balayage électronique (SEM) est présentée en chapitre 3 pour étudier les argiles compactées et contaminées avec différents produits chimiques. Les principes de la

modélisation de transport de contaminant sont également présentés dans ce chapitre, avec la conception de la maille d'éléments finis et la spécification d'états de borne.

Le chapitre 4 présente les résultats de l'étude de la structure de la kaolinite compactée à la teneur en eau optimum et des interactions de sol-contaminant. Les caractéristiques de compaction et le comportement hydraulique diffèrent des argiles ont été obtenus et sont discutés en se basant sur la microstructure indiquée par les micrographes de SEM. Les effets d'exposition de l'échantillon aux composés organiques en imbibant, en ce qui concerne la structure du sol et la microstructure, sont également présentés et discutés en chapitre 4. Les réactions géochimiques produites entre les particules d'argile et les fluides de pore pendant la lixiviation et le trempage sont discutées dans ce chapitre. Les résultats de la simulation numériques sont également présentés et comparés aux résultats expérimentaux pour vérifier la validité de la modélisation numérique par la méthode d'éléments finis.

Le chapitre 5 récapitule les conclusions tirées en se basant sur les résultats de cette étude. L'importance de la microstructure d'argile à la conductivité hydraulique est soulignée. Les changements microstructurels résultant de la lixiviation et exposition au contaminant sont vérifiés, et l'effet des procédures de mesure sur la conductivité hydraulique est proposé. En conclusion, les avantages et les inconvénients de différentes méthodes, y compris la microscopie à balayage électronique et la simulation numérique par éléments finis, sont récapitulés dans ce chapitre.

L'annexe A compile et récapitule la plupart des principes de base liés à la structure d'argile et l'interaction de sol-contaminant.

4. Conclusions de l'étude

Parmi les propriétés du sol nécessaires pour la solution de la plupart des problèmes d'ingénierie geo-environnementale, aucune ne change tellement sur un intervalle considérable

ou est si difficile à déterminer sûrement comme la conductivité hydraulique. La conductivité hydraulique et sa susceptibilité aux changements avec le temps ou l'exposition aux produits chimiques sont les facteurs principaux dans la sélection de l'argile pour l'usage dans les barrières de retenue de déchets. Un sol donné, cependant, peut montrer de grandes variations de la conductivité hydraulique en raison des changements de microstructure (arrangement de particules), de densité, et de teneur en eau. Comprendre comment les différents produits chimiques peuvent influencer la conductivité hydraulique des sols argileux, et aussi, comment des variations d'une grandeur importante de la conductivité hydraulique peuvent se produire dans des petites marges de densité et de teneur en eau exige la considération de l'importance de structure de l'argile et les facteurs qui l'affectent.

La recherche actuelle exécutée sur deux argiles de kaolin ayant des particules de dimensions différentes, compactées statiquement à la teneur en eau optimum et imprégnées avec un éventail des contaminants, mène aux conclusions suivantes en ce qui concerne la structure du sol et la conductivité hydraulique:

❑ En dépit des avances récemment réalisées dans notre connaissance au sujet du domaine des interactions de sol-contaminant et de la compatibilité, le besoin est encore persistant pour l'évaluation du transport des polluants à travers les sols et son impact sur la structure du sol; par conséquent, remettant en cause l'intégrité des barrières d'argiles compactées aux sites d'enfouissements.

❑ Une recherche exceptionnelle est fondée sur une caractérisation minutieuse et complète des matériaux employés dans la recherche. La caractérisation des argiles et des produits chimiques utilisés comme permeants dans cette étude est accomplie. Les différentes méthodes adoptées pour conduire le programme expérimental et l'analyse numérique sont discutées et justifiées.

❏ La kaolinite compactée à la teneur en eau optimum se caractérise par une microstructure ordonnée, composée d'agrégats floculés et de matrice dispersée. La matrice est constituée d'un empilement dense des domaines dont les contacts sont face-à-face ayant comme résultat la structure appelée turbostratique. La densité sèche maximum est atteinte par la matrice de l'argile compactée à la teneur en eau optimum. Les agrégats sont disposés par des groupes de domaines ayant des arrangements tête-à-tête et tête-à-face. La microstructure ayant la forme d'un escalier fournit la forte résistance à l'effort de compaction. La résistance forte des agrégats à la contrainte de compaction mène à l'existence de grands pores en argile compactée à la teneur en eau optimum. Par conséquent, des valeurs minima de la conductivité hydraulique ne peuvent pas être atteintes quoique le sol possède sa densité sèche maximum, et ainsi l'indice de vide minimum.

❏ Les contaminants organiques purs peuvent causer la floculation des particules d'argile en rétrécissant la double couche dû à leurs constantes diélectriques relativement basses. Cependant, les composés non polaires et hydrophobes n'ont pas pu substituer l'eau dans les petits pores, et n'ont ainsi aucun effet sur la structure d'argile comme indiqué par les micrographes du microscope à balayage électroniques. D'ailleurs, les changements observés de la microstructure des échantillons imbibés ont été limités aux zones localisées. Le phénomène de dissolution-précipitation est confirmé par l'attaque de l'acide organique sur les échantillons lixiviés et imbibés. Bien qu'un nombre significatif d'études aient été effectués pour évaluer la conductivité hydraulique des sols avec les fluides organiques comme permeants, il est toujours extrêmement difficile de choisir un seul facteur qui peut être identifié comme étant le responsable du changement de la perméabilité quand un fluide organique substitue l'eau.

❏ La microstructure modifiée et/ou la structure floculée ne mène pas nécessairement à une augmentation de la conductivité hydraulique, particulièrement si l'argile a été correctement compactée et est gardée sous confinement. Des réductions de la conductivité hydraulique ont été mesurées quand les colonnes de sol ont été imprégnées avec les divers

produits chimiques. La valeur de cette propriété macroscopique devrait être influencée par beaucoup d'autres facteurs comprenant: les constituants du sol et la composition minérale, les propriétés de permeant, les procédures de préparation de l'échantillon, l'état des contraintes, l'échelle de gradient hydraulique, et les méthodes de mesure de la conductivité hydraulique.

❏ La filtration d'un sel inorganique fortement concentré par les kaolinites compactées n'a pas eu comme conséquence un changement substantiel de perméabilité intrinsèque. Les investigations de SEM sont conformées aux résultats des mesures de conductivité hydrauliques. L'augmentation de la concentration d'électrolyte ne modifie pas la structure d'une argile correctement compactée et confinée.

❏ L'acide et la base inorganiques avec des pH extrêmement bas et haut ont un léger effet sur la structure des argiles de kaolin. Des réactions géochimiques, cependant, ont été détectées. La capacité tampon des particules d'argile pourrait avoir joué un rôle plus significatif en empêchant les particules d'être dissoute pendant la lixiviation, comme illustré par les observations de SEM de la microstructure.

❏ Les échantillons imbibés dans les dissolvants organiques pour examiner l'impact du transfert de contaminant sous la diffusion pure sur la structure des argiles compactées ont confirmé les conclusions tirées sur les essais de lixiviation. Excepté les échantillons imbibés en acide organique pur, on n'a observé aucune différence perceptible dans la microstructure de l'argile avec le Hydrite Flat-D ou le Hydrite R.

❏ La méthode d'éléments finis est utilisée pour accomplir l'analyse analytique de cette recherche. La simulation numérique a servi comme passerelle en évaluant la corrélation entre les propriétés macroscopiques et microscopiques. Elle a également jeté plus de lumière sur l'ampleur de la validité de simuler le transfert de polluant à travers les sols par la méthode d'éléments finis.

❏ La microscopie à balayage électronique s'est avérée être un outil puissant pour étudier la structure des sols au niveau microscopique. Le SEM met à jour la haute résolution sous le rapport optique et produit un champ de profondeur des images. Les ombres et la perspective des micrographes fournissent des informations topographiques abondantes de valeur inestimable aux études microscopiques des sols. Les plus petites particules peuvent être discernées des particules éloignées sur la photo. Les particules superposantes peuvent également être identifiées. Néanmoins, l'application de SEM à l'observation microstructurelle des argiles compactées est provocante dû aux techniques compliquées, et parfois pénibles, de préparation des specimens et aux exécutions de SEM.

TABLE OF CONTENTS

Page

LIST OF TABLES

Table   **Page**

LIST OF FIGURES

Figure   Page

LIST OF SYMBOLS AND ABBREVIATIONS

A	cross section area normal to the direction of flow
A_f	area of flow passages
a	cross sectional area of the tube
C_S	concentration of the source
C_s	shape coefficient
c	concentration of the solute
c_0	equilibrium concentration
D	diffusion coefficient
D^*	effective diffusion coefficient
D^*_A	apparent diffusion coefficient
D_h	hydrodynamic dispersion coefficient
D_0	"free solution" diffusion coefficient
e	void ratio
EC	Electrical Conductivity
f_{OC}	fraction (by weight) of organic carbon in the soil
h	total hydraulic head
I	electrical flow rate per unit area
i, i_h	dimensionless hydraulic gradient
i_c	chemical gradient
i_e	electrical gradient
i_t	thermal gradient
J_A	advective mass flux
J_D	diffusive mass flux
J_M	mechanical dispersive flux
J_i	flow rate or flux
K	intrinsic or absolute permeability
K_d	distribution coefficient

K_{OC}	organic carbon partition coefficient
K_{OW}	octanol-water partition coefficient
K_p	intrinsic permeability of the permeant
K_w	intrinsic permeability of water
k, k_h	hydraulic conductivity
k_p	hydraulic conductivity of the permeant
k_t	thermal conductivity
k_w	hydraulic conductivity of water
k_0	pore shape factor
L	length of flow channel in the direction of flow
L_e	effective distance of transport between 2 points
m	total mass of solute per unit volume of soil
N	number of particles per cluster
n	porosity
n_e	effective porosity
P	wetted perimeter
PVF	Pore Volume of Flow
Q	mass flux
Q_d	dispersive flux
Q_m	total nodal mass flux
Q_w	nodal water flux
q	volumetric flow rate of water per unit time
q_{cm}	flow rate for the cluster model
q_h	water flow rate per unit area
q_{KC}	flow rate predicted by Kozeny-Carman equation
q_t	heat flow rate per unit area
R	tube radius
R_H	hydraulic radius
R_d	dimensionless retardation factor

S   adsorbed concentration, or mass of solute adsorbed per mass of soil

S_0 wetted surface per unit volume of particles

SEM   Scanning Electron Microscope

T   tortuosity factor

TOC   Total Organic Carbon

t   transit time

t_0 time required for the solute to reach the effluent end of the column

V_s volume of solids

V_w volume of water

v   Darcian (discharge) velocity, or flux of water

v_R transport rate or velocity of the reactive solute

v_{ave} average flow velocity

v_h flow velocity

v_s seepage, advective or average linear velocity

α dispersivity of the porous medium

α_L longitudinal dispersivity

α_T transverse dispersivity

β empirically determined constant

γ_p unit weight of the permeant

Δt incremental time step

Δx nodal spacing in the x-direction

Δy nodal spacing in the y-direction

θ volumetric water content

μ dynamic or absolute viscosity

ρ_b, ρ_d bulk (dry) density of the soil

σ_e electrical conductivity

τ dimensionless tortuosity factor

ω empirical dimensionless coefficient

CHAPTER 1

INTRODUCTION

1.1 Problem Statement

In the 1940s to 1960s, the industrialized countries of the world underwent an enormous expansion in capacity for manufacturing goods, processing petroleum, and making new chemicals. Geotechnical engineers and earth scientists played an important role in that expansion by identifying mineral and petroleum resources, investigating subsurface stratigraphy and soil conditions, designing foundations for complex structures and machinery, and developing earthwork specifications.

Despite the advances made in the field that we now call geotechnical engineering in the 1950s and 1960s, there was practically no emphasis on environmental matters in geotechnical engineering practice during this period. By the end of the 1970s, though, the situation began to change markedly and irrevocably. The production of ever increasing volumes of solid wastes and hazardous materials in that period poses a serious challenge for civil engineers, in general, and geotechnical engineers, in particular; specifically: *how to treat these wastes properly to eliminate or, at least, minimize their potential threat to public health and the environment*. Despite various recently developed chemical, physical, and biological techniques of waste treatment, ground burial of wastes is still a common practice all over the world, especially in North America, for economic and technological reasons. Regulations, performance standards, and technical guidelines for the design, construction, and operation of these waste disposal facilities have been issued by the concerned authorities, notably the U.S. Environmental Protection Agency (U.S. EPA, 1985).

The engineered double liner containment system is recommended for hazardous waste landfills, with leachate collection and leak detection layers located above and between the two liners, respectively, as shown in Fig. 1.1. These liners may be flexible membrane liners
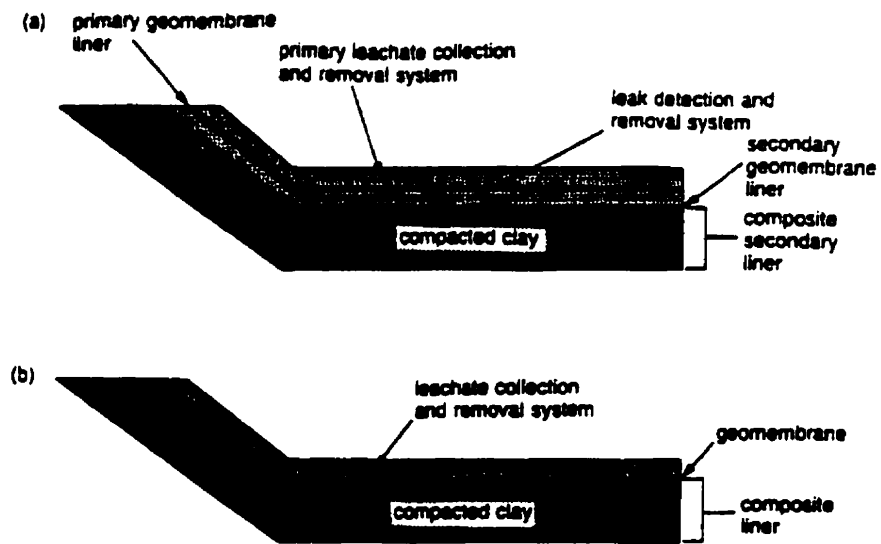
Figure 1.1 Minimum liner requirements of the US Environmental Protection Agency: (a) for hazardous waste landfills, and (b) for non-hazardous waste landfills (after U.S. EPA, 1985; Daniel, 1993).

NOMENCLATURE		MATERIAL	DIMENSIONS & SPECIFICATIONS
Solid waste			
Filter medium		Graded granular filter medium	Recommended thickness > 6 in (152 mm)
Primary leachate collection and removal system		Granular drain material	Recommended thickness > 12 in (305 mm). Hydraulic conductivity > 1 x10^{-2} m/s
Primary geomembrane liner		Flexible membrane liner (FML)	Recommended thickness of FML > 30 mils (0.76 mm)
Leak detection and removal system		Granular drain material	Recommended thickness > 12 in (305 mm). Hydraulic conductivity > 1 x10^{-2} m/s
Composite secondary liner	Secondary geomembrane liner	Flexible membrane liner (FML)	Recommended thickness of FML > 30 mils (0.76 mm)
	Compacted clay	Low permeability soil, compacted in lifts	Recommended thickness > 36 in (914 mm). Recommended hydraulic conductivity < 1 x10^{-9} m/s, prepared in 6 in. lifts, surface scarified between lifts
Native soil foundation/sub-base		In-situ soil	Unsaturated zone
			Saturated zone

Figure 1.1 Minimum liner requirements of the US Environmental Protection Agency (after U.S. EPA, 1985; Daniel, 1993) [continued].

(FMLs), compacted soil layers, or a composite of both. Because of their extremely low values of hydraulic conductivity after proper compaction, fine-grained soils have always been opted for as the preferred construction material of the hydraulic barriers for engineered landfills and surface impoundments. The recommended compacted clay liner has a minimum thickness of 0.90 m (3 ft) and a hydraulic conductivity (k) of less than 1×10^{-9} m/s. Its purpose is to serve as the final barrier to waste leachate migration into surrounding environment for at least 30 years after the closure of a landfill, even if the FML fails. The importance of these compacted clay liners (CCLs) in the confinement of hazardous materials is evident.

As a macroscopic parameter quantifying the integrity of a CCL, hydraulic conductivity has long been known to be a function of compaction water content and compactive effort (Lambe, 1958b). Hydraulic conductivity values between a clay compacted dry of optimum and one compacted wet of optimum can differ by several orders of magnitude. Previous studies have indirectly demonstrated the dominant control of this property by the structure of compacted clay (Lambe, 1958a). Direct observations and detailed calculations, however, have yet to be made on the fabric and pore characteristics of compacted clay.

The preliminary purpose of this research is to examine the relation between the structure and the hydraulic conductivity of kaolinite compacted at optimum moisture content by direct observation using scanning electron microscopy (SEM) method. Simulation of contaminant transport in soils by finite element method (FEM) is expected to serve as a bridge in evaluating the correlation between macroscopic and microscopic properties.

The chemical compatibility of compacted soil has been of major concern for geo-environmental engineers and soil scientists since early 1980s when serious leakage of hazardous chemicals was discovered through ground burial facilities of solid and hazardous wastes. Intensive studies have been performed on soil-chemical interactions and their effects on soil hydraulic conductivity. Due to the complexity of the problem, the different methods used in testing, and the variety of tested soils and chemicals, the results and conclusions made

by different researchers are difficult to compare and some are even contradictory to each other. Changes in hydraulic conductivity due to chemical permeation are usually postulated to be the result of fabric changes by virtue of a different pore fluid chemistry. The diffuse double layer theory is often used as a qualitative explanation. A main goal of this research is to investigate the influence of various pollutants on both the structure and hydraulic conductivity of compacted clay.

1.2 Research Objectives

Specific objectives of this research are to:

❏ better understand the structure of compacted clays at maximum dry density;

❏ assess the compatibility of compacted clay with different contaminants and its impact on both the fabric and hydraulic conductivity;

❏ explore quantitative relationships between physical properties of permeants and hydraulic conductivity of compacted soils, and between clay characteristics and intrinsic permeability;

❏ shed more light on the pore characteristics responsible for the hydraulic behavior of compacted clays;

❏ explore the extent of validity of simulating the contaminant migration through soils by finite element method;

❏ adopt scanning electron microscopy to study clay structure; and

❏ establish viable protocols for chemical characterization of soils, leaching of compacted clays and preparation of contaminated specimens for SEM observations.

1.3 Dissertation Organization

Chapter 2 provides a complete review of previous developments in our knowledge regarding compaction theory and conduction phenomena. Also included in this chapter is a summary of previous studies of hydraulic conductivity with chemicals as permeants reported during the past decade. A presentation of the basic concepts for describing contaminant

transport in and through porous materials is also covered in chapter 2. The chapter ends off with the purpose of the study defined and specified.

Chapter 3 describes the properties of the materials used in the study. Advantages and drawbacks of adopted methods are also discussed, with their limitations cited. Special attention is paid to the methodology of the investigation and the unique approaches to accomplish the research objectives. Procedures of chemical characterization, static compaction, and hydraulic conductivity measurements have been established and are discussed. Test equipment and different protocols followed to conduct both leaching and soaking tests are presented in this chapter, and the termination criteria for the compatibility tests are discussed in detail. Distinct methods are adopted to analyze various leachates depending on the contaminant properties. Scanning electron microscopy (SEM) method is introduced in chapter 3 to study compacted clays contaminated with different chemicals and compounds. Principles of contaminant transport modeling are also presented in this chapter, along with the design of the finite element mesh and the specification of the boundary conditions.

Chapter 4 presents the results of the study of both the structure of compacted kaolinite at optimum moisture content and the soil-contaminant interactions. The compaction characteristics and different hydraulic behavior of the clays have been obtained and are discussed based on microfabric features revealed by SEM micrographs. The effects of sample exposure to organic compounds upon soaking with respect to soil structure and microfabric are also presented and discussed in chapter 4. Geochemical reactions occurring between clay particles and the pore fluids during leaching and soaking are discussed in this chapter. Numerical simulation results are also presented and compared with the experimental results to verify the validity of numerical modeling by finite element method.

Chapter 5 summarizes the conclusions reached based upon the results of this study. The importance of clay microfabric to hydraulic conductivity is emphasized. Microfabric

changes resulting from contaminant leaching and exposure are verified, and the effect of measurement procedures on hydraulic conductivity is proposed. Finally, advantages and disadvantages of different methods, including scanning electron microscopy and finite element numerical simulation, are summarized in this chapter.

Appendix A compiles and summarizes most of the basic principles related to the structure of clay and soil-contaminant interaction.

CHAPTER 2
OVERVIEW OF PREVIOUS STUDIES

2.1 Introduction

Whilst disposal of waste, in the general context used in North America, refers to the discharge of waste forms into the atmosphere, receiving waters and land, the subject of concern to the geotechnical engineering community is land disposal of waste. The immediate and particular concerns regarding landfilling technology relate to the availability, or lack thereof, of proper specifications and technical information regarding disposal standards and criteria which are critical in the establishment of the basic land disposal/containment design standards and technological requirements.

Regardless of how the waste material is generated (produced), and regardless of the procedures taken to neutralize or treat the waste material, the final resting place for the industrial or consumer waste that cannot be recycled, or has been recycled, is in the ground. Burial in the ground is the ultimate disposal mode for most waste products. Therefore, special care must be exercised if we are to avoid problems created by land disposal of waste.

In geoenvironmental technology, the problem of waste management requires solution of waste containment (in the ground) in a manner that can satisfy criteria designed to protect both human health and the environment. This requires attention not only to waste water quality and treatments needed to improve the quality of the discharge streams to meet environmentally acceptable standards, but also to ground water protection and the various problems of safe ground containment and isolation of waste and its leachates. The choice of solution, together with the emphasis, detail, and scope of attention to the various constituent parts of the problem of waste management requires proper study of waste characteristics and substrate material. In particular, the interaction between waste and substrate soil must be well understood.

A necessary function of the ground in containment of waste material, and in protection of the quality of groundwater, is to provide the capability to buffer the waste leachates such that the contaminating constituents are retained within the soil matrix. For proper design considerations or analysis, it is indispensable to study and understand the many kinds of interactions established between the various contaminants and soil constituents. To do so, one needs to understand what constitutes the waste material being disposed of, and in turn understand what the soil constituents are, since interactions established are directly related to the characteristics and properties of the interacting partners.

As illustrated in the previous chapter (cf. Division 1.1), one of the principal features of a secure landfill is an impermeable base and sides to prevent the escape of leachates. This is accomplished by using double- or single-membrane synthetic liners (e.g., polyethylene) with filter separations to permit drainage, along with a compacted natural clay liner to create engineered barriers (Fig. 1.1). The basic intent in safe landfilling can be expressed in one of two forms: 1) Providing a totally secure leakproof side and bottom liner system which will contain *"forever"* the waste material and whatever leachates generated within the waste pile, or 2) Using the ground substrate system, i.e. the substrate soil underlying the landfill, as a physical and chemical buffer to accumulate and attenuate contaminant leachates emanating from the waste pile. In the second intent, it is accepted that no liner system can fully contain the waste leachates "forever." Thus, the second intent requires the physical and chemical buffer system of the substrate soil to reduce the concentration of pollutants such that when (or if) the pollutants reach the groundwater system, the concentrations will be below acceptable limits. This requirement places a large burden of responsibility on the landfill constructor to properly determine the capability of the soil to perform its buffering functions. Two absolutely important conditions need to be fulfilled:

1. Development of a proper understanding of the contaminant migration process in compacted clays; and

2. Development of a viable and reliable analytical model which can accurately predict transport performance of the contaminant plume for the time period of concern.

This study is focused on contributing to the fulfillment of the first condition.

An extensive literature review focusing on the aspects relevant to the migration of contaminants through compacted clay liners is compiled and summarized in this chapter. These are discussed and criticized in the following divisions: theory of compaction, conduction phenomena, soil-chemical interactions, contaminant transport, and purpose of study. It has to be noted that the basic principles comprising the foundation for a better understanding of these topics and the present study are presented in appendix A of the dissertation.

2.2 Theory of Compaction

Compaction is the process of increasing the density of a soil by packing the particles closer together with a reduction in the volume of *air*; there is no significant change in the volume of water in the soil. It is an ancient technique by which the mechanical and hydraulic properties of a soil can greatly be improved making use of some combinations of water content and compactive effort. The fact that soils compacted dry of optimum and wet of optimum behave in significantly different ways has inspired relentless investigations. The importance of fabric to the engineering behavior of compacted clay was first studied in the 1950s by Lambe (1958), and Seed and Chan (1959). Less swell-shrinkage and higher as-compacted shear strength can be found in soil compacted dry of optimum. The flocculated structure of soils compacted dry of optimum contributes to hydraulic conductivities two to three orders of magnitude higher than those soils compacted wet of optimum. Dispersed fabric would make the soil compacted wet of optimum much less permeable (Mitchell *et al.*, 1965). Structure is considered to be the most important variable influencing the hydraulic conductivity of a compacted soil.

Lambe (1958a) was one of the first investigators to hypothesize a model for the fabric of compacted clay. He postulated that individual clay particles are the predominant units that

influence the compaction characteristics and behavior of a soil mass (Lambe, 1958b). By adopting the diffuse double layer theory, Lambe (1958a) proposed the fabric model of soil compacted at different water contents and different compactive efforts as shown in Fig. 2.1. At the same compactive effort, with increasing water content, the soil fabric becomes increasingly oriented. Dry of optimum the soils are always flocculated, whereas wet of optimum the fabric becomes more oriented or dispersed. In Fig. 2.1, for example, the fabric at point C is more oriented than at point A. Now, if the compactive effort is increased, the soil tends to become more oriented, even dry of optimum. Again, referring to Fig. 2.1, a sample at point E is more oriented than at point A. Wet of optimum, the fabric at point D will be somewhat more oriented than at point C, although the effect is less pronounced compared to that at dry of optimum. At point B, that is near or at optimum, the fabric is a combination of flocculated and dispersed structures.

According to Lambe (1958a) an increase in molding water content would increase the dispersion tendency of clay particles because a decrease in electrolyte concentration tends to increase the thickness of the diffuse double layer leading to a relatively high repulsive force. As a result, soil compacted dry of optimum exhibits a flocculated structure with the clay particles contacting each other in randomly face-to-edge configurations and a corresponding low compacted dry density. Soil compacted at the optimum water content possesses a more dispersed fabric and a maximum dry density. Though soil compacted wet of optimum has a totally dispersed fabric composed of face-to-face arranged particles, its compacted dry density decreases due to the added water occupying more space in the soil mass. The increase in compactive effort would result in more preferentially oriented clay particles, and thus increase soil density by virtue of more energy input into the system. Limitations to the application of the diffuse double layer theory to soil have been described in Lambe (1958a). Because the theory was derived for very dilute colloidal suspensions, higher particle concentrations, extremely small interparticle spacing, and externally applied forces are among the factors that invalidate direct application of the theory to soil. Furthermore, the amount of water used in clay compaction is always less than what is needed for a fully developed diffuse double layer
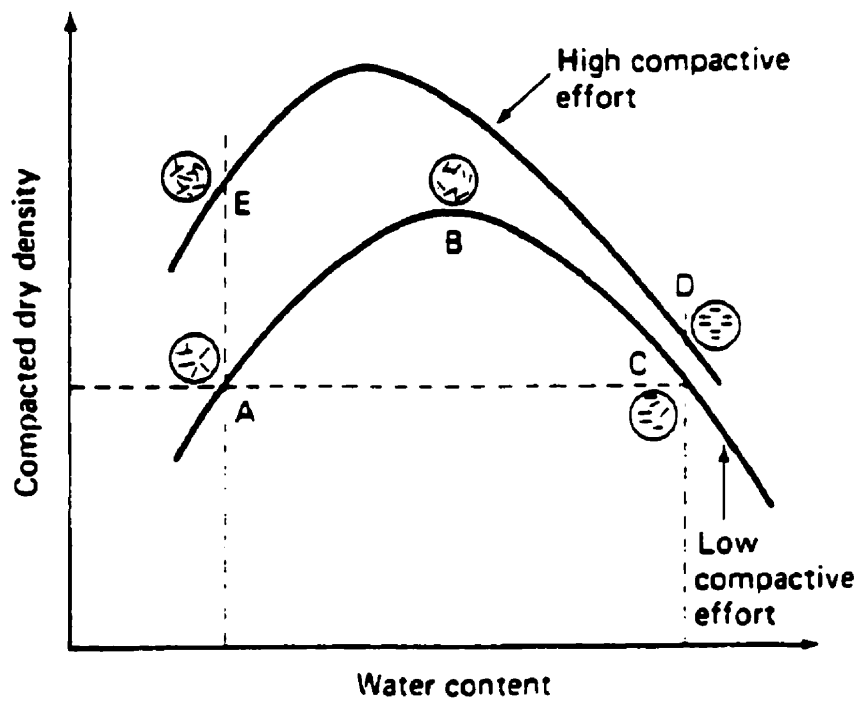
Figure 2.1 Effect of compaction on soil structure (after Lambe, 1958a).

around particles (Lambe, 1958a). The compaction theory was confirmed by measurements of particle orientation as a function of compaction water contents using Mitchell's (1956) optical microscope method. Higher compaction water content leads to a more parallel arrangement of clay particles.

Seed and Chan (1959) emphasized the effect of the compaction process on the structure, and thus on the engineering behavior, of compacted clays. Compaction was considered to be a dispersion process by which the induced shear strain would produce a great degree of particle orientation, and even a flocculated fabric could be changed into a dispersed one. Comparatively, soil compacted dry of optimum tends to retain its flocculated fabric resulting from mixing due to stronger attractive force between particles. However, soil compacted wet of optimum would suffer greater shear deformation, and hence tends to be more dispersed with particles preferentially oriented as a result of increase in repulsive forces between particles leading to a reduction in shear strength. Mitchell *et al.* (1965) attributed the extremely high hydraulic conductivity of soils compacted dry of optimum to the existence of large flow channels. The dispersion process, caused by either increase in water content or compactive effort, reduces the number of large channels. Consequently, the average pore size decreases and the hydraulic conductivity is drastically reduced.

When it was possible to examine particle-to-particle relationships of a clay by carbon replica using a transmission electron microscope, the hypothetical fabric composed of individual clay particles (either oriented or random) was rejected (Sloane and Kell, 1966). Instead, the fabric was found to consist of parallel and random arrangements of packets of oriented clay flakes. Apparently, the packets are domains of oriented clay platelets as described by Aylmore and Quirk (1960). Though the degree of parallel orientation of the packets increases with increasing water content, the effect of shear strain induced on the fabric during compaction was found to be partial remolding; that is, trajectories of parallel packets with essentially randomly oriented zones of packets. The bookhouse structure was

proposed as an analog to the cardhouse fabric to describe the randomly arranged fabric composed mainly of packets (Sloane and Kell, 1966).

Aggregation and its effect on engineering behavior of compacted clay was studied by Barden and Sides (1970), in which they have proposed a revision of Lambe's compacted clay model and reached the conclusion that the behavior and characteristics of a compacted clay can be explained in terms of a deformable aggregate soil model. In their low magnification scanning electron microscope investigation, Barden and Sides (1970) observed pellet-like macropeds in soils compacted dry of optimum, but a homogeneous structure was apparent in soils compacted wet of optimum. Prior to compaction, the soil particles are grouped in agglomerations or "peds" whose size and strength characteristics are influenced by the molding water content. During compaction at low water contents (below optimum), these peds or aggregates have a high strength and are better able to resist the compaction pressures without much distortion. Thus, there exist two networks of pore space in the clay mass: a network of large inter-aggregate pores, and a network of small intra-aggregate pores. As the molding water content increases (dry of optimum), the aggregates decrease in strength and suffer greater deformation during compaction. This results in a decrease in inter-aggregate pore space and an increase in dry density. Olson (1963), Langfelder et al. (1968), and Barden and Sides (1970) have all found that clays compacted near their optimum moisture contents have zero air permeability, which could indicate that the inter-aggregate pore network is no longer continuous. With increasing water content above optimum, the aggregates are easily distorted and fuse together making them indistinguishable. Individual particle reorientation and dispersion may occur at this stage. Pore size distribution measurements of compacted clays by Diamond (1970, 1971), Sridharan et al. (1971), and Ahmed et al. (1974) have also provided strong evidence for a deformable aggregate soil model.

Other studies have found that increasing the compactive effort on the dry side of optimum for a given soil decreases the total porosity and diminishes the fraction of large

pores. However, increasing the compaction effort on the wet side of optimum had little effect on either the total porosity or the distribution of pore sizes.

Diamond (1971) investigated the importance of pore size distribution by comparing scanning electron microscope images to mercury intrusion porosimetry data of compacted kaolinite and illite. Regardless of compaction water content and compactive effort, there were always small pores with modal diameters between 0.02-0.08 μm existing in compacted kaolinite. Nevertheless, large modal pore diameters between 0.1 and 5.0 μm were observed in clay compacted dry of optimum or at lower compactive efforts. The large pores are believed to be constituted by domains or aggregates composed of individual kaolinite flakes in approximately parallel orientation. Diamond (1971) concluded that soil compacted dry of optimum is composed of domains or aggregates randomly touching each other at peripheral points to form large interdomain void spaces. Domains in soil compacted wet of optimum are in close contact and boundaries between domains are difficult to distinguish. Very few interdomain spaces are thus formed. On the other hand, small pores, formed irrespective of compactive conditions, were assumed to be intradomain pores between individual clay platelets. No attempt was made to distinguish the difference between domain and aggregate.

Porosimetry tests also revealed bimodal pore size distributions in a series of compacted silt-kaolinite mixtures (Garcia-Bengochea et al., 1979). Large modal pore diameters occurring from 1.0 μm to 10.0 μm were assumed to be intersilt and inter-aggregate pores. The volumetric frequency distribution and dominant pore sizes were sensitive to changes in molding water content, compactive effort, and silt content. Yet, the small modal pore diameter occurs consistently at 0.1 μm regardless of compaction conditions in a given soil. It was hypothesized that these were intra-aggregate pores. As a matter of fact, the dominant size and the characteristic volumetric frequency of the large pores provide a bridge connecting the macrostructure of compacted soil to its hydraulic conductivity. Increasing compaction water content, increasing compactive effort, and decreasing silt or increasing clay content result in lower hydraulic conductivity by virtue of reducing the percentage of pores

and/or decreasing the size of large pores. Though a quantitative relationship was given based on several models relating pore size distribution to intrinsic permeability, no direct observation was made to confirm the existence of aggregation in the soils.

Scanning electron microscopy (SEM) observations can be used to correlate the characteristics of compacted kaolinite obtained from pore size measurements by mercury porosimetry (Acar and Olivieri, 1989). Both bimodal and unimodal distributions were revealed by the different methods in kaolinite compacted dry of optimum and wet of optimum, respectively. SEM photomicrographs of compacted kaolinite and Ca-montmorillonite showed that clay compacted dry of optimum was composed of a flocculated fabric with individual flakes randomly arranged in edge-to-face contacts; while clay compacted wet of optimum was characterized by a dispersed fabric with dominant face-to-face association between individual flakes. Though the difference of surface roughness between soils compacted dry and wet of optimum hinted the existence of micropeds (aggregates), no details were provided about the aggregates and their internal structure.

In this research, emphasis is on correlating the structure of compacted clay at optimum moisture content with its hydraulic behavior. The particular fabric of compacted clay is exposed by means of detailed direct observations using scanning electron microscopy, which also helps in defining the difference between domain and aggregate. The existence of aggregation in clays compacted at their maximum dry density is verified to weigh its role in the conduction process. The present study puts in place the final block of compaction theory in regard to soil structure.

2.3 Conduction Phenomena

Virtually all geotechnical problems involve soil (or rock) deformation and stability, volume change, and/or the flow of fluids, chemicals, and energy in various forms. Furthermore, the flows often play a vital role in the deformation, volume change, and stability

behavior itself. Water flow has been extensively studied because of its important role in problems of seepage, consolidation, and stability, which form a major part of soil and rock engineering analysis and design. As a result, much is known about the hydraulic conductivity and permeability of earth materials.

Chemical, thermal, and electrical flows in soils are also important. Chemical transport through the ground is of a major concern in connection with groundwater pollution, waste disposal and storage, remediation of contaminated sites, corrosion, leaching phenomena, osmotic effects in clay layers, and soil stabilization. Heat flows are important relative to frost action, construction in permafrost areas, insulation, underground storage, thermal pollution, temporary ground stabilization by freezing, permanent ground stabilization by heating, underground transmission of electricity, and other problems. Electrical flows are important to the transport of water and ground stabilization by electroosmosis, insulation, corrosion, and subsurface investigations.

In addition to the above four flow types, i.e., hydraulic, chemical, thermal, and electrical flows, each driven by its own potential gradient, coupled flows may be important under a variety of circumstances. A coupled flow is a flow of one type, such as hydraulic, driven by a potential gradient of another type, such as electrical.

2.3.1 Flow Laws and Relationships

Fluids, electricity, chemicals, and heat all flow through soils. It has been well established that, provided the flow process does not change the state of the soil, each flow rate or flux J_i (as shown in Fig. 2.2) relates linearly to its corresponding driving force X_i according to

$$J_i = L_{ii} X_i$$

(2.1)

FLUID

$$q_h = k_h \frac{\Delta H}{L} A$$

Darcy's Law

ELECTRICITY

$$I = \sigma_e \frac{\Delta V}{L} A$$

Ohm's Law

HEAT

$$q_t = k_e \frac{\Delta T}{L} A$$

Fourier's Law

CHEMICALS

$$J_D = D \frac{\Delta c}{L} A$$

Fick's Law

ΔH

L

q_h

V_1 V_2

L

$\oplus$ $\ominus$

T_1 T_2

L

$T_1 > T_2$

q_t

L

C_1 J_D C_2
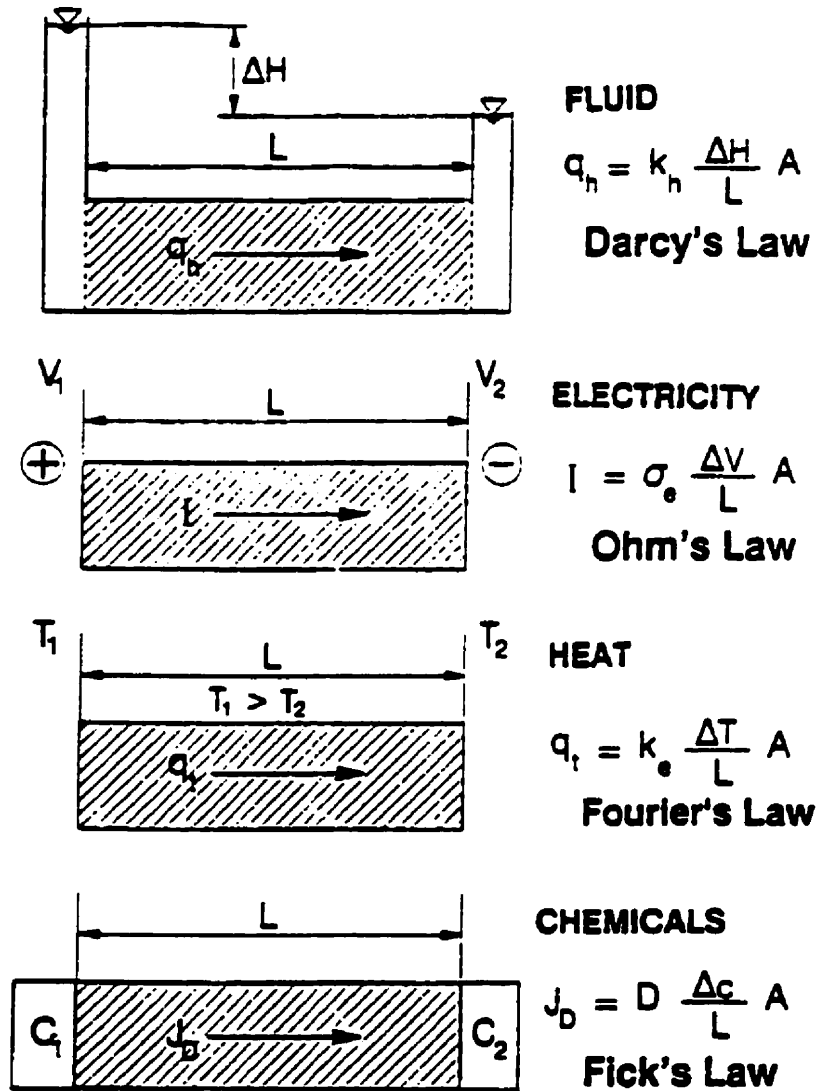
Figure 2.2 Four types of direct flow through a soil mass (Mitchell, 1993).

in which L_n is the conductivity coefficient for flow. When written specifically for a particular flow type and in terms of familiar phenomenological coefficients, Eq. 2.1 becomes

Water flow	$q_h = k_h\, i_h$	Darcy's law
Heat flow	$q_t = k_t\, i_t$	Fourier's law
Electrical flow	$I = \sigma_e\, i_e$	Ohm's law
Chemical flow	$J_D = D\, i_c$	Fick's law

(2.2)

In these equations q_h, q_t, I, and J_D are the water, heat, electrical, and chemical flow rates per unit area, respectively. The coefficients k_h, k_t, σ_e, and D are the hydraulic, thermal, electrical conductivities and the diffusion coefficient, respectively. The driving forces for flow are given by the respective hydraulic, thermal, electrical, and chemical gradients, i_h, i_t, i_e, and i_c.

The terms in Eqs. 2.2 are identified in Fig. 2.2, which shows analogs between the various flow types. As long as the flow rates and gradients are linearly related, the mathematical treatment of each flow type is the same, and solutions for flow of one type may be used for problems of another type provided the property values and boundary conditions are properly represented. A well-known practical illustration of this is the use of electrical analogies for the study of seepage problems.

In most cases, however, there are simultaneous flows of different types, even when only one type of driving force is acting. For example, when pore water containing chemicals flows under the action of a hydraulic gradient, there is a concurrent flow of chemical through the soil. This type of chemical transport is termed advection. In addition, owing to the existence of surface charges in soil minerals, especially the clays, there are nonuniform distributions of cations and anions within soil pores resulting from the attraction of cations to and repulsion of anions from the negatively charged particle surfaces. Because of the small pore sizes in fine-grained soils and the electrical fields within them, clay layers may exhibit membrane properties, which means that the passage of certain ions and molecules through the clay may be restricted in part or in full on both microscopic and macroscopic levels.

Owing to the internal nonhomogeneities in ion distributions, restrictions on ion movements caused by electrostatic attractions and repulsions, and the dependence of these interactions on temperature, a variety of microscopic and macroscopic effects may be observed when a wet soil mass is subjected to flow gradients of different types. In particular, it has been observed that a gradient of one type can cause a flow of another type, according to

$$J_i = L_{ij} X_j \qquad (2.3)$$

The L_{ij} are termed coupling coefficients. They are properties that may or may not be of significant magnitude in any given soil. The types of coupled flow that can occur are listed in Table 2.1, along with the terms commonly used to describe them.

Of the twelve coupled flows shown in Table 2.1, several are known to be significant in soil-water systems, at least under some conditions. *Thermoosmosis*, which is water movement under a temperature gradient, is important in partly saturated soils, but of limited influence in fully saturated soils. *Electroosmosis* has been used for many years as a means for control of water flow and for consolidation of soils. *Chemical osmosis*, the flow of water caused by a chemical gradient acting across a clay layer, is being studied in some detail presently, owing to its importance in waste containment systems.

Isothermal heat transfer, caused by heat flow along with water flow, has caused great difficulties in the creation of frozen soil barriers in the presence of flowing groundwater. Electrically driven heat flow, the *Peltier effect*, and chemically driven heat flow, the *Dufour effect*, are not known to be of significance in soils; however, they appear not to have been studied in any detail in relation to geotechnical problems.

Streaming current, the term applied to both hydraulically driven electrical current and ion flows, has importance to both chemical flow through the ground (advection) and the development of electrical potentials, which may, in turn, influence both fluid and ion flows as

Table 2.1 Direct and coupled flow phenomena (Mitchell, 1993).

| Flow J | Gradient X | | | |
	Hydraulic head	Temperature	Electrical	Chemical concentration
Fluid	Hydraulic conduction *Darcy's law*	Thermoosmosis	Electroosmosis	Chemical osmosis
Heat	Isothermal heat transfer	Thermal conduction *Fourier's law*	Peltier effect	Dufour effect
Current	Streaming current	Thermoelectricity *Seebeck effect*	Electric conduction *Ohm's law*	Diffusion and membrane potentials
Ion	Streaming current	Thermal diffusion of electrolyte *Soret effect*	Electrophoresis	Diffusion *Fick's law*

a result of additional coupling effects. The complete roles of *thermoelectricity or Seebeck effect* and *diffusion and membrane potentials* are not known; however, electrical potentials generated by temperature and chemical gradients are important in corrosion and in some groundwater flow and stability problems.

Whether thermal diffusion of electrolytes, the *Soret effect*, is important in soils has not been evaluated; however, since chemical activity is highly temperature dependent, it may be a significant process in some systems. Finally, *electrophoresis*, the movement of charged particles in an electrical field, has been used for concentration of mine waste and high water content clays.

2.3.2 Hydraulic Conductivity

Darcy's "law" which was established empirically by Darcy (1856) based on the results of flow tests through sands, and whose general validity for the description of hydraulic flow through most soil types has been verified by many subsequent studies, states that there exists a direct proportionality between flow velocity v_h or flow rate q_h and hydraulic gradient i_h; i.e.,

$$v_h = k_h \, i_h$$
$$q_h = k_h \, i_h \, A \qquad\qquad (2.4)$$

where A is the cross section area normal to the direction of flow. The constant k_h is a property of the material. Virtually all steady-state and transient flow analyses in soils are based on Darcy's law. In many instances, more attention is directed at the analysis, rather than at the value of k_h. This is unfortunate, since no other property of importance in geotechnical problems is likely to exhibit such a great range of values, up to ten orders of magnitude, from coarse to very fine grained soils, or show the variability in a given deposit as does the hydraulic conductivity. Even a given soil may exhibit a few orders of magnitude variation in hydraulic conductivity as a result of changes in fabric, void ratio, and water content. A

comparison of hydraulic conductivities measured in the laboratory and *in situ* which highlights the remarkable variation in hydraulic conductivity, even for the same soil deposit, is presented by Olson and Daniel (1981).

2.3.2.1 The Validity of Darcy's Law

Darcy's law is not universally valid for all conditions of liquid flow in porous media. The two conditions implied in the Darcy relationship are: (a) flow rate is directly proportional to hydraulic gradient, and (b) the relationship between flow rate and hydraulic gradient is linear through the origin. It has long been recognized that the linearity of the flow rate versus hydraulic gradient relationship fails at high flow velocities, where inertial forces are no longer negligible compared to viscous forces. Darcy's law applies only as long as flow is laminar, and where soil-water interaction does not result in a change of fluidity or permeability with a change in gradient.

Deviations from Darcy's law may also occur at the opposite end of the flow-velocity range, namely, at low gradients and in small pores. The condition of linearity between flow rate and hydraulic gradient is valid for porous media and for many clay soils. However, the condition specifying linearity through the origin has been shown not to be valid for all clays. The saturated flow tests performed by the Swedish Geotechnical Institute (Hansbo, 1960, 1973) on undisturbed natural clays show the existence of both a critical gradient and an apparent threshold gradient (Fig. 2.3).

The reported deviations from linearity between flow rate and hydraulic gradient are most significant in the lower range of gradients. In the field, the hydraulic gradients are seldom much greater than one. Thus, deviations from Darcy's law, if real, could have very important implications for the applicability of steady-state and transient flow analyses that are based on this law. Furthermore, gradients that are typically used in laboratory testing are high, commonly more than 10, and often up to several hundred. This brings the suitability of laboratory test results as indicators of field behavior into question.
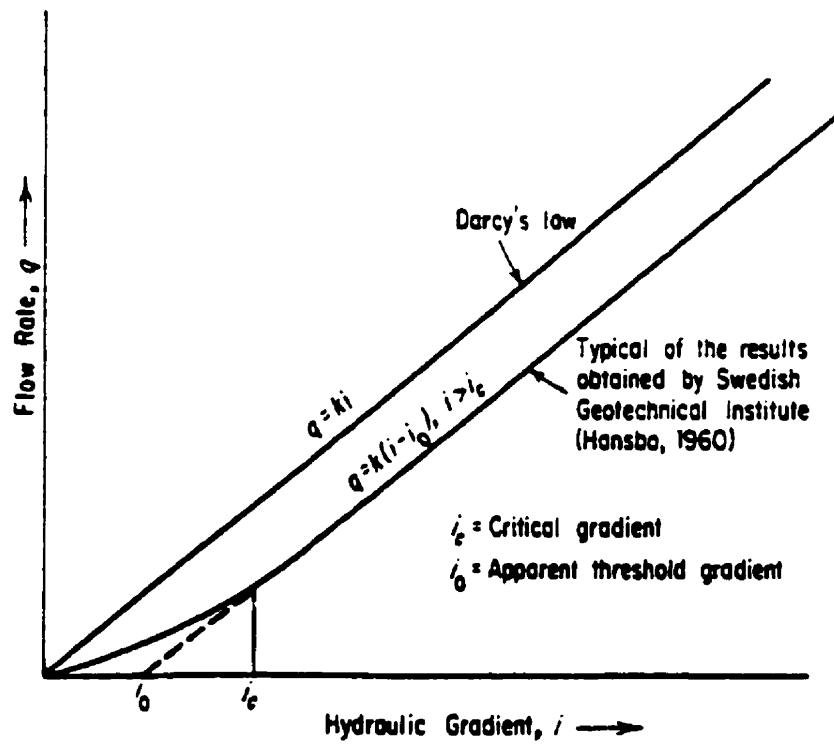
Figure 2.3 Hydraulic flow rates vs. hydraulic gradients (after Hansbo, 1960).

Three hypotheses have been advanced to account for nonlinearity between flow velocity and gradient:

(1) non-Newtonian water flow properties;

(2) particle migrations that cause blocking and unblocking of flow passages; and

(3) local consolidation and swelling that is inevitable when hydraulic gradients are imposed across a compressible soil at the start of hydraulic conductivity testing.

The apparent existence of a threshold gradient below which flow was not detected was attributed to a quasi-crystalline water structure. It is now known, however, that many of the effects interpreted as due to unusual water properties can be ascribed to undetected experimental errors arising from contamination of measuring systems (Olsen, 1965), local consolidation and swelling, and bacterial growth (Gupta and Swartzendruber, 1962). Additional careful measurements by a number of investigators (e.g., Olsen, 1969; Gray and Mitchell, 1967; Mitchell and Younger, 1967; Miller *et al.*, 1969; Chan and Kenney, 1973) failed to confirm the existence of a threshold gradient in clays.In fact, Darcy's law was obeyed exactly in several of these studies. Therefore, it is unlikely that unusual water properties can lead to non-Darcy flow behavior.

On the other hand, particle migrations leading to void plugging and unplugging, electrokinetic effects, and chemical concentration gradients can cause apparent deviations from Darcy's law. Analysis of interparticle bond strengths in relation to the magnitude of seepage forces shows that particles that are not participating in the load-carrying skeleton of a soil mass can be moved under moderate values of hydraulic gradient. Soils with open, flocculated fabrics and soils with a relatively low content of clay appear particularly susceptible to the movement of fine particles during permeation. Internal swelling and dispersion of clay particles during permeation can also cause changes in flow rate and apparent non-Darcy behavior.

Nevertheless, available evidence indicates that Darcy's law is valid, *provided that all system variables are held constant.* Unless fabric changes, particle migrations, and internal

void ratio redistributions caused by effective stress and chemical changes can be shown to be negligible, hydraulic conductivity measurements in the laboratory should be made under conditions of temperature, pressure, hydraulic gradient, and pore fluid chemistry as closely approximating those in the field as possible. This has become a particularly important issue in connection with the testing of clays as potential waste containment barriers, such as liners for landfills and impoundments.

Unfortunately, duplication of field conditions is not always possible, especially as regards the hydraulic gradient. If hydraulic gradients low enough to duplicate those in most field situations are used, then the testing time usually becomes unacceptably long. In such cases, tests over a range of gradients are desirable in order to assess the stability of the soil to structure changes due to seepage forces.

2.3.2.2 Theoretical Equations for Hydraulic Conductivity

Fluid flow through soils finer than coarse gravel is laminar. Equations have been developed to relate the hydraulic conductivity to properties of the soil and permeating fluid. A usual starting point for derivation of such equations is Poiseuille's law for flow through a round capillary, which gives the average flow velocity v_{ave}, according to

$$v_{ave} = \frac{1}{8} \frac{\gamma_p}{\mu} R^2 i_h \tag{2.5}$$

where μ is viscosity, R is tube radius, and γ_p is unit weight of the permeant. Because the flow channels in a soil are of various sizes, a characteristic dimension is needed to describe average size. The hydraulic radius R_H

$$R_H = \frac{flow\ channel\ cross\ section\ area}{wetted\ perimeter} \tag{2.6}$$

is useful.

For a circular tube flowing full,

$$R_H = \frac{\pi R^2}{2\pi R} = \frac{R}{2} \tag{2.7}$$

so Poiseuille's equation becomes

$$q_{cir} = \frac{1}{2} \frac{\gamma_p}{\mu} R_H^2 \, i_h \, a \tag{2.8}$$

where a is the cross-sectional area of the tube. For other shapes of cross section, an equation of the same form will hold, differing only in the value of a shape coefficient C_s

$$q = C_s \frac{\gamma_p}{\mu} R_H^2 \, i_h \, a \tag{2.9}$$

For a bundle of parallel tubes of constant but irregular cross section contributing to a total cross-sectional area A (comprising soilds and voids), the area of flow passages A_f filled with water is

$$A_f = S \, n \, A \tag{2.10}$$

where S is the degree of saturation, and n is the porosity. For this condition the hydraulic radius is given by

$$R_H = \frac{A_f}{P} = \frac{A_f L}{P L} = \frac{\text{volume available for flow}}{\text{wetted area}} = \frac{V_{water}}{V_s S_0} \tag{2.11}$$

where P is the wetted perimeter, L is the length of flow channel in the direction of flow, V_s is the volume of solids and S_0 is the wetted surface per unit volume of particles. The wetted surface depends on the particle sizes and the soil fabric. It is less than the total specific surface area of the soil, since flow will not occur adjacent to all particle surfaces.

For void ratio e and volume of solids V_s, the volume of water is

$$V_w = e \ V_s \ S \tag{2.12}$$

Thus, Eq. 2.9 becomes

$$q = C_s \left(\frac{\gamma_p}{\mu}\right) R_H^2 \ S \ n \ i_h \ A = C_s \left(\frac{\gamma_p}{\mu}\right) R_H^2 \ S \left(\frac{e}{1+e}\right) i_h \ A \tag{2.13}$$

and substitution for R_H gives

$$q = C_s \left(\frac{\gamma_p}{\mu}\right) \frac{1}{S_0^2} \ S^3 \left(\frac{e^3}{1+e}\right) i_h \ A \tag{2.14}$$

By analogy with Darcy's law,

$$k_h = C_s \left(\frac{\gamma_p}{\mu}\right) \frac{1}{S_0^2} \left(\frac{e^3}{1+e}\right) S^3 \tag{2.15}$$

For the case of full saturation, $S = 1$, and denoting C_s by $1/(k_0 \ T^2)$, where k_0 is a pore shape factor and T is a tortuosity factor, Eq. 2.15 becomes

$$K = k_h \left(\frac{\mu}{\gamma_p}\right) = \frac{1}{k_0 \ T^2 \ S_0^2} \left(\frac{e^3}{1+e}\right) \tag{2.16}$$

This is the well-known Kozeny-Carman equation for the permeability of porous media (Kozeny, 1927; Carman, 1956).

In principle, the effects of permeant properties are accounted for by the $(\mu \ / \ \gamma_p)$ term. The pore shape factor k_0 has a value of about 2.5 and the tortuosity factor has a value of about $\sqrt{2}$ in porous media containing approximately uniform pore sizes. The hydraulic conductivity k_h has units of velocity (LT^{-1}), and the absolute or intrinsic permeability K has units of area (L^2).

Although the Kozeny-Carman equation accounts well for the dependency of permeability on void ratio in uniformly graded sands and some silts, serious discrepancies are found in clays. The main reason for these discrepancies is that most clays do not contain uniform pore sizes. Particles in clays are grouped in clusters or aggregates that produce large intercluster pores and small intracluster pores.

Provided comparisons are made using samples having the same fabric, the influence of permeant on hydraulic conductivity is quite well accounted for by the $(\mu \quad \gamma_p)$ term. If, however, a fine-grained soil is molded or compacted in different permeants, then the fabrics may be quite different, and the hydraulic conductivities for samples at the same void ratio can differ greatly.

Despite the inability of the theoretical equations to predict the hydraulic conductivity accurately in many cases, they do reflect the overwhelming importance of pore size. Flow velocity depends on the square of pore radius, and hence, the flow rate depends on radius to the fourth power. The specific surface in the Kozeny-Carman equation is a measure of the pore size. For a soil having a homogeneous fabric, the hydraulic conductivity depends more on the fine particles than on the large. A small percentage of fines can clog the pores of an otherwise coarse material and result in a manyfold lower hydraulic conductivity. On the other hand, the presence of fissures, cracks, etc. can result in enormous increases in the rate of water flow through an otherwise compact soil layer.

Finally, Eq. 2.15 predicts that the hydraulic conductivity should vary with the cube of the degree of saturation, and experimental data support this, even in the case of fine-grained soils.

2.3.2.3 Fabric and Hydraulic Conductivity

The theoretical relationships developed in the previous subsection indicate that the flow velocity should depend on the square of the pore radius, and the flow rate is proportional

to the fourth power of the radius. Thus, for a given soil, fabrics with a high proportion of large pores are much more pervious than those with small pores. For example, remolding undisturbed soft clays has been found to reduce the hydraulic conductivity by as much as a factor of 4, with an average of about 2 (Mitchell, 1956). This can be explained by the breakdown of a flocculated open fabric and the destruction of large pores.

A typical illustration of the profound influence of compaction water content on the hydraulic conductivity of a fine-grained soil is shown in Fig. 2.4. For the case shown, all samples were compacted to the same density. For samples compacted using the same compactive effort, curves such as those in Fig. 2.5 are typical. For compaction dry of optimum, clay particles and aggregates are flocculated (Fig. 2.1), the resistance to rearrangement during compaction is high, and a fabric with comparatively large pores is formed. For higher water contents, the particle groups are weaker, and fabrics with smaller average pore sizes are formed. Considerably lower values of hydraulic conductivity are obtained wet of optimum in the case of kneading compaction than by static compaction (Fig. 2.5), because the high shear strains induced by the kneading compaction method break down flocculated fabric units.

Three levels of fabric are important when considering the hydraulic conductivity of fine-grained soils (cf. Subsection A.3.1.3), namely, the microfabric, minifabric, and macrofabric (Collins and McGown, 1974).

All the above considerations are of particular importance when it comes to the hydraulic conductivity of compacted clays used as barriers for waste containment in environmental applications. The controlling units in these materials are the clods, which would correspond to the minifabric units. It has been shown (Benson and Daniel, 1990) that acceptably low values of hydraulic conductivity can be obtained only if clods and interclod pores are eliminated during compaction. This requires that compaction be done wet of
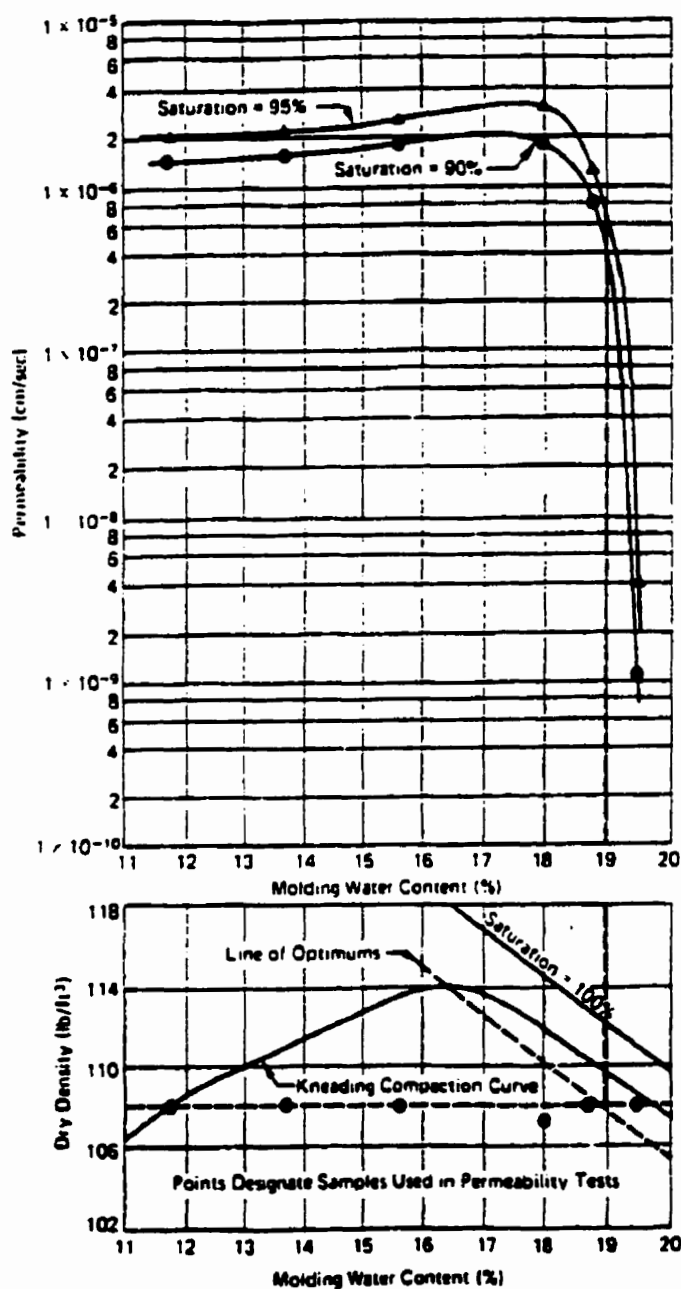
Figure 2.4 Hydraulic conductivity as a function of molding water content for samples of silty clay prepared to constant density by kneading compaction (Mitchell, 1993).
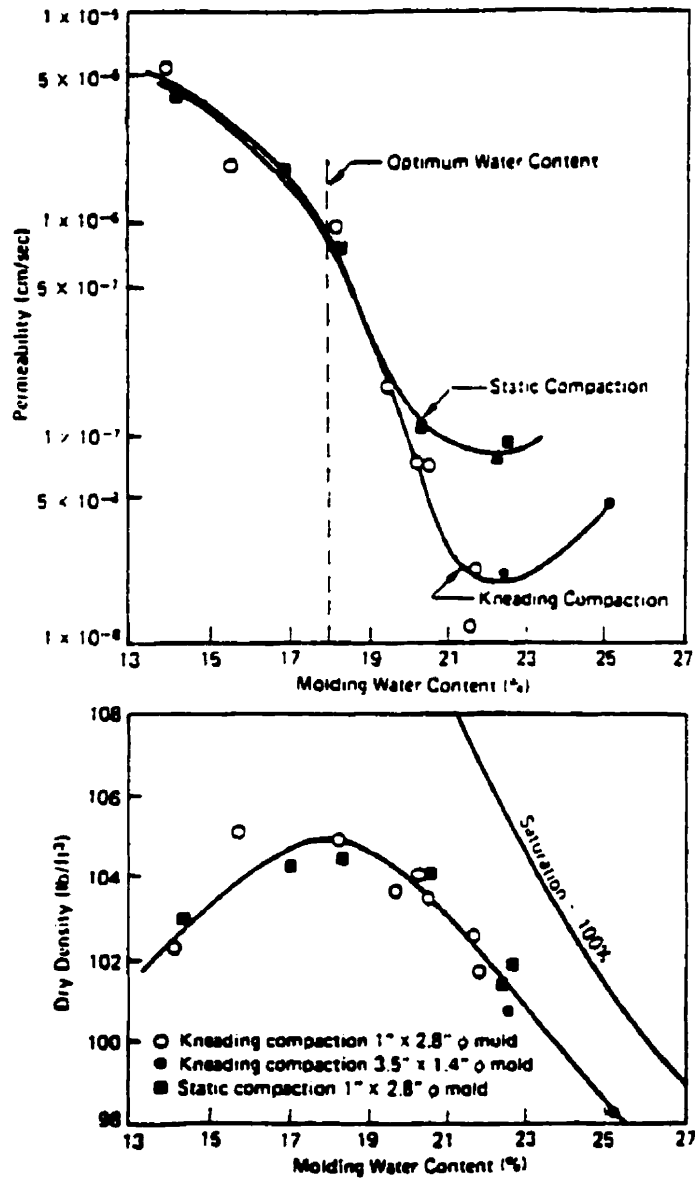
Figure 2.5 Influence of compaction method on the hydraulic conductivity of silty clay. Constant compactive effort for all samples (Mitchell, 1993).

optimum using a high effort and a method that produces large shear strains, such as sheepsfoot rollers.

The wide range of values of hydraulic conductivity of compacted fine-grained soils resulting from the large differences in fabric associated with compaction to different water contents and densities is illustrated by Fig. 2.6. The grouping of contours means that selection of a representative value for use in a seepage analysis is difficult and that precise predictions cannot usually be made. In addition, if it is required that the hydraulic conductivity of earthwork not exceed a certain value, such as may be the case for a clay liner, then specifications must be carefully drawn. In so doing, it must be recognized also that other properties, such as strength, also vary with compaction water content and density, and that the compaction conditions that are optimal for one property may not be suitable for the other. A procedure for the development of suitable specifications for compacted clay liners is given by Daniel and Benson (1990).

In a classic study, Olsen (1962) showed that the reason equation such as Eq. 2.16 fails to account quantitatively for the variation of the hydraulic conductivity of fine-grained soils with void ratio was the existence of unequal pore sizes. A typical soil will have a fabric composed of small aggregates or clusters as shown schematically in Fig. 2.7, having an intracluster void ratio e_c. The spaces between the aggregates comprise the intercluster voids and are responsible for the intercluster void ratio e_p. The total void ratio e_T is equal to the sum of e_c and e_p. The clusters and intracluster void ratio correspond to the microfabric; whereas, the assemblage of clusters (including intercluster void ratio) comprises the minifabric. Fluid flow in such a system is dominated by flow through the intercluster pores.

The size of clusters that form depends on the mineralogical and pore fluid compositions and the formational process. These conditions that favor aggregation of individual clay plates produce larger clusters than deflocculating, dispersing environments, and there is a general consistency with the interparticle double layer interactions discussed in
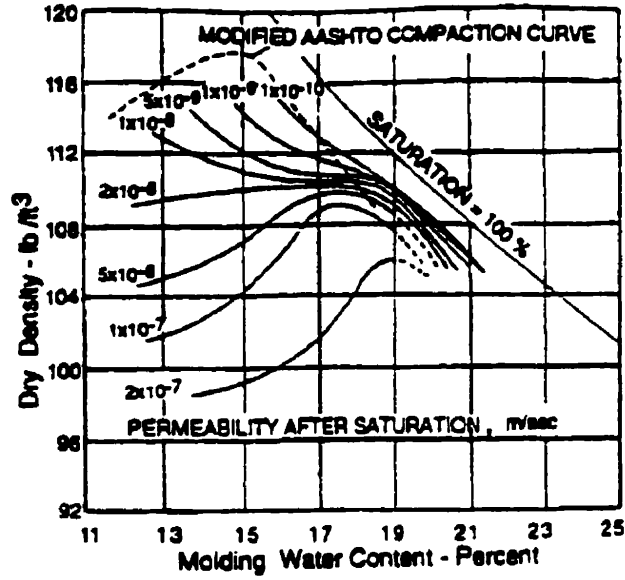
Figure 2.6 Contours of constant hydraulic conductivity for silty clay compacted using kneading compaction (Mitchell, 1993).
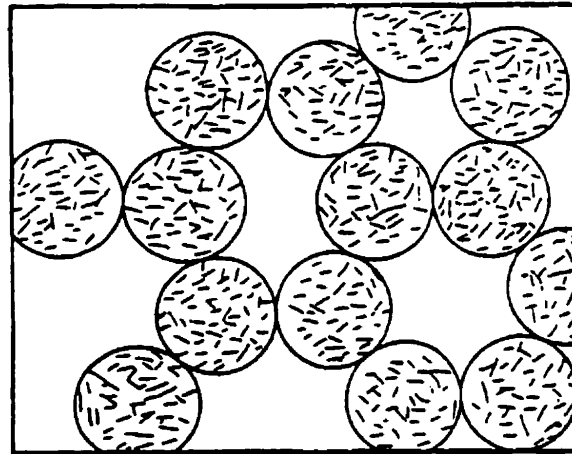
Figure 2.7 Cluster model for permeability prediction (after Olsen, 1962).

section A.2.3. When a given fine-grained soil is sedimented in or mixed with water of different electrolyte concentration or type, or with fluids of different dielectric constants, quite different fabrics result. This explains why the $(\mu \cdot \gamma_p)$ term in the Kozeny-Carman equation is inadequate to account for pore fluid differences, unless comparisons are made using samples having identical fabrics. This is likely to be the case only when a pore fluid of one type replaces one of another type without disturbance to the soil.

The cluster model developed by Olsen (1962) accounts for discrepancies between the predicted and measured variations in flow rates through different soils such as those shown in Fig. 2.8 for several clays. The following equation can be derived for the ratio of estimated flow rate for a cluster model q_{CM} to the flow rate predicted by the Kozeny-Carman equation (Eq. 2.16) q_{KC} :

$$\frac{q_{CM}}{q_{KC}} = N^{\frac{2}{3}} \frac{[1 - e_c / e_T]^3}{[1 - e_c]^{4 \cdot 3}}$$

(2.17)

with N the number of particles per cluster.

Application of Eq. 2.17 requires assumptions for the variations of e_c with e_T that accompany compression and rebound. Such assumptions, shown in Fig. 2.9, were based on considerations of the relative compressibilities of individual clusters and cluster assemblages. The compressibility of individual clusters is small at high total void ratios, so compression is accompanied by reduction in the intercluster pore sizes, but with little change in intracluster void ratio. As a result, the actual hydraulic conductivity decreases more rapidly with decreasing void ratio during compression than predicted by the Kozeny-Carman equation until the intercluster pore space is comparable to that in a system of closely packed spheres, when the clusters themselves begin to compress. Further decreases in porosity involve decreases in both e_c and e_T. As the intercluster void ratio now decreases less rapidly, the hydraulic conductivity decreases at a slower rate with decreasing porosity than predicted by the Kozeny-Carman equation. The behavior during rebound, Fig. 2.8b, reflects the fact that the
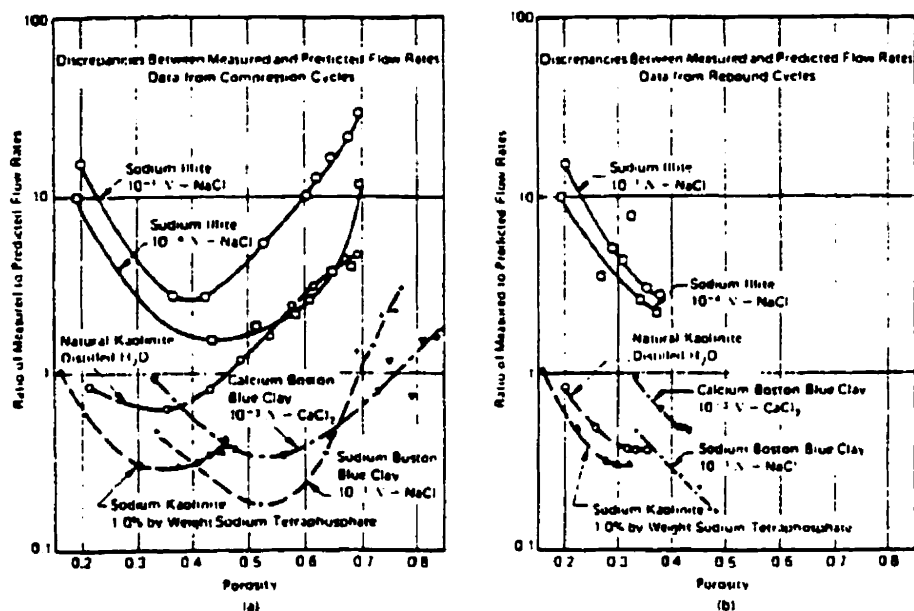
Figure 2.8 Discrepancies between measured and predicted flow rates (Olsen, 1962). (a) Compression cycles. (b) Rebound cycles.
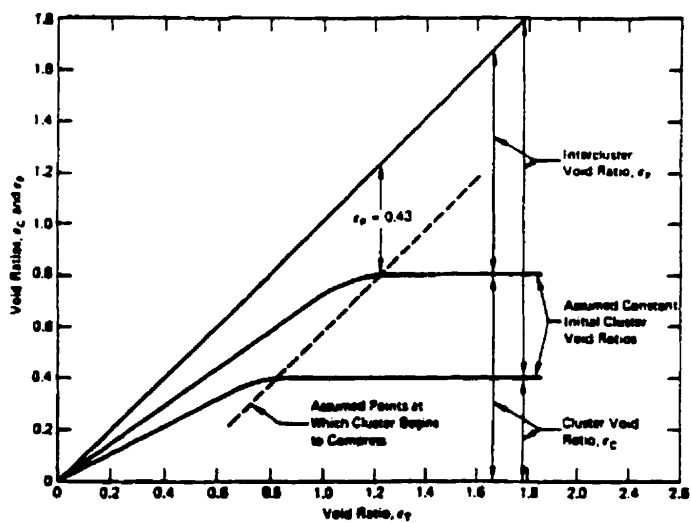
Figure 2.9 Assumed relationships between the total, cluster, and intercluster void ratios (Olsen, 1962).

increase in porosity develops mainly by swelling of the clusters; whereas, the flow rate continues to be controlled primarily by the intercluster voids.

The discrepancies between predicted flow through a cluster model as a function of porosity and that predicted by the Kozeny-Carman equation are shown in Fig. 2.10. The agreement between the actual behavior shown in Fig. 2.8 and the predicted behavior shown in Fig. 2.10 is surprisingly good.

One of the main contributions of the present study is the examination of the structure of compacted clay responsible for conducting fluids through the porous material by direct observation using high-resolution, high-magnification scanning electron micrographs.

2.4 Soil-Chemical Interactions

The study of soil-chemical interactions and their effects on engineering properties of soils began in the 1950s. Michaels and Lin (1954) found that the intrinsic permeability of kaolinite at any void ratio decreases with increases in the polarity of different organic permeants. Soil for the column tests was obtained by mixing dried kaolinite with the permeants, then the suspension was compacted in permeameter cells under slight vacuum and top loading. The dispersion and orientation of clay particles are the major factors responsible for the low hydraulic conductivity when water is used as permeant. The high values of hydraulic conductivity with organic chemicals of low permittivity are caused by the rearrangement and flocculation of clay particles. Shrinkage and the accompanying cracks of soil column, and side-wall leakage were considered by Michaels and Lin (1954) to be the main cause of increased hydraulic conductivity.

Systematic reductions of hydraulic conductivity were measured when a series of inorganic salt solutions of decreasing concentrations were permeated through a natural silty loam composed of 80% sand and silt, and 20% kaolinite and illite clays (Quirk and Schofield,
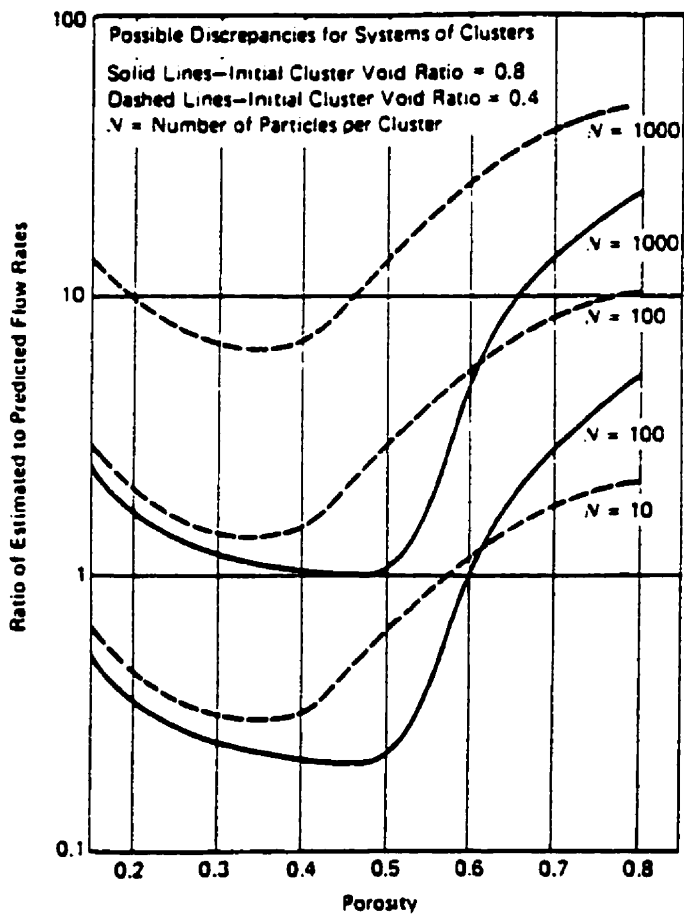
Figure 2.10 Hydraulic conductivity discrepancies according to the cluster model (Olsen, 1962).

1955). The soil was loosely placed in a permeameter with no compaction, except for tapping the permeameter to get a uniform pack of soil. Though no definite mechanism was given, three possible processes were inferred:

- Swelling resulting in the blocking, or partial blocking, of the larger conducting pores.

- Failure of the soil aggregates caused by stress resulting from unequal swelling throughout the soil mass.

- Occurrence of deflocculation or dispersion of clay particles when the charged particles are separated from each other due to the dominance of repulsive forces between them.

Intensive investigations on the compatibility of compacted soil to chemicals were not conducted until the early 1980s when extensive leakage of chemical waste was detected through hydraulic barriers of landfills and surface impoundments. Except for field operation-related macroscopic defects, such as cracks, rootholes, slickensides, and sand pockets, there is considerable concern for the integrity of the barriers resulting from waste-soil interactions. Numerous laboratory tests have been performed to detect changes in hydraulic conductivity when soil columns are permeated by various chemicals. There has been a considerable increase in our knowledge on soil-chemical compatibility and its effects on the engineering behavior of soil, notably the hydraulic conductivity. A review of our contemporary knowledge regarding liquid-soil compatibility used in evaluating waste-soil interactions is presented in Shackelford (1994). However, there has been large variations, and sometimes even contradictions, between the published results of these studies. Factors, such as difference in soil constitution and mineralogical composition, chemical permeants, soil column preparation methods, hydraulic conductivity measurement procedures, all have significant influences on the results.

When permeated by a spectrum of pure organic liquids, four types of natural soil, namely, non-calcareous smectite, calcareous smectite, kaolinite, and illite, showed two to

three orders of magnitude increase in hydraulic conductivity over baseline results obtained with 0.005 M CaSO$_4$ solution (Anderson *et al.*, 1985a). After compaction, the soil columns were tested in compaction-mold permeameters without back-pressuring saturation, and thus no information on sample saturation was provided. The change of a massive structure of the soil to a blocky one after the treatment indicated the dominance of flocculation of clay particles caused by shrinkage of the diffuse double layer around the particles. Lower permittivities of the organic chemicals relative to water were attributed to soil-chemical reactions resulting in cracks and macropores for easier passage of fluids.

Fernandez and Quigley (1985) further showed that water-insoluble hydrocarbons of low permittivity (benzene, cyclohexane, and xylene) do not cause a dramatic increase in hydraulic conductivity, except when the water-soluble alcohol was first introduced into the soil column to expel the pore water. The hydrophobic nature of the non-polar hydrocarbons restricted them to the inter-connected macropores (about 10% of total pores) during permeation. Hydrophilic alcohol acts as a medium to replace pore water and was then removed by the hydrocarbons.

Bowders and Daniel (1987) concluded that dilute organic chemicals had little effect on soil fabric, and thus hydraulic conductivity, when a commercial kaolinite and a natural illite-chlorite were tested using different organic chemicals of various concentrations. Sedimentation tests were first performed and the results showed that the suspensions of the two types of soil settled rapidly in concentrated chemicals due to the formation of flocculated aggregates, but very slowly or not at all in dilute organic solutions as well as water. The low permittivities of concentrated chemicals were believed to cause shrinkage of clay particles. On the other hand, the permittivity of dilute solutions are so high (greater than 60-70) that no flocculation took place. It was logically suggested that if an organic liquid does not cause soil particles to flocculate in a suspension, it will not cause neither an alteration in the fabric of compacted clay nor an increase in hydraulic conductivity. This assumption was seemingly confirmed by the results obtained from compaction-mold permeameter tests. The results

showed that dilute organic chemicals could not cause significant changes in the hydraulic conductivity of most soils, but pure organic chemicals do.

The results of soil-organic chemical interaction were found to be very sensitive to the apparatus and testing procedures (Foreman and Daniel, 1986). Three types of permeameter, compaction-mold, consolidation cell, and flexible-wall permeameters, were used for permeating both commercial kaolinite and two natural soils with methanol and heptane. Similar hydraulic conductivity values with baseline water were obtained by all three permeameters. The soils in compaction-mold showed significant increases in hydraulic conductivity when they were permeated by concentrated organic chemicals. Comparatively, no significant changes in intrinsic permeability for methanol permeation were observed in flexible-wall permeameter while the hydraulic conductivity of soils was practically zero for heptane permeation. The high hydraulic conductivity values obtained by compaction-molds were ascribed to the combination of lower confining stresses and sidewall leakage. The fact that hydraulic conductivity decreased with increasing effective stress applied on the samples in flexible-wall permeameters suggests that the cracks or macropores caused by flocculation of soil particles were forced to close.

The importance of testing procedures on the hydraulic conductivity of fine-grained soil resulting from chemical permeation was also emphasized by Acar et al. (1985a), and Acar and Olivieri (1989). Their results showed that flexible-wall permeameters always yield decreased or insignificantly increased hydraulic conductivities when both commercial kaolinite and Ca-montmorillonite were permeated by a spectrum of pure organic chemicals with different permittivities. Back pressures of 414 to 449 kPa (60-65 psi) were used to saturate the specimens during the tests, and an effective stress of 69 kPa (10 psi) was maintained in the samples (Acar et al., 1985a). A specific trend was not observed between the hydraulic conductivity values and the permittivities of organic fluids in the study (Acar and Olivieri, 1989). By comparison, fixed-wall cell tests on compacted kaolinite permeated by acetone revealed hydraulic conductivity values almost two orders of magnitude higher than that

obtained in the flexible-wall cell. The difference was attributed exclusively to sidewall leakage due to the shrinkage of the specimen during the test (Acar at al., 1985a). Furthermore, hydraulic conductivity would increase by nearly an order of magnitude when the effective stress in the sample was decreased from 69 kPa (10 psi) to 13.8 kPa (2 psi). The insolubility of the organic chemicals, pH value, and confining pressure are among other factors affecting the hydraulic conductivity (Acar and Olivieri, 1989).

Hydraulic conductivity of soil is considered to be the most variable soil parameter in geotechnical engineering (Dunn and Mitchell, 1984). Among the factors important to test results are: (1) the compaction method used; (2) the effect of increased hydraulic gradient; (3) the saturation procedure and verification of the degree of saturation; (4) the use of the proper permeant; (5) consideration of the sample consolidation state throughout the test; and (6) the time (thixotropic) effect. Their hydraulic conductivity results showed that there is significant difference between values obtained when permeating soils with distilled water, tap water, and a synthetic lead-zinc tailing leachate. Static compaction, which is considered to produce less dispersed fabric by virtue of lower level shear strain, was used to prepare two natural clayey soils predominantly composed of montmorillonite and kaolinite, respectively. The fact that the hydraulic conductivity obtained by the permeation of tap water and distilled water decreased with time was believed to be caused by leaching of soluble salts in the soil resulting in a more dispersed fabric. Permeation of the lead-zinc tailing leachate with a pH of 2.5 resulted in an increase in hydraulic conductivity over that measured using tap water by 1 to 2 orders of magnitude. Ion exchange of divalent Pb and Zn for monovalent Na and the low pH of the permeant were considered to contribute to the flocculation of clay particles (Dunn and Mitchell, 1984).

The importance of initial soil fabric and confining pressure during tests of the hydraulic conductivity of clays was recognized by Yang and Barbour (1992) and Barbour and Yang (1993). A Ca-montmorillonitic glacial clay soil from western Canada was permeated by a concentrated NaCl brine in a fixed-wall permeameter. The soil was thought to be

composed of aggregates of elementary clay particles. This soil fabric can be described in terms of microfabric as referring to an association within individual aggregates, and mini- or macrofabric considering the arrangement of the aggregates. Soils prepared by kneading compaction, static compaction, and slurring have different arrangement of aggregates, and consequently different distributions of interaggregate pores while clay aggregates have the same internal structure. The permeation of samples prepared from slurry by brine results in shrinkage of the diffuse double layer causing contraction of individual clay aggregates, but it does not change the microfabric. Any change in hydraulic conductivity is caused by change in minifabric and macrofabric, opening of interaggregate pores, and formation of fracturing or fissuring, resulting from a reduction in the net physico-chemical repulsive force. The increase in hydraulic conductivity due to the permeation of brine was restricted by an increase in vertical confining pressure in the permeameter. This confirms the fact that external stress is able to limit the opening of macropores caused by shrinkage of the diffuse double layer and contraction of clay aggregates.

The interaction between clay particles and chemicals, and its possible effects on soil engineering properties have been justified theoretically by a change in pore fluid chemistry. Evans *et al.* (1985) summarized the influence of various factors in pore fluid on the thickness of the diffuse double layer and soil fabric. The summary tabulated in Table 2.2 was extended to include the potential effects of these factors on the hydraulic conductivity of fine-grained soils by Madsen and Mitchell (1987).

In practice, however, other factors related to soil properties and testing procedures seem to play a key role in the determination of hydraulic conductivity. Madsen and Mitchell (1987) emphasized the importance of the constrained condition to the flocculation-dispersion of clay particles in a soil mass.

Table 2.2 Effect of relative changes in major pore fluid parameters on hydraulic conductivity of clay soils based on fabric (adapted from Madsen and Mitchell, 1987).

Pore Fluid Parameter	Effect of Relative Change in Parameter	
	Decrease in DDL thickness, flocculated fabric, and an increase in hydraulic conductivity	Increase in DDL thickness, dispersed fabric, and a decrease in hydraulic conductivity
Electrolyte Concentration	Increase	Decrease
Cation Valence	Increase	Decrease
Permittivity	Decrease	Increase
pH	Decrease	Increase
Cation Size	Decrease	Increase
Anion Adsorption	Decrease	Increase

DDL = diffuse double layer

2.4.1 Chemical Compatibility and Hydraulic Conductivity

Of special concern in recent years has been the compatibility between waste chemicals, especially liquid organics, and compacted clay liners and slurry wall barriers constructed to contain them. Numerous studies have been done to evaluate chemical effects on clay hydraulic conductivity, because of fears that prolonged exposure may compromise the integrity of the liners and barriers and because tests have shown that under certain conditions clays can shrink and crack when permeated by some classes of chemicals. Summaries of the results of chemical compatibility studies are given by Quigley and Fernandez (1994, 1989) and Mitchell and Madsen (1987), and factors controlling the long-term stability of clay liners are discussed by Mitchell and Jaber (1990).

Rigid-wall (including consolidometers) and flexible-wall permeameters are used for compatibility testing in the laboratory. These types of test apparatus are described and discussed in detail by Daniel et al. (1985) and Daniel (1994). In the past several years a controversy has developed over the use of fixed-wall versus flexible-wall permeameters for measuring the hydraulic conductivity of clayey soils. All permeameters have important advantages and serious limitations (Daniel et al., 1985; Daniel, 1994). The rigid-wall system overestimates hydraulic conductivity whenever chemical-clay interactions cause shrinkage and cracking; however, it is well suited for qualitative determination of whether or not there may be adverse interactions. In the flexible-wall system, the lateral confining pressure prevents cracks from opening; thus there is risk of underestimating the hydraulic conductivity of some soils. The consolidometer permeameter system allows for testing clays under a range of confining stress states that are representative of those in the field and for quantitative assessment of the effects of chemical interactions on volume stability and hydraulic conductivity. A summary of hydraulic conductivity cells used in over 50 conducted studies, published between 1980 and 1992, is given by Daniel (1994). The literature suggests a mix (roughly 50-50) of rigid- and flexible-wall permeameters. Several investigators used both types of cells. Daniel (1994) also presented a comparison of hydraulic conductivity

determined in rigid-wall, compaction-mold permeameters to the hydraulic conductivity determined in flexible-wall permeameters. All specimens were permeated with de-aired water to strip air from specimens during permeation and the tests continued for a sufficient period of time to ensure equal inflow and outflow as well as steady hydraulic conductivity. Under these circumstances, there is good agreement between the results of rigid-wall and flexible-wall permeameters.

The effects of chemicals on the hydraulic conductivity of high water content clays, as used in slurry walls, are likely to be much greater than on lower water content, high density clays, as those used in compacted clay liners. This is because of the greater particle mobility and easier opportunity for fabric changes in the higher water content system. A high compactive effort or an effective confining stress greater than about 70 kPa can make a properly compacted clay invulnerable to attack by concentrated organic chemicals (Broderick and Daniel, 1990). Unfortunately, it is not always possible to insure high-density compaction or to maintain high confining pressures, so it is useful to know the general effects of different chemical types on hydraulic conductivity.

2.4.1.1 Inorganic Chemicals

The effects of inorganic chemicals on hydraulic conductivity are consistent with (1) their effects on the double-layer and inter-particle forces that promote flocculation, dispersion, shrinkage, and swelling; (2) their effects on surface and edge charges on particles and the influences of these charges on flocculation and deflocculation; and (3) their effects on pH.

Acids cause solutioning of carbonates, iron oxides, and the alumina octahedral layers of the clay minerals. Bases cause solutioning of silica tetrahedral layers, and to a lesser extent, alumina octahedral layers of clay minerals. Removal of dissolved material can cause increases in hydraulic conductivity; whereas, precipitation of this material can cause pore clogging and hydraulic conductivity decreases.

2.4.1.2 Organic Chemicals

Clay-organic reactions have been studied for many years because of their importance in such fields as agriculture and petroleum engineering. They are important in the technology of drilling fluids, in the stability control of clay suspensions, and in the manufacture of lubricants. In recent years, clay-organic interactions have become of great interest to geo-environmental engineers because of the need to solve problems in the migration, containment, and cleanup of toxic wastes.

Organics interact with clays by adsorption on particle surfaces, ion exchange, and intercalation (Lagaly, 1984). *Intercalation* involves the entry of organic molecules between silicate layers, and is particularly important to the kaolin minerals. Adsorption of organic compounds on clay surfaces in aqueous systems depends on the available surface and the ability of the organic molecules to displace water molecules. Cationic organics can exchange for inorganic adsorbed cations; however, if the organic cation is larger than the cation site, then all exchangeable cations cannot be displaced. Attraction of large organic molecules to clay surfaces by van der Waals forces may contribute to the total amount of organics held (Raussell-Colom and Serratosa, 1987).

The most important factors controlling the effects of organic chemicals on hydraulic conductivity are (1) their water solubility, (2) their dielectric constant, (3) their polarity, and (4) whether or not the clay is exposed to the pure organic or a dilute solution. In practice, exposure of clay barriers to water-insoluble pure or concentrated organics is likely only in the case of spills, leaking tanks, and with dense nonaqueous phase liquids (DNAPLs) or "sinkers" that accumulate above low spots in liners. Some general conclusions about the influences of organics on the hydraulic conductivity are (Mitchell, 1993):

1. Solutions of compounds having a low solubility in water, such as the hydrocarbons, have no large effect on the hydraulic conductivity. This is in contrast to dilute

solutions of inorganic compounds that may have significant effects as a result of their influence on flocculation and dispersion of the clay particles.

2. Water-soluble organics, such as the simple alcohols and ketones, have no effect on hydraulic conductivity at concentrations less than about 75 to 80 percent.

3. Many water-insoluble organic liquids can cause shrinkage and cracking of clays, with concurrent increases in hydraulic conductivity.

4. Hydraulic conductivity increases caused by permeation with organics are partly reversible when water is reintroduced as the permeant.

5. Concentrated hydrophobic compounds permeate soils through cracks and macropores. Water remains within mini- and micropores.

6. Hydrophilic compounds permeate the soil more uniformly, as the polar molecules can replace the water in hydration layers of the cations and are more readily adsorbed on particle surfaces.

7. Organic acids can dissolve carbonates and iron oxides. Buffering of the acid can lead to downstream precipitation and pore clogging. However, after long time periods, these precipitates may be redissolved and removed, thus leading to an increase in hydraulic conductivity.

8. Pure bases can cause a large increase in the hydraulic conductivity; whereas, concentrations at or below the solubility limit in water have no effect.

9. Organic acids do not cause large scale dissolution of clay particles.

The combined effects of confining pressure and concentration, as well as permeant density and viscosity, are illustrated by Fig. 2.11 (Fernandez and Quigley, 1988). The data are for water-compacted, brown Sarnia clay permeated by solutions of dioxane in domestic landfill leachate. Increases in hydrocarbon concentration cause decreases in hydraulic conductivity up to concentrations of about 70 percent, after which the hydraulic conductivity increased by about three orders of magnitude for pure dioxane (Fig. 2.11a), for samples that were unconfined by a vertical stress (σ_v = 0). On the other hand, the data points for samples maintained under a vertical confining stress of 160 kPa indicate no effect of the dioxane on
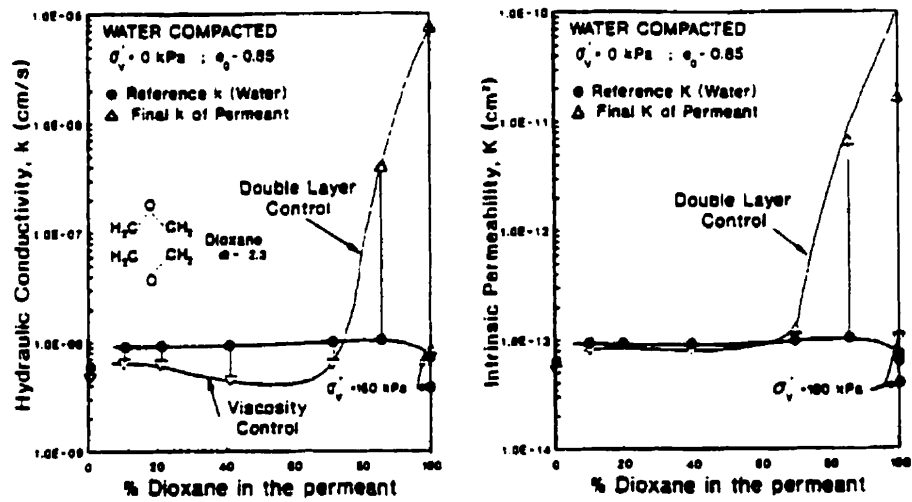
Figure 2.11 (a) Hydraulic conductivity and (b) intrinsic permeability of compacted Sarnia clay permeated with leachate-dioxane mixtures (Fernandez and Quigley, 1988).

hydraulic conductivity relative to water. The decreases in hydraulic conductivity for dioxane concentrations up to 70 percent can be accounted for in terms of fluid density and viscosity, as may be seen in Fig. 2.11b where the intrinsic values of permeability are shown. As noted earlier in the previous division, in connection with the development of Eq. 2.16, the intrinsic permeability is defined by $K = k (\mu / \gamma)$.

While many researchers seem content to find out the variations associated with transport of contaminants through soils, scrutinizing the structure of leached specimens in order to understand the genuine nature of these variations is the focal point of this study. As a result, the primary objective of the present research is to investigate clay-contaminant interactions, like intercalation and dissolution-precipitation phenomena, by detecting their influence on the fabric of compacted clays. Even though the importance of soil fabric on hydraulic conductivity values has long been recognized, and justified theoretically, there are not enough studies devoted to providing sound experimental evidence of structural alteration caused by contaminant migration through soils. It is in this context that this research occupies its own distinctive place among others contributing to the advancement of our knowledge in the field called geoenvironmental engineering.

Although many chemicals do not have a significant effect on the hydraulic conductivity of clay barriers, this does not mean that they will not be transported through the clay. Unless adsorbed by the clay or by organic matter within the clay, the chemicals will be transported by advection and diffusion. Furthermore, the actual *transit time* through a barrier by advection; i.e., the time for chemicals moving with the seepage water, may be far less than estimated using the conventional seepage velocity. The seepage velocity is usually defined by the Darcy velocity $(k_h \cdot i_h)$, divided by the total porosity n. In systems with unequal pore sizes, however, the flow is almost totally through mini- and macropores, which comprise the effective porosity n_e, which may be several times smaller than the total porosity. Thus compaction of clay barriers that eliminates clods and aggregates has the added advantage of

increasing the proportion of the porosity that is effective porosity, thereby increasing the transit time.

2.5 Contaminant Transport

The main driving forces in contaminant transport in soils are advective and diffusive in nature. Advective flow can be described by groundwater flow models, and dispersion of molecules during advective flow will depend on several constraints dictated by pore geometry and continuity in the porous media (soil), and the hydrogeological setting. It is important that attention be given to a proper description of the hydrogeological setting because the control and propagation of the contaminant plume will be highly dependent on this setting. Attenuation of advective-driven contaminants in the substrate soil will be primarily due to physical constraints dictated by the setting, and to a lesser extent to the chemically driven interactions as a result of the relative velocity of flow of the soil water.

When advective flow is not a significant component of the problem, diffusion-driven contaminants are more likely to develop physico-chemical interactions with the soil constituents. Adsorption isotherms can be obtained and the chemistry of adsorption can be studied for particular soil compositions and specific types of contaminants. Several major difficulties must be faced, however, in using this information to model contaminant transport under natural soil conditions. The boundary conditions are often difficult to specify. Moreover, many reactions, especially slow reversible reactions, are not at equilibrium and hence the thermodynamic descriptions that assume equilibrium are not valid. The error in using thermodynamic equilibrium constants is not known. Also, of greater concern is the variability of soil characteristics, such as hydraulic conductivity, in space and time. This leads to errors when using deterministic models; probability functions in stochastic models lead to better predictions of contaminant transport (Yong *et al.*, 1992).

The purpose of the following discussion is to present the basic concepts for describing contaminant transport in and through porous materials. The material covered, however, is limited to one-dimensional transport of miscible contaminants (i.e., solutes) in saturated porous media.

2.5.1 Transport Processes

Transport processes include advection, diffusion, coupled flow, mechanical dispersion, and combined transport.

2.5.1.1 Advection

Advection is the process by which solutes are transported along with the flowing fluid or solvent, typically water, in response to a gradient in total hydraulic head. Due to advection, non-reactive solutes (i.e., solutes which are not subject to chemical or biological reactions) are transported at an average rate equal to the seepage velocity of the fluid, or

$$v_s = \frac{v}{n} \qquad (2.18)$$

where v_s is the seepage or average linear velocity of the water (solvent), n is the total porosity of the porous material, and v is the flux of water (i.e., quantity of flow per unit area per unit time). Equation 2.18 presupposes that all of the voids in a porous material are equally effective in conducting flow. The flux is given by Darcy's law which, for one-dimensional flow, can be written as (cf. Eq. 2.4)

$$v = \frac{q}{A} = -k \frac{\partial h}{\partial x} = k\,i \qquad (2.19)$$

where q is the volumetric flow rate of the water per unit time, A is the total cross-sectional area (solids plus voids) perpendicular to the direction of flow, k is the hydraulic conductivity, h is the total hydraulic head, x is the direction of flow, and i is the dimensionless hydraulic

gradient. The seepage velocity, v_s, reflects the fact that the fluid actually can flow only through the void space of the porous material, whereas the flux, v, represents the volumetric flow of fluid through the total cross-sectional area of the material.

The time required for a nonreactive solute to migrate through a saturated soil of thickness L, known as the solute transit time, due to advection can be estimated using the seepage velocity as follows:

$$t = \frac{L}{v_s} = \frac{nL}{ki} \tag{2.20}$$

where t is the transit time. When Eq. 2.20 is used to estimate the transit time of the solute, it is implied that all solute constituents are carried along with the fluid at the velocity v_s. Under these conditions, the advective mass flux of a particular chemical species can be calculated as

$$J_A = v\,c = ki\,c = nv_s\,c \tag{2.21}$$

where J_A is the advective mass flux (mass flowing through a unit cross-sectional area in a unit of time), and c is the concentration of the solute in the liquid phase of the porous material (i.e., mass of solute per unit volume of mixture).

With some porous materials, e.g., fractured soil or rock, most of the advective flow occurs through only part of the total void space of the material. For these materials, an effective porosity, n_e, is defined as the volume of fluid conducting pores divided by the total volume (pores plus solids) of the material. For materials with $n_e < n$, n_e should be substituted for n in Eqs. 2.18, 2.20 and 2.21.

2.5.1.2 Diffusion

Diffusion may be thought of as a transport process in which a chemical or chemical species migrates in response to a gradient in its concentration, although the actual driving force for diffusive transport is the gradient in chemical potential of the solute (Robinson and Stokes, 1959). A hydraulic gradient is not required for transport of contaminants by diffusion.

The fundamental equation for diffusion is Fick's first law which, for one-dimensional transport, can be written as

$$J_D = -D_0 \frac{\partial c}{\partial x} \qquad (2.22)$$

where J_D is the diffusive mass flux, x is the direction of transport, and D_0 is the "free-solution" diffusion coefficient. Equation 2.22 represents the one-dimensional form of Fick's first law describing diffusion in aqueous or free solution (i.e., no porous material).

For diffusion in saturated porous material, a modified form of Fick's first law is used;

$$J_D = -\tau \, D_0 \, n \, \frac{\partial c}{\partial x} \qquad (2.23)$$

or

$$J_D = -D^* \, n \, \frac{\partial c}{\partial x} \qquad (2.24)$$

where τ is a dimensionless tortuosity factor, and D^* is the "effective" diffusion coefficient. The porosity term is required in Eq. 2.24 since the diffusive flux, J_D, is defined with respect to the total cross-sectional area of the porous medium. The tortuosity factor accounts for the increased distance of transport and the more tortuous pathways experienced by solutes diffusing through porous media. Tortuosity is expressed as

$$\tau = \left(\frac{L}{L_e}\right)^2 \qquad (2.25)$$

where L is the macroscopic, straight-line distance between two points defining the flow path, and L_e is the actual, microscopic or effective distance of transport between the same two points. Since $L_e > L$, $\tau < 1.0$ and $D^* < D_0$. Therefore, mass transport due to diffusion in porous materials is slower than mass transport due to diffusion in free or aqueous solution. Typical values of τ are reported in the range 0.01 to 0.67 (Freeze and Cherry, 1979; Shackelford, 1989; Shackelford and Daniel, 1991). In some instances, however, the porosity term in Eq. 2.24 is included in the definition of the effective diffusion coefficient (Shackelford and Daniel, 1991; Shackelford, 1991).

2.5.1.3 Coupled Flow Processes

As was discussed in section 2.3.1, water can flow through porous media not only in response to a gradient in total hydraulic head but also in response to gradients in chemical composition (chemical osmosis), electricity (electroosmosis), and temperature (thermoosmosis) [cf. Table 2.1]. Also, in the absence of advective flow, solutes can migrate through porous materials not only in response to a concentration gradient but also in response to an electrical gradient (electrophoresis) and a thermal gradient (thermal diffusion). Solutes may also be filtered (ultrafiltration) by some porous materials. These additional flow processes typically are referred to as *coupled flow processes* in order to distinguish them from the direct flow processes represented by advection and diffusion.

The description of coupled flow processes is based on the theory of the thermodynamics of irreversible processes. A description of this theory is beyond the scope of the current presentation, but an excellent review of the relation of the theory to coupled and direct flow processes can be found in Bear (1972). Mitchell (1993) provides examples of the application of coupled flow processes to typical geotechnical engineering problems.

In the formulation of the contaminant transport equations, coupled flow processes often are neglected or are considered to be insignificant for at least two reasons (Shackelford, 1993). First, coupled flow processes are significant only at the relatively low flow rates which typically are associated with flow through fine-grained soils (e.g., clays and silts). Since most of the applications of contaminant transport theory traditionally have been associated with problems pertaining to the transport of contaminants through highly permeable, granular materials (e.g., aquifers), the effects of coupled flow processes typically have been assumed to be negligible. Nevertheless, coupled flow processes may be significant in materials with high activity and/or low void ratio (Olsen, 1969; Greenberg et al., 1973). Second, the determination of the phenomenological coefficients associated with the equations describing coupled flow processes is difficult, at best. As a result, such determinations usually can be performed only under highly controlled conditions in the laboratory, and extrapolation of the results to field situations is uncertain.

2.5.1.4 Mechanical Dispersion

In traditional contaminant transport theory, a *mechanical dispersive* flux, J_{Mf}, is added to the total mass flux of the solute to account for the spreading of the solute due to variations in the seepage velocity, v_s, which occur during transport in and through porous materials. On a microscopic level, these variations are thought to be related to the three different effects illustrated in Fig. 2.12 (Fried, 1975; Bear, 1979; Freeze and Cherry, 1979). First, the velocity of flow across any given pore channel within the material will be greater in the middle of the pore channel than it is near the walls of the pore channel (Fig. 2.12a). This is the same effect which is known to occur in fluid flow through pipes and in rivers, streams, and channels. Second, the equation of continuity predicts that the flow velocity across a smaller pore opening will be greater than that across a larger pore opening as illustrated in Fig. 2.12b. Finally, velocity variations will result due to the tortuous nature of the flow paths existing in nearly all porous materials (Fig. 2.12c).

(a)

pore wall

direction of flow

velocity distribution across pore channel

pore wall

(b)

A_1

pore channel

A_2

direction of flow

$v_2 > v_1$

equation of continuity: $A_1 v_1 = A_2 v_2$

(c)

soil particles

direction of flow
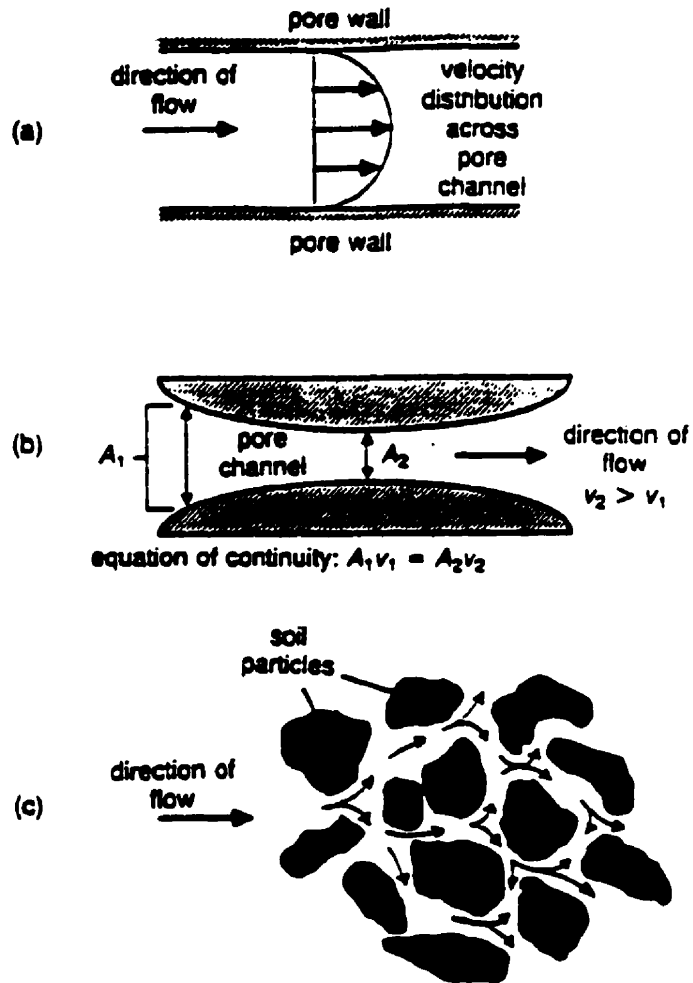
Figure 2.12 Microscopic dispersion in soil: (a) effect of velocity distribution across single pore; (b) effect of variation in pore sizes; and (c) effect of tortuous nature of flow paths (after Freeze and Cherry, 1979).

On a larger scale, mechanical dispersion is thought to be caused by the different flow rates resulting from heterogeneities that typically are encountered whenever transport occurs over relatively large areas or regions. This type of dispersion is illustrated in Fig. 2.13 where flow through the bulk sand medium is shown to be interrupted by the existence of the low-hydraulic-conductivity clay lenses dispersed throughout the sand layer. Due to the existence of the clay lenses, the transport proceeds around rather than through the clay resulting in a situation which is analogous to that shown in Fig. 2.12c for microscopic dispersion. Therefore, the dispersion illustrated in Fig. 2.13 may be thought to be due to a 'macroscopic tortuosity effect.'

The mechanical dispersive flux typically is assumed to be a Fickian process which, for one dimension, can be expressed as

$$J_M = -D_m \, n \, \frac{\partial c}{\partial x} \tag{2.26}$$

where J_M is the mechanical dispersive flux, and D_m is the mechanical dispersion coefficient. Since mechanical dispersion results from variations in the magnitude of the seepage velocity, the mechanical dispersion coefficient often is assumed to be a function of the seepage velocity, or

$$D_m = \alpha_L \, v_s^\beta \tag{2.27}$$

where α_L is the longitudinal dispersivity of the porous medium in the direction of transport, and β is an empirically determined constant between 1 and 2 (Freeze and Cherry, 1979). In most applications, the exponent, β, is assumed to be unity, i.e., D_m is assumed to be a linear function of v_s in Eq. 2.27. However, β may be greater than unity in many situations (Anderson, 1984; Bear and Verruijt, 1987). Also, the dispersivity, α_L, is probably scale dependent with larger values for α_L being associated with greater transport distances (Pickens and Grisak, 1981). For example, values of dispersivity reported from the results of field
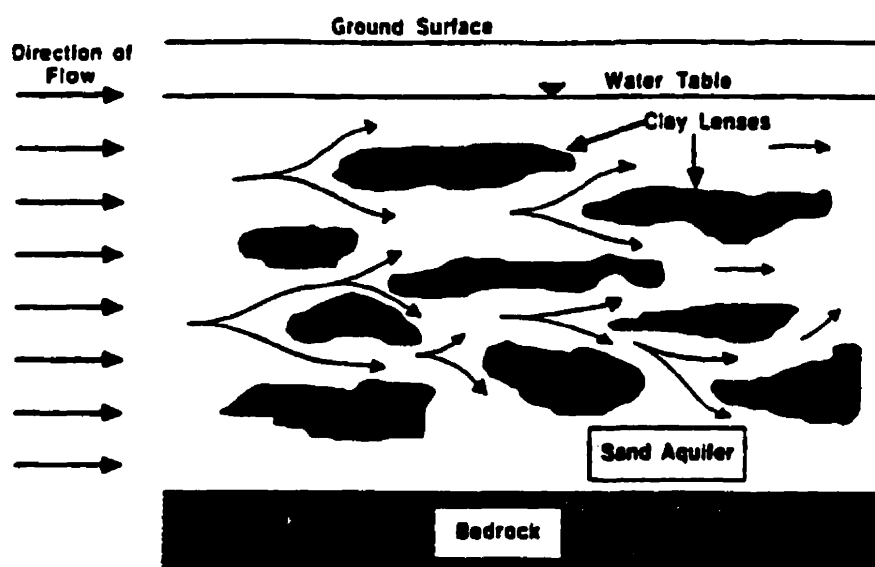
Figure 2.13 Mechanical dispersion on large or regional scale (Shackelford, 1993).

studies may be as much as four to six orders-of-magnitude greater than the corresponding laboratory measured values (Freeze and Cherry, 1979).

Regardless of the appropriate values for α_L and β, the relationship for D_m in Eq. 2.27 indicates that the effect of mechanical dispersion increases as the seepage velocity increases and vice versa. As a result, for typical problems involving low-hydraulic-conductivity barrier materials, mechanical dispersion does not appear to be significant due to the relatively low flow rates (Rowe, 1987).

2.5.1.5 Combined Transport

In the absence of coupled flow processes, the total mass flux, J, of the solute or contaminant species is the sum of the advective, diffusive, and dispersive fluxes, or

$$J = J_A + J_D + J_M \tag{2.28}$$

Based on Eqs. 2.21, 2.24, and 2.26, the total mass flux for one-dimensional transport in saturated porous material is

$$J = n \, v_s \, c - D^* \, n \, \frac{\partial c}{\partial x} - D_m \, n \, \frac{\partial c}{\partial x} \tag{2.29}$$

or

$$J = n \, v_s \, c - D_h \, n \, \frac{\partial c}{\partial x} \tag{2.30}$$

where D_h is the hydrodynamic dispersion coefficient given by

$$D_h = D^* + D_m = D^* + \alpha_L \, v_s \tag{2.31}$$

The exponent β in Eq. 2.27 has been assumed to be unity in the formulation of Eq. 2.31. The hydrodynamic dispersion coefficient accounts for dispersion of the solute due to both diffusion and mechanical dispersion.

2.5.2 Transient Transport

2.5.2.1 Conservation of Mass

The transient transport of a chemical species through saturated material is based on the *conservation of mass* for a representative elementary volume (REV) of soil, or (Freeze and Cherry, 1979)

net rate of mass increase within the REV = mass flux into the REV − mass flux out of the REV ± increase (or decrease) in mass due to chemical reactions occurring within the REV

A REV is the minimum volume that will allow for the application of the continuum approach to flow or transport through porous media (Bear, 1972, 1979; Bear and Verruijt, 1987). In mathematical terminology, the conservation of mass is reflected by the continuity equation, or

$$\frac{\partial m}{\partial t} = -\nabla \cdot J \pm R \pm \lambda m \tag{2.32}$$

where m is the total (adsorbed plus liquid phase) mass of solute per unit volume of soil, λ is a general rate constant used to describe such reactions as radioactive and/or biological decay and R is a general term representing all other chemical and biological reactions. The positive signs (+) in Eq. 2.32 are used for concentration source terms (e.g., mineral dissolution), whereas the (−) signs are used for terms representing concentration sinks (e.g., precipitation).

2.5.2.2 Advection-Dispersion Equation

A number of simplifying assumptions often are required in practice to reduce Eq. 2.32 to a more usable form. For instance, the porous medium often is assumed to be homogeneous, isotropic, and non-deformable, and transport is assumed to be governed by steady flow of an incompressible fluid. Also, only trace concentrations of solutes typically are considered so that changes in fluid density due to changes in solute concentrations can be neglected. Coupled flow processes usually are neglected and only equilibrium exchange reactions (e.g., reversible sorption reactions) are included routinely in the modeling of the transport of reactive solutes through porous media. When these assumptions are acceptable, and transport is assumed to occur only in one direction (say, the x-direction), Eq. 2.30 can be used for the flux term, J, and Eq. 2.32 can be reduced to (Freeze and Cherry, 1979)

$$\frac{\partial c}{\partial t} = \frac{D_h}{R_d} \frac{\partial^2 c}{\partial x^2} - \frac{v_s}{R_d} \frac{\partial c}{\partial x} \qquad (2.33)$$

where R_d is the dimensionless retardation factor. In the study of contaminant transport, Eq. 2.33 commonly is referred to as the one-dimensional *advection-dispersion equation*. When the seepage velocity is sufficiently low such that mechanical dispersion is negligible, the advection-dispersion equation (Eq. 2.33) effectively reduces to an advection-diffusion equation since the hydrodynamic dispersion coefficient from Eq. 2.31 is dominated by the effective diffusion coefficient (i.e., $D_h \approx D^*$).

The retardation factor represents the relative rate of fluid flow to the transport rate of a reactive solute (Freeze and Cherry, 1979), or

$$R_d = \frac{v_s}{v_R} \qquad (2.34)$$

where v_R is the transport rate, or velocity, for the center of mass of the reactive solute. For nonreactive (nonadsorbing) solutes, such as chloride (Cl^-), the retardation factor is unity and the solute is transported at the rate of the seepage velocity in accordance with Eq. 2.34. As a result, Eq. 2.33 may be written as

$$\frac{\partial c}{\partial t} = D_h \frac{\partial^2 c}{\partial x^2} - v_s \frac{\partial c}{\partial x}$$

(2.35)

However, for reactive (adsorbing solutes), the retardation factor is greater than unity, i.e., R_d > 1. Therefore, Eq. 2.34 indicates that adsorbing solutes are transported at a reduced rate, v_R, relative to nonadsorbing solutes. In such cases, it often is convenient to rewrite the advection-dispersion equation, Eq. 2.33, for adsorbing solutes by utilizing Eq. 2.34 as

$$\frac{\partial c}{\partial t} = D_R \frac{\partial^2 c}{\partial x^2} - v_R \frac{\partial c}{\partial x}$$

(2.36)

where $D_R = D_h \cdot R_d$.

The value of R_d typically is determined in the laboratory from the results of either column tests or batch equilibrium tests using the relationship (Shackelford, 1993):

$$R_d = 1 + \frac{\rho_b}{n} K_p$$

(2.37)

where ρ_b is the bulk (dry) density of the soil, and K_p is the 'partition coefficient.' The partition coefficient relates the change in the adsorbed concentration relative to a change in the equilibrium concentration of the chemical species as

$$K_p = \frac{dS}{dc}$$

(2.38)

where S is the adsorbed concentration, or mass of solute adsorbed per mass of soil. Equation 2.38 represents the slope of a plot of S versus c, also known as an adsorption isotherm. The term 'partition coefficient' applies when the adsorption isotherm is nonlinear and, therefore, when K_p is dependent on the equilibrium concentration, i.e., $K_p = f(c)$. Therefore, the partition coefficient of a nonlinear adsorption isotherm is equal to the tangential slope of the adsorption isotherm evaluated at a specific value for the equilibrium concentration, c. When the

adsorption isotherm is linear, the partition coefficient is constant and is called the 'distribution coefficient, K_d.'

In general, there are two types of nonlinear adsorption isotherms - concave and convex - as well as the linear adsorption isotherms which are of interest in contaminant transport (Melnyk, 1985; Shackelford and Daniel, 1991). In chemical engineering, concave and convex adsorption isotherms often are referred to as favorable and unfavorable isotherms, respectively (Weber and Smith, 1987). Concave isotherms are the more common type of nonlinear isotherms for transport in soils. The difference in the three types of isotherms is illustrated schematically in Fig. 2.14. In a concave isotherm, the slope of the isotherm at a lower equilibrium concentration is greater than it is at a higher equilibrium concentration, whereas the opposite is true for a convex isotherm (compare points for c_1 and c_2 in Fig. 2.14). Since the rate of transport for a reactive solute (v_R) is inversely proportional to the retardation factor (R_d) and, therefore, the partition coefficient (K_p) [compare Eqs. 2.34, 2.37, and 2.38], a reactive solute will be transported faster at a higher concentration for a concave isotherm, whereas the opposite is true for a convex isotherm (see Figs. 2.15a and 2.15b). As a result, the concentration profile described by a convex isotherm (Fig. 2.15b) tends to spread out more during transport and forms what is known as a 'concentration wave.'

However, since it is physically impossible for a higher concentration of a given solute to reach a specified distance before a lower concentration of the same solute reaches the same distance, the concentration profile shown in Fig. 2.15a for concave adsorption behavior tends to form what is known as a 'concentration step.' As a result, the limiting partition coefficient for reactive solutes described by concave isotherms is based on the use of secant lines instead of tangent lines, as shown in Fig. 2.15c (Melnyk, 1985). The use of secant lines forces all equilibrium concentrations of a solute up to the value at the intersection of the secant line and the adsorption isotherm (i.e., c_2 in Fig. 2.15c) to have the same value for the partition coefficient and, consequently, the same transport rate. In essence, the slope of the secant line
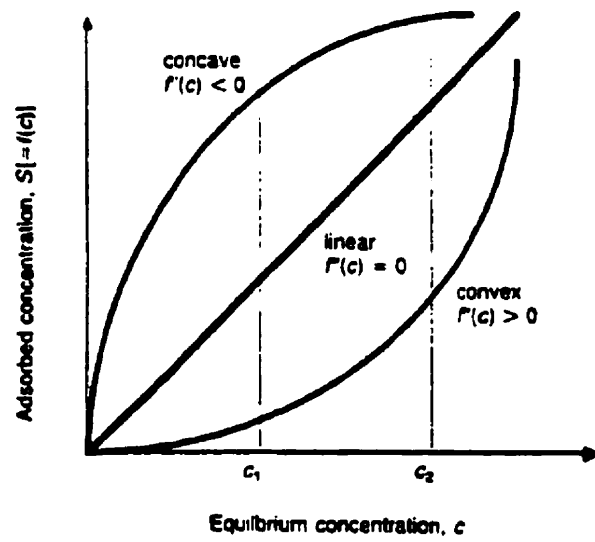
Figure 2.14 General types of adsorption isotherms (after Shackelford and Daniel, 1991).
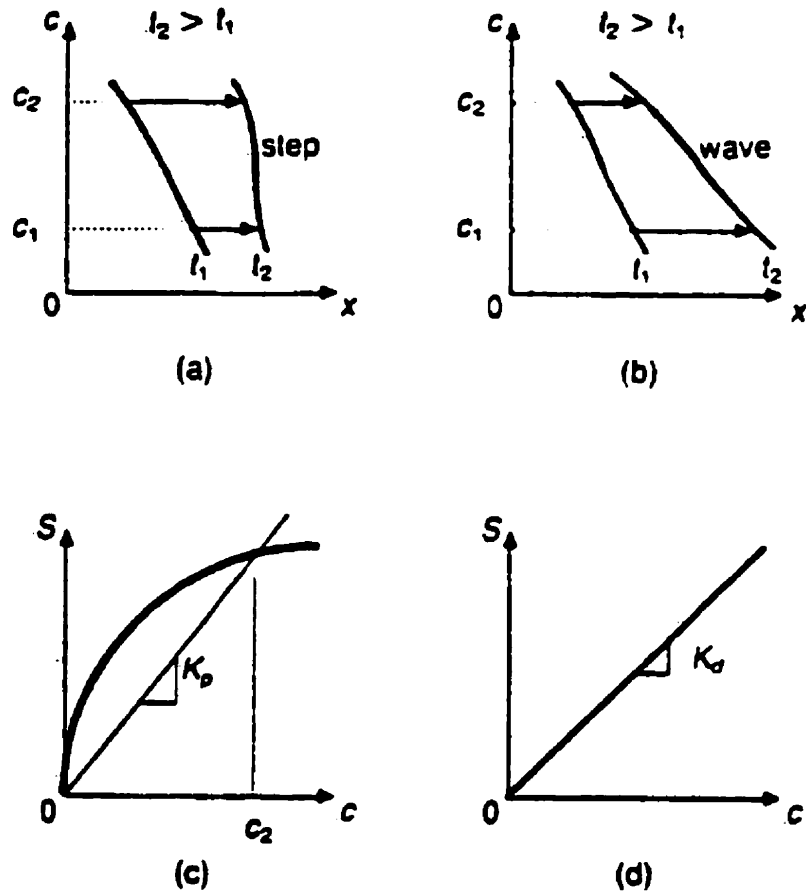
Figure 2.15 Effects of different types of adsorption isotherms: (a) concentration-distance curve for concave adsorption behavior; (b) concentration-distance curve for convex adsorption behavior; (c) secant formulation for concave isotherm; and (d) distribution coefficient for linear adsorption isotherm (Shackelford, 1993).

is analogous to the slope associated with a constant, distribution coefficient for a linear isotherm (Fig. 2.15d). The above concepts are described in more detail by Melnyk (1985).

In most applications, nonlinear adsorption behavior is described by either a Freundlich or a Langmuir isotherm equation, as

$$S = K_f c^N \tag{2.39}$$

or

$$S = \frac{K_L M c}{1 + K_L c} \tag{2.40}$$

where S is the adsorbed concentration, K_f and N are the Freundlich isotherm equation parameters, and K_L and M are the Langmuir isotherm equation parameters.

For the cases of a nonlinear, convex adsorption isotherm described by a Freundlich or a Langmuir isotherm, the retardation factor becomes, respectively

$$R_d = 1 + \frac{\rho_b}{n} K_f N c^{N-1} \tag{2.41}$$

or

$$R_d = 1 + \frac{\rho_b}{n} \frac{K_L M}{(1 + K_L c)^2} \tag{2.42}$$

When the adsorption behavior is described by nonlinear, concave isotherms, the limiting partition coefficient can be evaluated using a secant formulation, or

$$K_p = \left.\frac{\Delta S}{\Delta c}\right|_{c_0} \tag{2.43}$$

where c_0 is the equilibrium concentration which defines the particular slope of the secant line used for the evaluation of K_p (e.g., c_2 in Fig. 2.15c). For secant lines passing through the origin of the adsorption isotherm, the limiting retardation factors based on the Freundlich and Langmuir isotherm equations are, respectively

$$R_d = 1 + \frac{\rho_b}{n} K_f c_0^{N-1}$$

(2.44)

and

$$R_d = 1 + \frac{\rho_b}{n} \frac{K_L M}{1 + K_L c_0}$$

(2.45)

Retardation factors based on Eqs. 2.44 or 2.45 can be used to estimate the extent of migration of the center of mass of a contaminant plume in the case of nonlinear, concave adsorption behavior. However, it is unlikely that accurate estimates of the distribution of contaminants in the soil can be made using retardation factors based on Eqs. 2.44 or 2.45 due to the approximation of the nonlinear adsorption behavior by linear secant formulations.

For the case of a linear adsorption isotherm (Fig. 2.15d), the retardation factor is written simply as

$$R_d = 1 + \frac{\rho_b}{n} K_d$$

(2.46)

As a result, all concentrations have the same transport rate, i.e., the slope of the isotherm is constant at all equilibrium concentrations.

2.5.2.3 Transport of Reactive (Adsorbing) Organic Compounds

The adsorption of hydrophobic organic contaminants at relatively low concentrations also can be described adequately by Eq. 2.46, provided that the distribution coefficient is defined as

$$K_d = f_{oc} \cdot K_{oc} \tag{2.47}$$

where f_{oc} is the fraction (by weight) of organic carbon in the soil, and K_{oc} is the organic carbon partition coefficient (Karichoff et al., 1979). The organic carbon partition coefficient has been correlated empirically with a number of parameters, particularly the octanol-water partition coefficient, K_{ow}. These empirical correlations are covered in more detail by Griffin and Roy (1985).

2.5.2.4 Fick's Second Law

At low values for the seepage velocity, diffusion is more significant relative to advection. In the limit, i.e., as $v_s \to 0$, Eqs. 2.33 and 2.35 reduce to the following two expressions for *Fick's 2nd law* for diffusion of adsorbing and nonadsorbing solutes, respectively:

$$\frac{\partial c}{\partial t} = \frac{D^*}{R_d} \frac{\partial^2 c}{\partial x^2} = D_A^* \frac{\partial^2 c}{\partial x^2} = D_s \frac{\partial^2 c}{\partial x^2} \tag{2.48}$$

and

$$\frac{\partial c}{\partial t} = D^* \frac{\partial^2 c}{\partial x^2} \tag{2.49}$$

where D_A^* in Eq. 2.48 is referred to as an 'apparent diffusion coefficient' (Li and Gregory, 1974) and D_s is known as the 'effective diffusion coefficient of the reactive solute' (Gillham et al., 1984; Quigley et al., 1987b). The result of using D_A^* or D_s in Eq. 2.48 is that only one unknown must be solved instead of the two unknowns, since $D_A^* = D_s = D^*/R_d$. Shackelford (1991) and Shackelford and Daniel (1991) discuss the use of D_A^* or D_s in application and summarize several other expressions for Fick's 2nd law of diffusion which exist due to differences in the definitions of D^* and differences in the expression of the solute concentration.

2.5.3 Effects of Material Properties

The effects of several material properties (R_d, D_m, D^*, k, and n) on the transport of solutes in saturated porous media can be illustrated with the aid of solute breakthrough curves. Breakthrough curves represent the temporal variation in the concentration of a solute at the effluent end of a column of porous material. Breakthrough curves can be measured using laboratory columns by:

1. establishing steady-state fluid flow conditions;

2. continuously introducing at the influent end of the column a liquid containing a solute at concentration c_0; and

3. monitoring the solute concentration at the effluent end.

A schematic representation of a solute breakthrough curve for a continuous source concentration for a column of length L is presented in Fig. 2.16a. The effluent concentration, c, is expressed for convenience as a relative concentration, c/c_0.

With respect to Fig. 2.16a, the breakthrough curve can be divided into three distinct zones. Zone 1 represents the time (t_0) required for the solute to reach the effluent end of the column. Zone 3 represents the steady-state transport condition with respect to the solute, which occurs after time t_f, where the effluent concentration is the same as the influent concentration, c_0. It is important to note that it takes some time before steady-state solute transport occurs, whereas steady-state fluid (solvent) flow is a pre-condition for the column test. Zone 2 is a transient, transitional zone wherein the effluent concentration is gradually rising from zero to c_0.

Due to the spreading effect of the solute front in zone 2, there are an infinite number of possible transit times depending on the particular choice of the relative concentration, c/c_0. However, the 'usual' practice has been to define the transit time with respect to a relative concentration of 0.5, which is time t_L in Fig. 2.16a (Bowders *et al.*, 1986). The concentration-
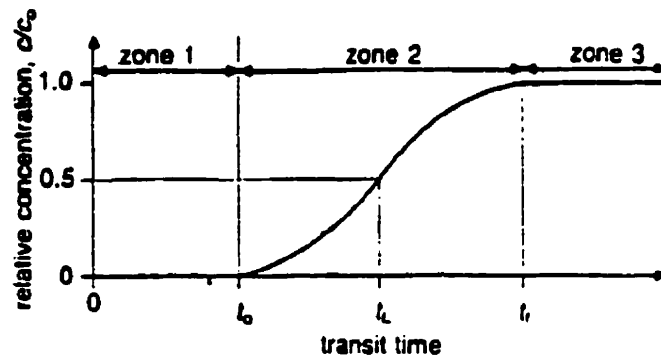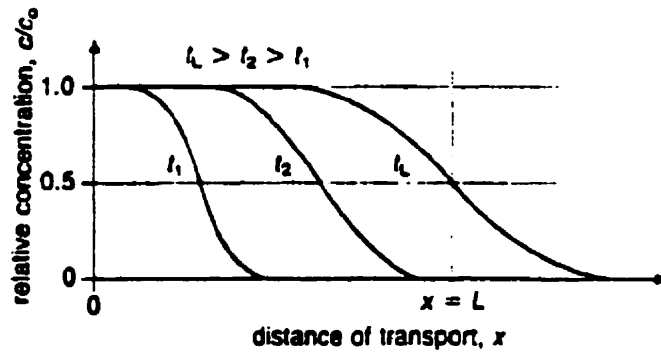
Figure 2.16 Solute breakthrough curve for constant source concentration: (a) concentration-time profile; and (b) concentration-distance profiles for different times (Shackelford, 1993).

distance curves for this case are illustrated in Fig. 2.16b for three different elapsed times after the introduction of the solute at the influent end of the column.

2.5.3.1 Effect of Retardation

The effect of retardation on the transport of a solute is illustrated in Fig. 2.17a. The abscissas for the breakthrough curves in Fig. 2.17 have been defined in terms of pore volumes of flow instead of time. The number of pore volumes of flow (PVF) is equal to the cumulative volume of flow through the sample divided by the volume of void space in the material, or

$$PVF = \frac{vAt}{LAn} = \frac{vt}{Ln} = \frac{v_s}{(L/t)} = \frac{v_s}{v_R} \tag{2.50}$$

where A is the cross-sectional area of the material and L is the length of the column. Under steady-state fluid flow conditions, Eq. 2.50 indicates that the number of pore volumes of flow is directly proportional to time. For purely advective transport of nonreactive solutes, the velocity of the solute, v_R, is the same as the seepage velocity, v_s, and (provided $n_e = n$) complete breakthrough of the solute will occur at one PVF (curve 1 in Fig. 2.17a). This ideal condition is often referred to as 'piston' or 'plug' flow since there is no spreading of the solute front.

For solutes subject to reversible sorption reactions, i.e., reactive solutes, $v_R < v_s$ and the solute will be retarded. This retardation effect is manifested as an offset in the solute breakthrough curve of the reactive solute relative to the nonreactive solute (distance A in Fig. 2.17a). With respect to the advective transport of an adsorbing solute, v_R ($=L/t$) in Eq. 2.50 represents the 'velocity' of the retarded solute. The transit time based solely on the advective transport of adsorbing solutes can be estimated from the retarded solute velocity as

$$t = \frac{L}{v_R} = \frac{L\,R_d}{v_s} = \frac{n\,L}{k\,i}\,R_d \tag{2.51}$$
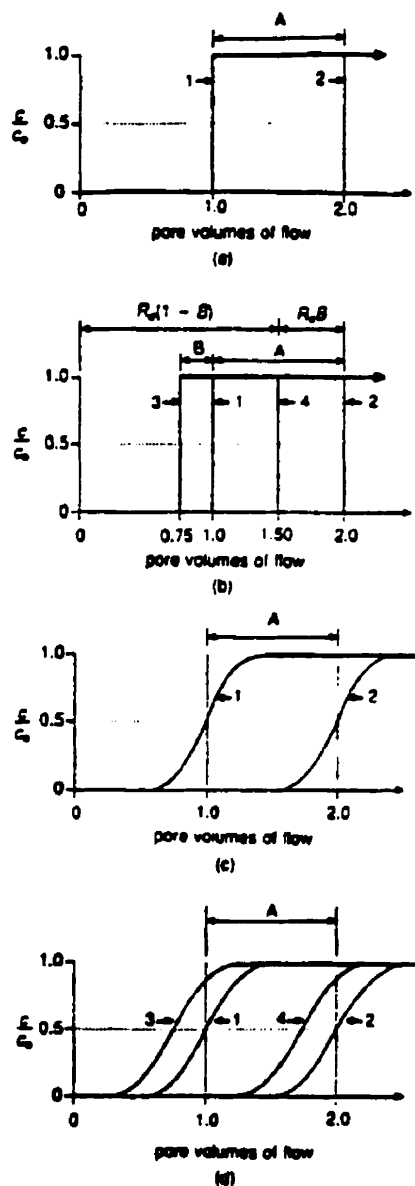
Figure 2.17 Effect of material properties on solute breakthrough curves for constant source concentration: (a) effect of retardation - piston flow; (b) effect of effective porosity - piston flow; (c) effect of mechanical dispersion; and (d) effect of diffusion. Note: curves 1&3 - nonreactive solutes; curves 2&4 - reactive solutes (Shackelford, 1993).

Since $R_d > 1.0$ for retarded solutes, the transit time based on Eq. 2.51 for adsorbing solutes will be greater than the transit time for nonadsorbing solutes (Eq. 2.20).

Again, it is important to distinguish clearly between steady-state fluid flow and steady-state solute transport. The retardation factor R_d as defined by Eq. 2.34 is a measure of how much slower a retarded solute moves relative to the steady-state movement of the fluid, or solvent. Once complete breakthrough of the solute has occurred, the solute is no longer retarded (as the term is used here) since 'steady-state' solute transport, by definition, means that the influent and effluent mass fluxes of the solute are equal. As a result, steady-state transport is achieved only after the liquid-phase concentration of the solute is in equilibrium with the solid-phase concentration of the solute throughout the entire length of the column.

A comparison of Eqs. 2.34 and 2.50 reveals that the retardation factor, R_d, is equal to the number of pore volumes of flow, PVF, it takes for the solute to break through the effluent end of the column. This relationship can be utilized to determine the value for the retardation factor for an adsorbing solute. For example, the breakthrough curve in Fig. 2.17a for the retarded solute is given by curve 2, so the retardation factor is 2.0, i.e., $R_d = PVF = 2.0$.

2.5.3.2 Effective Porosity

In fine-grained soils, some of the fluid in the pore space may be immobile due to dead-end pores and/or attraction of fluid molecules to the surface of the soil particles (Bear, 1972, 1979). As a result, the portion of the pore space available for solute transport may be significantly less than the total pore space. In such cases, an effective porosity, n_e, should be used instead of the total porosity, n, in Eq. 2.18 to determine the seepage velocity. Effective porosities on the order of 2-100% of the total porosity have been measured in compacted soils (Horton *et al.*, 1985; Liao and Daniel, 1989).

The effect of effective porosity on purely advective (piston) transport of solutes is illustrated by the offset B in Fig. 2.17b. Since $n_e < n$, the seepage velocity is greater than that predicted using the total porosity, and actual breakthrough of the solutes occurs earlier than expected. For the case shown in Fig. 2.17b, B represents 0.25 PVF, and, therefore, only 75% of the total pore space is effective in conducting the fluid flow (i.e., $n_e = 0.75\ n$). As a result, breakthrough of nonreactive (nonadsorbing) solutes will occur after only 0.75 PVF (curve 3) rather than after one PVF (curve 1).

On the other hand, complete breakthrough (i.e., assuming piston transport) of reactive solutes occurs after $\{R_d(1 - B)\}$ pore volumes of flow, or $(R_d \cdot B)$ pore volumes sooner than expected. For example, R_d for the reactive solute in Fig. 2.17 is 2 and, therefore, breakthrough of the reactive solute is expected at 2 PVF (curve 2). However, due to the effective porosity effect, breakthrough of the reactive solute actually occurs after only 1.5 PVF (curve 4).

2.5.3.3 Mechanical Dispersion

In general, complete breakthrough of a solute will not occur instantaneously. Instead, there is a gradual rise in the solute concentration from $c = 0$ to $c = c_0$ due to the spreading effect caused, in part, by mechanical dispersion. This spreading effect gives the solute breakthrough curve its characteristic S-shape shown in Fig. 2.16a. The effects of mechanical dispersion on the breakthrough curves illustrated in Fig. 2.17a are shown in Fig. 2.17c. At relatively high seepage velocities, mechanical dispersion dominates the mixing process and the solute breakthrough curves, including the effects of mechanical dispersion, intersect those for piston flow at a relative concentration, c/c_0, of 0.5, as shown in Fig. 2.17c.

2.5.3.4 Effect of Diffusion

The breakthrough curves illustrated in Fig. 2.17c represent spreading of the solute front primarily due to mechanical dispersion, i.e., spreading due to diffusion is negligible. This is the case commonly referred to in groundwater hydrology textbooks because the primary

concern is with contaminant migration in aquifers, i.e., coarse-grained, water-bearing strata subject to relatively high seepage velocities. Curves 3 and 4 in Fig. 2.17d represent breakthrough curves for nonreactive and reactive solutes, respectively, when the seepage velocity is sufficiently low such that the effect of diffusion is not masked by the effect of advection, including mechanical dispersion. For comparison, the breakthrough curves of Fig. 2.17c are also provided in Fig. 2.17d. The spreading effect is still noticeable in Fig. 2.17d, but curves 1 and 3 and curves 2 and 4 do not intersect each other at $c/c_0 = 0.5$. Instead, curves 3 and 4 are displaced to the left of curves 1 and 2, respectively. This displacement due to diffusion can result in transit times (at $c/c_0 = 0.5$) which, in some cases, can be much less than those predicted by considering only advection. This effect previously has been recognized analytically by De Weist (1965) and experimentally by Biggar and Nielsen (1960).

The decrease in the transit time, illustrated in Fig. 2.17d, due to diffusion is a function of the magnitude of the seepage velocity. This dependence is illustrated in Fig. 2.18 where the transit time for purely advective, purely diffusive, and advective-dispersive transport is presented as a function of the logarithm of the seepage velocity. Figure 2.18a presents the qualitative relationship between transit time and seepage velocity for nonreactive solutes (R_d = 1), while Fig. 2.18b demonstrates the same relationship for reactive solutes ($R_d > 1$). Although no data are provided in Fig. 2.18, the general trends are apparent from previous analyses (Shackelford, 1988, 1989). The horizontal distance between the purely advective and the advective-dispersive curve in Fig. 2.18 represents the offset distance in Fig. 2.17d for a given seepage velocity. The independence of pure diffusion on hydraulic conductivity is indicated by the vertical line.

From the trends presented in Fig. 2.18, it is apparent that the effect of diffusion on transit time increases as the seepage velocity decreases. The seepage velocity at which diffusion begins to dominate solute transport is indicated by the inflection point in the advective-dispersive curve. Available evidence indicates that diffusion can be a significant transport process when the seepage velocity is in the range 0.064-0.09 m/yr (Rowe *et al.*,
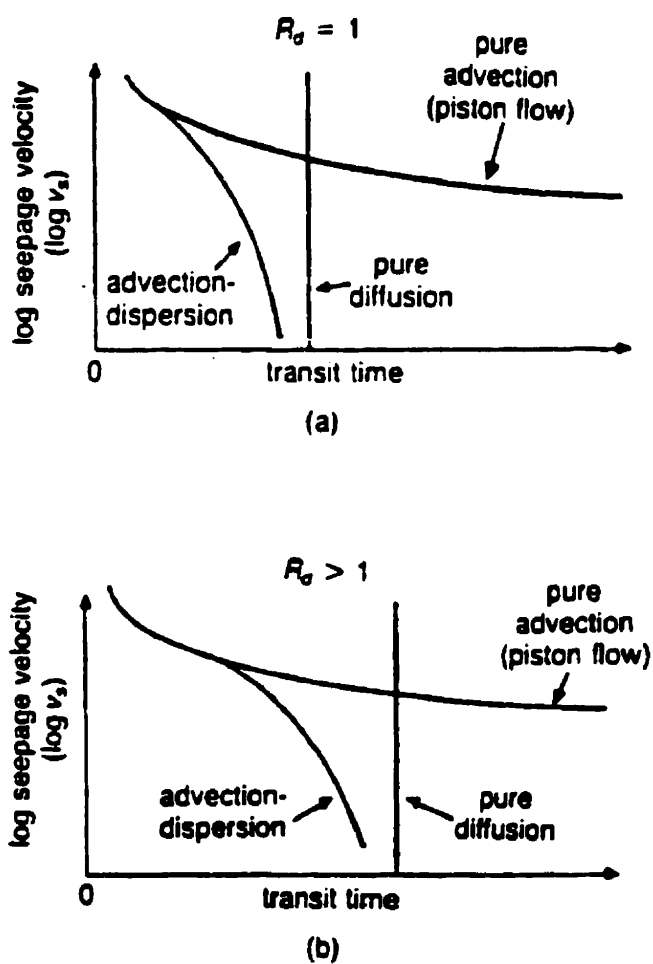
Figure 2.18 Schematic relationship between transit time and seepage velocity for a transport distance L and a constant source concentration: (a) nonreactive solutes; and (b) reactive solutes (after Shackelford, 1989, 1991).

1988), and a dominant transport process when v_s is $\leq$ 0.005 m/yr (Gillham *et al.*, 1984; Shackelford, 1988, 1989).

The effect of diffusion on solute breakthrough curves is similar to the effect of effective porosity (cf. Figs. 2.17b and 2.17d). Whereas the effect of diffusion is noticeable only at relatively low seepage velocities, the effect of effective porosity is expected to be independent of the seepage velocity. However, there is some indication that the value of n_e can be a function of the hydraulic gradient (and, consequently, v_s) imposed in the study, with lower values of n_e being observed at lower hydraulic gradients (Liao and Daniel, 1989). Thus, attempts to discern the effective porosity of a soil, e.g., by performing column tests at elevated seepage velocities, may not prove successful.

The analytical phase of the present study is accomplished by means of finite element analyses of the transport of contaminants through the clay soils. The correlation between macroscopic properties, as obtained from the leaching tests, and microscopic features, as revealed by the scanning electron micrographs, is cross-referred and evaluated through the numerical modeling to explore the extent of validity of simulating leachate migration in compacted clays.

2.6 Purpose of Study

Based on a review of the literature related to the migration of contaminants and compacted clays, it can be concluded that a great deal is known about hydraulic conductivity and the interrelationships between specimen characteristics, permeant properties, and the equipment needed to conduct the compatibility tests. Excluding the impact of test equipment, relatively fast permeability rates (10^{-4} to 10^{-7} m/s) appear to be a function of the variables associated with the macrostructure of the soil. Mineralogy and stress history allow assemblages of soil particles that exhibit high porosity and low dry unit weight. The

macrofabric provides a highly interconnected void space that allows permeants to flow easily through soils.

Conversely, relatively low permeability rates (10^{-9} to 10^{-12} m/s) seem to be controlled by those variables directly affecting the microfabric of clays and the diffuse double layer. Such factors become evident and have a significant impact on hydraulic conductivity. For low flow situations, it appears that alteration of any one variable may lead to physico-chemical changes in the other variables, therefore inducing changes in the response variable, namely, hydraulic conductivity. Organics in the permeant and/or soil interact with the clay-water system by varying the rate of ion exchange, hence altering the magnitude of the forces acting at the soil particles interface and ultimately affecting the structure of clays. Expanded exposure time between the pore fluid and the clay particles also results in opportunity for increased ion exchange. The effects of surface force interactions and small particle size of clays are manifested by a variety of interparticle attractive and repulsive forces, which, in turn, influence the flocculation-deflocculation behavior of clays in suspension. It is these forces that this research is focused on investigating and detecting by means of direct observations of the structure of compacted clay after permeation with and exposure to a wide range of contaminants.

The rigid-wall permeameters simulate a worst case scenario for a clay liner. In such a situation, there is no vertical overburden applied to the soil; for instance, a liner for a liquid impoundment facility. The lack of overburden results in low-effective stresses in the liner. Soils under low-effective stresses being leached with contaminants that are susceptible to altering their structure can develop shrinkage stresses, shrinkage cracks, and increased hydraulic conductivity. Consequently, the use of rigid-wall cells could help in the detection of the influence of contaminants on soil structure. On the other hand, flexible-wall permeameters apply a confining stress to the soil specimen that results in the specimen having increased effective stress and resistance against development of cracks when undergoing volume change. Such a situation is representative of a soil liner overlain by solid waste and

a soil cover. The increased stress due to the overburden lessens the chance of developing shrinkage cracks during volume change, thus masking the impact of contaminant transport on the soil fabric.

Although much care and study have been directed to the question of permeability of soils, not enough research has been performed for the purpose of figuring out what sort of contaminants would have a detrimental effect on the structure of compacted clays, thus calling into question the integrity of compacted clay liners commonly employed in waste containment facilities. Indeed, it is possible that soil-contaminant interactions may result in a substantial alteration of the compacted soil structure, which can lead to catastrophic failures of clay barriers in engineered landfills and surface impoundments, and dangerous outcomes threatening the environment and public health. Nonetheless, it is rare to find published studies that have focused on examining the subtle differences in the structure of compacted clay associated with different permeants, and the impact these pollutants have upon migration through soils. The purpose of the present study is to fill in the lack of research dedicated to investigating this crucial point.

CHAPTER 3

MATERIALS AND METHODS

Chapter 3 presents the materials used in the research, their properties and characteristics. The chapter also discusses and justifies the methods employed in the study through its various divisions. The divisions of the chapter include: materials, leaching tests, soaking tests, scanning electron microscopy, and contaminant transport modeling.

3.1 Materials

The materials used in this research include kaolinite as a clay mineral, and a spectrum of fluids representing a variety of contaminants.

3.1.1 Soils

Two types of Hydrite$^{\circledR}$ Kaolin (HK) clays, produced by the Dry Branch Kaolin Company of Dry Branch, Georgia, are used for the current investigation. The trade name of these processed clay soils is *Hydrite Flat-D*, and *Hydrite R*, respectively. They were chosen because they cover a wide range of particle size, even though their principal mineral is kaolinite.

3.1.1.1 Physical and Geotechnical Properties

The Dry Branch Kaolin Company reports that HK soil consists, on average, of 96% (dry weight) kaolinite mineral. The physical and geotechnical properties of the processed kaolin soils are shown in Table 3.1. Those were determined by performing the respective tests following the ASTM standards (ASTM, 1995). The particle-size distribution curves for the two types of kaolinite are illustrated in Fig. 3.1. It can readily be seen from that figure that the *Hydrite Flat-D* is identified by a well-graded silt- and clay-sized materials, whereas the *Hydrite R* is composed of 20% silt-size particles and 80% clay-size particles. Based on the

Table 3.1 Physical and geotechnical properties of the processed clay soils.

Trade Name	Hydrite Flat-D	Hydrite R
Principal Mineral	Kaolinite	Kaolinite
Color	White	White
Water Content, % (ASTM D 2216)	0.30	0.40
Specific Gravity (ASTM D 854)	2.6	2.5
Liquid Limit, % (ASTM D 4318)	41	58
Plasticity Index, % (ASTM D 4318)	12	28
Particle Size: silt (74-2 μm) clay (< 2 μm)	75 % 25 %	20 % 80 %
Activity*	0.48	0.35
Classification by USCS (ASTM D 2487)	ML	CH
Max. Dry Density, Mg/m³ (ASTM D 698[A])	1.42	1.31
Opt. Moisture Cont., % (ASTM D 698[A])	29	33

* Activity = Plasticity Index (%) / % < 2 μm
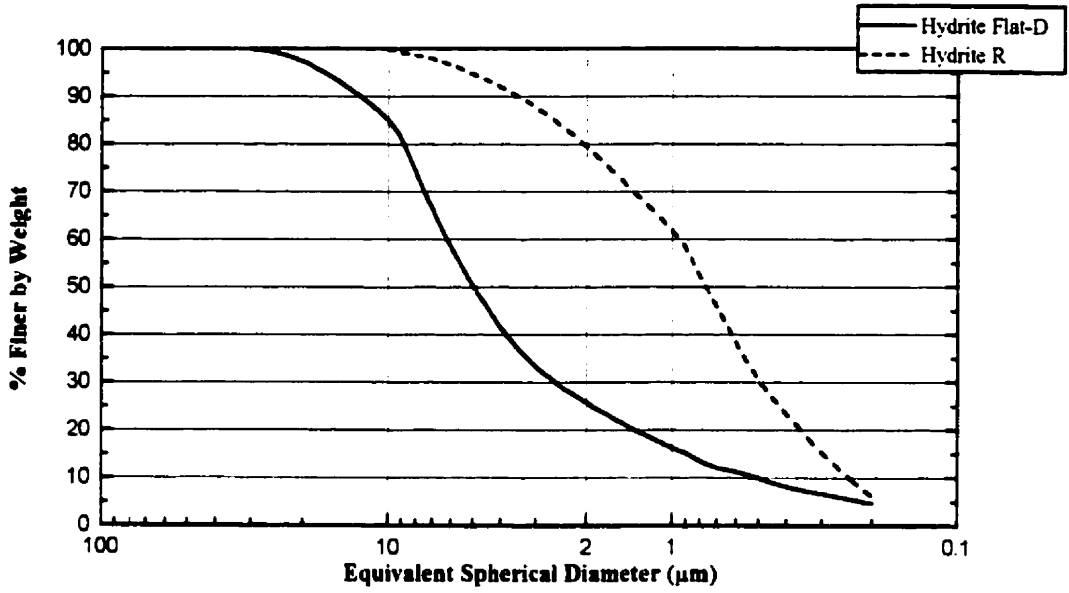
Figure 3.1 Typical particle-size distribution curves
of the processed clay soils (ASTM D 422).
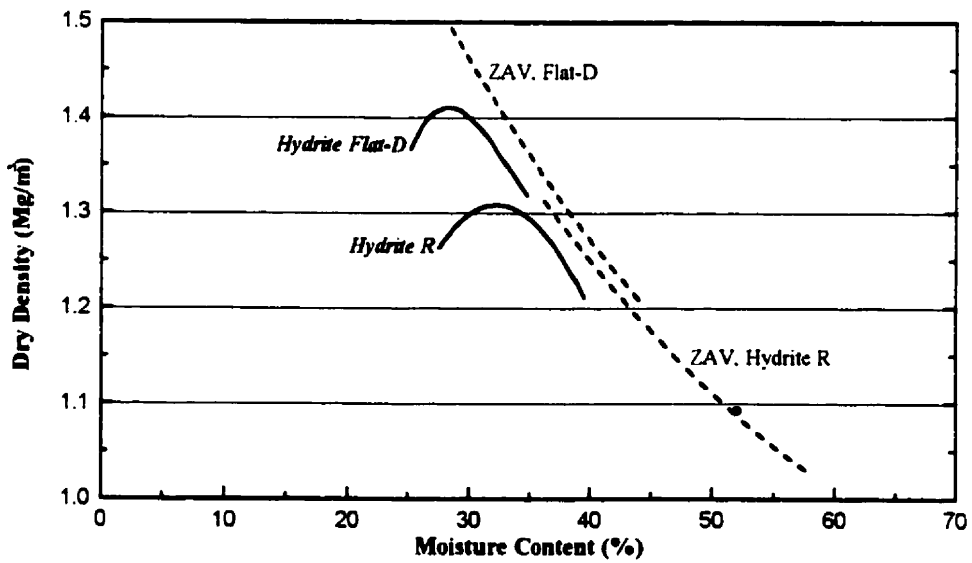
Figure 3.2 Compaction curves of the processed clay soils
by the standard Proctor test (ASTM D 698[A]).

determined liquid limit and plasticity index of *Hydrite R*, it is classified as fat clay (CH) according to the Unified Soil Classification System (USCS) (ASTM D2487). The *Hydrite Flat-D*, on the other hand, is classified as silt (ML) following the same classification system.

The moisture content of the clay as-supplied was found to range between 0.3 and 0.4%. The specific gravity, however, varies from 2.5 to 2.6 for the two types of kaolin clays. Activity is used as an index for identifying the swelling potential of clay soils. The greater the activity of a given soil, the higher its swelling potential is expected to be. The activity of *Hydrite Flat-D* was calculated to be 0.48, whereas it is 0.35 for the *Hydrite R*.

Standard Proctor compaction tests were conducted following ASTM standard, method D698, procedure A. Tap water was used as the molding fluid. The specifications for compaction are

- Mass of manual rammer: 2.5 kg (5.5 lb);
- Height of free fall: 305 mm (12 in);
- Volume of compaction mold: 944×10^{-6} m^3 (1/30 ft^3);
- Number of sample layers: 3; and
- Number of blows per layer: 25.

The clay was prepared for compaction by uniformly spraying the air-dried kaolinite with tap water. Following the gradual moistening, the sample was further mixed manually to break clay clods or peds, making it as homogenous as possible. The total mass of the clay was measured after compaction. Specimens were taken from the top, middle, and bottom of the compacted clay for water content measurements. Dry density of each compacted clay was then calculated. Consequently, a plot of dry density versus molding water content can be obtained for a given clay. The compaction curves of the two processed clay soils are shown in Fig. 3.2 along with their saturation curves. The maximum dry density and optimum moisture content values of *Hydrite Flat-D*, and *Hydrite R*, respectively, are presented in Table 3.1.

3.1.1.2 Chemical Properties

The chemical properties of the processed clay are shown in Table 3.2. The reported values are averages of, at least, three measurements. The chemical analyses were performed at the Analytical Geochemistry laboratory.

HK clays are water processed soils, according to the Dry Branch Kaolin Co., to reduce soluble salt contents to extremely low levels. The measured Na^+ concentrations of the supplied kaolinite, however, were far from being low as indicated in Table 3.2. The soluble salts in the two types of kaolin clays were determined by the saturation extract method (Rhoades, 1982b). The ammonium acetate (NH_4OAc), on the other hand, was used to determine the exchangeable cation concentrations based on the procedure of Thomas (1982).

The saturated paste properties of *Hydrite Flat-D*, and *Hydrite R*, respectively, were determined following the appropriate methods of chemical analyses (Hesse, 1971). The saturation percentage is defined as the loss in weight of the oven-dried saturated soil paste multiplied by 100 and divided by the oven-dry weight. The high values of electrical conductance of the saturated pastes reflect the fact that both soils contain high concentrations of Na^+. Major chemical constituents and carbonate content of the two types of kaolin clay, included in Table 3.2, were found to be almost identical, confirming the uniformity of the parent kaolinite.

The cation exchange capacity (CEC) was determined following a procedure adapted after Chapman's (1965) ammonium saturation method (Cabral, 1992). The test was conducted, in part, at the Environmental Engineering laboratory. The Atomic Absorption Spectrometer (AAS) of the Analytical Geochemistry laboratory was used, however, to analyze the collected supernatants. The results of such analyses, along with the CEC for each kaolin clay, are shown in Table 3.3. The CEC values for the two types of kaolinite used in this study vary from 2.19 to 5.82 meq/100 g, falling in the lower range of those values reported

Table 3.2 Chemical properties of the processed clay soils.

Trade Name	Hydrite Flat-D	Hydrite R
a) Saturated Paste:		
- Percent Saturation, g/g	96	188
- pH at 25°C	4.4	4.0
- Electrical Conductance at 25°C, mS/m	50	135
b) Soluble Salts, mg/L:		
Ca^{2-}	3.5	18.7
Mg^{2-}	0.5	2.6
Na^-	72	423
K^-	0.8	2.6
Cl^-	< 5	< 5
c) Exchangeable Cations, meq/100 g:		
Ca^{2-}	0.39	0.76
Mg^{2-}	0.09	0.18
Na^-	0.53	2.52
K^-	0.01	0.02
d) Major Constituents, percentage by mass:		
Silicon Dioxide (SiO_2)	49.50	49.50
Aluminum Oxide (Al_2O_3)	34.00	34.00
Iron Oxide (Fe_2O_3)	0.43	0.57
e) Carbonate Content, %	< 0.01	< 0.01

Table 3.3 Cation exchange capacity of the supplied kaolinite.

Trade Name	Hydrite Flat-D	Hydrite R
Exchangeable Cations, meq/100 g		
Na^-	0.45	2.46
K^-	0.01	0.02
Ca^{2-}	0.34	0.63
Mg^{2-}	0.08	0.15
Al^{3-}	1.31	1.46
H^-	0.00	1.10
CEC, meq/ 100 g	2.19	5.82

in the literature, namely, 3 to 15 meq/100 g (e.g., Grim, 1968; Lambe and Whitman, 1979; Mitchell, 1993).

3.1.1.3 Morphology and Specific Surface

The Dry Branch Kaolin Company reports that HKs finer than 2 μm are thin, flat, hexagonal plates, whereas those coarser than 2 μm consist of particles occurring as stacks of such plates and are bound together as a single particle. This statement was confirmed by subsequent scanning electron microscopy observations.

Surface area largely determines many physical and chemical properties of materials. Physical adsorption of molecules, heat loss or gain resulting from that adsorption, swelling and shrinkage, water retention and movement, and cation exchange capacity, to name just a few, are all physical and chemical processes closely related to the specific surface (defined as the surface area per unit mass of soil). Specific surface is usually expressed in square meters per gram of dry soil (m²/g).

Soils vary widely in their reactive surface because of differences in mineralogical composition and in their particle-size distribution. Clay-size particles, and particularly some layer silicate minerals, contribute most of the inorganic surface area to soils. Nonexpanding layer silicates such as kaolinite and some micas have only external surfaces. The specific surface of these minerals ranges from 10 to 70 m²/g. Expanding layer silicates, such as montmorillonites, other smectites, and vermiculites, have extensive internal as well as external surface, giving specific surfaces up to 810 m²/g, depending upon the amount of internal surface exposed by expansion. Consequently, the types of minerals present in a given soil largely determine its specific surface and related properties.

The purpose of surface-area measurements is commonly to determine the accessibility of internal surfaces of the clay mineral complex to molecules or ions which can be adsorbed thereon. Many methods and approaches have been employed to measure the specific surface

of soils and minerals. Some methods are thermodynamically sound but too time-consuming, or they require too much specialized apparatus to be used on a routine basis. Therefore, other relatively rapid but less accurate methods have been developed. The assumptions required and the several factors influencing results from most of these latter procedures give us merely an assessment but not a real measure of the specific surface. Absolute measurements are difficult to attain and interpret because of the interactions of several factors such as the adsorbed cation, the orientation of the adsorbed molecules, mono- or duo-layer coverage in the interlayer spacing, and sample water-content.

Ethylene glycol monoethyl ether (EGME) appears to be adsorbed on clay mineral surfaces and to adsorbed cations to essentially the same extent, and probably by the same mechanisms, as is water in hydrated systems (Carter *et al.*, 1986). For this particular reason, the EGME was opted for as the adsorbate for determining the specific surface of the processed soil in hand. The guidelines mentioned by Carter *et al.* (1986) were followed in carrying out the test which was performed in the Environmental Engineering laboratory. The specific surface of *Hydrite Flat-D* and *Hydrite R* was found to be 11 and 16 m^2/g, respectively. The obtained results are averages of three measurements for each type of kaolinite. The resulted values of the test fall well in the range of the recognized values of specific surface for kaolinite, which varies from 10 to 20 m^2/g (e.g., Grim, 1968; Lambe and Whitman, 1979; Mitchell, 1993). Moreover, the reported trend is in the right direction, i.e., the finer the particle size, the higher the specific surface.

3.1.2 Permeants

Waste liquids in the environment may result from several sources, e.g., uncontrolled dumping of pure solvents, spills, or infiltration of water through solid waste resulting in leachate. Waste liquids may be categorized as aqueous liquids or solutions containing contaminants which are miscible in water (also known as hydrophilic or "water-loving"), non-aqueous liquids consisting of organic compounds immiscible in water (also known as

hydrophobic or "water-hating"), or mixtures of both aqueous and non-aqueous liquids resulting in the formation of two separate liquid phases. The migration of mixtures containing two separate liquid phases in liquid saturated soil, referred to as "two-phase flow," requires special consideration for the interaction between the two liquid phases. This interaction is particularly important in the case of permeation of a water saturated soil by a non-polar organic liquid. Due to surface and interfacial tension effects, the non-polar liquid (a "non-wetting fluid") can displace the free water (or "wetting fluid") in the pore space of the soil only after a minimum pressure, known as the "entry pressure," for the non-wetting fluid is reached.

In some cases, the actual waste liquid is either unknown or is not readily available for use in laboratory tests. In such cases, a synthetic liquid made to simulate the properties expected for the actual waste liquid typically is used. The chemical properties of the synthetic waste liquid which typically are measured or controlled include: (1) the concentration and types of chemicals present in the liquid; (2) the density and viscosity of the liquid; (3) the pH and specific (or electrical) conductance (EC) of aqueous liquids; and (4) the polarity, solubility, and dielectric constant (or relative permittivity) of organic compounds. Other parameters, such as the electron potential (Eh), total dissolved solids (TDS), total organic carbon (TOC), chemical oxygen demand (COD), and biological oxygen demand (BOD), also may be important.

In the present research, tap water is used to set up a baseline in laboratory soil-chemical compatibility tests. It also serves as the standard fluid for compaction, saturation, and all reference hydraulic conductivity measurements. The type and concentration of electrolytes are among the most important characteristics of tap water. The quality of tap water was determined by the Atomic Absorption Spectrometer (AAS) of the Analytical Geochemistry laboratory, and is presented in Fig. 3.3.
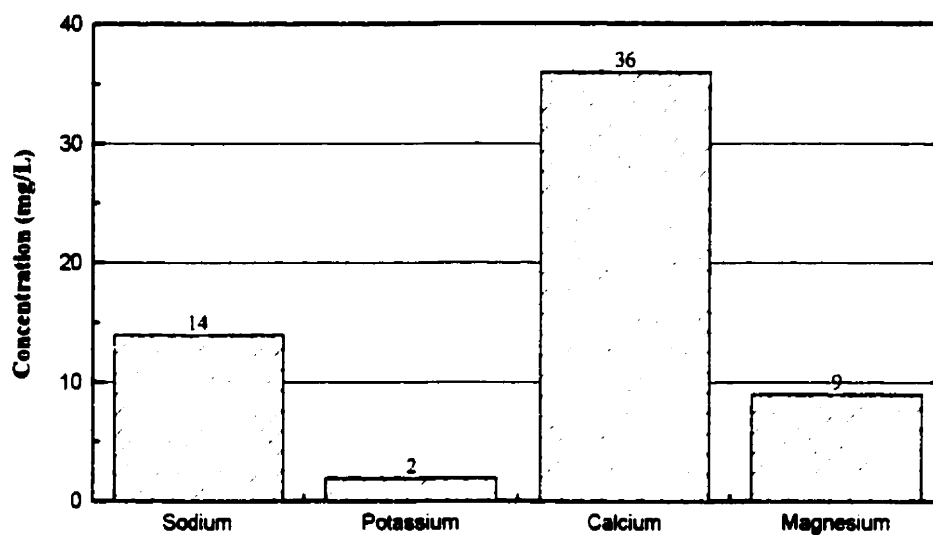
Figure 3.3 Quality data of tap water determined by Atomic Absorption
Spectrometer.

Inorganic salt solution, inorganic acidic and basic solutions, neutral polar alcohol, neutral non-polar hydrocarbon, and organic acid and base, are selected to permeate the compacted clay samples to study the effects of these chemicals on clay structure and hydraulic conductivity. The magnitude of the significant properties of the selected chemicals at 25°C is listed in Table 3.4. The ambient temperature, however, in which the tests are conducted varies from 22°C to 24°C. The main purpose of using NaCl solution of such high concentration is to explore the influence of electrolyte concentration on the hydraulic conductivity of compacted kaolinite and, ultimately, its internal structure. Permeation with inorganic and organic acids and bases is expected to provide insight into the effect of hydrogen ions on the thickness of the diffuse double layer and on dissolution-precipitation processes of kaolin mineral. The use of organic contaminants also helps to investigate the influence of permittivity, solubility, and the interfacial tension of the pore fluid on the microscopic and macroscopic properties of compacted clay.

3.2 Leaching Tests

3.2.1 Test Equipment

The experimental set-up of the leaching test comprises two major parts, namely, a hydraulic control system, and a permeameter cell. A schematic diagram of the test equipment is shown in Fig. 3.4.

3.2.1.1 Hydraulic Control System

Hydraulic control systems are needed to control the delivery of fluid to a permeameter cell. Darcy's law (Eq. 2.4) relates the rate of flow, q, to the hydraulic gradient, i. It may be assumed that in all hydraulic conductivity tests, the length, L, and cross-sectional area, A, of the test specimen are known. Thus, in order to determine the hydraulic conductivity, one must measure the flow rate, q, and head loss, ΔH. To accomplish this task, several approaches are possible:

Table 3.4 Properties of chemicals selected as permeants.

(a) Inorganic chemicals

Permeant	Tap Water	NaCl	HCl	NaOH
Concentration		5 M	0.01 M	0.25 M
Density (kg/m³)	1000	1290	1000	1010
Viscosity (mPa.s)	0.89	1.70	0.89	0.89
pH	5.4-6.2	8.3	2.6	13.2
Electrical Conductivity (S/m)	0.03	24.1	0.58	4.5

(b) Organic compounds

Permeant	Ethanol	Heptane	Acetic Acid	Aniline
Concentration	Pure	Pure	Pure	Pure
Density (kg/m³)	790	680	1050	1020
Viscosity (mPa.s)	1.07	0.39	1.06	3.85
Dipole Moment (Debye)	1.69	0	1.74	1.55
Relative Permittivity	24.30	1.90	6.15	6.89
Solubility in Water (kg/m³)	∞	< 0.3	∞	36
Surface Tension (mN/m)	22	20	27	4
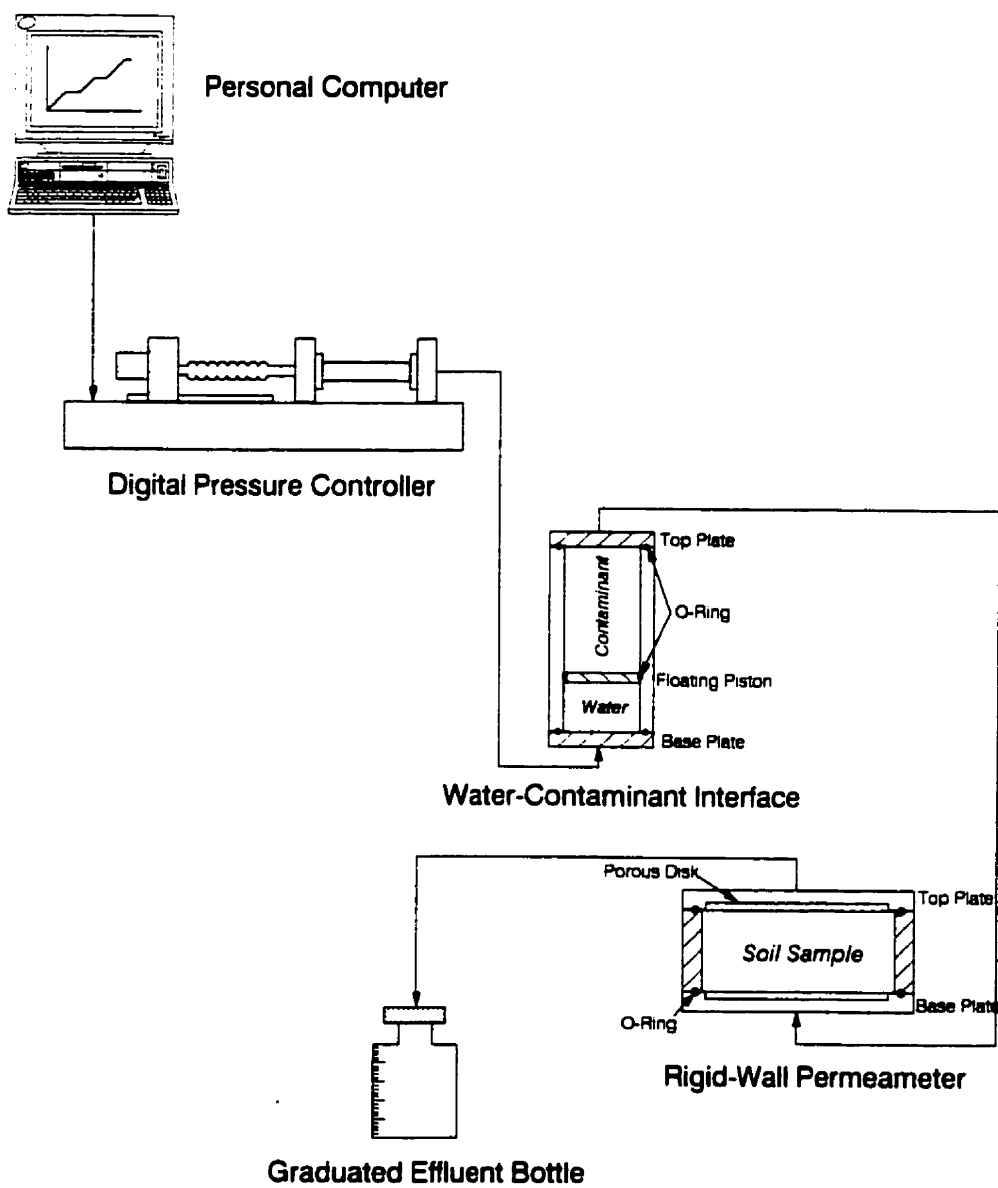
Figure 3.4 Test equipment of the leaching tests.

- Constant-head test in which the head loss is kept constant and the corresponding rate of flow is measured.

- Varying-head test in which the head loss declines with time in a measured manner and the rate of flow is computed from the change in water level and the area of the tube in which the head falls.

- Constant-rate-of-flow test in which the rate of flow is kept constant and the corresponding head loss is measured.

For the present research, a constant-head hydraulic control system was adopted. The main advantages of a constant head test are: (1) the relative simplicity of calculation of hydraulic conductivity, and (2) the maintenance of constant water pressure in the test sample. If the water pressure in the test sample varies, air bubbles can change volume and the soil sample itself can change volume in certain types of permeameters.

There are several ways, though, of maintaining a constant head. An overflow drain in the influent reservoir would sustain a constant water level in the influent reservoir, provided the supply line feeds enough water to the reservoir to supply the permeameter and drain. Alternatively, one can simply use a very large reservoir of influent liquid such that the water level in the reservoir does not change significantly during the permeation stage. A small change in head occurs, but if the reservoir is large enough, the change would be trivial and can be ignored.

Another way for maintaining a constant head is achieved by applying a constant pressure gradient through the sample. A computer-controlled digital pressure controller of GDS Instruments Ltd. (Fig. 3.4) was employed in the current investigation to conduct constant-head tests (Menzies, 1988; Olsen et al., 1988b). The used pressure controllers have an accuracy of 1 kPa. The target pressure was introduced and maintained by entering its specific value through a program built with HP's *visual engineering environment* (HP VEE) programming language. The program allows communication with instruments from the visual

environment running on an MS-Windows platform. The measured flow rates, while the test was in progress, were recorded to the nearest 1 mm³, at equal specified time intervals, using the same program.

A water-contaminant interface was necessary to separate physically the various chemicals from the pressurized water, and also to minimize human exposure to hazardous contaminants, as shown in Fig. 3.4. Such interface may also help to reduce the dissolved air content in the contaminant liquid relative to the pressurized water. An elevated dissolved air content in the contaminant liquid may result in non-representative oxidation-reduction reactions in the test sample during permeation. A high grade stainless steel cylinder, equipped with a floating piston, was adapted and calibrated to work as the water-contaminant interface in this study. Viton* O-rings were employed to sustain the attack of aggressive chemicals.

3.2.1.2 Rigid-Wall Permeameter

The second major part of the experimental set-up of the leaching tests is the hydraulic conductivity cell. Several types of hydraulic conductivity cells are available for testing the chemical compatibility and hydraulic conductivity of soils. The cells may be divided, however, into two broad categories: rigid-wall and flexible-wall permeameters. The advantages and limitations of these permeameters were elaborately discussed in chapter 2 (cf. Section 2.4.1).

The principal drawback of rigid-wall permeameters was reported by many researchers to be the sidewall leakage. Sidewall leakage, however, is not a problem for laboratory-compacted clay soils that are permeated with water (no backpressure) in a rigid-wall, compaction-mold permeameter. Swelling of the soil upon wetting seems to seal off potential sidewall leaks (Daniel, 1994). Another major disadvantage of the rigid-wall permeameter is the fact that stresses on specimen are unknown and uncontrollable. To overcome the inconveniences of rigid-wall permeameters, Mitchell and Madsen (1987) recommend the use of the consolidation-cell permeameter. The vertically applied stress conditions help to minimize sidewall leakage and allow for measurement of hydraulic conductivity under a range

of stress conditions. While this capability for the consolidation-cell permeameter is recognized, the question as to which permeameter is "best" depends on the intended purpose. For instance, a rigid-wall test may be the best permeameter to indicate the potential for excessive shrinkage of the soil sample upon exposure to the contaminant liquid, and therefore to examine the impact of contaminant migration on soil fabric. For measurement of saturated hydraulic conductivity at a prescribed effective stress, the flexible-wall permeameter would be preferred since the test sample can be backpressure-saturated relatively easily and the stresses can be controlled.

On the other hand, the main advantages of the rigid-wall permeameters are: (1) simplicity of construction and operation of cell, (2) low cost of cell, (3) useful for compacted soil, (4) wide range of materials can be used (including chemically resistant materials), (5) very large permeameters can be constructed fairly conveniently, (6) no confining pressures required, (7) unrestrained vertical swelling can be allowed, (8) zero vertical stress can be applied, if desired, and (9) sidewall leakage may provide rapid indication of incompatibility between soil and contaminant.

Based on the specific considerations of the current investigation, a rigid-wall permeameter was opted for as the hydraulic conductivity cell for the present research, as shown in Fig. 3.4. The internal diameter of the cells used for the leaching tests of this study measures 76.2 mm (3 in). The cells, which have a clear height of 30 mm, are made from high-molecular weight polyethylene (HMWPE); a non-corrosive, non-reactive material capable of resisting the attack of the selected contaminants for this research. Moreover, the valves, fittings and tubing of the cells are all made from Teflon® for the very same reason.

Nalgene® narrow-mouth Boston round bottles of Nalge Company, Rochester, New York, served as the leachate collecting system in the present research (Fig. 3.4). This type of bottles is highly reliable and durable for long-term use. It is made from high-density polyethylene (HDPE), which is a resin known for its excellent chemical resistance, thus

making the bottles suitable for use with most corrosives. Two sizes of capacity 125 and 175 mL, respectively, were used and calibrated to the nearest 2 mL. The bottles were thoroughly cleaned before usage. They were washed in a mild detergent, followed by a rinse with tap water, and then distilled water. A dilute solution of nitric acid (50% concentration) was also used to avert any possible contamination of the collecting bottles.

3.2.2 Sample Preparation

Sample preparation consists of statically compacting the soil at its optimum moisture content or slightly wet of optimum (i.e., optimum + 1%). Tap water is used as the standard fluid for compaction. The processed kaolin clays are supplied by the manufacturer in 22.7 kg (50 lb) sacks each. Before compaction, the soil was air-dried. Referring to Fig. 3.2, the exact weight of soil for each type of kaolinite could be determined at a given moisture content, provided the volume of soil is known. The volume of molding water could also be defined after consulting Table 3.1 for the optimum moisture content value of the respective kaolinite, and based on the selected water content.

The soil was then hydrated manually to obtain the desired moisture content (near optimum). Hydration was completed by spraying water onto the soil and then mixing the soil with a trowel. Water was sprayed in stages to prevent the soil from lumping together and producing clod-size particles. Preventing clods formation produced a relatively uniform soil material that was necessary to prepare test samples with similar porosity, dry unit weight, and hydraulic conductivity. The hydrated soil was wrapped in plastic bags and stored for at least 24 hours in a temperature- controlled room (humid chamber) to equilibrate prior to compaction.

3.2.3 Static Compaction

A hydraulic jack was adapted to statically compact the soil in its leaching cell to the desired thickness (30 mm). A wet filter paper was placed on both the top and bottom of the sample before compaction. They prevent the sticking of soil on the piston after removing the static charge. The hydraulic jack was modified in a manner to allow an even application of the pressure on the top and bottom faces of the sample during compaction. The transmitted static pressure measures 12.4 MPa (1,800 psi). This charge was applied on the sample for 30 minutes to minimize the effects of soil rebound after compaction.

After the completion of compaction, the 30-mm thick clay sample in its leaching cell was mounted between the cap and base of the rigid-wall permeameter. Two saturated porous stones were placed on the top and bottom sides of the sample, respectively, and overlain by a filter paper. The permeameter was then assembled by evenly tightening the clamping rods connecting the cap, cell, and base.

3.2.4 Test Procedures

3.2.4.1 Saturation Procedure

After static compaction and before saturation, the clay samples were found to have a degree of saturation varying around 91%. In principle, one could eliminate gas bubbles in a rigid-wall cell with backpressure. "Backpressure" means pressurization of both the influent and effluent liquid. Pressurizing the water in the test specimen reduces the volume of air present by compressing air bubbles and dissolving air into the pore water (backpressure dissolves air because the amount of air that can be dissolved in water increases linearly with pressure in accord with Henry's law). Although it is physically possible to back pressure rigid-wall specimens, backpressure has not been found to work well in rigid-wall cells and is not recommended (Edil and Erickson, 1985).

One of the most important characteristics of the permeant water is the amount of dissolved air in the water. Whenever rigid-wall permeameters are used, it is recommended that de-aired water be employed to strip air from the specimen during saturation and permeation. "De-aired water" means water whose dissolved air has been substantially removed. A dissolved oxygen meter was used in this study to confirm proper de-airing. At atmospheric pressure, water contained approximately 8-10 mg/L of dissolved oxygen. Properly de-aired water contained less than 3 mg/L of dissolved oxygen. Water is de-aired by either boiling the water or by placing the water in a container that is subjected to vacuum. With a vacuum chamber, it is best to stir the water while in the evacuated chamber (e.g., with a spinning motor) to expose a large surface area of the water to vacuum and to facilitate rapid de-airing. If the tap water is boiled, care must be taken not to increase the salinity too much. In the present research, tap water was de-aired by using a vacuum container equipped with a spinning engine.

In an attempt to saturate the soil as thoroughly as possible, the following steps were undertaken when permeating the laboratory-compacted kaolinite in the rigid-wall permeameter: (1) direction of flow is upward (from bottom-to-top) to facilitate the removing of entrapped air during saturation; (2) permeant water is thoroughly de-aired so that the water is constantly dissolving, and thereby removing, entrapped air; (3) saturation continues until outflow and inflow rates are equal; and (4) saturation continues until hydraulic conductivity is steady. The latter two requirements usually force testing times of 1 to 8 weeks for soils having hydraulic conductivities of 1×10^{-9} m/s or less (Daniel, 1994). For each sample of the current investigation, at least 15 Pore Volumes of Flow (PVF) were allowed to percolate through the compacted kaolinite before starting the hydraulic conductivity measurements. At the end of saturation, the degree of saturation was calculated to be approximately 98%.

3.2.4.2 Hydraulic Conductivity Measurements

There currently is no official standard test procedure for evaluating the effect of soil-contaminant interactions on hydraulic conductivity. However, the unofficial "standard"

laboratory test procedure typically is performed by permeating a soil specimen with water to establish a reference value for the hydraulic conductivity followed by permeation of the same specimen with the contaminant liquid to determine the change in hydraulic conductivity. These tests frequently are referred to as "compatibility tests" since the purpose of the test is often to determine whether or not the soil and the contaminant permeant are compatible with respect to hydraulic conductivity. As a result of this test procedure, the final hydraulic conductivity value after permeation with the contaminant permeant, k_p, is measured relative to a reference hydraulic conductivity value, k_w, established by permeating the soil with water. A large change in hydraulic conductivity ($k_p / k_w \gg 1$) is an indication that the contaminant and soil are not compatible. If there is a significant difference between the properties of the contaminant permeant and water, the evaluation of compatibility should be made in terms of the ratio of intrinsic permeability values, K_p / K_w.

The above described test procedure was followed in performing the laboratory leachate tests of this research. All tests were conducted by flowing liquid upward through the 76-mm (3-in) diameter, 30-mm height, statically compacted clay samples. The effluent pressure at the outflow end of the permeameter was essentially at atmospheric pressure for all tests and, therefore, the effective stress at the effluent interface between the soil sample and the porous stone should have been greater than zero in all cases. The reference hydraulic conductivity value, k_w, was obtained using de-aired tap water as recommended by Chapuis *et al.* (1989), Daniel (1994) and ASTM D2434 and D5084. Yet, one has to keep in mind that the use of de-aired water may result in the artificial inducement of anaerobic conditions within the test specimen and influence the effects, if any, of chemical reactions (e.g., oxidation-reduction) on the hydraulic conductivity (Shackelford, 1994).

Hydraulic conductivity defines the capacity of a porous medium to conduct a particular fluid, and is a function of both the medium and the fluid. Permeability (ASTM, 1985), also known as the intrinsic or absolute permeability, expresses the capacity of flow in terms of the properties of the porous medium only. The intrinsic permeability (K, in square

meters) and the coefficient of hydraulic conductivity (k, in meters per second) are related by the following equation:

$$K = k \mu / \gamma \quad\dotfill (3.1)$$

in which μ = absolute or dynamic viscosity of the permeant liquid (Pa.s), and γ = unit weight of the permeant liquid (N.m^{-3}). In this investigation, the form of Darcy's law used to calculate the hydraulic conductivity value, k, is as follows:

$$k = q/(A.i) \quad\dotfill (3.2)$$

where q = rate of flow (m^3.s^{-1}), A = cross-sectional area of specimen perpendicular to direction of flow (m^2), and i = hydraulic gradient (dimensionless) = $\Delta H / L$ with ΔH = head loss across specimen (m) and L = length of specimen (m).

Based on the adopted approach of a constant-head test employed in the present research, the head loss was kept constant and the corresponding rate of flow was measured. Using the previously described computer automated data acquisition system (cf. Subsection 3.2.1.1), the measured flow rates were recorded to the nearest 1 mm^3 at pre-set time intervals. Plots of hydraulic conductivity as a function of pore volumes of flow (*PVF*) are plotted to illustrate and evaluate the hydraulic conductivity trend of the compacted clay soils permeated with various contaminants. A pore volume of flow (*PVF*) is the cumulative quantity of flow relative to the volume of void space conducting flow in the soil specimen, or:

$$PVF = \frac{qt}{n_e AL} \quad\dotfill (3.3)$$

where t = cumulative time (s), n_e = effective porosity (dimensionless), and other terms as defined before. The effective porosity represents the pore space in the soil available for flow relative to the total volume of the test specimen. An effective porosity might exist, for example, when the soil specimen is characterized by dead-end pore space or as a result of resistance of highly viscous, adsorbed water in tightly packed clay soils (Bear, 1972; Freeze and Cherry, 1979). However, in most cases, the effective porosity is assumed to be equal to

the total porosity, n. In the present research, the total porosity, n, for the *Hydrite Flat-D* and *Hydrite R* were found to be 0.45 and 0.47, respectively.

The permeation of immiscible, non-polar liquids (e.g., heptane of this study) may require excessively large entry pressures to achieve permeation. Large entry pressures correlate to large hydraulic gradients in hydraulic conductivity tests. For example, Foreman and Daniel (1986) found that the entry pressure for permeating water saturated kaolin with non-polar heptane to be greater than 324 kPa (47 psi) for flexible-wall tests, corresponding to hydraulic gradients of more than 300. For similar tests in compaction-mold permeameters, Foreman and Daniel (1986) found that the heptane would enter the water saturated kaolin at an entry pressure of only 55 kPa (8 psi), or a hydraulic gradient of 50. The difference was attributed to a few relatively larger pores in the compaction-mold permeameter relative to the flexible-wall permeameter, presumably due to the absence of confinement in the rigid-wall permeameter.

Fernandez and Quigley (1985) describe constant-flow hydraulic conductivity tests in which two pore volumes of hydrophobic organic compounds (benzene, xylene, and cyclohexane) were forced through saturated compacted natural soils over a period of 4.2 days. The flow rates resulted in induced hydraulic gradients of about 500, apparently due to the high entry pressures of the non-polar organics. Acar and Seals (1984) report that benzene could not be permeated through a water saturated Ca-montmorillonite at a hydraulic gradient of 150.

Based on the above discussion, an entry pressure of 115 kPa for permeating the compacted water-saturated kaolin of this research with non-polar heptane seems to be justified. An entry pressure of 115 kPa for heptane corresponds to a hydraulic gradient of about 578. The entry pressure of heptane was the major factor for selecting a specific hydraulic gradient throughout the leaching tests, as investigating the influence of different hydraulic gradients on the test results for rigid-wall permeameters was beyond the objectives

of the present study. A hydraulic gradient of about 578 was maintained for all hydraulic conductivity measurements, corresponding to pressure gradients ranging from 115 kPa, in the case of heptane, to 220 kPa, for 5M NaCl solution, depending on the density of the different permeants (cf. Table 3.4). For tap water, a pressure of 170 kPa was necessary to uphold the hydraulic gradient at 578. Even though ASTM D5084 recommends limits on hydraulic gradient for testing low-hydraulic-conductivity soil, allowances for higher hydraulic gradients may have to be made for compatibility testing involving chemicals or leachate, where a minimum number of pore volumes of flow are required and where the only practical way of achieving this in a realistic time is to use elevated hydraulic gradients (Daniel, 1994).

3.2.4.3 Termination Criteria

After saturation, the sample was permeated with tap water to establish the reference value of hydraulic conductivity to water. The termination criteria proposed by Peirce and Witter (1986) for this initial step of the compatibility test procedure seem to be acceptable. They suggest that clay permeability tests be continued until: (1) at least one pore volume of permeant is passed through the clay specimen; and (2) the slope of hydraulic conductivity versus the number of cumulative pore volumes does not differ significantly from zero. Bowders (1988) noted that the termination criteria proposed by Peirce and Witter (1986) were sound when the permeant is water, but suggested that the criteria are unacceptable in terms of compatibility tests because the criteria account only for hydraulic conductivity equilibrium, not chemical equilibrium.

Bowders *et al.* (1986) suggest that compatibility tests should continue until: (1) at least two pore volumes of flow (*PVF*) are achieved to ensure that the original soil-water in the test specimen is replaced by the leachate; and (2) the effluent concentration ratio (i.e., the effluent concentration, c, of each principal chemical species relative to the influent concentration, c_0, of the same chemical species) approaches unity when c_0 is maintained constant. However, in his discussion on Peirce and Witter's (1986) paper, Bowders (1988) presented data which indicated that a significant increase (17X) in the hydraulic conductivity

of a compacted specimen of kaolin clay to acetic acid occurred suddenly and only after more than six PVF. In addition, the hydraulic conductivity had stabilized essentially after six PVF. The test was performed in a rigid-wall "Proctor" mold permeameter. There was no mention though of the flow direction. Based on this example, both criteria proposed by Peirce and Witter (1986), as well as the criterion proposed by Bowders *et al.* (1986) requiring the passage of a minimum of two PVF, would not have been adequate.

Bowders (1988) suggested that a number of chemical parameters, besides the relative effluent concentration of principal solutes, could be monitored, such as the pH of acid solutions and the total organic carbon (TOC) content of organic liquids. However, TOC is not always a reliable indicator of the potential impacts of organic liquids since two organic liquids with the same TOC can have different impacts depending on the composition of the organic liquids (Shackelford, 1994).

Based on these considerations, the criteria proposed by Peirce and Witter (1986) seem to be reasonable for the initial stage of the compatibility test procedure, i.e., establishing the reference value of hydraulic conductivity to water, k_w. However, with respect to the second stage of the leaching test procedure involving the use of a different permeant than water and the measurement of the final hydraulic conductivity value after permeation with the waste liquid, k_p, a criterion based on an arbitrary minimum number of PVF does not appear suitable. Therefore, the primary criterion for termination of compatibility tests should be the establishment of chemical equilibrium between the effluent and influent ends of the test. The establishment of hydraulic conductivity equilibrium for k_p should be considered only after the chemical equilibrium criterion has been achieved (Shackelford, 1994).

For the tests of this research, the permeant solutions were only introduced after fulfilling the requirements suggested by Peirce and Witter (1986) regarding the establishment of k_w. A minimum of 10 PVF of de-aired tap water was allowed to percolate through the clay specimen to establish a reference value for the hydraulic conductivity before permeating the

same specimen with the contaminant liquid to determine the change in hydraulic conductivity. The primary criterion for termination of the leaching tests of the present study, however, was the establishment of chemical equilibrium between the effluent and the influent of the test. The establishment of hydraulic conductivity equilibrium for k_p was only considered after the chemical equilibrium criterion has been achieved. Moreover, seven pore volumes of contaminant liquid (7 PVF), at least, were leached through the compacted clay soils before terminating the test.

3.2.5 Leaching Analysis

Aqueous liquids contain inorganic chemicals (acids, bases, salts) and/or hydrophilic organic compounds. Hydrophilic organic compounds are distinguished from hydrophobic organic compounds based on the concept of "like dissolves like," i.e., polar organic compounds usually will readily dissolve in water, a polar molecule; whereas non-polar organic compounds are repelled by water. A hydrophobic compound also is further separated into either a LNAPL (Light Non-Aqueous Phase Liquid) or DNAPL (Dense Non-Aqueous Phase Liquid) based on whether the density of the compound is lower or greater than water, respectively.

The concentration and type of solutes in the pore fluid play an important role in determining the fabric of soil, and consequently its hydraulic conductivity (cf. Table 2.2). In addition, available evidence indicates that only pure organic solvents significantly alter soil hydraulic conductivity (e.g., Acar *et al.*, 1985a; Fernandez and Quigley, 1985, 1988; Foreman and Daniel, 1986; Bowders and Daniel, 1987; Acar and Olivieri, 1989). The significance of the density and viscosity of the liquid already has been mentioned in terms of Eq. 2.16, as well as in the migration of DNAPLs and LNAPLs. This particular point was further discussed in the previous chapter (cf. Fig. 2.11).

Two parameters which always should be measured are the electrical conductivity (EC) and the pH. Both of these parameters are relatively easy to measure using electrodes and provide fairly reproducible results. However, in the case of pH, care should be taken to measure the effluent pH soon after the leachate sample is recovered because release of aqueous phase carbon dioxide, $CO_{2(aq)}$, into the atmosphere will result in a continual increase in the measured pH with time. Shackelford (1994) reported data which illustrate the influence of delay in measurement of pH and EC on a backpressure saturated specimen of compacted kaolin permeated in a flexible-wall permeameter with 0.01M NaCl solution. These results demonstrate that the "delayed" pH values are consistently higher than the "immediate" pH values (measured within minutes after collection), despite the fact that the samples which were analyzed for pH and EC at a later date (i.e., delayed) were carefully preserved in "air-tight" containers. However, the EC measurements are very similar regardless of the elapsed time before measurement. Therefore, in order to measure an accurate pH of the pore liquid in the test specimen, the pH of the effluent sample should be measured as rapidly as possible after collection. Otherwise, elevated pH values should be expected resulting in improper interpretation of the test results, such as in the case of exposure of soils to acidic permeants.

The pH of solutions ranges from 0 to 14. Solutions which are highly reactive with soils include strong acids (pH ≤ 2) and strong bases (pH ≥ 12). Neutral solutions are characterized by pH values between about 5 and 9. The pH of a solution not only characterizes chemical reactions (e.g., dissolution/precipitation) which are important in terms of soil hydraulic conductivity, but also can affect significantly soil fabric.

The EC of a solution is a measure of the ability of the solution to carry an electrical current, and varies directly with the number and type of ions in solution. As a result, the electrical conductivity is an indirect indication of the strength of the solution, and is particularly useful for indicating the relative strength of a solution when detailed characterization of the concentration and types of chemical constituents is not possible.

Moreover, EC provides an indirect measure of the potential for an electrolyte solution to affect the fabric of a clay soil.

Concentrations of the chemical influents are measured before they are permeated through the compacted kaolin soils of the present research and monitored on the effluent end during hydraulic conductivity testing. The main purpose of these measurements is to obtain the source loading and breakthrough curves. Those curves illustrate how relative concentrations of chemicals in the influent and effluent ends vary with time or pore volumes of flow, *PVF*.

Typically, the breakthrough curve would not be stepped like the source loading function due to chemical diffusion and mechanical dispersion as shown in Fig. 2.17. A zone of mixing between the baseline fluid and chemical permeant is inevitably created due to the hydrodynamic dispersion effect. As a result, some chemicals leave the soil column in advance of the advective front (Fig. 2.17). Chemical analysis of the effluent is also expected to reveal other reactions taking place between the soil and permeants, such as cation exchange, acid-base and sorption reactions. Different measurement approaches, however, are adopted for the distinct permeants of the current study.

i. *Sodium Chloride*

For electrolytes, a certain relationship exists between the concentration of inorganic salt solutions, like sodium chloride, and their electrical conductivity (EC). Standard salt solutions of known concentrations were first prepared and their corresponding EC was measured using the conductivity meter CDM 83 of the Environmental Engineering laboratory. The concentrations are plotted versus EC values to create a standard curve as shown in Fig. 3.5. The main advantages of this method are its simplicity and relative ease of measurement.

Electrical conductivity of the collected leachate at different *PVF* is also measured to monitor the breakthrough of the chemical permeant. The results, however, give only the total
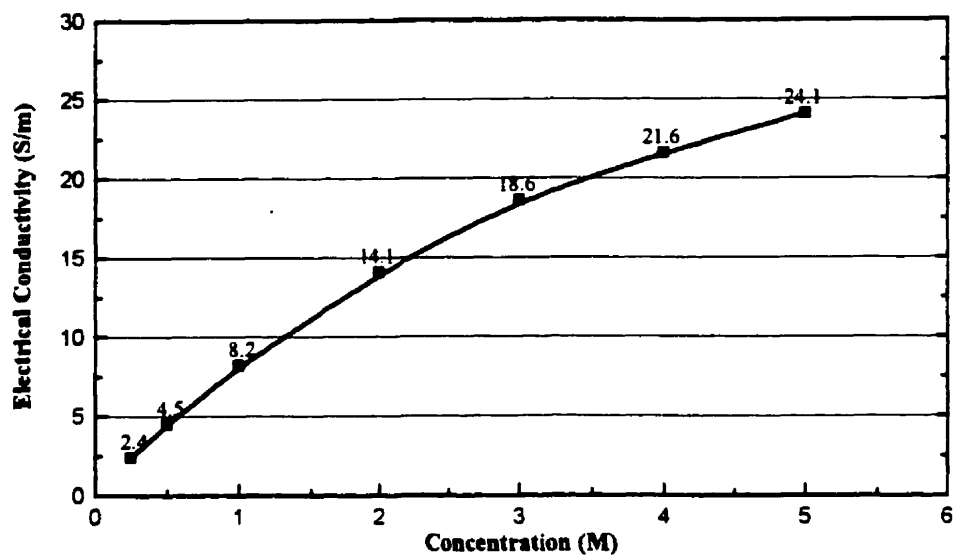
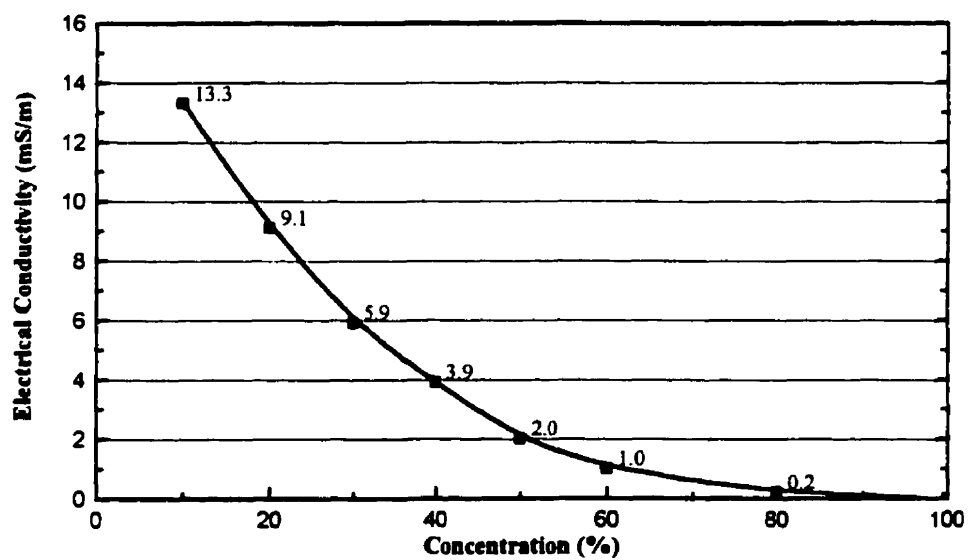Figure 3.5 Electrical conductivity of NaCl solutions.

Figure 3.6 Electrical conductivity of Ethanol solutions.

concentration of all ions. Further advanced measurements are necessary to determine the specific concentration of certain ions. In this investigation, the ion analyzer of the Environmental Engineering laboratory was employed to determine chloride concentrations (Cl⁻) of the 5M NaCl leaching test. The analyzer consists of an Accumet model 825MP, from Fisher Scientific, and a halide electrode from Orion Research Inc. The readings were recorded in millivolts and then, based on standard curves, converted to Cl^- concentrations in ppm $(ppm=mg/L=g/m^3)$.

ii. *Hydrochloric Acid and Sodium Hydroxide*

Acid and base solutions permeated through a soil sample attack the clay particles by virtue of their extremely high and low concentration of hydrogen ions, respectively. Monitoring the pH of the effluent is a must for the tests conducted using acid and base permeants. The pH of the collected leachate was measured by a pH meter within minutes after collection to avert the detrimental effect of time on pH measurements. The pH meter Accumet 10 of Fisher Scientific, equipped with a polymer body gel-filled electrode, was used for all pH measurements of this study. The results are presented by plotting the pH values versus the *PVF* of the respective permeant.

In addition to the pH measurements, the inorganic acid and base leachates of the present research were monitored during the tests by measuring their electrical conductivity. The results of the relative EC between the inflow and outflow are plotted against the pore volumes of flow.

iii. *Acetic Acid and Aniline*

The previously described pH meter is used to monitor the breakthrough of the organic acid and base selected for this investigation. The obtained pH values are plotted for each pore volume of flow to indicate the establishment of chemical equilibrium.

Furthermore, the establishment of chemical equilibrium between the effluent and the influent of the test was cross-checked by determining the total organic carbon (TOC) content of the effluent. A more sophisticated analysis using a TOC analyzer from Dohrmann-Rosemount, USA, was conducted to determine the total organic carbon content of the effluent . The DC-190 TOC analyzer uses the combustion tube method to analyze the leachate. TOC contents are gauged by the device infrared gas analyzer, which has a capacity up to 2500 ppm. The variation of the relative concentrations of TOC in the influent and effluent ends with pore volumes of flow, PVF, are reported in plots of the obtained results.

iv. Ethanol (Ethyl Alcohol)

Because of the high polarity and nearly complete ionization of alcohols, standard curves as the one shown in Fig. 3.6 could be generated. The electrical conductivity of the different prepared concentrations was measured using the same conductivity meter mentioned earlier. The breakthrough of ethanol during the leaching tests was also monitored by measuring EC of the collected leachate at different PVF. Those measurements are reported relative to the electrical conductivity of reference tap water, which varies around 320 mS/m, to indicate the establishment of chemical equilibrium between the effluent and the influent of the test.

The establishment of chemical equilibrium was further verified by the measurement of TOC in the leachate. The same procedure that are used to monitor the effluent of acetic acid and aniline is employed for monitoring TOC concentration of ethanol leachate.

v. Heptane

Heptane is characterized by an extremely low solubility in water as a result of its non-polar properties. Volume measurements of chemical and water were performed by introducing the effluent into a titration burette after every $1.0\ PVF$. The contact face between heptane and water permits calculation of their respective volumes. The relative accumulated volume of heptane, V_p / V, is calculated by the following equation:

$$\frac{V_p}{V} = \frac{V_p}{V_p + V_{water}} \qquad \qquad \qquad \qquad \qquad (3.4)$$

where V_p = volume reading of heptane, V_{water} = volume reading of water, and V = total volume reading of heptane and water. The results are plotted versus the pore volumes of flow.

Similar to the other organic compounds of this research, the breakthrough curve of heptane and the establishment of chemical equilibrium between the effluent and influent ends of the test were double-checked by the determination of TOC. The total organic carbon content of the leachate was determined using the above described TOC analyzer. The relative TOC concentrations between the influent and effluent are presented in plots versus *PVF*.

3.3 Soaking Tests

The main purpose of conducting the soaking tests is to investigate the compatibility of compacted kaolin clays with organic contaminants and its impact on the fabric under pure diffusion conditions. Diffusion may be thought of as a transport process in which a chemical or chemical species migrates in response to a gradient in its concentration, although the actual driving force for diffusive transport is the gradient in chemical potential of the solute (Robinson and Stokes, 1959).

Both *Hydrite Flat-D* and *Hydrite R* kaolin clays are used as the testing soils to carry out the soaking tests of the present research. Acetic acid, aniline, ethanol, and heptane are the selected organics in which the soils were soaked. The properties of those contaminants are listed in Table 3.4.

3.3.1 Test Equipment

The test equipment of the soaking test consists of a rigid-wall cell. The rigid-wall cell is made from high-molecular weight polyethylene (HMWPE); a non-corrosive, non-reactive material capable of resisting the attack of the selected organic contaminants. The valves, fittings and tubing of the cells are all made from Teflon® for the very same reason. The height of the cells used for the soaking tests measures 75 mm whereas their internal diameter measures 76.2 mm (3 in).

3.3.2 Sample Preparation

The preparation of clay samples for the soaking tests involves preparing the soil for compaction at its optimum moisture content or slightly wet of optimum (i.e., optimum + 1%). Tap water is used as the standard fluid for compaction. The same procedures used to prepare the test samples for leaching tests were duplicated for the soil samples of the soaking tests (cf. Section 3.2.2).

3.3.3 Static Compaction

The same hydraulic jack that was used to compact the samples of the leaching tests is employed to perform the static compaction of kaolin clays for the soaking tests. The soil was compacted in its soaking cell following the same protocol for the compaction of leaching test samples (cf. Section 3.2.3).

After the completion of compaction, the 30-mm thick clay sample in its cell was mounted between the cap and base of the rigid-wall soaking cell. The soaking cell was then assembled by tightening the clamping rods connecting the cap, cell, and base.

3.3.4 Test Procedures

To assess the compatibility of compacted kaolin clays with the selected organic contaminants under pure diffusion, the soil was kept submerged beneath a 20-mm depth of contaminant liquid. A hydraulic gradient is not required for transport of contaminants by diffusion. The concentration of contaminant liquids was periodically refreshed at equal time intervals of 4 weeks each.

The establishment of chemical equilibrium between the fresh contaminant liquid and the 4-weeks-old leachate of the same contaminant was the principal criterion for termination of the soaking tests. The soaking tests of *Hydrite Flat-D* lasted 24 consecutive weeks, while it took the tests with *Hydrite R* almost 8 months (32 weeks) to establish the requirement of chemical equilibrium and terminate the test.

3.3.5 Leaching Analysis

The establishment of chemical equilibrium was confirmed by determining the total organic carbon (TOC) content of the leachate at the predetermined time intervals. The previously described DC-190 TOC analyzer was employed to analyze the 4-weeks-old leachate. The target ratio between TOC of the leachate and that of the fresh contaminant liquid should be close to unity. All soaking tests of this study were terminated only when the target ratio was just about unity.

3.4 Scanning Electron Microscopy

Of the available techniques for soil-fabric study, only the electron microscope can reveal clay particles and their arrangements directly (cf. Fig. A.18). The practical limit of resolution of the transmission electron microscope (TEM) is now less than 10 Å, and atomic planes can be seen. The practical limit of the scanning electron microscope (SEM) is about

100 Å; however, lesser magnification is sufficient to resolve details of clay particles and other very small soil constituents. The major advantages of the SEM relative to the TEM are the very great depth of field (some 300 times greater than that with the light microscope), the wide, continuous range of possible magnifications (about ×20 to ×20,000), and the ability to study surfaces directly. Either surface replicas or ultrathin sections are needed for the TEM.

Many successful scanning electron microscopy observations have been made on different soils to study their micromorphology (Fitzpatrick, 1993). In this instrument, the SEM that is, soil fragments are examined. The beam of high energy electrons hits the surface of the sample causing secondary electrons to be emitted. These can be detected by a secondary electron detector to form an image of the specimen which can be recorded photographically. Conventional SEMs use tungsten filaments as a source of electrons, but field emission increases the brightness by a factor of about 1000 times allowing much finer details to be observed. This is a very popular and useful technique for studying the morphology of a number of features such as clay coatings. It is particularly useful in the study of soluble salts that may be lost in the preparation of thin sections for transmission electron microscopy analysis. A few attempts have been made, however, to examine thin sections of soils with the SEM, but generally these have not been very successful because of the flat polished surface of the specimens. Nevertheless, the application of SEM to microfabric observation on compacted clays is challenging due to the complicated, and sometimes tedious, specimen preparation procedures and SEM operations.

3.4.1 Sample Preparation

Sample preparation techniques differ according to the purpose of a particular study. The "best" method of sample preparation should be selected after consideration of scale of the fabric features of interest, method of observation to be used, and the soil type and state as regards water content, disturbance, strength, etc. With these factors in mind, the probable effects of the different preparation methods on the fabric can be assessed. For this

investigation, the adopted procedures are thought to most suite the research objectives. Sectioning, pore fluid removal, and preparation of surfaces for study constitute the main procedures preceding the analysis of the kaolinite specimen by SEM to examine the influence of contaminant migration on the clay structure.

Sectioning of the soil sample is conducted in a manner to study as few surfaces as possible, yet reflecting the structure of the whole sample. The various sections obtained at the end of the preparation procedures are shown in Fig. 3.7. Specimens representing the cross-section surface at three different levels, the influent, middle, and effluent, are examined. Another three specimens at different radii from the center enable studying the fabric of the plan surface. Ordinary trimming equipment, such as a wire saw, a sharp edge knife, etc., are used to carry out the sectioning operation; however, a certain degree of art and finesse is needed to obtain relatively undisturbed samples.

Electron microscopy requires that the pore fluid be removed, replaced, or frozen. To accomplish this without disturbance of the original fabric is difficult, and in most cases there is no way to determine how much disturbance there may have been. Air drying, as a technique for pore fluid removal, may be suitable for very stiff soils and other soils that do not undergo significant shrinkage. For soft samples at high water content, oven drying may cause less fabric change than air drying, evidently because the longer time required for air drying allows for greater particle rearrangement (Tovey and Wong, 1973; Smart and Tovey, 1982). On the other hand, the stresses induced during oven drying may result in some particle breakage (Mitchell, 1993).

Water removal by critical-point drying has also been used. The high temperature and pressure involved in this technique, however, may change the arrangement of clay particles. To avoid this, replacement by carbon dioxide has been suggested. Still, the procedure requires prior impregnation of the sample with acetone which may alter the soil structure (Smart and Tovey, 1982). Pore fluid replacement may be necessary, though, where thin sections are
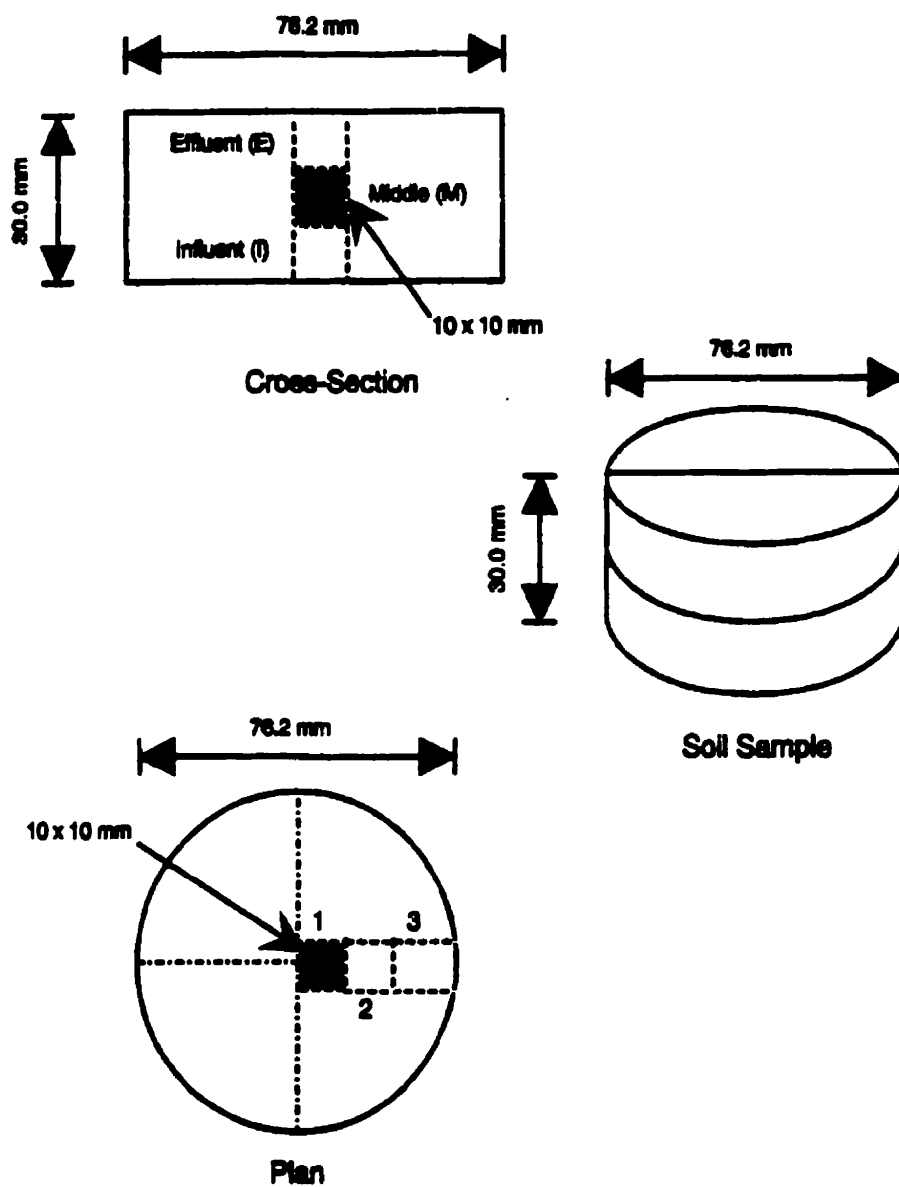
Figure 3.7 Sectioning of the soil sample for scanning electron microscopy.

required or where drying shrinkage must be minimized, but the presence of a material in pore spaces is not objectionable. Various resins and plastics have been used for this purpose.

Freeze-drying is a commonly used technique for removal of pore water. Sublimation of the ice in a rapidly frozen soil avoids the problem of air-water interfaces and shrinkage which accompanies water removal by drying. Sample size must be small, though, if disruption due to nonuniform freezing is to be avoided. The quick freezing of the kaolinite sample in this research is performed by direct immersion in liquid nitrogen at $-196°C$. The freezing temperature should be less than $-130°C$ to avoid formation of crystalline ice. At this point, the sample is fractured to expose the surface for examination by the SEM. Sublimation of the ice is accomplished by preserving the sample in a desiccator connected to the vacuum system.

The freezing process has been shown to produce fabric changes in very high water content systems such as a 10 percent by weight slurry of bentonite in water (Mitchell, 1993). However, with more typical saturated clays at consistencies likely to be encountered in geotechnical investigations, the effects of freeze-drying on the fabric are minimal. The freeze-drying-fracture technique adopted in this study appears to be the most suitable of the available alternatives.

The main difficulty in the study of soil structure using SEM is the preparation of a sample surface that retains the undisturbed fabric of the original soil. In general, the higher the water content and void ratio of the original sample, the greater the likelihood of disturbance. The surfaces chosen for study should reflect the original fabric of the soil and not the preparation method. Grinding or cutting air-dried samples, for instance, may result in substantial particle rearrangement at the surface, thus making them of little value for study by the electron microscope. In the current investigation, the fractured surface of frozen wet specimen is considered as representative as possible of the undisturbed fabric of compacted kaolin clays. Additional preparation such as gentle blowing of the surface is needed following

fracture, because there may be loose particles on the surface. The freeze-dried samples are further cut into blocks of approximately 10 mm thick without touching the finished surface.

3.4.2 Scanning Electron Micrographs

Until recently, wet soils could not be studied directly, because electron microscopes require an evacuated sample chamber (1×10^{-5} torr). A newly developed technique, known as "variable pressure" scanning electron microscope (VPSEM), provides the operator with control over the specimen chamber vacuum level and environment. Technically, any specimen may be inserted directly into the VPSEM and observed in its natural state. Properly controlled chamber vacuum pressure allows high resolution imaging of wet, oily, or nonconductive type specimens without the need for tedious specimen preparation techniques. The variable pressure mode of the VPSEM is expected to greatly expand the application limits of the conventional SEM.

In this research, however, a conventional SEM model JEOL JSM-840 of the Centre for Microscopic Characterization of Materials (CM)² at École Polytechnique is used to examine the impact of contaminant migration on the structure of compacted kaolinite. Because of the requirement of an evacuated sample chamber, wet soils cannot be studied directly with this type of microscope. Cold stages are available, however, so that frozen materials may be examined. It is also necessary for that model to coat the sample surface of interest with a conducting film to prevent surface charging and loss of resolution. Gold placed as a very thin layer (20-30 nm) in a vacuum evaporator is usually used to provide that coat. Before coating, the specimen is fixed on a metallic stub by means of a conducting graphite paint. This paint assures sufficient electrical conductivity between the stub and specimen.

After the coating operation, the specimen on its metallic stub is placed on the sample block of the SEM and attached to it using an electrical tape to ensure a certain electrical conductance between the sample seat and the specimen stub. The sample seat, with the coated

specimen on top, is then inserted into the sample chamber of the SEM. At this point, the specimen is ready to be examined by SEM.

A series of calibration and adjustment is necessary before getting a high resolution image of the investigated surface. Once a clear image is obtained, the surface is scrutinized before being recorded photographically. During the present study, many scanning electron micrographs of the *Hydrite Flat-D* and *Hydrite R* were recorded at normalized magnifications. The normalized magnification enables the detection of substantial changes in clay fabric that may result from contaminant migration. Kaolinite samples micrographs before (as-compacted) and after permeation with the different contaminants are examined and compared to correlate the structure changes, if any, with the variation in hydraulic conductivity.

3.5 Contaminant Transport Modeling

Modeling the movement of contaminants through soil is a complex type of analysis. The contaminant transport process is not only governed by water movement, but also is influenced by dispersion, molecular diffusion, adsorption, and radioactive decay, if any. With so many factors involved, it can be confusing and difficult to resolve the contribution of each component in the transport process.

CTRAN/W is a finite element software that can be used to model the movement of contaminants through porous materials such as soil. The comprehensive formulation of the software makes it possible to analyze problems varying from simple particle tracking in response to the movement of water, up to complex processes involving diffusion, dispersion, adsorption, and radioactive decay. Even though a finite difference method (FDM) analysis would have been sufficient in studying the one-dimensional transport problem of this research, exploiting the capacity and examining the validity of a finite element method (FEM) analysis were the main driving forces behind opting for CTRAN/W.

CTRAN/W is integrated with SEEP/W, another software product from Geo-Slope Int'l. Ltd. of Alberta, Canada, that computes the flow velocity for a problem. CTRAN/W utilizes the SEEP/W flow velocities to compute the movement of dissolved constituents in the pore-water. CTRAN/W version 4.2 which was used to simulate the contaminant migration through the compacted kaolin clays of this research operates under the MS-Windows graphical user interface.

3.5.1 Contaminant Migration Processes

The factors which govern the migration of a contaminant can be considered in terms of *transport* processes and *attenuation* processes. The transport processes can be mathematically represented by equations based on flow laws. These equations can be combined into a mass balance equation with those processes causing the attenuation of the contaminant; this yields the general governing differential equation for contaminant migration.

3.5.1.1 Transport Processes

The two basic transport processes are *advection* and *dispersion*. Advection is the movement of contaminant with the flowing water. Dispersion is the apparent mixing and spreading of the contaminant within the flow system. While the advection process is simply migration in response to the flowing water, the dispersion process consists of two components. One is an apparent "mixing" and the other is *molecular diffusion*.

The mixing component, often called *mechanical dispersion*, arises from velocity variations in the porous media. Velocity variations may occur at the microscopic level due to the friction between the soil particles and the fluid, and also due to the curvatures in the flow path (cf. Fig. 2.12). These velocity variations result in concentration variations. When the concentration variations are averaged over a given volume, the contaminant appears to have dispersed.

Molecular diffusion results in the spreading of contaminant due to concentration gradients. This process occurs even when the seepage velocity is zero. Molecular diffusion is dependent on the degree of saturation or volumetric water content of the porous medium.

In equation form, the dispersion process is characterized as:

$$D_h = D^* + \alpha \ v_s \qquad (3.5)$$

where D_h = coefficient of hydrodynamic dispersion ($m^2.s^{-1}$), D^* = coefficient of molecular diffusion ($m^2.s^{-1}$), α = dispersivity of the porous medium (m), and v_s = seepage or average linear velocity of the flow system ($m.s^{-1}$).

The diffusion coefficients for electrolytes in aqueous solutions are well known. The major ions in groundwater (Na^+, K^+, Ca^{2+}, Mg^{2+}, Cl^-) have diffusion coefficients in the range 1×10^{-9} to 2×10^{-9} m^2/s at 25°C (Robinson and Stokes, 1959). The coefficients are temperature-dependent. At 5°C, for example, the coefficients are about 50 % smaller. Moreover, the effect of ionic strength is negligible.

In porous media, the apparent diffusion coefficients for these ions are much smaller than in water because the ions follow longer paths of diffusion caused by the presence of particles in the solid matrix and because of adsorption on the particles. The apparent diffusion coefficient for nonadsorbed species in porous media D^* is represented by the relation:

$$D^* = \omega \ D_0 \qquad (3.6)$$

where D_o = aqueous solution diffusion coefficient ($m^2.s^{-1}$), and ω, which is less than 1, is an empirical dimensionless coefficient that takes into account the effect of the solid phase of the porous medium on diffusion. In laboratory studies on diffusion of nonadsorbed ions in porous geologic materials, ω values between about 0.5 and 0.01 are commonly observed (Freeze and Cherry, 1979). In this research, ω is assumed to have a value ranging between 0.05 and 0.025, resulting in a coefficient of molecular diffusion D^* of about 5×10^{-11} m^2/s. This value is

considered a representative value of a typical molecular diffusion coefficient for nonreactive chemical species in clayey geologic deposits.

Nearly all studies of dispersion reported in the literature have involved relatively homogeneous sandy materials under controlled conditions in the laboratory. These studies have indicated that the dispersivity of these materials is small. Dispersivity values reported from laboratory measurements are commonly found to range between 0.1 and 10 mm. Whether or not these values are at all indicative of dispersivities in field systems is subject to considerable controversy at the present time. Many investigators have concluded that values of longitudinal and transverse dispersivities in field systems are significantly larger than values obtained in laboratory experiments on homogeneous materials or on materials with simple heterogeneities. Values of longitudinal dispersivity α_L as large as 100 m and lateral dispersivity α_T values as large as 50 m have been used in mathematical simulation studies of the migration of large contaminant plumes in sandy aquifers (Freeze and Cherry, 1979).

Based on the above considerations, a transverse dispersivity value of 10 mm for the kaolin clays of this research seems to be justifiable. The ratio between the longitudinal (α_L) and transverse (α_T) dispersivity values are typically in the range of 5-20 (Freeze and Cherry, 1979). Therefore, the longitudinal dispersivity α_L of the soils analyzed by finite element method to model the contaminant migration through compacted clays was taken as 50 mm.

3.5.1.2 Attenuation Processes

The migration of a contaminant in a porous medium is attenuated by chemical reactions taking place during the migration process. These reactions can occur between the contaminant mass and the soil particles, or between the contaminant mass and the pore fluid. Among these reactions, the process of *adsorption* is believed to be the most important factor in attenuating the migration of contaminant.

The effect of adsorption is that contaminant mass is withdrawn from the moving water, reducing the dissolved concentration and rate of movement. The amount of adsorption that occurs is a function of the contaminant concentration within the porous medium. This relationship is described by an adsorption function or an adsorption isotherm, as illustrated qualitatively in Fig. 2.14.

The slope of the adsorption isotherm $\partial S/\partial c$ is the partition coefficient, where S is the mass of contaminant adsorbed per unit mass of soil particles, and c is the concentration of contaminant in the porous medium. In the case of a linear adsorption isotherm, the partition coefficient is constant and is called the distribution coefficient, K_d. The slope represents the partitioning of the contaminant mass between the solid (soil particles) and fluid phases of the porous medium. The chemical reactions that cause the partitioning are assumed to be instantaneous and reversible.

For equilibrium controlled ion exchange, where the concentration of one exchange ion is relatively low, the adsorption of this species can often be approximated by a linear relationship between the contaminant adsorbed and the concentration in the pore fluid (Rowe and Booker, 1985). For the contaminant migration modeling of the current study, and whenever adsorption was taken into account, a linear adsorption function defined as a straight line with a slope of 1.0 was considered to be representative of all geochemical reactions taking place during the migration process. The linear relationship is a simplification of the real situation; however, this approach can be shown to be adequate for many practical applications, provided that the parameter K_d is determined over a representative range of concentrations (Rowe and Booker, 1985). The use of this linear approximation is analogous to the use of secant elastic moduli in settlement predictions.

3.5.2 Governing Equation

Consideration of the above transport and attenuation processes, and the application of the principle of mass balance in an element of porous medium leads to the following *advection-dispersion equation* (in one-dimensional form):

$$\theta \, D_h \frac{\partial^2 c}{\partial x^2} - v \frac{\partial c}{\partial x} = \left(\theta + \rho_d \frac{\partial S}{\partial c} \right) \frac{\partial c}{\partial t} \qquad\qquad (3.7)$$

where θ = volumetric water content (dimensionless), x = distance in the x direction (m), v = Darcian or discharge velocity ($m.s^{-1}$), ρ_d = bulk or dry mass density of the porous medium ($g.m^{-3}$), t = time (s), and other terms as previously defined.

The first term in the equation represents transport by dispersion, while the second represents transport by advection. The term on the right side of the equation represents storage of mass in the fluid phase and in the solid phase due to a change in concentration.

3.5.2.1 Flow Velocity

SEEP/W version 4.2 was used to compute the Darcian or discharge velocity. The Darcian velocity is the total flux Q divided by the full cross-sectional area A (voids and solids alike). However, the actual cross-sectional area available for flow is less than the full area A due to the presence of solids. Consequently, the actual rate of flow is higher than the Darcian velocity.

By definition, the porosity n is the volume of voids divided by the total volume. Therefore, the actual cross-sectional area available for flow is the porosity times the total cross-sectional area, and the seepage or average linear velocity of the pore fluid would be:

$$v_s = \frac{Q}{nA} = \frac{v}{n} \qquad\qquad (3.8)$$

where all terms as defined before. The volume of water per unit volume of the porous material is the volumetric water content θ. Under saturated conditions, as is the case for the present simulation, the volumetric water content θ is equal to the porosity. The seepage velocity then is also equal to:

$$v_s = \frac{v}{\theta} \quad\quad\quad (3.9)$$

CTRAN/W is formulated on the assumption that the seepage velocity can be related to the volumetric water content for both saturated and unsaturated conditions. SEEP/W, being a saturated/unsaturated flow model, computes the volumetric water content. The SEEP/W Darcian or discharge velocity divided by the SEEP/W volumetric water content is taken in the CTRAN/W formulation as the seepage or average linear velocity.

3.5.2.2 Mass Flux

SEEP/W has the ability to compute the seepage quantity that flows across a user-defined section. This quantity can be computed from the nodal heads and the coefficients of the finite element equation.

From Darcy's law, the total flow between two points is:

$$Q = k\,A\frac{\Delta H}{L} = c\,\Delta H \quad\quad\quad (3.10)$$

The coefficient c in Eq. 3.10 is a representation of the term $(k\,A\ \ L)$, with all other terms being defined elsewhere. The flow from node i to node j is therefore:

$$Q_{ij} = c_{ij}\left(H_i - H_j\right) \qu\quad\quad (3.11)$$

CTRAN/W can also compute the total mass flux across a user-specified section. The mass flux across a section is composed of four components; the dispersive mass flux, the advective mass flux, the stored mass flux, and the decayed mass flux, if any. The total mass

flux Q across a section is the sum of all four components, as represented by the following equation:

$$Q = Q_{dis} + Q_{adv} + Q_{sto} + Q_{dec} \qquad \dots\dots\dots\dots\dots\dots\dots\dots\dots\dots\dots\dots \quad (3.12)$$

i. *Dispersive Mass Flux*

The dispersive mass flux is computed in the same way as SEEP/W computes the water flux across a section. For an element in the finite element mesh, the dispersive mass flux from node i to node j is:

$$\left(Q_{dis}\right)_{ij} = d_{ij}\, c_i - d_{ji}\, c_j \qquad \dots\dots\dots\dots\dots\dots\dots\dots\dots\dots\dots \quad (3.13)$$

The d coefficients in the above equation are a representation of the dispersive properties of the element, and c is the concentration.

ii. *Advective Mass Flux*

For an element in the finite element mesh, the advective mass flux from node i to node j is:

$$\left(Q_{adv}\right)_{ij} = a_{ij}\, c_i - a_{ji}\, c_j \qquad \dots\dots\dots\dots\dots\dots\dots\dots\dots\dots\dots \quad (3.14)$$

The a coefficients in the above equation are a representation of the advective properties of the element, and c is the concentration.

iii. *Stored Mass Flux*

In general, the average change of concentration from node i to node j can be expressed as:

$$\Delta c_{ij} = \frac{\Delta c_i + \Delta c_j}{2} \qquad \dots\dots\dots\dots\dots\dots\dots\dots\dots\dots\dots\dots\dots\dots \quad (3.15)$$

Therefore, the stored mass flux from node i to node j due to a change in storage is:

$$\left(Q_{sto}\right)_{ij} = s_{ij} \frac{\Delta c_{ij}}{\Delta t} \quad \dots \dots \dots \dots \dots \dots \dots \dots \dots \dots \dots \dots \dots \dots \dots \quad (3.16)$$

The s coefficient in the above equation is a representation of the storage properties of the element, and Δt is the time difference between the start and end of a time step.

3.5.3 Modeling Progression

CTRAN/W is a powerful analytical tool, but it will only provide valid solutions if the boundary conditions, material properties, and time sequence are appropriately defined. A rule of thumb to follow in contaminant transport modeling is to progress from the simple to the complex. It is a good practice to define a simplified version of the problem and then build complexity in stages. Moving from the simple to the complex makes it easier to pinpoint difficulties with the model when the results of the analysis are unrealistic.

3.5.3.1 Numerical Dispersion and Oscillation

Numerical dispersion and oscillation are inherent in the finite element solution of the advection-dispersion equation. Numerical dispersion tends to spread out the contaminant more than what is predicted by analytical solutions. Numerical oscillation produces concentrations higher or lower than the maximum and minimum specified values.

Numerical dispersion and oscillation cannot be eliminated; they can only be controlled or minimized. Two widely used criteria for controlling the phenomena of numerical dispersion and oscillation are the Peclet Number and the Courant Number constraints.

3.5.3.2 Peclet and Courant Number Criteria

The Peclet and Courant Number criteria are usually expressed in the one-dimensional form as follows:

$$Peclet \ Number = \frac{v_s \Delta x}{D_h} \leq 2$$

$$Courant \ Number = \frac{v_s \Delta t}{\Delta x} \leq 1 \qquad \qquad \qquad \qquad \qquad \qquad \qquad \qquad \qquad \text{(3.17)}$$

where v_s = seepage or advective velocity (m.s^{-1}), D_h = hydrodynamic dispersion coefficient (m^2.s^{-1}), Δx = nodal spacing (m), and Δt = incremental time step.

The Peclet Number constraint requires that the spatial discretization of the flow regime is not larger than twice the dispersion potential of the porous medium. The Courant Number constraint requires that the distance traveled by advection during one time step is not larger than one spatial increment (i.e., one element). The Peclet and Courant Number constraints provide the necessary conditions for the finite element mesh design and the selection of time steps in transport modeling.

3.5.3.3 Mesh Design

In order to obtain stable solutions in a transport analysis, both the Peclet Number and Courant Number criteria must be considered in the design of the finite element mesh. Rearranging Eq. 3.17, the spatial discretization requirements would be:

1. $\Delta x \leq 2 \dfrac{D_h}{v_s}$;

2. $\Delta y \leq 2 \dfrac{D_h}{v_s}$;

3. $\Delta x \geq v_s \Delta t$; and

4. $\Delta y \geq v_s \Delta t$

The above requirements indicate that the spatial discretization of the flow regime should not be larger than twice the dispersion potential of the porous medium, and should not also be smaller than the distance traveled by advection during one time step.

As a broad rule, the discretization in the major flow direction should be about twice the longitudinal dispersivity α_L of the soil, and the discretization in the minor flow direction should be about twice the transverse dispersivity α_T of the soil. This will provide a starting point for estimating the required spatial discretization.

A 25-element mesh was designed to simulate the contaminant migration through the compacted kaolin clays of this study, as shown in Fig. 3.8. The soil sample measures 76 mm in the x-direction and 30 mm in the y-direction, with an upward flow movement. A pattern of four-noded quadrilateral elements with one node at each corner and a thickness of 60 mm was selected as the finite element pattern for the soil cross-section. At the end of each simulation of the current research, the actual Peclet and Courant Numbers computed by CTRAN/W were checked to confirm that both the Peclet and Courant Number criteria are satisfied.

3.5.3.4 Time Step Design

Numerical dispersion and oscillation are affected by the size of the time step. To control the numerical dispersion and oscillation, the Courant Number constraint must be satisfied. The Courant Number constraint requires that the distance traveled by the advective component of the transport process during one time step ideally should not be larger than one element; that is, the advective component should not jump across elements in one time step.

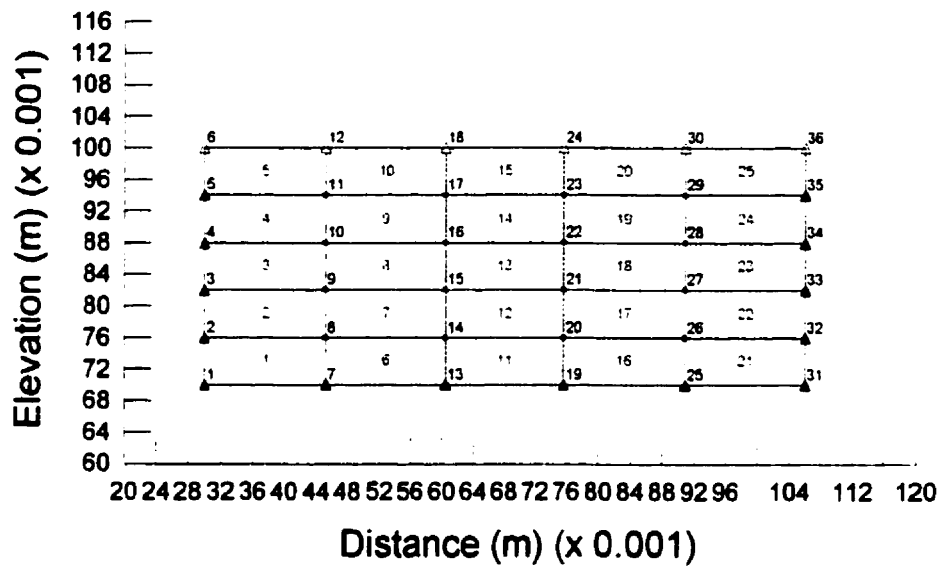In order to satisfy the Courant Number constraint (cf. Eq. 3.17), the time increment should be:

Figure 3.8 Finite element mesh of contaminant transport modeling.

$$\Delta t \leq \frac{\Delta x}{v_s}; \text{ and } \Delta t \leq \frac{\Delta y}{v_s}$$

As a first approximation, the time step increment could be estimated based on the average size of the elements and the advective velocity.

The design of time steps to analyze the transport of contaminants by finite element method for this study was conceived based on the above Courant Number criterion. The Courant Numbers computed by CTRAN/W were checked at the end of each analysis to confirm that the Courant Number constraint is satisfied in all time steps.

3.5.3.5 Boundary Conditions

When specifying boundary conditions in a contaminant transport analysis, it is important to recognize that there are two processes by which mass is carried across a boundary: one is by advection and the other is by dispersion. The advective component is due to the water movement across a boundary, while the dispersive process is due to the chemical (concentration) gradients between the boundary nodes and the nodes immediately inside the boundary.

The advective component of the boundary mass flux is related to the water flux (Q_w) across the boundary. This information is obtained from the SEEP/W analysis. CTEAN/W uses the nodal Q_w values from the SEEP/W head (H) file to compute the advective boundary flux. A clear understanding of the boundary water flux is essential in the specification of boundary conditions and the interpretation of computed results.

In the SEEP/W simulation of this analysis, the influent and effluent boundaries were specified as total head or H boundaries with a magnitude of 17.4 m and 0.10 m, respectively, acting at the boundary nodes. The vertical boundaries of the finite element mesh were set as

zero total nodal mass flux boundaries (no-mass flux condition), or $Q_w = 0$ in the SEEP/W analysis and $Q_m = 0$ for the CTRAN/W modeling, as shown in Fig. 3.8.

Source Concentration

Whenever the concentration of the contaminated fluid is known, the boundary condition can be specified as C_S (the concentration of the source) type. For the C_S boundary condition type, CTRAN/W uses the concentration of the source to compute a nodal mass flux at the boundary. The mass flux is calculated as:

$$Q_m = Q_w * C_S \dotfill (3.18)$$

where Q_m = total nodal mass flux, Q_w = nodal water flux from SEEP/W, and C_S = specified concentration of the source.

Specifying a C_S boundary at the nodes is different than specifying a concentration boundary C equal to C_S. Setting a node to C_S implies that the computed nodal concentration will be less than C_S during the early stage of the transport process. After some time, the computed concentration will become equal to C_S. On the other hand, if the boundary condition is specified as a value C equal to C_S, the computed nodal concentration would be equal to C_S immediately. In other words, specifying C_S at a boundary is actually equivalent to defining a mass flux type boundary, whereas setting C equal to C_S means specifying a concentration type boundary.

In the contaminant transport modeling of this study, a C_S boundary type was specified at the influent nodes. Using C_S as a boundary condition is a more realistic option than simply specifying concentration at the nodes. In addition, it has the advantage of not creating excessive initial concentration gradients as does the concentration specification. The gradual build-up of concentration at the nodes tends to reduce numerical difficulties that may arise from excessively-high concentration gradients.

Exit Condition

At a boundary where neither the mass flux nor the concentration are known, or where the nodal water flux may reverse in direction during the transport process, an exit review boundary may be specified. When a boundary node is specified with exit review, the node is checked to see if an exit boundary should be applied at each time step. If the water flux of the node is negative (i.e., water flux is exiting at the boundary), the boundary condition of the node will be changed to an exit boundary. If the water flux of the node is zero or positive, the boundary condition of the node is not changed.

CTRAN/W offers two types of exit boundaries. The first and simplest option is one that ignores the dispersive flux across the exit boundary ($Q_d = 0$), and is often referred to as a zero dispersive mass flux exit boundary. With this type of exit boundary, contaminant mass is assumed to leave the exit boundary by advection only. As a result, the concentration gradients at the boundary are forced to be zero, which causes the concentration contours to be perpendicular to the exit boundary. The second type of exit boundary condition accounts for both advective and dispersive mass flux at the boundary ($Q_d > 0$), and is referred to as a free exit boundary. A free exit boundary accounts for both advective and dispersive mass flux across the boundary, which generally gives more realistic results.

Since neither the mass flux nor the concentration are known at the exit boundary of the present simulation, the boundary is specified as $Q_m = 0$ conditions with review for free exit boundary ($Q_d > 0$), as shown in Fig. 3.8.

CHAPTER 4

RESULTS AND DISCUSSIONS

Chapter 4 presents the results obtained throughout this research using the materials and methods described in the previous chapter. The chapter also discusses the significance of those results through its four divisions. Compaction characteristics, leaching test results, soaking test results, and contaminant transport simulation constitute the four divisions of the chapter.

4.1 Compaction Characteristics

Compaction is a dispersing process by which large shear strains are induced in clay soils resulting in the dominance of deformed and smaller interdomain pores. Interestingly, minimum value of hydraulic conductivity could not be achieved in clays compacted at their optimum water content, even though the dry density is at its maximum and, thus, the void ratio is at its minimum. Instead, it appears that soils compacted wet of optimum have the minimum value of hydraulic conductivity. Numerous studies have revealed this phenomenon (e.g., Lambe, 1954, 1958b; Mitchell *et al.*, 1965). Compacting at the optimum water content does not guarantee minimum hydraulic conductivity of compacted clay, although a minimum void ratio can be obtained. Mitchell *et al.* (1965) reported that hydraulic conductivity values of clay soil compacted at optimum water content were 150 times higher than the minimum values obtained with soil compacted wet of optimum. This phenomenon has not been investigated in detail due to lack of direct observations of the compacted clay microfabric. On the basis of SEM investigations, this behavior can be explained by examining the microfabric and pore characteristics of the soil. The well-stacked aggregates of the clay compacted at optimum water content are certainly responsible for the higher hydraulic conductivity. Because of the high resistance of aggregates to compaction stress, relatively large pores still exist after compaction. These pores formed between the aggregates serve as preferred passages for fluid during permeation. The maximum dry density at optimum water content

is achieved by the densely stacked matrix while the aggregated portion of the soil keeps the compacted clay relatively porous. Microfabric plays a more important role than compacted dry density in controlling the hydraulic property of a compacted clay.

A microfabric model proposed to describe the hydraulic behavior of a compacted clay is presented in chapter 2 (cf. Division 2.2). The structure of a compacted clay is a function of both compactive effort and molding water content. Hydraulic conductivity of a compacted clay is controlled by its pore characteristics including void ratio and pore size distribution. Under a given compactive effort, clay samples compacted dry of optimum are composed of as-mixed aggregates. The aggregates are constructed by randomly arranged clay particles in edge-to-face contacts, making the aggregates resistant to deformation. Relatively weak repulsive forces caused by the poorly developed diffuse double layer around clay particles are responsible for the flocculated structure due to low molding water content and low degree of saturation. Comparatively high values of hydraulic conductivity can be measured in clay compacted dry of optimum due to the existence of large inter-aggregate pores. Increase in moisture content will result in an increase in repulsive forces between clay particles and thus a decrease in the rigidity of the as-mixed aggregates. The deformation of the aggregates caused by compactive shear strain reduces both void ratio and large inter-aggregate pores, leading to a decrease in hydraulic conductivity.

When clay is compacted at optimum water content, or slightly wet of optimum (i.e., optimum + 1%) as in this research, its microfabric is composed of both dispersed matrix and flocculated aggregates due to nonuniform distribution of water content. The matrix is characterized by densely stacked clay particles in face-to-face contacts; whereas aggregates are formed by stepped face-to-face and edge-to-face arrangements of clay particles. The maximum dry density of the clay compacted at optimum water content is achieved by dense stacking of clay particles in the matrix. However, a minimum hydraulic conductivity cannot be reached simultaneously due to the existence of large pores resulting from the high

resistance of aggregates to compactive stress, even though an overall minimum void ratio is attained in the clay.

Dispersed structure occurs in clay samples compacted wet of optimum due to the relative dominance of repulsive forces between clay particles as a result of the increased molding water content. Only few of as-mixed aggregates exist due to large shear strains induced by the compaction process. The microfabric of clay compacted wet of optimum is characterized by face-to-face and edge-to-edge arrangements of clay particles preferentially aligned in the direction perpendicular to the compactive stress. Minimum hydraulic conductivity is obtained in a clay with dispersed structure when compacted wet of optimum water content. Increase in water content on the wet side of the optimum will make compacted clay more permeable by increasing its void ratio while retaining a dispersed structure.

The standard compaction curves of the kaolinites of this study are shown in Fig. 3.2. The optimum water content and maximum dry density are reported in Table 3.1. When the clay is compacted dry of optimum, the degree of saturation is sensitive to molding water content. When molding water content exceeds optimum, however, the degree of saturation is slightly above 90% regardless of the moisture content. Such value can be taken as the maximum degree of saturation the soil can obtain naturally. Soaking after compaction increases water content of samples, but does not change their structure (Seed and Chan, 1959).

SEM micrographs of *Hydrite Flat-D* and *Hydrite R* statically compacted are presented in Figs. 4.1 and 4.2, respectively. Three samples of each kaolin clay were examined by SEM following the procedures outlined in the previous chapter (cf. Division 3.4). As predicted by engineering properties (Lambe, 1954, 1958a, 1958b; Seed and Chan, 1959; Mitchell *et al.*, 1965) and inferred from pore size distribution studies (Diamond, 1970, 1971; Sridharan *et al.*, 1971; Ahmed *et al.*, 1974; Garcia-Bengochea *et al.*, 1979) kaolinite samples compacted at optimum water content show a more complex structure compared with soils compacted dry-
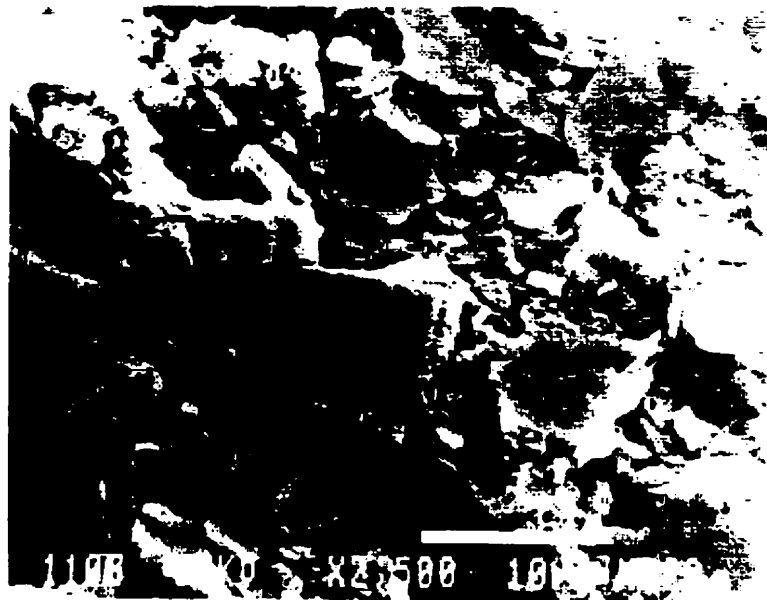
(a) cross-section: influent (bottom)

(b) cross-section: effluent (top)

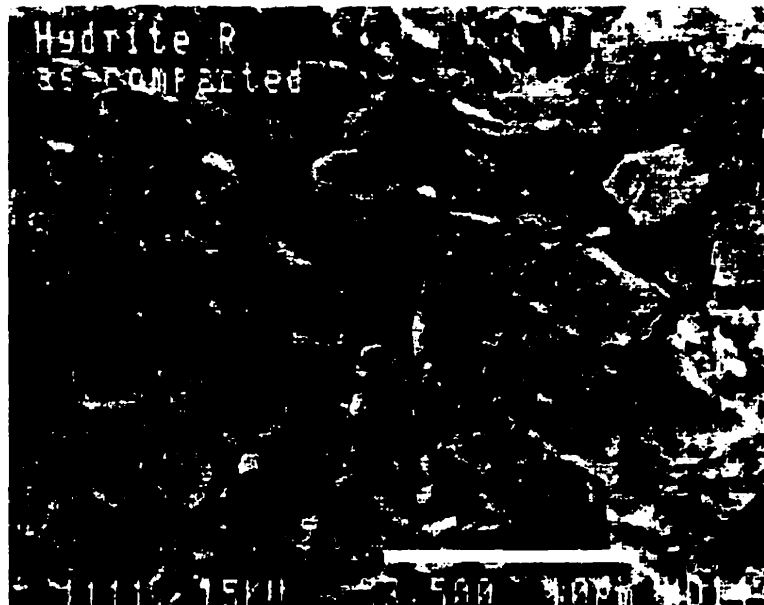Figure 4.1 Scanning electron micrographs of compacted Hydrite Flat-D.
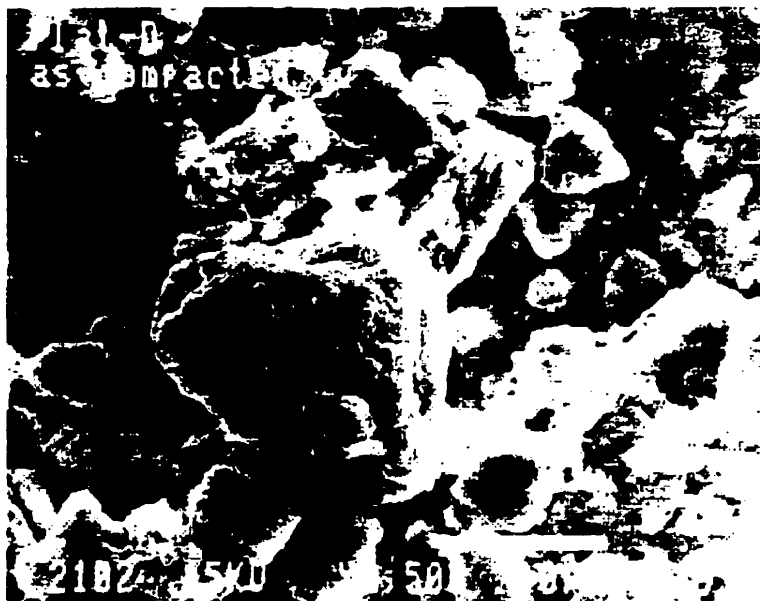
(c) plan: core

(d) plan: edge

Figure 4.1 Scanning electron micrographs of compacted
Hydrite Flat-D [continued].

(a) cross-section: influent (bottom)

(b) cross-section: effluent (top)

Figure 4.2 Scanning electron micrographs of compacted Hydrite R.

(c) plan: core

(d) plan: edge
Figure 4.2 Scanning electron micrographs of compacted
Hydrite R [continued].

or wet-of-optimum. Clays compacted dry of optimum exhibit flocculated structures; whereas those compacted wet of optimum demonstrate dispersed fabric.

The microfabric of both kaolin clays is composed of a dispersed matrix and flocculated aggregates as shown in Figs. 4.1 and 4.2. Single domains in the matrix seem to be much more sensitive to compactive effort, as indicated by a very dense stacking and perfectly oriented alignment. This dispersed arrangement of domains is called turbostratic structure (Barden, 1972). However, aggregates retain their arrangement in a much more porous stacking as shown in the scanning electron micrographs of both *Hydrite Flat-D* and *Hydrite R.* As a result, pore spaces in the soil are distributed nonuniformly with relatively large pores dominating within the flocculated portion of the specimen. The existence of those large inter-aggregate pores is probably caused as a result of friction between the aggregates and matrix, indicating the strong resistance provided by aggregates to compaction.

4.2 Leaching Test Results

Soil-chemical interactions are investigated by permeating compacted kaolinites with several organic and inorganic chemicals. The two soils involved in the research are presented in chapter 3, and the various chemicals are listed in Table 3.4. Leaching tests are performed following the procedures outlined in the previous chapter. The measured hydraulic conductivity k is plotted as a function of pore volumes of flow (PVF). The ratio between the hydraulic conductivity to permeant, k_p, and the reference hydraulic conductivity (hydraulic conductivity to water, k_w) is calculated and presented as a function of pore volumes of flow. The effluent liquid of each test is monitored and analyzed to obtain its particular breakthrough curves. Breakthrough curves are normalized by dividing the effluent measured values by the influent readings, and illustrated as a function of PVF.

To examine the effects of contaminant properties on hydraulic conductivity, the intrinsic permeability of the permeant K_p is computed and reported as a function of pore

volumes of flow. Moreover, K_p values are normalized by dividing by the permeability of water (reference intrinsic permeability, K_w), and the normalized values are plotted against the number of pore volumes of flow. After establishing the termination criteria for every leaching test, contaminated clays were sampled for SEM investigations. The SEM analysis is conducted following the protocol presented in chapter 3.

4.2.1 Organic Compounds

4.2.1.1 Acetic Acid

Leaching test results of compacted kaolinites permeated with acetic acid are presented in Figs. 4.3 through 4.8. Permeation of pure acetic acid resulted in a decrease in the hydraulic conductivity, as shown in Fig. 4.6. The decrease is almost one-half an order of magnitude for both kaolin clays. This decrease cannot be explained solely by differences in the density and viscosity between water and acetic acid as illustrated by Fig. 4.8. Using the properties of acetic acid and water as depicted in Table 3.4, the theoretical hydraulic conductivity ratio of acetic acid to water should be 0.88. Thus, if viscosity is the controlling factor, then the hydraulic conductivity of a soil at a given temperature and void ratio with acetic acid as the permeant will be lower by approximately 12% than that of the same soil with water as the permeant. Therefore, the permeability decreases of Fig. 4.7 indicate that factors other than density and viscosity are controlling the clay soils conductivity.

Four clay soils of different mineralogies were tested for compatibility with a wide variety of organic solvents by Anderson *et al.* (1985a) at Texas A&M University. Compacted samples were tested in a fixed-wall permeameter. In Anderson *et al.* (1985a) acetic acid test with compacted kaolinite, the soil showed continuous conductivity decreases throughout the test period. The main phenomenon observed by the authors was dissolution. According to Anderson *et al.* (1985a), dissolution resulted in smaller particles. As particles were transported by the permeant, they clogged the pores downstream, which caused the decrease in conductivity. Bowders and Daniel (1987) also noticed a relatively slight decrease in the
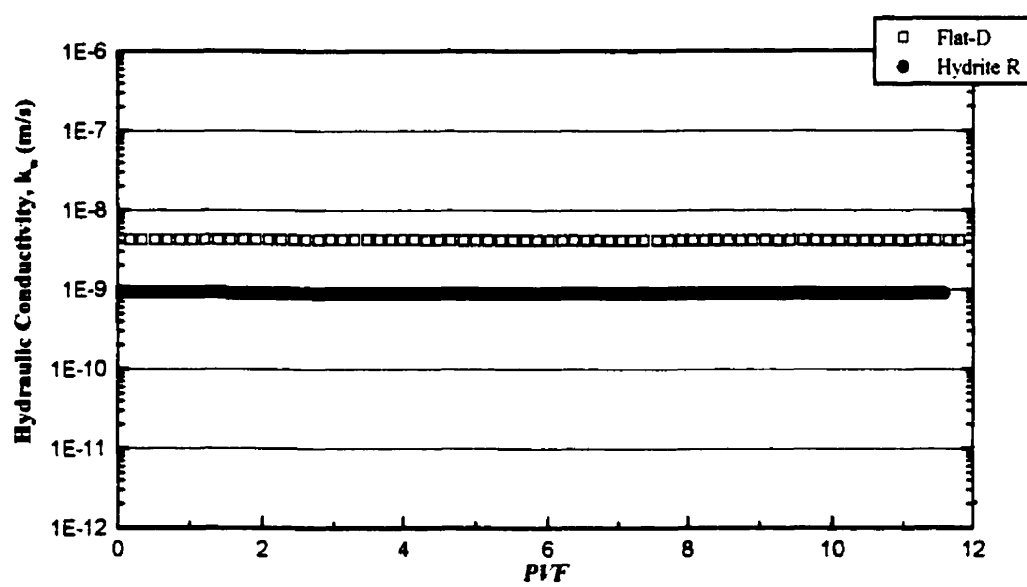
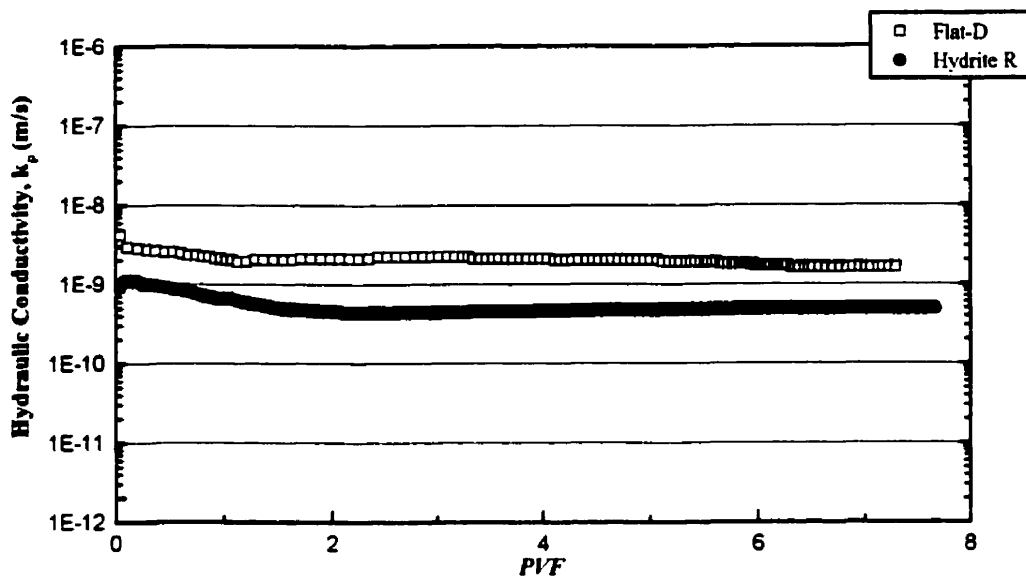Figure 4.3 Reference hydraulic conductivity of compacted kaolinites permeated with Acetic Acid.

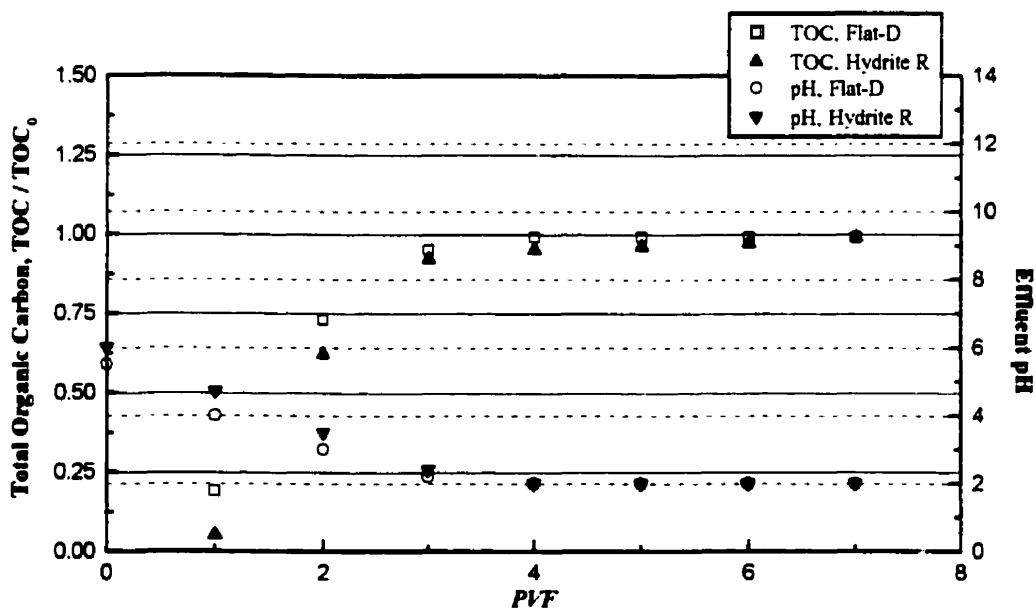Figure 4.4 Hydraulic conductivity of compacted kaolinites permeated with Acetic Acid.

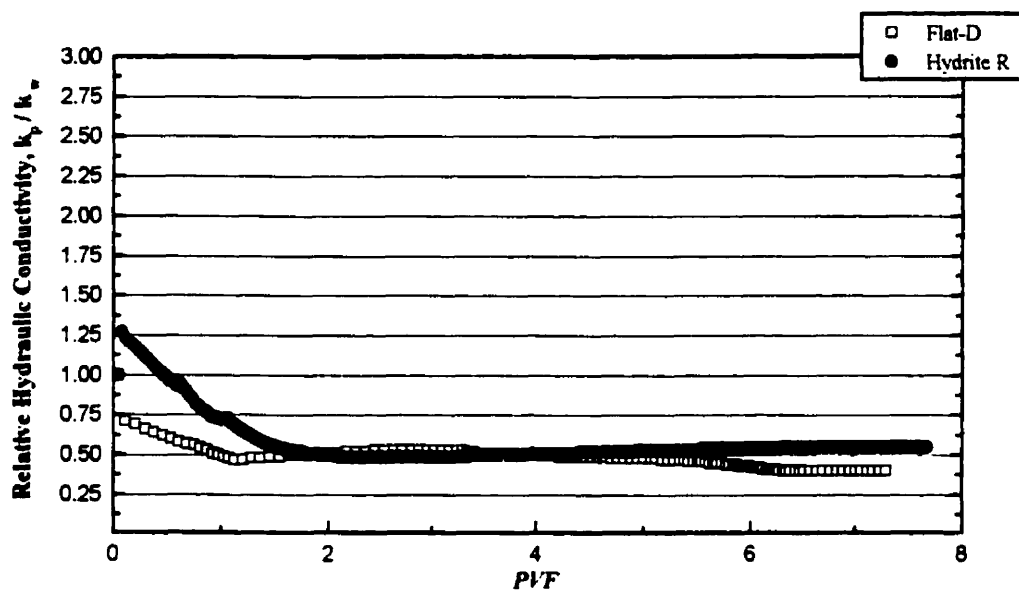Figure 4.5 Breakthrough curves of compacted kaolinites permeated with Acetic Acid.

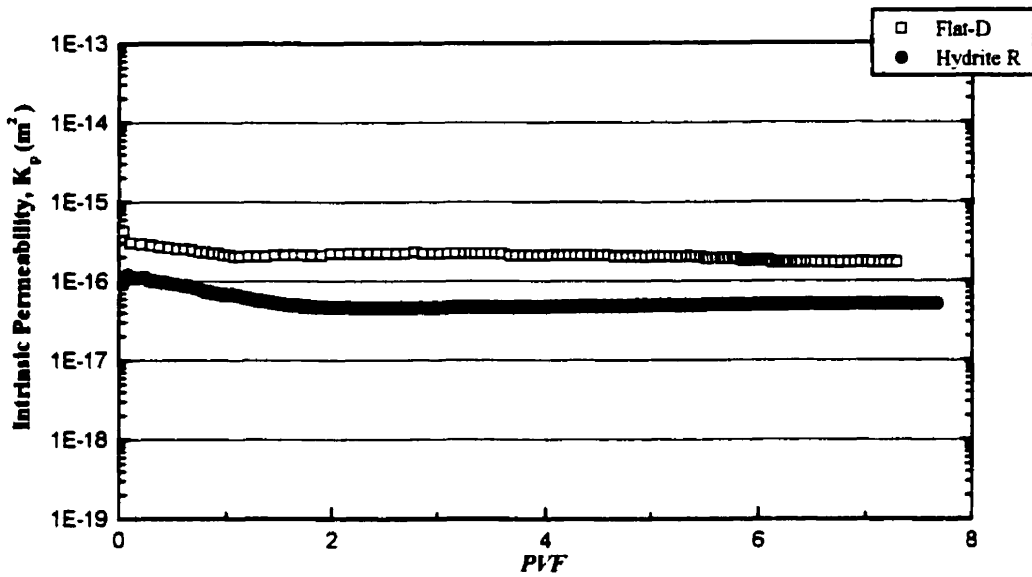Figure 4.6 Relative hydraulic conductivity of compacted kaolinites permeated with Acetic Acid.

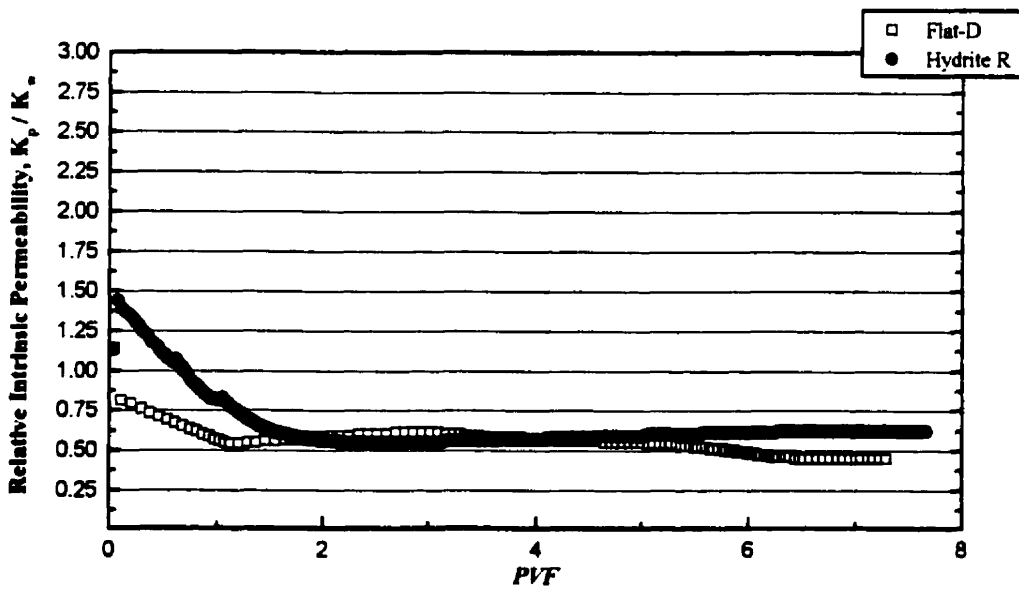Figure 4.7 Intrinsic permeability of compacted kaolinites
permeated with Acetic Acid.

Figure 4.8 Relative intrinsic permeability of compacted kaolinites
permeated with Acetic Acid.

hydraulic conductivity of compacted kaolinite permeated with different concentrations of acetic acid. The decrease was less than one-half an order of magnitude.

It is believed that the conductivity and permeability decreases of the present study are attributed to dissolution of some of the soil constituents at the influent end of the specimen followed by precipitation of these constituents further downstream. The precipitates clogged the soil pores and effectively reduced the hydraulic conductivity. The high volume of flow (>$7PVF$) seems to be not enough for exhausting the buffering capacity of the clay and re-dissolving the precipitates, despite the full breakthrough of acetic acid at 3 PVF as shown in Fig. 4.5. Scanning electron micrographs of both *Hydrite Flat-D* and *Hydrite R*, presented in Figs. 4.9 and 4.10, respectively, support the dissolution-precipitation phenomenon. The fabric of both clays is significantly altered after permeation with pure acetic acid, compared with the as-compacted structure of kaolinites shown in Figs. 4.1 and 4.2. The predominant factor affecting conductivity in this case appears to be the ability of acetic acid to alter the structural arrangement of soil particles.

4.2.1.2 Aniline

Hydraulic conductivity and intrinsic permeability to water for both kaolinites are presented in Figs. 4.11 and 4.12, respectively. The values shown in these figures are considered as representative values of the reference hydraulic conductivity and intrinsic permeability of the compacted kaolin clays used in the present research.

According to theory, a permeant liquid with the density and viscosity of aniline should result in a soil conductivity approximately 76% lower than that obtained with water. However, in this study there was no measurable flow of aniline through the clay samples during an entire 72-hour testing period, as shown in Figs. 4.13 and 4.14. The soil columns were permeated by only 0.5-0.6 pore volume of aniline resulting in a tremendous decrease in hydraulic conductivity, and the hydraulic conductivity measurements of this leaching test were consequently forced to be terminated prematurely. The clays virtually behaved as an

(a) cross-section: effluent

(b) plan: core

Figure 4.9 Scanning electron micrographs of compacted Hydrite Flat-D permeated with Acetic Acid.

(a) cross-section: influent

(b) plan: edge

Figure 4.10 Scanning electron micrographs of compacted
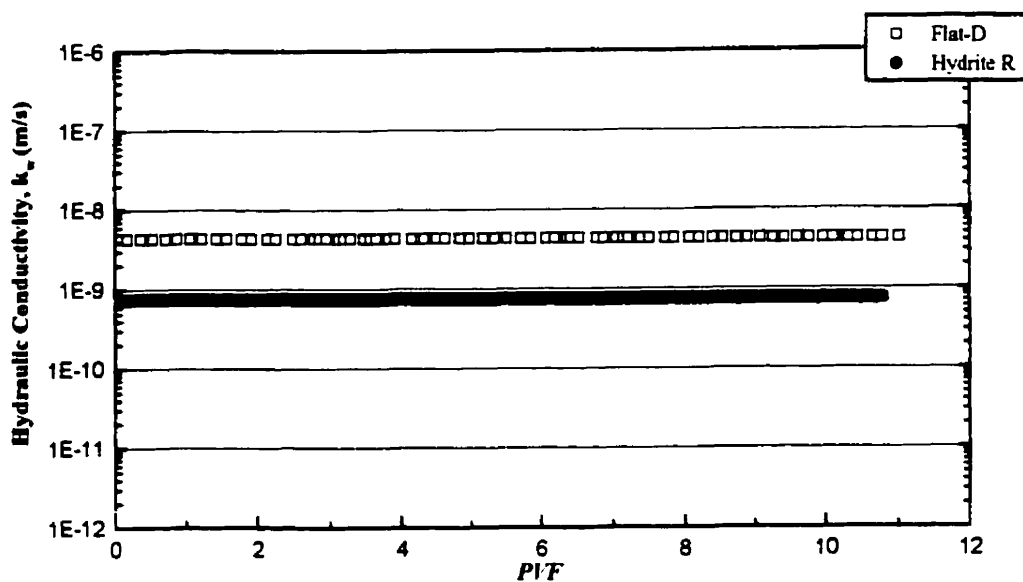Hydrite R permeated with Acetic Acid.

Figure 4.11 Reference hydraulic conductivity of compacted kaolinites permeated with Aniline.
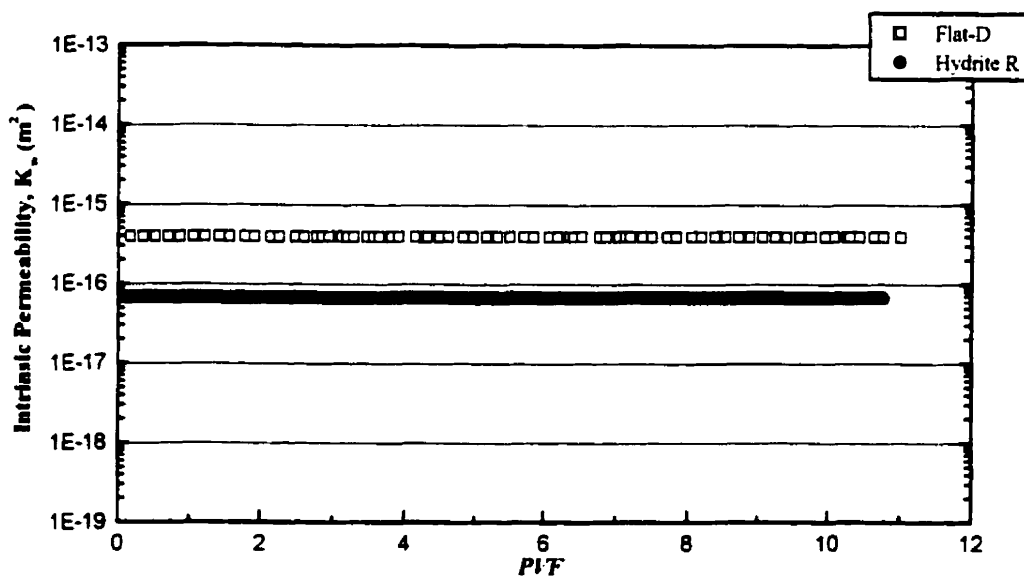

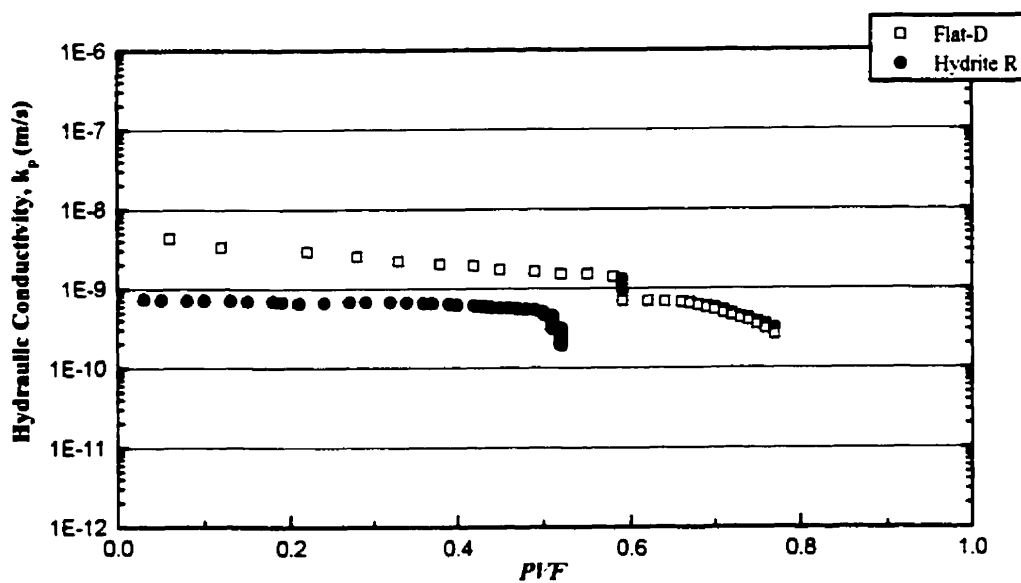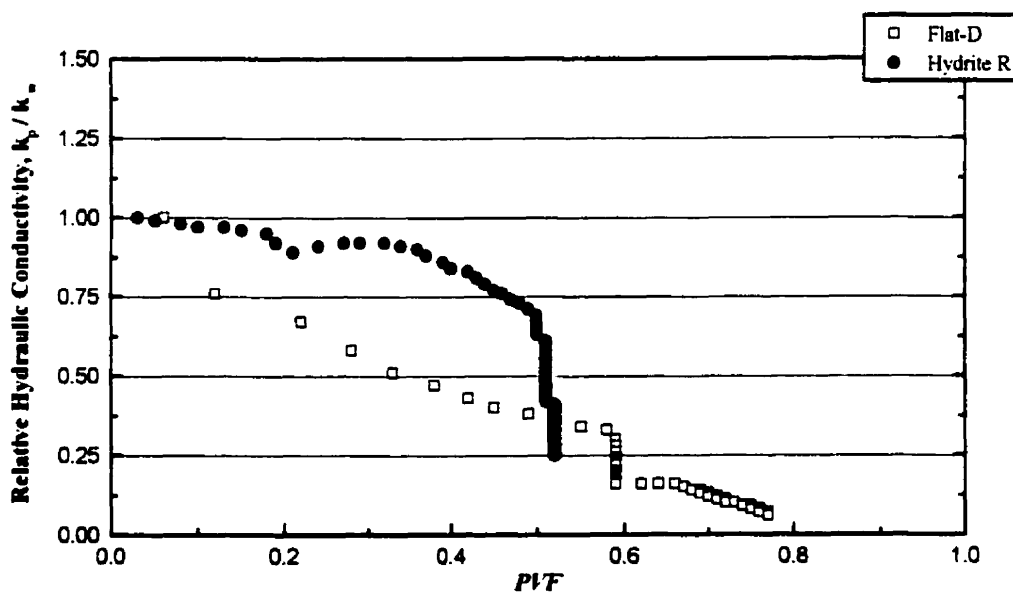Figure 4.12 Reference intrinsic permeability of compacted kaolinites permeated with Aniline.

Figure 4.13 Hydraulic conductivity of compacted kaolinites
permeated with Aniline.

Figure 4.14 Relative hydraulic conductivity of compacted kaolinites
permeated with Aniline.

impervious barrier. In fact, inspection of the samples after the test revealed that aniline did not penetrate the kaolinite samples. Because the flow through the samples was negligible, it is believed that no reaction took place between the permeant and the clay during the test, although aniline, an organic base, is positively charged and is capable of being adsorbed on the negatively charged clay surface, displacing the adsorbed water.

Aniline is more than four times more viscous than water and is of very low solubility in water. A similar mechanism by which heptane, a neutral non-polar hydrocarbon, interacts with clay can be drawn upon to explain the soil behavior with aniline. The hydrophobic nature of aniline, and let alone its significantly high viscosity, makes permeation at the best difficult. In this research, aniline permeated the porous stone, but could not flow (during the time of the test) through the kaolin clays apparently due to their small pore sizes.

Anderson *et al.* (1985a) reported conductivity increases in the various compacted clays of their study ranging between one and two orders of magnitude when subjected to a pure aniline permeant using rigid-wall permeameters. Contrary to their tests with acetic acid, Anderson *et al.* (1985a) observed no signs of migrating soil particles in any leachate samples collected from the aniline-treated soils. According to those authors, aniline is too weak a base to cause significant dissolution of clay soil constituents. The discrepancy between the study of Anderson *et al.* (1985a) and the present research could possibly emanate from the fact that the authors study was conducted on compacted soil specimens without sufficient prior saturation. Their specimens probably were not fully saturated during testing. This would allow aniline to permeate through the air voids within the non-saturated specimen and, possibly, cause chemical reactions, including particle aggregation, to take place. Such flow would not have taken place if the specimen were fully saturated due to the immiscibility of the two permeants. In another investigation by Uppot and Stephenson (1989) to study the change in clay permeability brought about by the soil-chemical interaction, the authors reported that aniline did flow through kaolinite, but at a significantly reduced permeability. The kaolinite clay subjected to pure aniline in a flexible-wall permeameter had a permeability of about 400

times less than the baseline permeability. Aniline did not flow at all through the montmorillonite clay in the study of Uppot and Stephenson (1989). The authors attributed this behavior to the specific properties of aniline, mainly its remarkably high viscosity and low water solubility, compared with water.

4.2.1.3 Ethanol

The relationships between flow and hydraulic conductivity for both kaolinites permeated with ethanol are shown in Figs. 4.15 and 4.16. Only a slight trend toward increase can be observed for the *Hydrite Flat-D* sample following its initial decrease to 62% of the conductivity to water, as illustrated by Fig. 4.18. On the other hand, for *Hydrite R*, there was an initial decrease in hydraulic conductivity to about 50% of the reference hydraulic conductivity by the end of the first pore volume of flow. At the end of the test, however, a reduction of only 42% was reached. Theoretically, the density to viscosity ratio of ethanol relative to water, which equals 0.66, infers that conductivity should decrease approximately 34% from the value obtained with water, presuming that no other factors than density and viscosity are controlling conductivity. Breakthrough curves for the leaching tests with ethanol are presented in Fig. 4.17. Visual inspection of both samples after the test revealed that they had become dehydrated and had lost much of their plasticity.

Ion exchange reactions with inorganic and organic cations in the new permeant, as well as adsorption of organic cations and neutral organic polar molecules in place of previously adsorbed water molecules, will change the thickness and composition of the adsorbed layer. A change in the thickness of the adsorbed layer and its composition in the clay may bring about: (1) a change in the effective pore space causing a variation in hydraulic conductivity; (2) an alteration in the fabric of the clay resulting in a modification in the pore system so that hydraulic conductivity is changed; (3) swelling, which, if confined, will decrease the hydraulic conductivity; (4) shrinking and cracking that will greatly increase the hydraulic conductivity; and (5) a loss in plasticity.
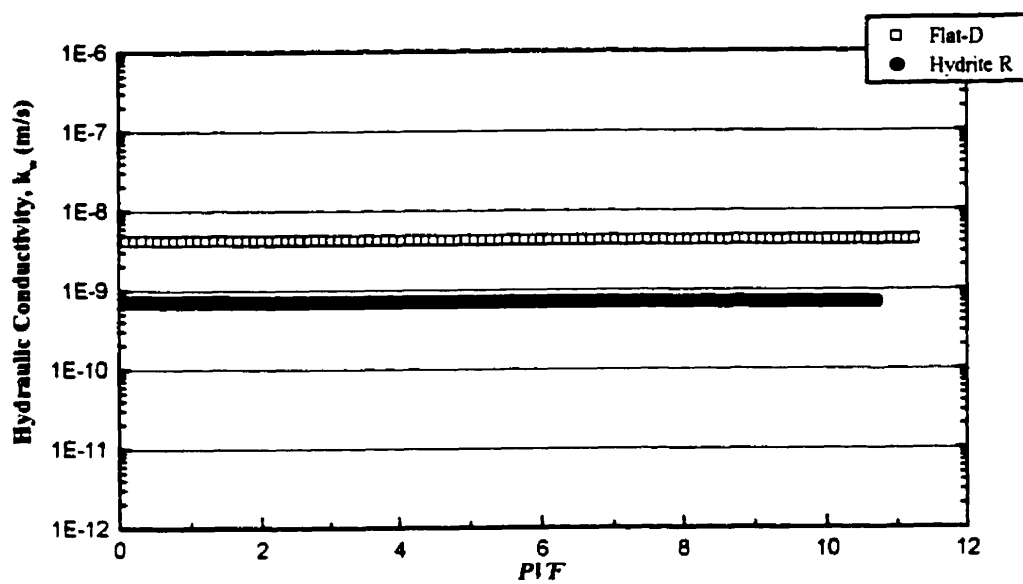
Figure 4.15 Reference hydraulic conductivity of compacted kaolinites permeated with Ethanol.
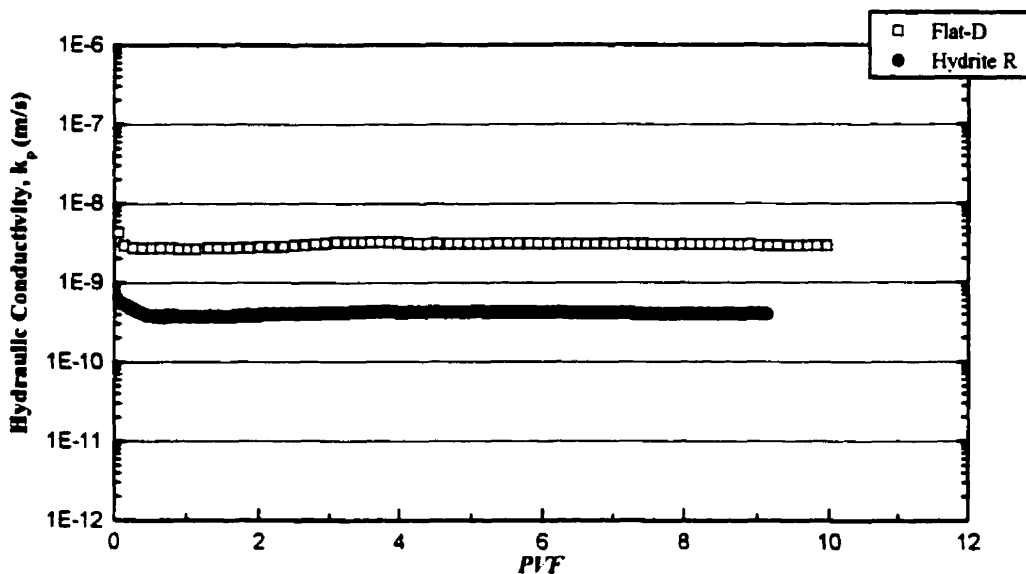
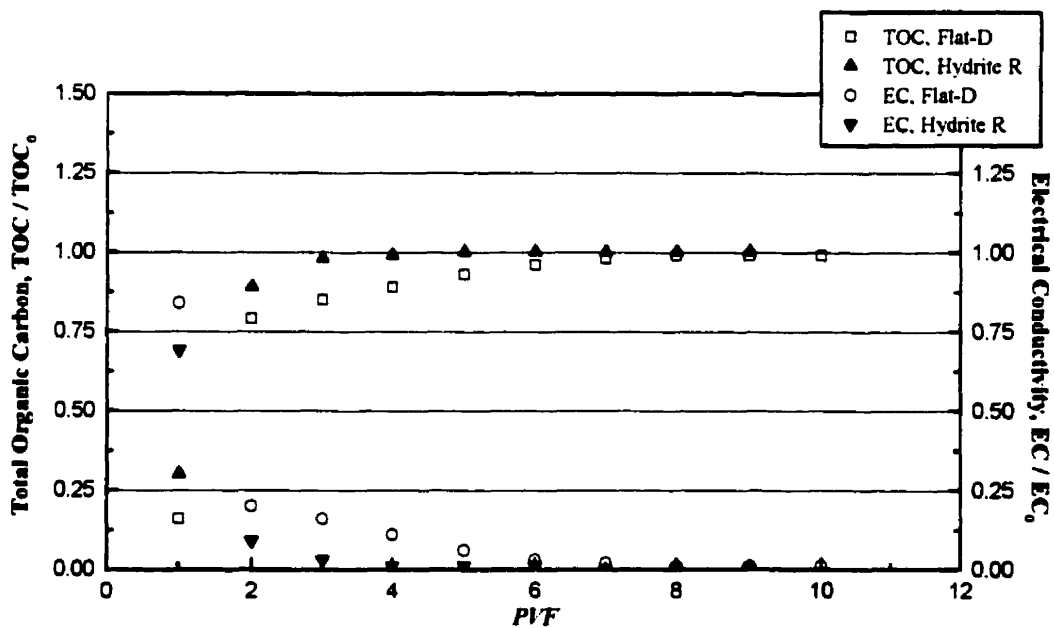Figure 4.16 Hydraulic conductivity of compacted kaolinites
permeated with Ethanol.

Figure 4.17 Breakthrough curves of compacted kaolinites
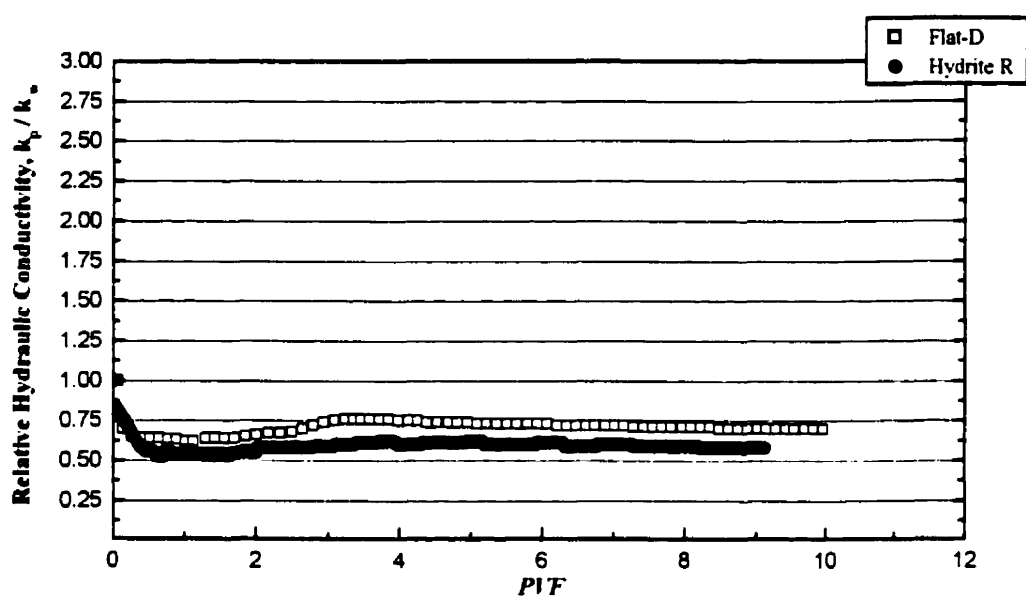permeated with Ethanol.

Figure 4.18 Relative hydraulic conductivity of compacted kaolinites
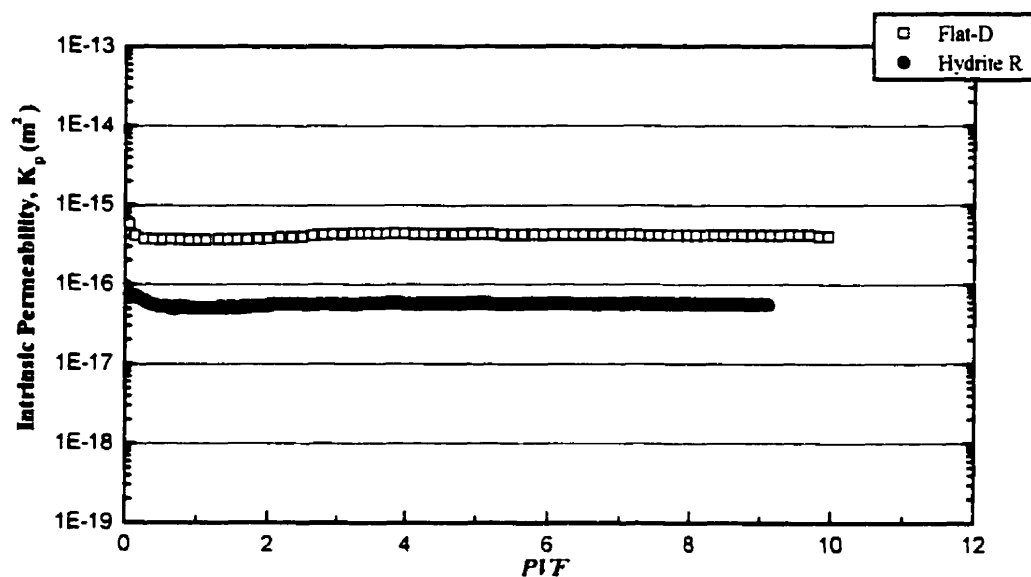permeated with Ethanol.

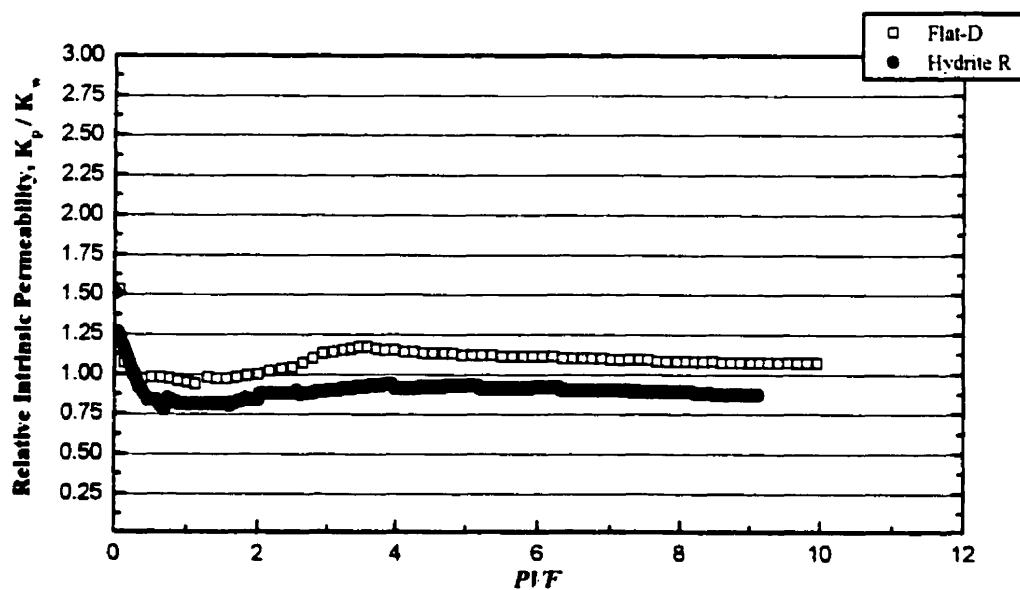Figure 4.19 Intrinsic permeability of compacted kaolinites permeated with Ethanol.

Figure 4.20 Relative intrinsic permeability of compacted kaolinites permeated with Ethanol.

According to Gouy-Chapman theory, the diffuse double layer thickness with ethanol will be smaller than that with water. This change will increase the effective pore space, thus increasing the hydraulic conductivity. The mineralogy, however, of the two clays examined in this study is identical. Kaolinite is a nonexpanding clay mineral with no layer charge. In addition, it has a 1:1 layer structure, and a low cation exchange capacity compared to other clay minerals. Interlayer space of the kaolinite particles cannot be changed. Therefore, the intrusion of ethanol will produce a minor increase, if any, in the effective pore space.

Relative intrinsic permeability of compacted clays permeated with ethanol is presented in Fig. 4.20. The values of K_p K_w for the clays approach unity, indicating that there was no substantial structural rearrangement of soil particles during permeation with ethanol. It is believed that the decrease in permeability for both clays during the first pore volume of flow is caused by the energy spent in replacing water by ethanol in the adsorbed layer. Scanning electron micrographs of the samples taken after leaching, shown in Figs. 4.21 and 4.22, and compared with Figs. 4.1 and 4.2, respectively, support the permeability results. Although trivial changes in fabric, induced by the replacement of water with ethanol, were observed, the soil structure appears to be the same before and after the test.

The simple alcohols whose effects on hydraulic conductivity have been reported in the literature (e.g., methanol) are lighter than water, are totally soluble in water, have dipole moments similar to that of water (about 1.7 Debye), and relative permittivities or dielectric constants in the range of 24 to 36. They should be able to replace the double layer water in clays and reduce the double layer thickness owing to their lower dielectric constant (Madsen and Mitchell, 1989). Fernandez and Quigley (1985) did tests on compacted illitic-smectitic soil with both ethanol and methanol in a rigid-wall permeameter under an initial gradient of 500. An increase in hydraulic conductivity of approximately one order of magnitude was measured in each case. In the tests by Anderson et al. (1985a), the neutral polar fluid, ethylene glycol, caused continuous conductivity decreases in the kaolinitic soil with no apparent tendency to stabilize. The same kaolinite treated with acetone, another neutral polar
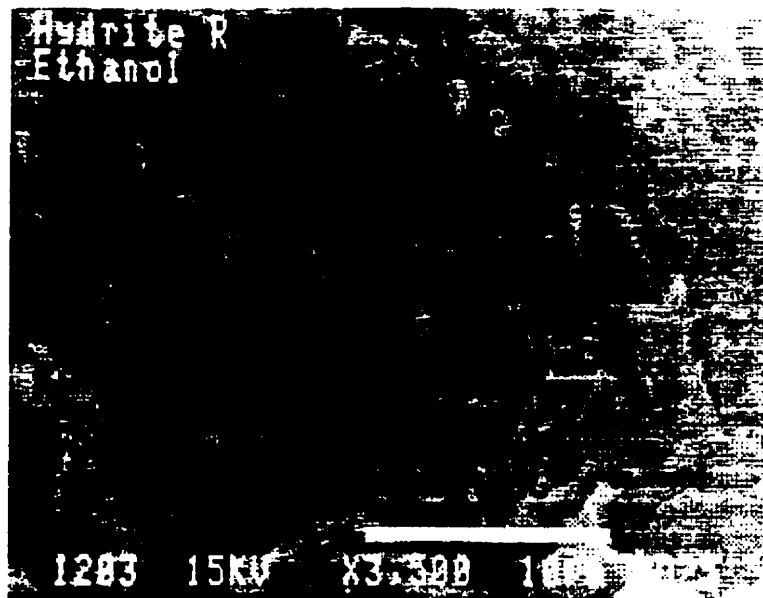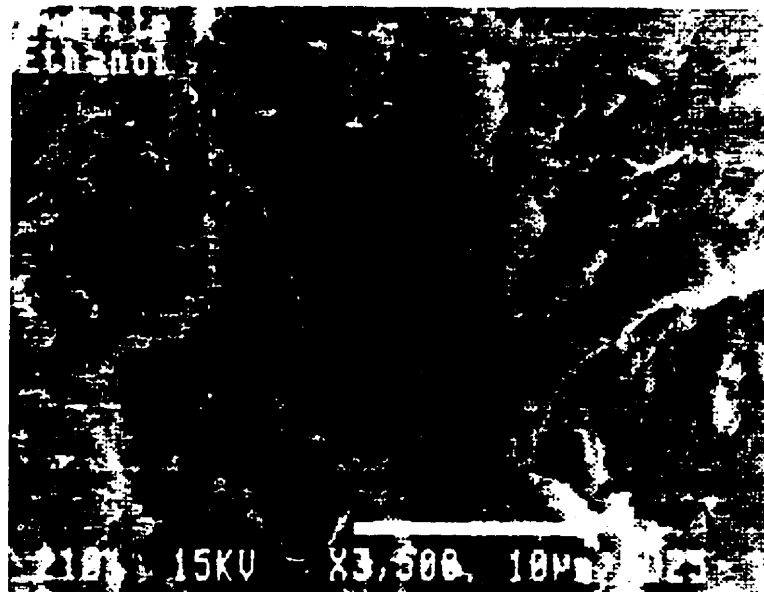
(a) cross-section: effluent
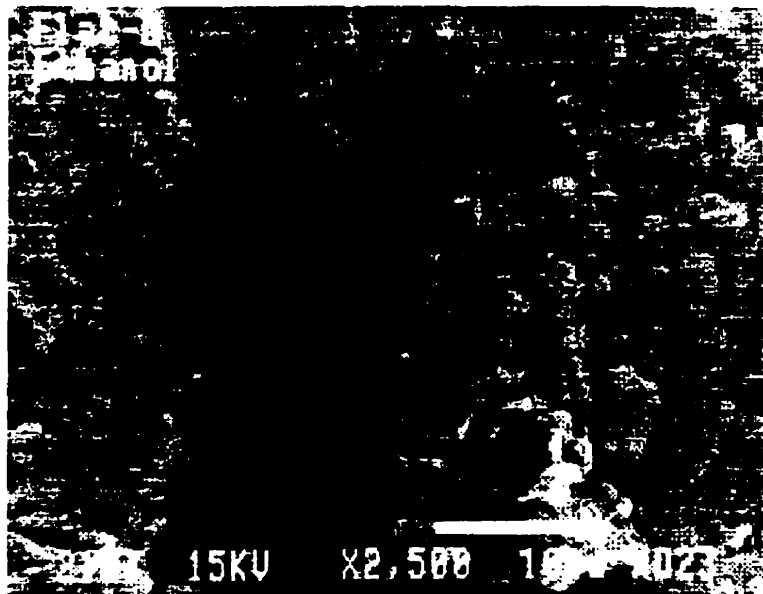
(b) plan: edge

Figure 4.21 Scanning electron micrographs of compacted
Hydrite Flat-D permeated with Ethanol.

(a) cross-section: influent

(b) plan: core

Figure 4.22 Scanning electron micrographs of compacted
Hydrite R permeated with Ethanol.

solvent, and methanol showed a conductivity increase of more than one order of magnitude after an initial decrease in the case of acetone. Such increases in conductivity were observed by Anderson *et al.* (1985a) before the passage of two pore volumes. The increase in conductivity was believed to have been brought about by structural changes in the clay produced by geochemical reactions between the permeant and the clay. Again, the use of specimen not fully saturated prior to testing could contribute to the inconsistency of these results with the results reported in this research.

Conductivity of kosse kaolin, montmorillonitic ranger shale, and fire clay was studied by Green *et al.* (1981). Several organic solvents were used as permeants. The authors found that the conductivity of all clays decreased under the flow of all organic solvents, including methanol and acetone. In most samples, the conductivity stabilized after 14-25 days. Green *et al.* (1981) attributed the difference in conductivity for various fluids to their dielectric constants. According to these authors, there was a good relationship between conductivity and the dielectric constant of the permeant: the greater the dielectric constant, the greater the conductivity. Not all the results agreed with this relationship, though.

4.2.1.4 Heptane

The hydraulic conductivities for both soils being permeated with water and heptane are shown in Figs. 4.23 and 4.24, respectively. Full breakthrough of heptane was confirmed by comparing TOC concentration of the effluent with that of the influent as presented in Fig. 4.25. The *Hydrite Flat-D* permeated with pure heptane underwent a 20% decrease in hydraulic conductivity compared to that with water, as illustrated by Fig. 4.26. The decrease is attributed to surface tension effects of immiscible liquids.

Heptane is a neutral, non-polar organic fluid, 0.4 times as viscous and 0.7 times as dense as water. It is practically immiscible with water, and the only way it could pass through a water-filled porous media is by physically displacing the water from the pores, unlike miscible liquids that can diffuse through the water. Being non-polar, it has no net charge and
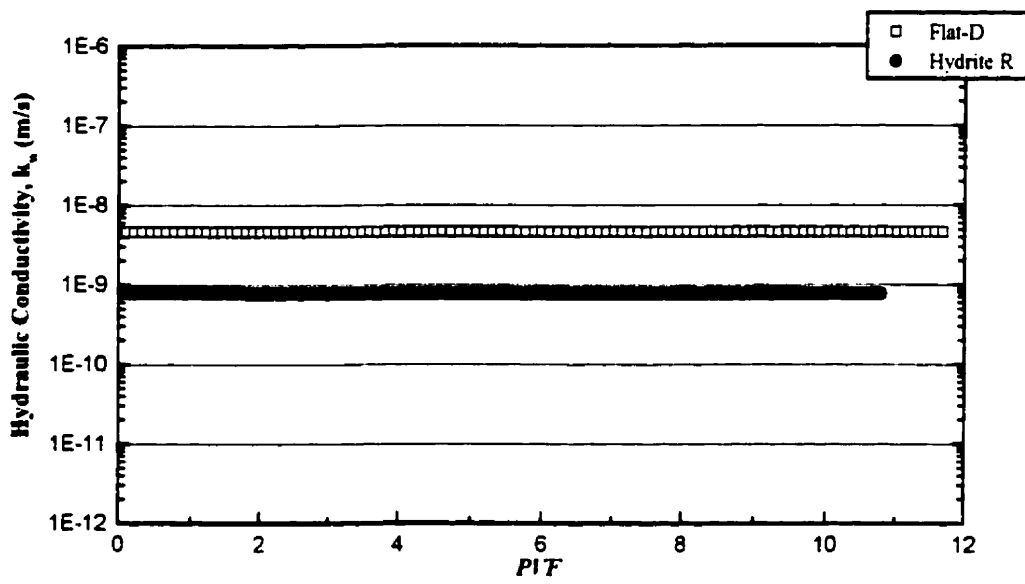
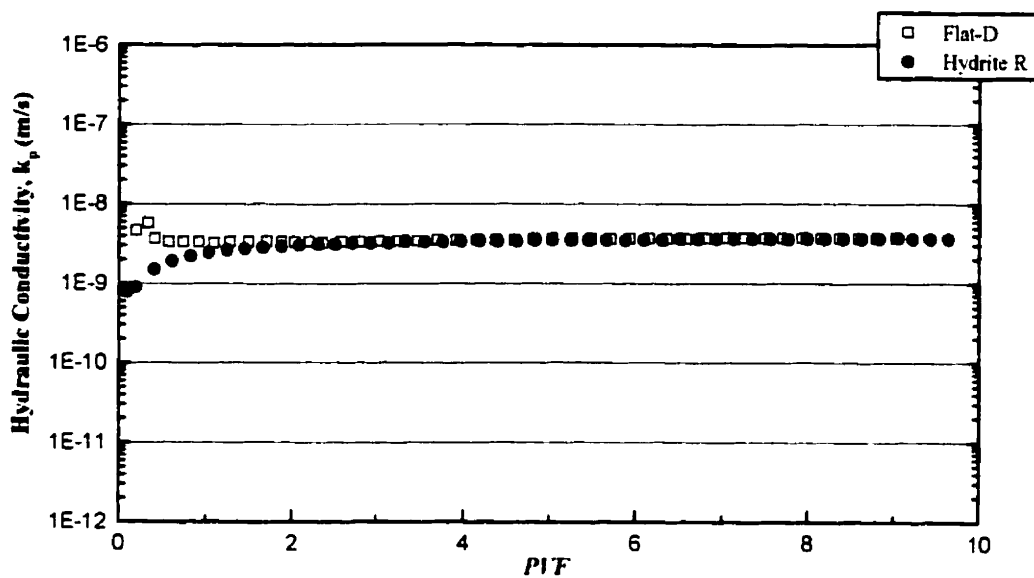Figure 4.23 Reference hydraulic conductivity of compacted kaolinites permeated with Heptane.

Figure 4.24 Hydraulic conductivity of compacted kaolinites
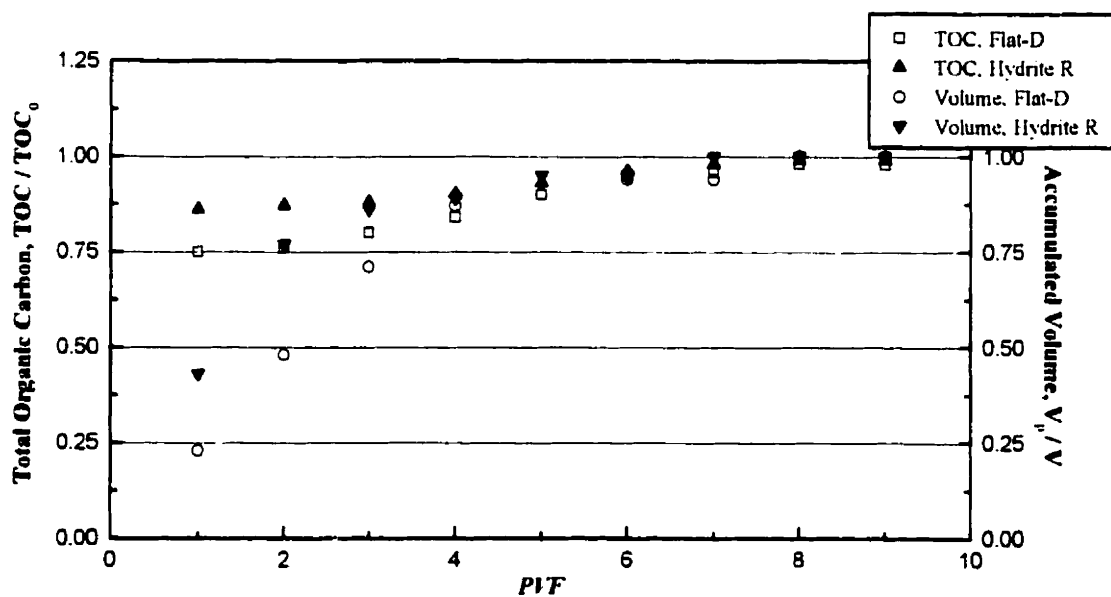permeated with Heptane.

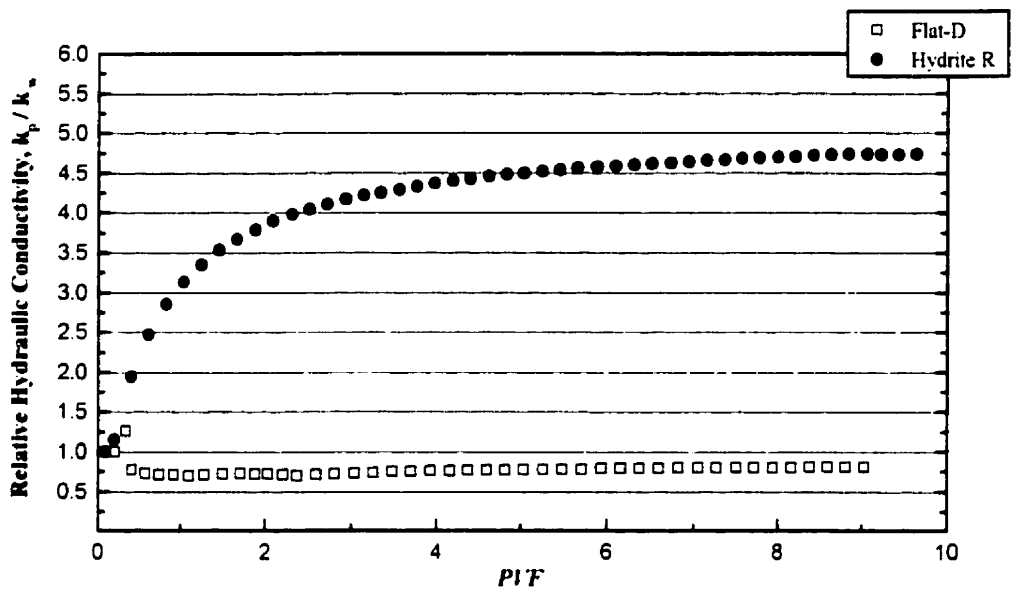Figure 4.25 Breakthrough curves of compacted kaolinites
permeated with Heptane.

Figure 4.26 Relative hydraulic conductivity of compacted kaolinites permeated with Heptane.
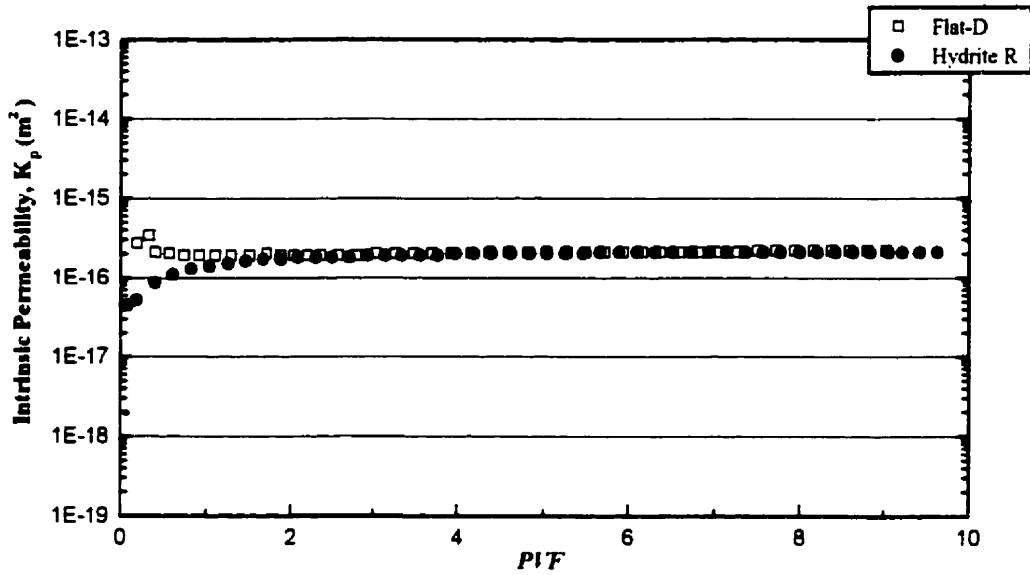
Figure 4.27 Intrinsic permeability of compacted kaolinites
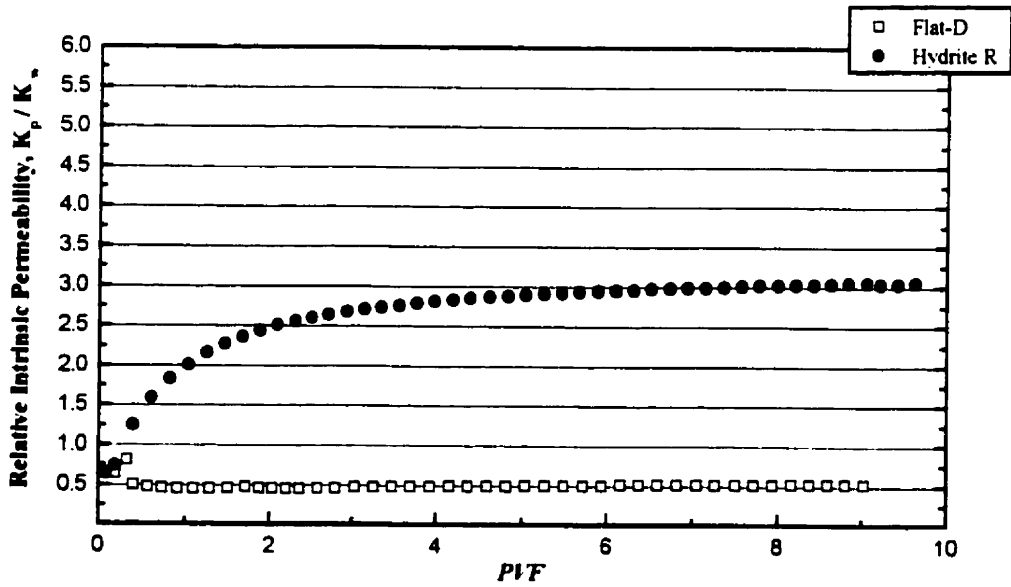permeated with Heptane.

Figure 4.28 Relative intrinsic permeability of compacted kaolinites
permeated with Heptane.

little, if any, dipole moment. Therefore, heptane cannot displace water and be adsorbed on the clay surface.

In a saturated porous medium, when one liquid replaces another with which it is immiscible, energy is expended. This is defined as the interfacial energy. Apart from the properties of the two liquids, such as the viscosity and density, the energy required depends on the pore size: the larger the pore size, the smaller the energy required. Thus, a liquid may be able to displace water from a porous stone and flow through the stone, yet may fail to flow through a saturated clay adjacent to the stone. In this case, the interfacial energy is provided by the pressure gradient.

Figure 4.26 shows an increase of almost 5 times the hydraulic conductivity to water for *Hydrite R*. Moreover, the intrinsic permeability of *Hydrite R* permeated with heptane is 3 times the intrinsic permeability to water, as presented by Figs. 4.27 and 4.28. Conductivity increases due to the density to viscosity ratio of heptane to water accounts for only a 55% increase in conductivity over values obtained with water. Other mechanisms than the density and viscosity of heptane are obviously involved. For the *Hydrite R* sample, it seems that the largest pores were small enough to prevent heptane entry even at a hydraulic gradient of 578 (a pressure gradient of 115 kPa). The reason for the lower heptane entry pressure in the case of *Hydrite Flat-D* is probably the presence of a few relatively large pores. It appears that the increase in k caused by heptane for the *Hydrite R* sample is the result of sidewall flow. The SEM examination of *Hydrite R* specimens supported this interpretation.

Scanning electron micrographs showing the structure of *Hydrite R* as-compacted before permeation with heptane, shown in Fig. 4.2, are compared with those of Fig. 4.30 obtained at the end of the leaching test. No features were observed that could be interpreted as indicating the alteration of the clay fabric. The same result is concluded after examining the micrographs of *Hydrite Flat-D* specimens.
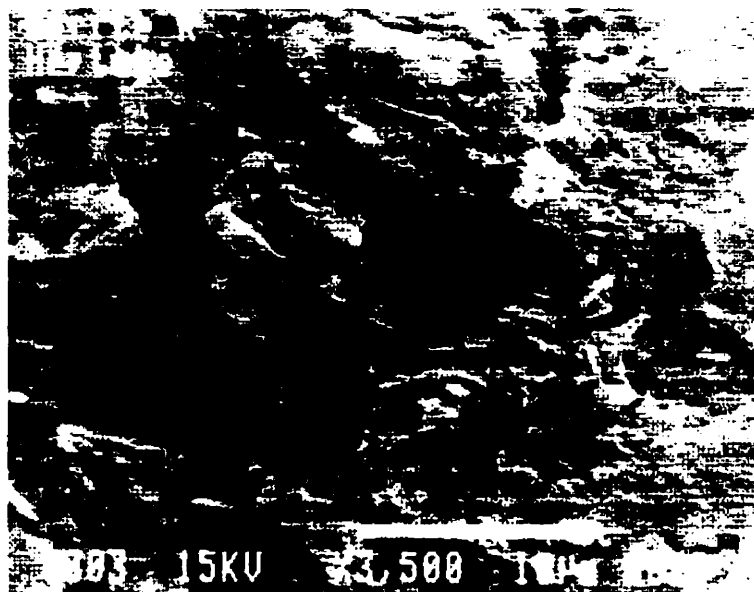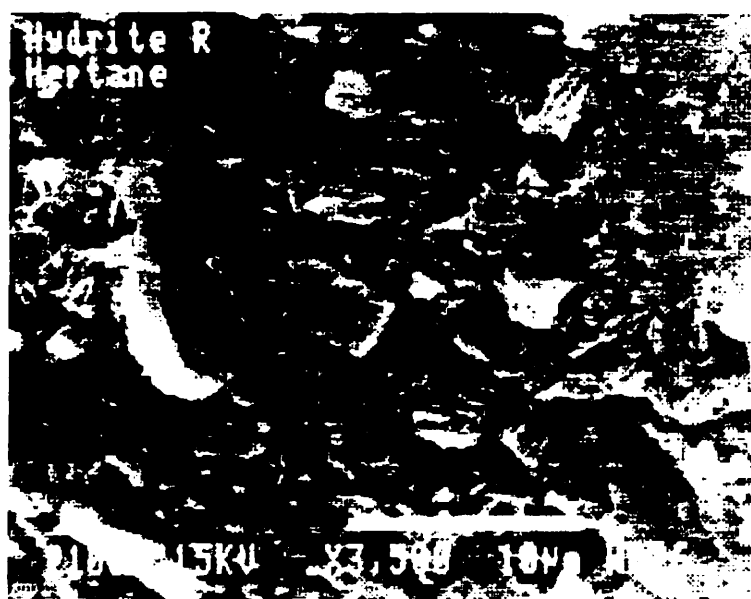
(a) cross-section: effluent

(b) plan: edge

Figure 4.30 Scanning electron micrographs of compacted Hydrite R permeated with Heptane.

Anderson *et al.* (1985a) reported conductivity increases of roughly two to three orders of magnitude in all of the samples, including kaolinite, permeated with the neutral non-polar fluids heptane and xylene even before the passage of half a pore volume. At that point, the soils tended to reach a relatively constant conductivity. Anderson *et al.* (1985a) believed that structural changes resulting from the reaction between the non-polar organic fluid and the clay caused the increase in conductivity. Since steady conductivity values were reached within a short time, unlike the continuous conductivity increases experienced with neutral polar permeants, the authors presumed that the reactions were limited.

The results of Anderson *et al.* (1985a) can be compared to those obtained for similar clays and permeants by Green *et al.* (1981) to note the contradictions. Green *et al.* (1981) show a continuous decrease in conductivity, whereas Anderson *et al.* (1985a) report a sharp increase in conductivity on the passage of half a pore volume of permeant. Attempts by Foreman and Daniel (1986) to permeate a *Hydrite R* kaolin clay from Georgia Kaolin Co., New Jersey, and two naturally occurring illitic and smectitic clays with pure heptane using flexible-wall permeameters and hydraulic gradients as large as 300 were unsuccessful. After some small quantity of flow of heptane, *k* dropped to essentially zero. Foreman and Daniel (1986) attributed the cessation of flow of heptane to the surface tension between heptane and water. The phenomenon is similar to the flow of oil in porous materials. Lambe (1956) states that the oil entry pressure for a water-saturated clay may be 689 to 1,034 kPa (100 to 150 psi). The entry pressure is a function of the radius of a pore (by analogy to a capillary) such that the oil entry pressure decreases as the pores in the soil become larger. Because the surface tension of heptane is similar to that of oil, the heptane entry pressure should be similar to the oil entry pressure.

The interaction between clay particles and organic compounds is considered to be the result of mainly the lower permittivity of the permeants. Mitchell (1993) showed that a decrease in relative permittivity from 80 to 24 when water was replaced by ethanol resulted in a reduction of the diffuse double layer thickness by 45%. The diffuse double layer tends to

shrink according to Eq. A.6, and the resulting decrease in repulsive force between particles is expected to lead to flocculation of clay particles in soil mass. This phenomenon has been proven experimentally for slurries prepared with organic chemicals (Michaels and Lin, 1954), and for compacted soils and slurries permeated by organic fluids (Anderson *et al.*, 1985a; Evans *et al.*, 1985). The SEM observations of this study confirm the alteration of clay fabric whenever the organic matter replaces the double layer water or at least encounters the clay particles at the microscopic level, as in the case of the leaching tests with acetic acid and, to some extend, with ethanol. Aniline and apparently heptane were unable to reach the surface of clay particles due to their hydrophobic nature, and thus failed to cause substantial structural rearrangement of soil fabric.

Green *et al.* (1981) also concluded from their work on the permeabilities of various clays with organic permeants that the differences in dielectric constant of the fluids are responsible for the changes in conductivities they observed. The results of Green *et al.* (1981) show that the greater the dielectric constant the greater the conductivity. Selected conductivity ratios (k_p k_w) published in the literature and those obtained by Budhu *et al.* (1991) from consolidation tests were plotted versus dielectric constant ratios for a group of organic fluids in three types of clay materials. Based on those plots, Budhu *et al.* (1991) proposed a single parameter relationship between the conductivity ratio and the dielectric constant of the permeant. Their proposed variable λ is a constant for a particular soil type with a given stress history. The authors were uncertain as to what soil properties determine the value of λ. Budhu *et al.* (1991) concluded that differences in dielectric constant between the organic fluids and pure water correlate better with changes in conductivity than does any other single parameter.

As a final note, an attempt was made to correlate the change in hydraulic conductivity with the relative permittivity of the different organic contaminants. The results obtained experimentally during the course of the research are plotted against the dielectric constant of the permeants in Fig. 4.31. Moreover, the theoretically calculated relative hydraulic
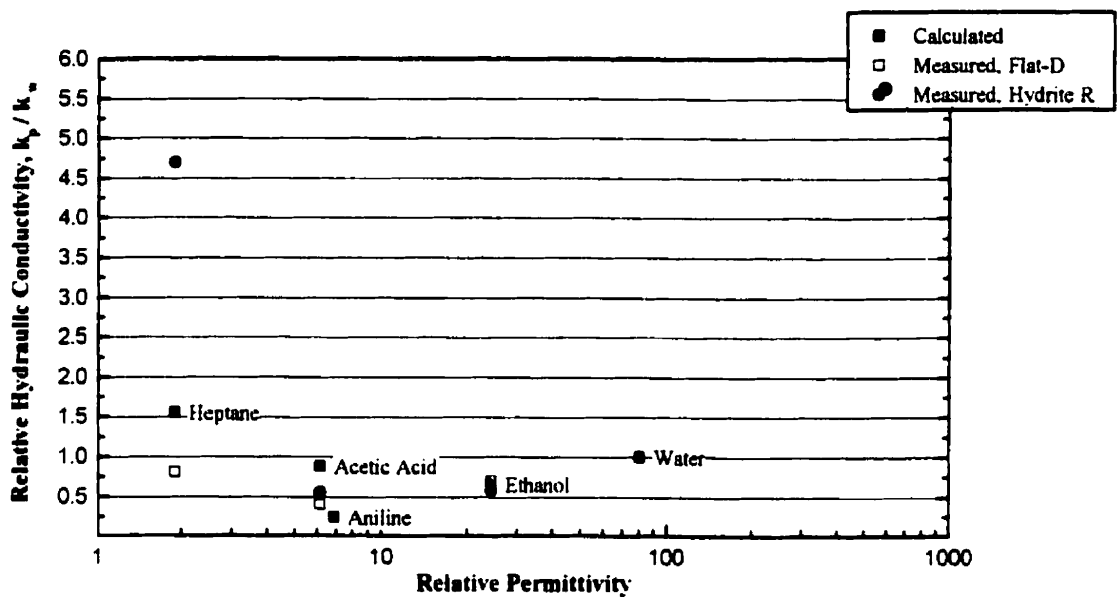
Figure 4.31 Relationship between relative hydraulic conductivity
of compacted kaolinites and relative permittivity of organic compounds.

conductivities for both clays are illustrated in the same figure. Examination of these plots revealed no convincing relationship between the conductivity ratio and the relative permittivity. The scatter in the results, partly owing to the limited number of data points, makes even a statistical evaluation intractable.

4.2.2 Inorganic Chemicals

4.2.2.1 Sodium Chloride

Figures 4.32 and 4.33 present the results of the hydraulic conductivity measurements for the compacted kaolinites. Monitoring of the effluent during the NaCl tests was accomplished by electrical conductivity measurements, and the establishment of breakthrough curves was realized by determining the chloride concentration of the effluent. Breakthrough curves of the clays permeated with 5M NaCl are shown in Fig. 4.34.

After a slight increase during the first pore volume of flow, the hydraulic conductivity of both kaolinites decreased steadily until reaching its respective equilibrium value, as shown in Fig. 4.35. The strong suppression of the diffuse double layer by virtue of an increase in electrolyte concentration can be demonstrated by Eq. A.6. Theoretically, a 100-fold decrease in sodium chloride concentration increases the thickness of the diffuse double layer 10 times, other parameters kept constant (Mitchell, 1993). For a slurry, the Gouy-Chapman theory postulates an increase in the hydraulic conductivity of clayey soils with the increase in electrolyte concentration. This prediction was confirmed experimentally by Alther et al. (1985). The authors conducted hydraulic conductivity measurements on a bentonite slurry using various inorganic salts. Hydraulic conductivity increased generally with the increase in salt concentration. Alther et al. (1985) considered the diffuse double layer theory to be generally consistent with their results: the higher the electrolyte concentration, the higher the hydraulic conductivity. The formation of flocculated structure in the case of a slurry, where the particles are free to move, is attributed to such behavior. However, the compacted

Figure 4.32 Reference hydraulic conductivity of compacted kaolinites permeated with 5M NaCl.

Figure 4.33 Hydraulic conductivity of compacted kaolinites
permeated with 5M NaCl.

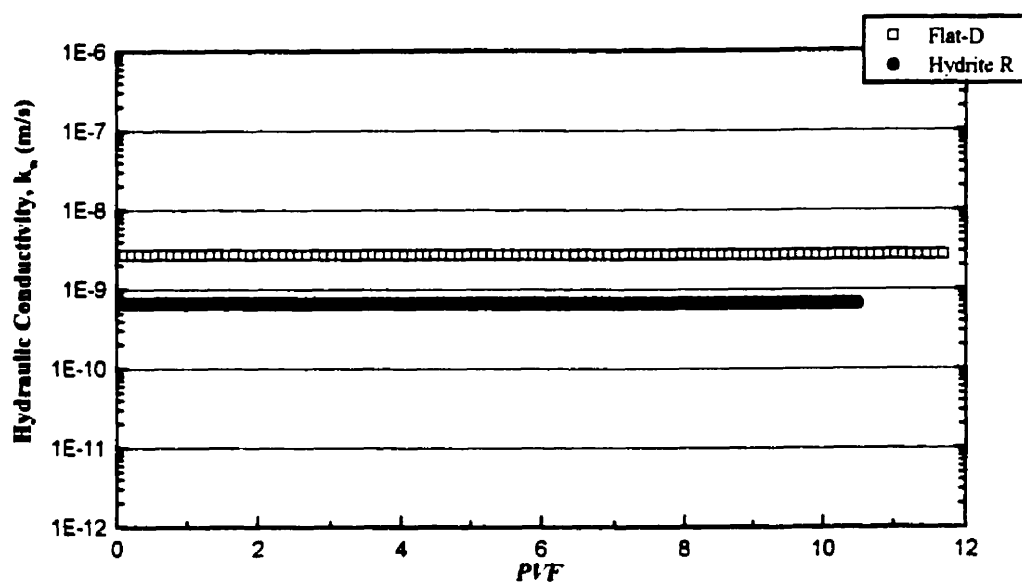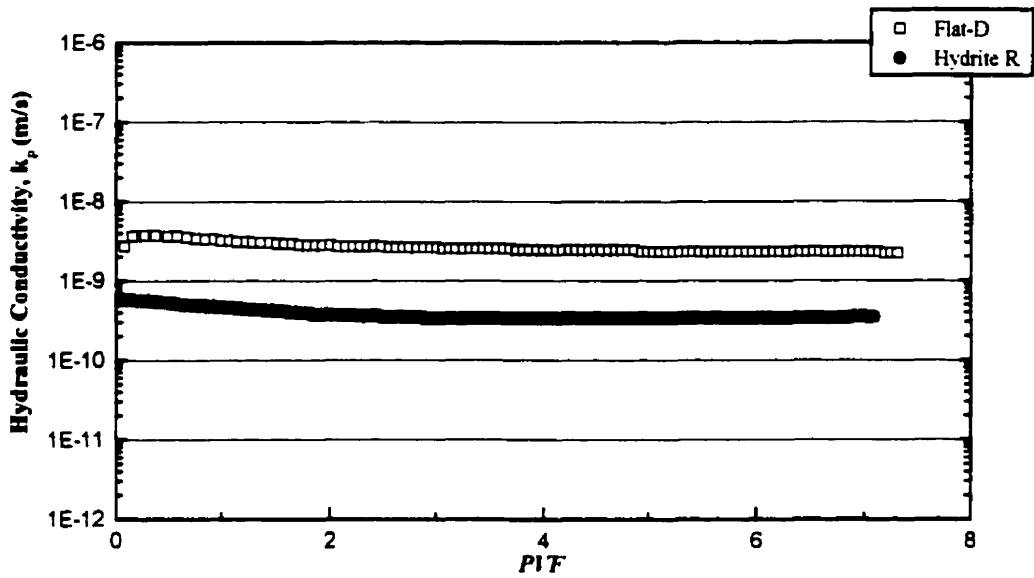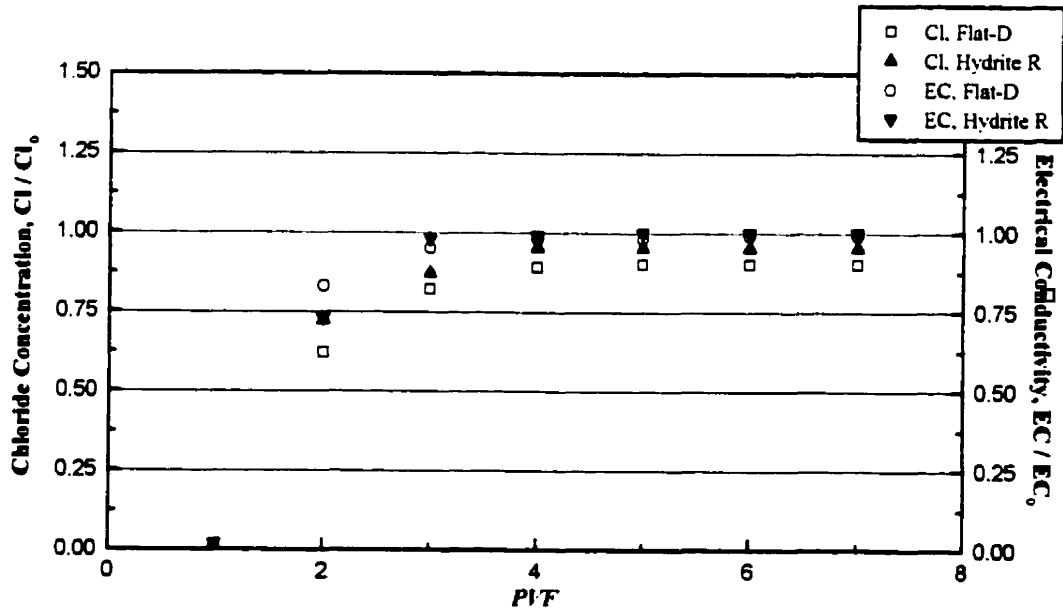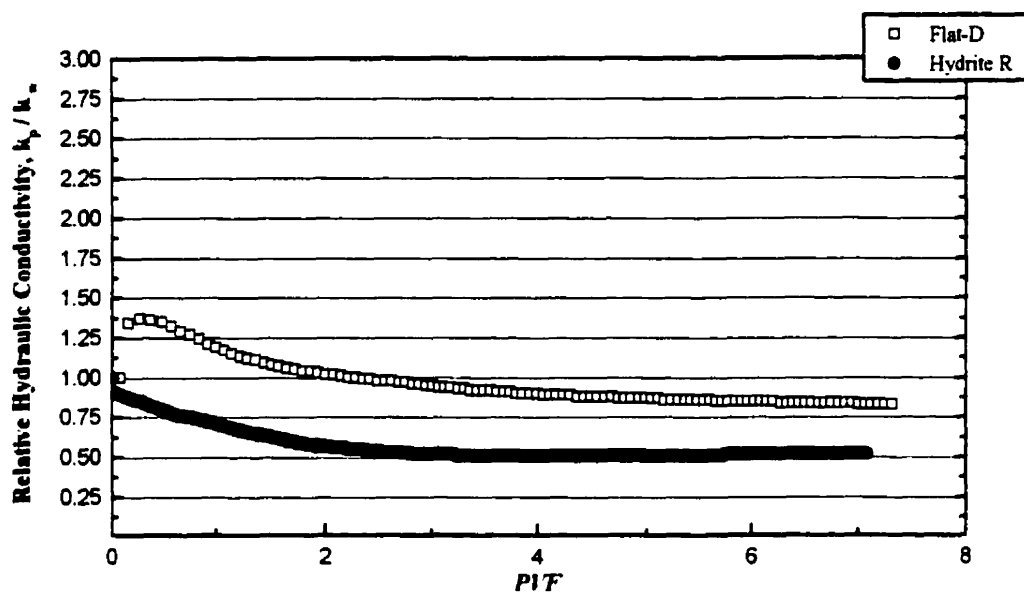Figure 4.34 Breakthrough curves of compacted kaolinites
permeated with 5M NaCl.

Figure 4.35 Relative hydraulic conductivity of compacted kaolinites
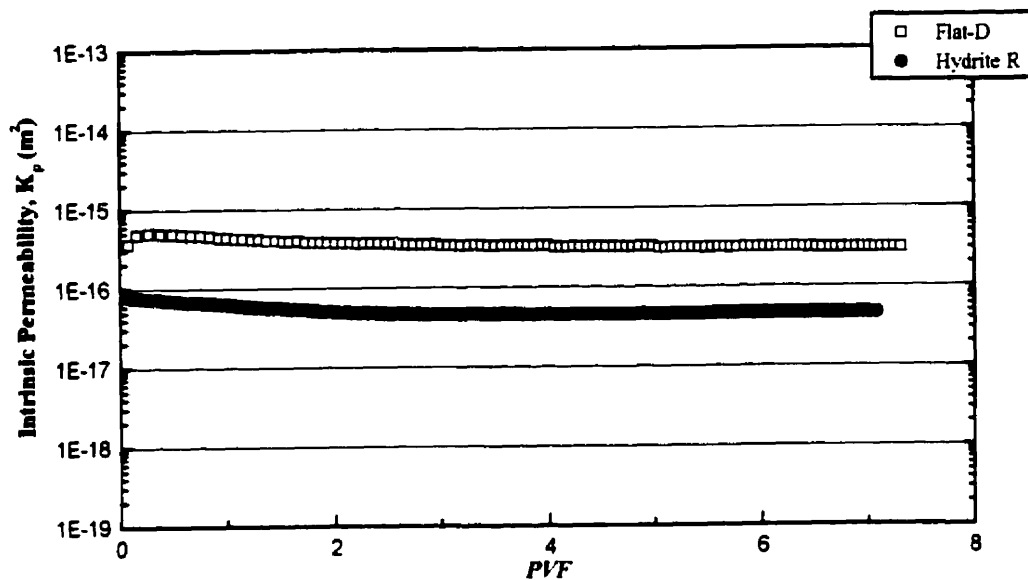permeated with 5M NaCl.

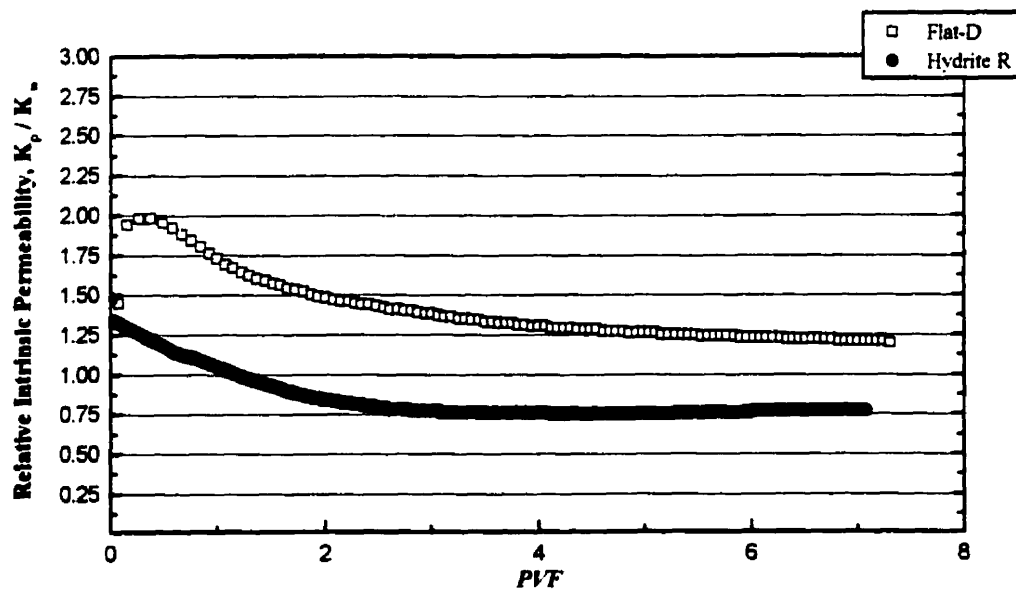Figure 4.36 Intrinsic permeability of compacted kaolinites permeated with 5M NaCl.

Figure 4.37 Relative intrinsic permeability of compacted kaolinites permeated with 5M NaCl.

kaolinites in this study are relatively confined by the rigid-wall permeameter, hence restricting the movement of clay particles.

When the effects of density and viscosity are corrected, the intrinsic permeability values can be obtained as presented by Fig. 4.36. The variation of K_p K_w for both kaolinites with the accumulated pore volumes of flow is shown in Fig. 4.37. The intrinsic permeability ratio at the end of the test varies from 1.20 to 0.77 for *Hydrite Flat-D* and *Hydrite R*, respectively. Such variation around unity indicates that the concentrated salt solution has no significant effect on the pore characteristics of compacted kaolinite. This observation is backed by the scanning electron micrographs of Fig. 4.38. No sever alteration in the fabric arrangement of the kaolinites before and after the salt transport through the samples could be detected when comparing SEM micrographs of the as-compacted clay (Figs. 4.1 and 4.2) with those of the contaminated soil. At higher SEM magnification, the disappearance of some of the smaller pores was revealed in the samples permeated by 5M NaCl. This might have been caused by the formation of salt crystals following the freeze-drying process for the preparation of SEM specimens. Compacted kaolinites used in this project appear to be much more resistant to the attack of concentrated salt as indicated by their stable structure.

During the course of this research, a leaching test was conducted on *Hydrite Flat-D* clay sample using Rowe cell as the permeameter and permeated with various concentrations of NaCl. To prevent potential sidewall leakage, a piston was applied to the soil column during hydraulic conductivity measurements. The same trend as the one shown in Fig. 4.33 for *Hydrite Flat-D* was obtained. It is well recognized that both compaction stress and lateral confining pressure play an important role in defining clay-electrolyte interaction, and consequently hydraulic conductivity results, by restricting the movement of clay particles. When clay particles are not constrained, there is a greater chance for clay-electrolyte interaction to take place, resulting in a change in conductivity as observed by Quirk and Schofield (1955). Yang and Barbour (1992) and Barbour and Yang (1993) reached similar conclusions.

(a) Hydrite Flat-D

(b) Hydrite R

Figure 4.38 Scanning electron micrographs of compacted
kaolinites permeated with 5M NaCl.

4.2.2.2 Hydrochloric Acid and Sodium Hydroxide

The effects of a change in pH of the pore fluids on compacted clays were investigated by permeating the soil columns with solutions of hydrochloric acid (0.01M HCl) and sodium hydroxide (0.25M NaOH). Permeation of 0.01M HCl solution resulted in the hydraulic conductivity changes presented in Figs. 4.39, 4.40, and 4.42. Limited neutralization reactions appear to have happened while permeating the kaolinites with HCl as indicated by the change in pH of the effluent shown in Fig. 4.41. No significant change in intrinsic permeability was recorded during the leaching test with the low concentration HCl as illustrated by Figs. 4.43 and 4.44, even though clay-chemical interactions are believed to have taken place, at least to some extend. SEM observations were all consistent with the leaching test results as shown by Fig. 4.45. Some local dissolution is revealed by the micrographs of the contaminated clays as a result of the geochemical reactions between the acid and soil.

When NaOH solution was introduced into the compacted clays, neutralization reactions appear to have occurred as indicated by the slow increase in pH of the *Hydrite Flat-D* leaching shown in Fig. 4.48. The clay particles of *Hydrite Flat-D* apparently possess certain buffer capacity. Permeation of 0.25M NaOH led to the conductivity changes presented in Figs. 4.46, 4.47, and 4.49. The changes in intrinsic permeability are also presented in Figs. 4.50 and 4.51. SEM micrographs shown in Fig. 4.52 do not reveal any significant alteration in the fabric of both contaminated soils compared with the particle arrangement of uncontaminated clay. It appears that the processed soils used in this research are neither capable of accepting nor releasing H⁺ as indicated by the SEM observations.

According to theory, a change in pH of a pore fluid should cause a change in the diffuse double layer thickness by altering the charge at the surface of clay particle. Adsorption of H⁺ onto the hydroxyl surface functional group tends to make the particles more positively charged, and thus results in a flocculated structure by virtue of reducing the repulsive energy potential. Adsorption of OH⁻ would have an opposite effect on clay particle interactions. When a bentonite slurry was tested, an increase of an order of magnitude in hydraulic
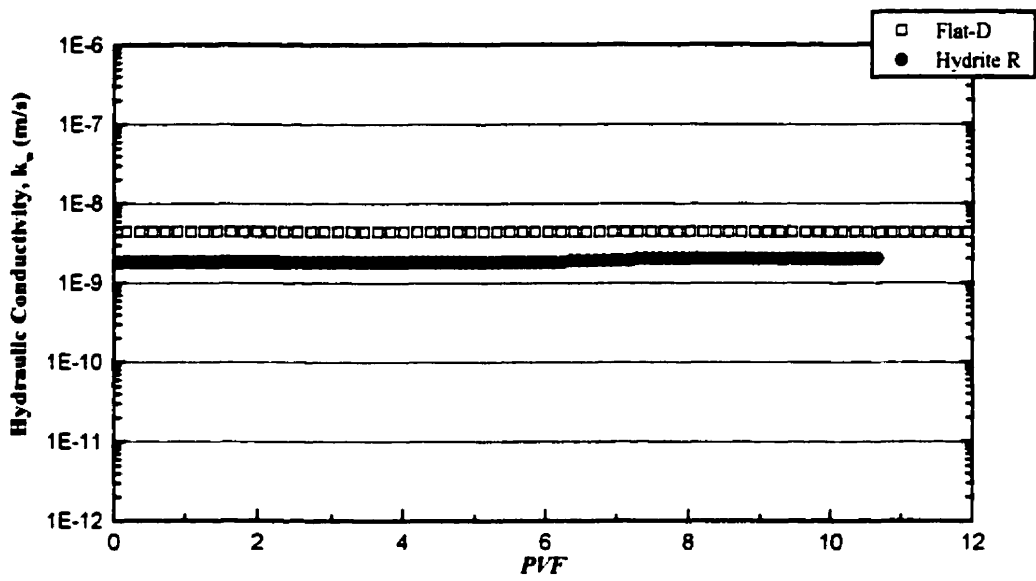
Figure 4.39 Reference hydraulic conductivity of compacted kaolinites permeated with 0.01M HCl.
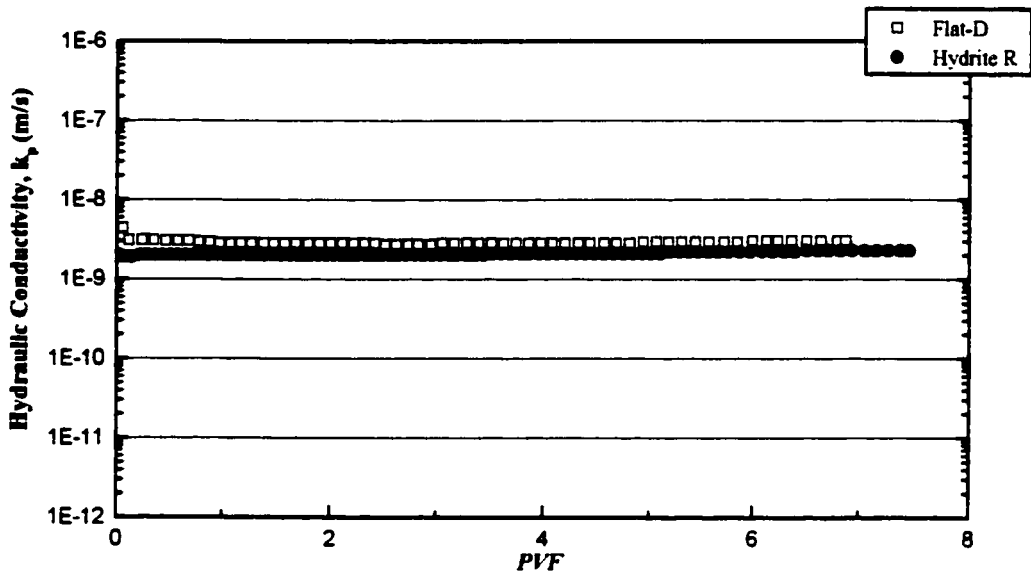
Figure 4.40 Hydraulic conductivity of compacted kaolinites
permeated with 0.01M HCl.
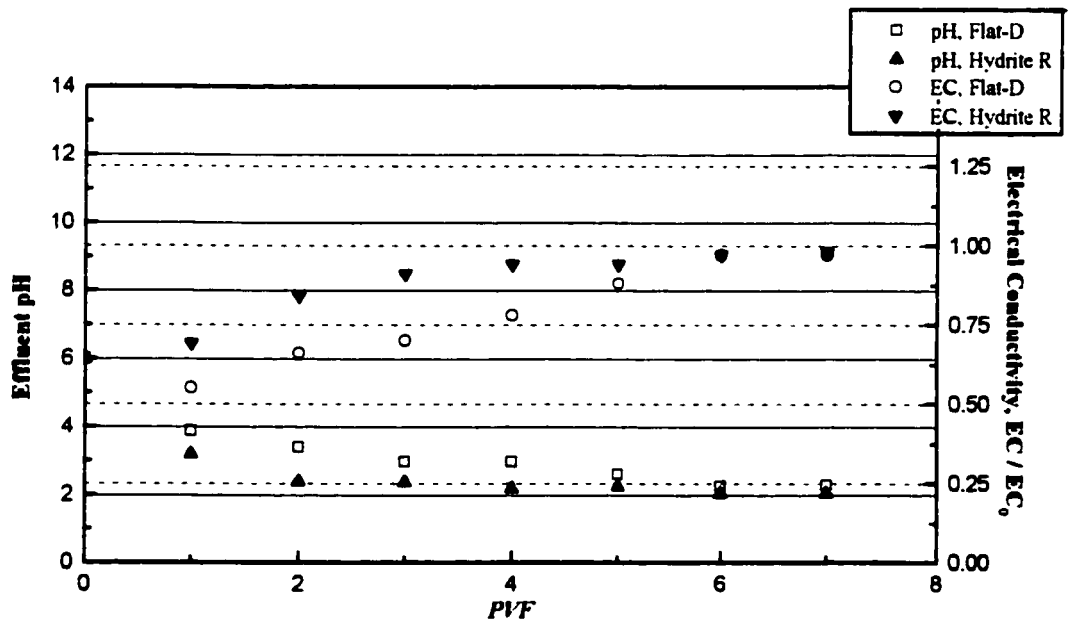
Figure 4.41 Breakthrough curves of compacted kaolinites
permeated with 0.01M HCl.

Figure 4.42 Relative hydraulic conductivity of compacted kaolinites permeated with 0.01M HCl.

Figure 4.43 Intrinsic permeability of compacted kaolinites
permeated with 0.01M HCl.

Figure 4.44 Relative intrinsic permeability of compacted kaolinites
permeated with 0.01M HCl.

(a) Hydrite Flat-D

(b) Hydrite R

Figure 4.45 Scanning electron micrographs of compacted kaolinites permeated with 0.01M HCl.
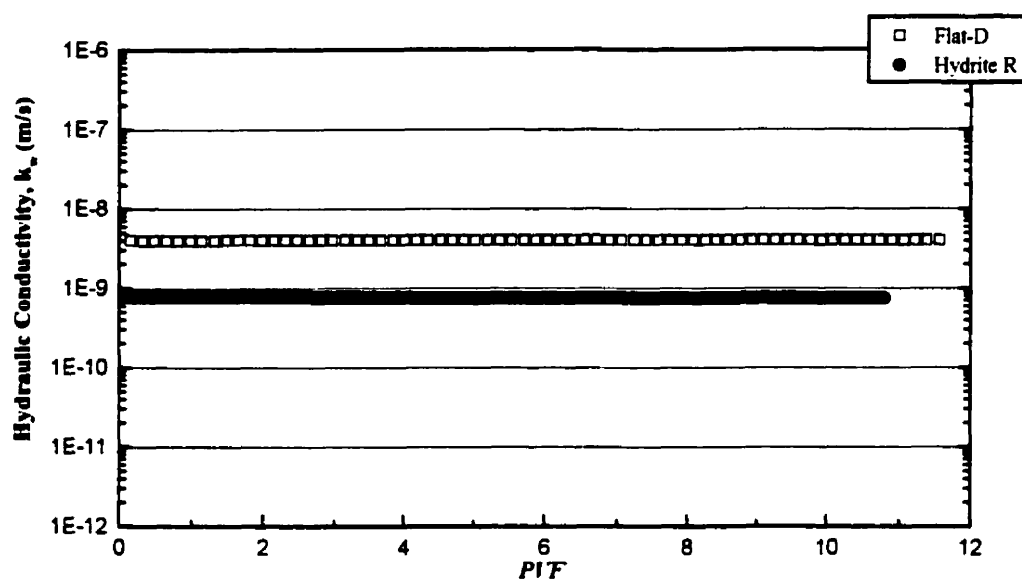
Figure 4.46 Reference hydraulic conductivity of compacted kaolinites
permeated with 0.25M NaOH.
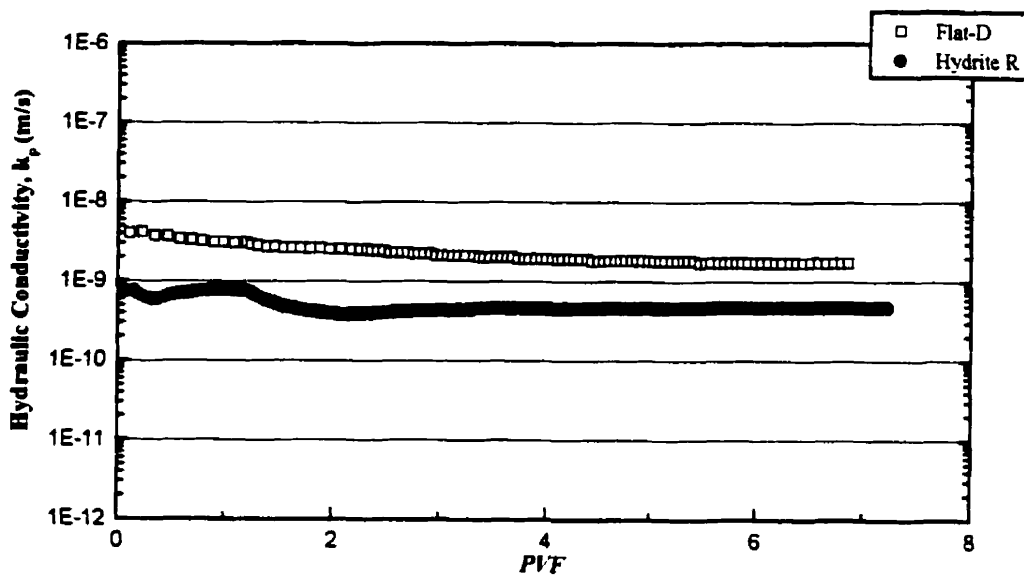
Figure 4.47 Hydraulic conductivity of compacted kaolinites permeated with 0.25M NaOH.
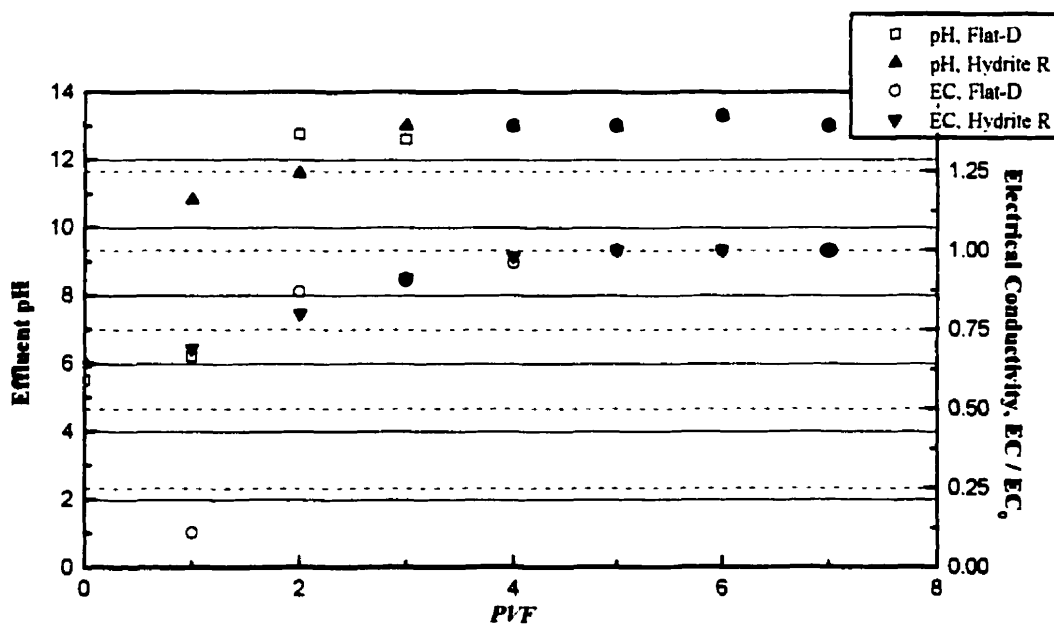
Figure 4.48 Breakthrough curves of compacted kaolinites permeated with 0.25M NaOH.
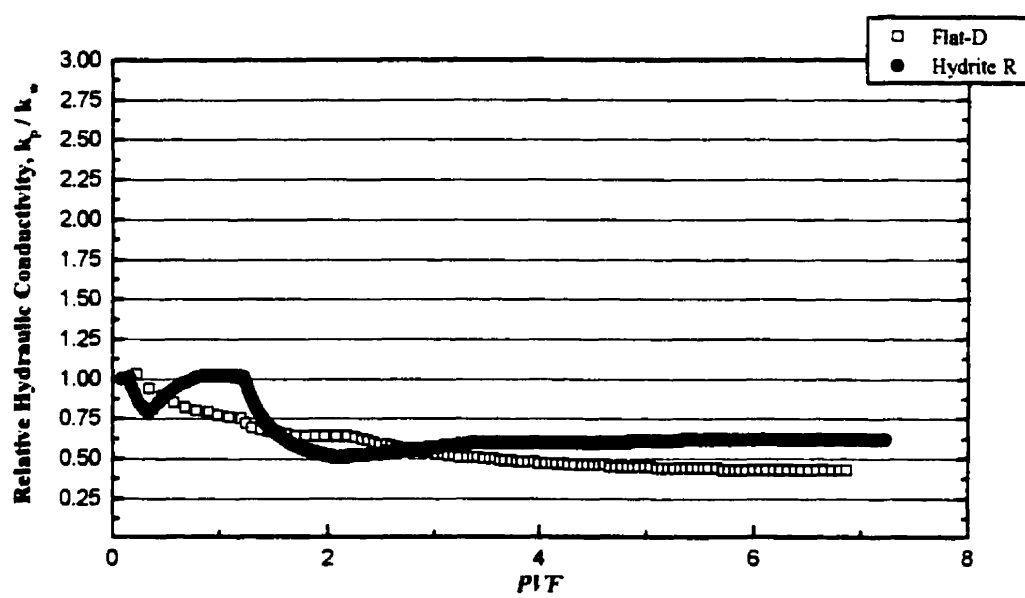
Figure 4.49 Relative hydraulic conductivity of compacted kaolinites
permeated with 0.25M NaOH.
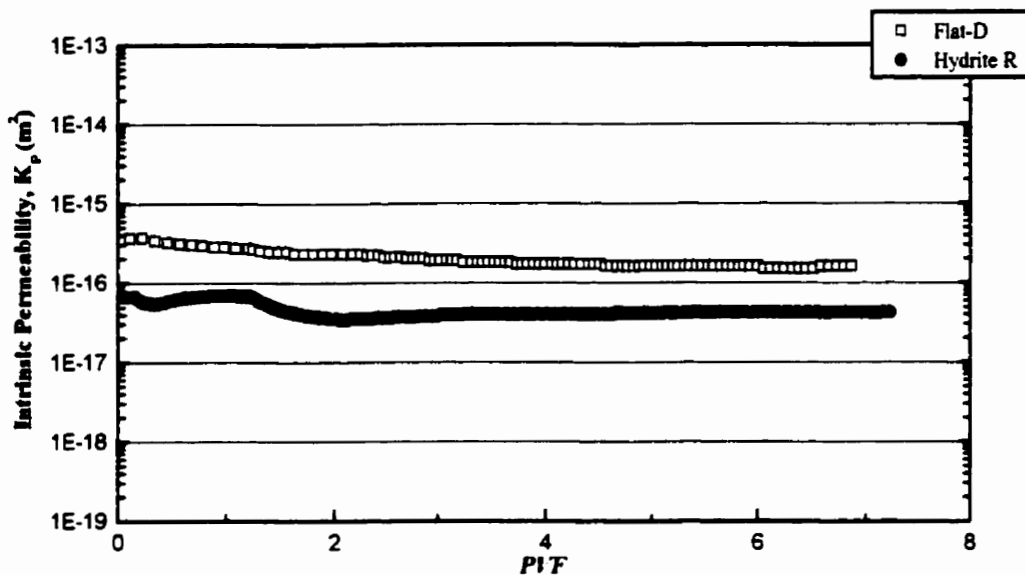
Figure 4.50 Intrinsic permeability of compacted kaolinites permeated with 0.25M NaOH.
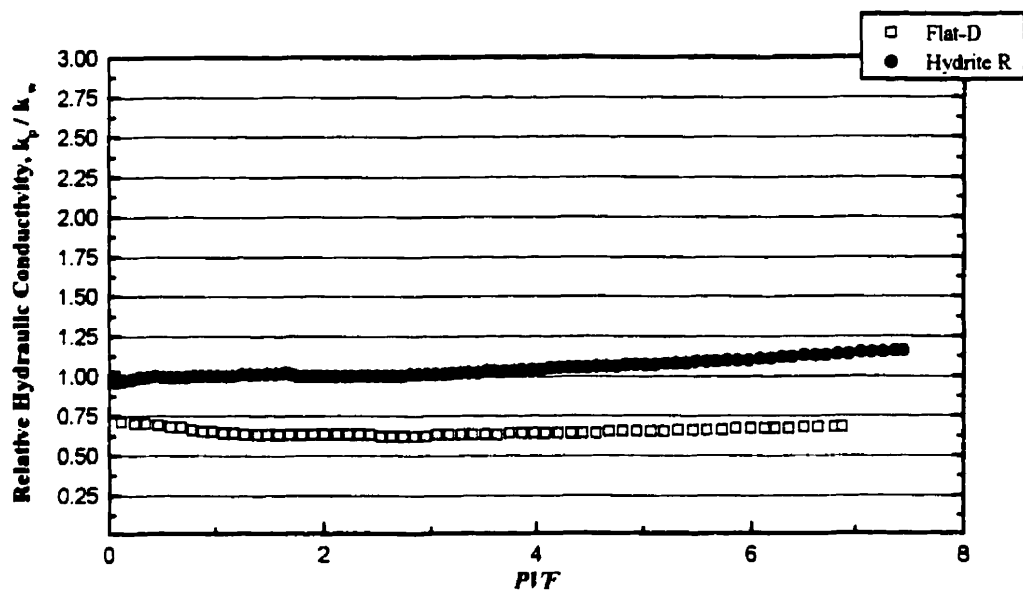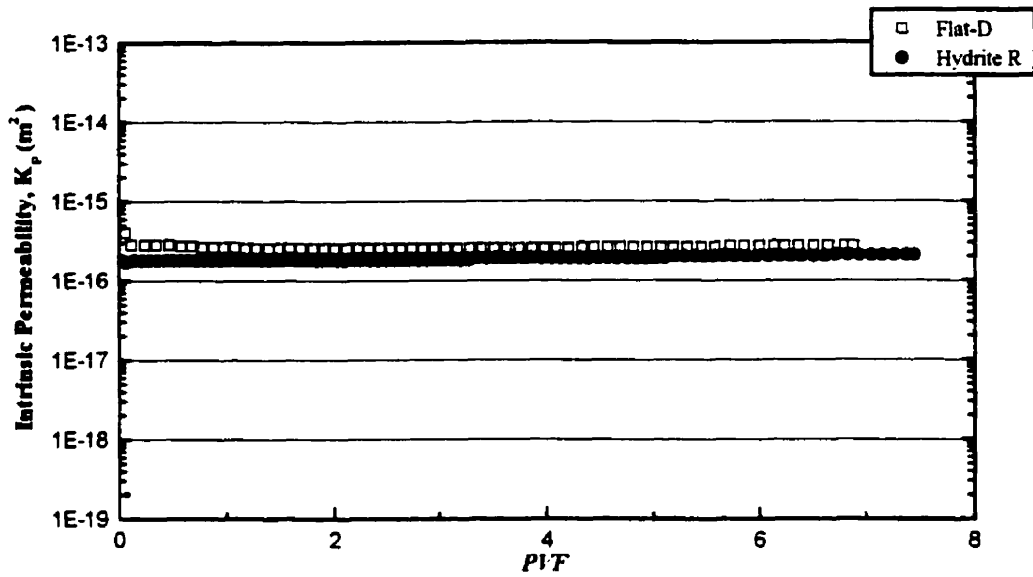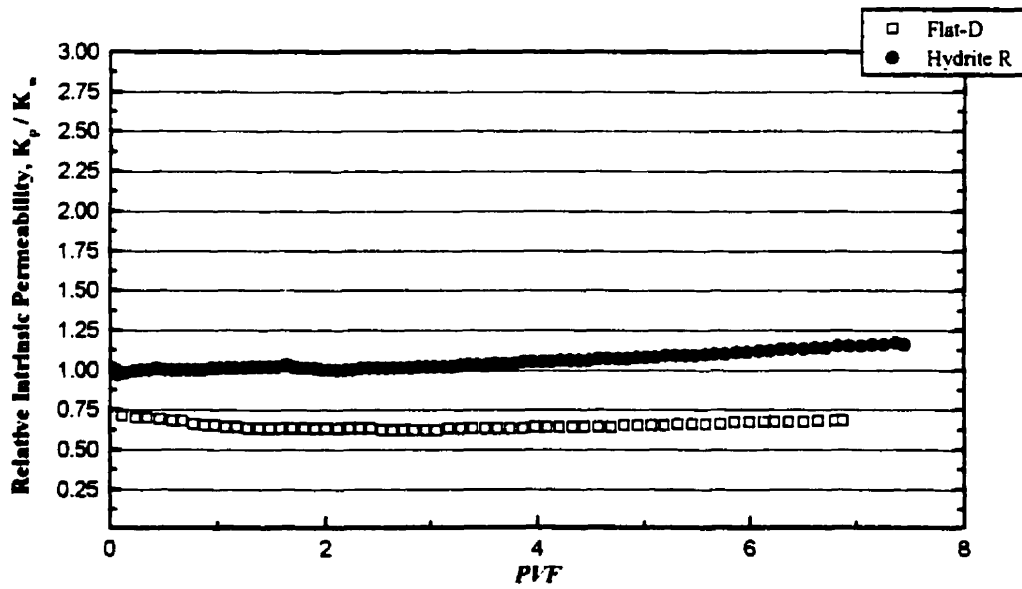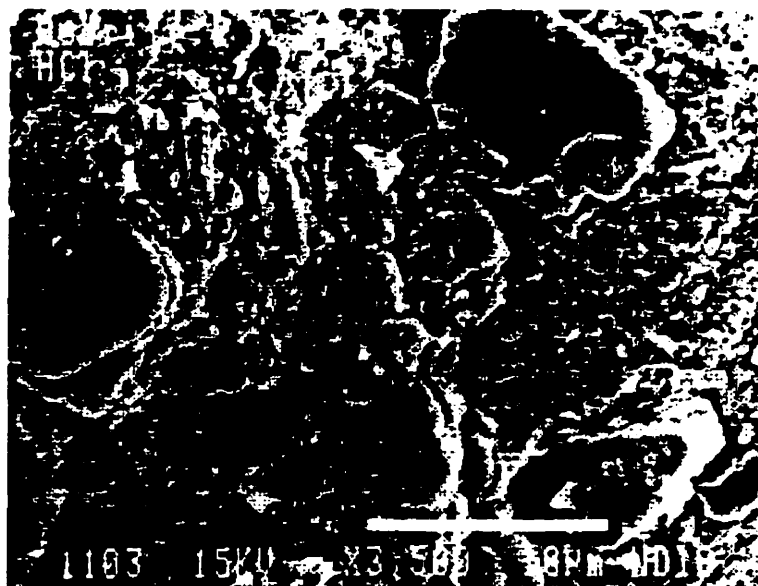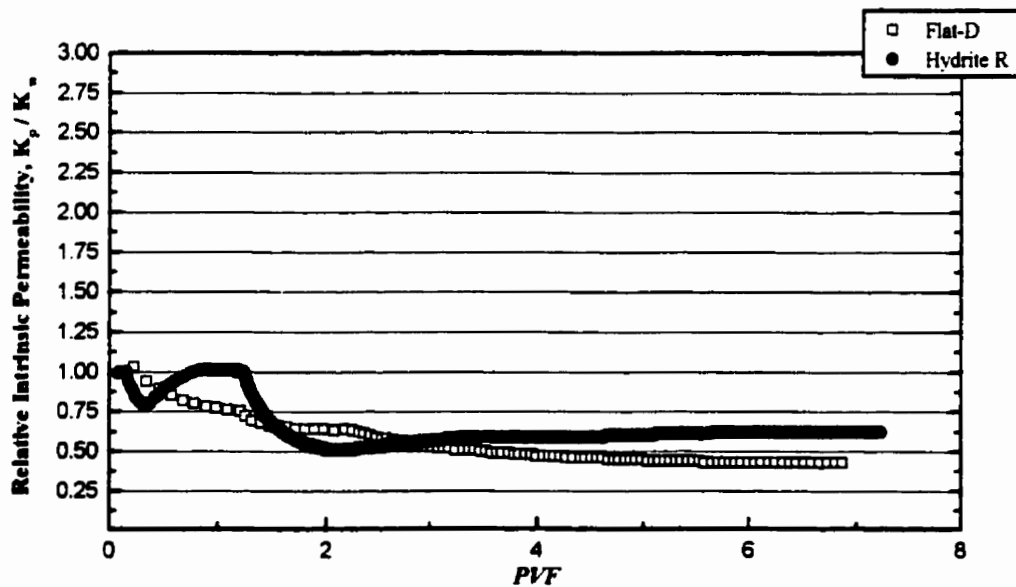

Figure 4.51 Relative intrinsic permeability of compacted kaolinites permeated with 0.25M NaOH.

(a) Hydrite Flat-D
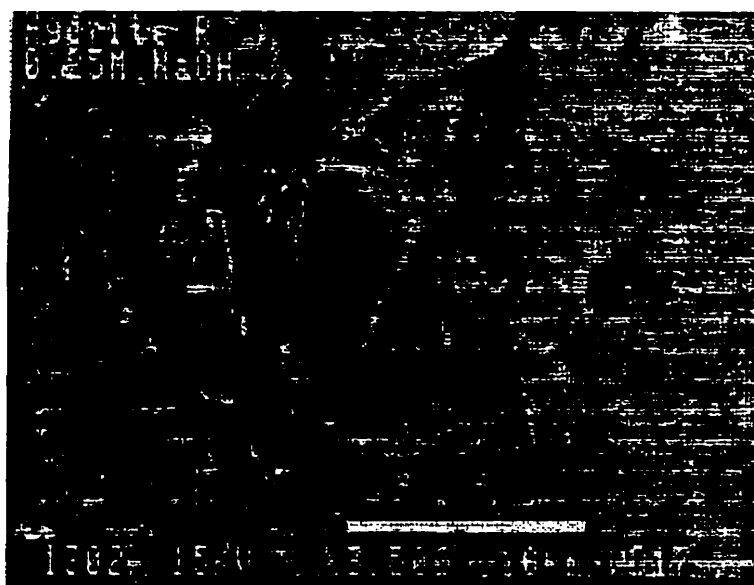
(b) Hydrite R

Figure 4.52 Scanning electron micrographs of compacted
kaolinites permeated with 0.25M NaOH.

conductivity was measured due to permeation of inorganic acid and base (D'Appolonia, 1980). However, the possible dissolution of bentonite particles was inferred as the mechanism responsible for the change in conductivity. For compacted clays, contradicting results have been reported and the dissolution-precipitation of other minerals contained in soil was frequently mentioned in most cases (Gordon and Forrest, 1981; Lentz et al., 1985). In this study, no significant dissolution of clay particles was detected from SEM observations, and the commercial clays used do not contain a large amount of soluble minerals. The pH changes at the effluent end of the tests appear to result from adsorption of either H^+ or OH^- onto the surfaces of clay particles. Under laterally constrained conditions, geochemical reactions seem not to cause substantial changes in soil fabric.

An effort was made to investigate the viability of Kozeny-Carman hydraulic model by correlating the theoretically calculated intrinsic permeability to the experimentally obtained values for inorganic chemicals, as presented in Fig. 4.53. The Kozeny-Carman equation, as defined by Eq. 2.16, expresses the intrinsic permeability K in terms of surface area, a flow factor, and void ratio (or porosity). Pore-size distribution and particle-size influence the porosity n or void ratio e. The role of void ratio may be readily seen in the form that e takes in Eq. 2.16. In computing the theoretical value of permeability for each kaolinite, flow is assumed to occur adjacent to only 80% of all particle surfaces. Therefore, the wetted surface S_0 of Eq. 2.16 is considered to represent 80% of the total specific surface area of the clay. The primary considerations needed for the valid application of Kozeny-Carman model are: (a) relatively uniform particle size, (b) laminar flow of liquid through the pores, (c) validity of Darcy's law, and (d) absence of long- and short-range forces of interaction.

Ideally, the quantitative prediction of permeability will be closest for granular particles. The Kozeny-Carman relationship represents a refinement of Darcy's law accounting for certain soil properties and characteristics. However, if the interaction characteristics known to exist in clay-contaminant systems, and add to that the fact that clay particles are platelike in shape and form fabric units such that overall permeability between and within
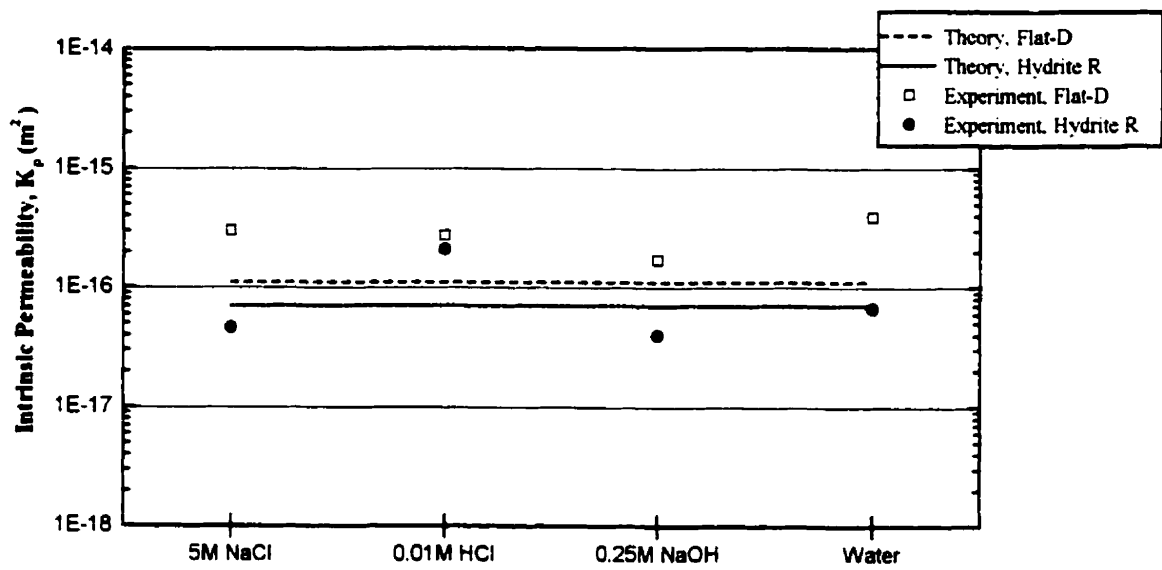
Figure 4.53 Theoretical and experimental permeability of compacted kaolinites permeated with inorganic chemicals.

fabric units are different, it is apparent that the Kozeny-Carman model becomes less valid. Figure 4.53 shows no solid relationship between the experimentally obtained permeabilities to inorganic permeants for the compacted clays of this study. The limited number of data points prevents further analysis through statistical regression.

Finally, a synthesis of the results for all leaching tests performed during the course of this study is presented in Table 4.1.

4.3 Soaking Test Results

To examine the influence of organic contaminants on the fabric of compacted kaolin clays under no flow conditions, a series of soaking tests was carried out following the protocol described in chapter 3. At the end of each test, the soaked samples were subjected to thorough visual inspections. Specimens of the contaminated soils were also scrutinized using SEM analysis. The resulted micrographs of the clay structure were compared with those of the as-compacted kaolinites. The SEM investigation was performed following the procedures discussed in the previous chapter.

4.3.1 Acetic Acid

The massive structure of the clays resulting from the static compaction was severely altered by exposure to the pure organic acid into an aggregated structure characterized by visible clod-size particles. The attack by acetic acid is clearly causing dissolution of soil components. A plug-like layer of approximately 10 mm thick was observed at the bottom of *Hydrite Flat-D* indicating partial precipitation following the dissolution process. SEM micrographs confirmed the alteration of the original compacted fabric into an aggregated one, as presented in Fig. 4.54.

Table 4.1 Results synthesis of the leaching tests.

Contaminant	Hydrite Flat-D		Hydrite R	
	K_w (x10^{-16} m^2)	K_p (x10^{-16} m^2)	K_w (x10^{-17} m^2)	K_p (x10^{-17} m^2)
Organics: Acetic Acid	3.7	1.7	8.2	5.1
Aniline	3.9	N/A	6.7	N/A
Ethanol	3.8	4.1	6.3	5.5
Heptane	4.2	2.2	7.0	21
Inorganics: 5M NaCl	2.5	3.0	6.0	4.6
0.01M HCl	4.0	2.7	18	21
0.25M NaOH	3.6	1.7	6.8	4.0

(a) Hydrite Flat-D
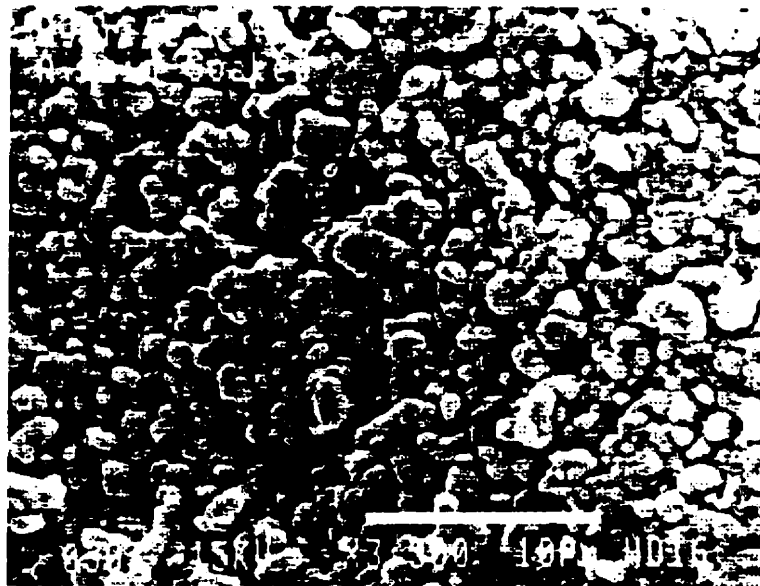
(b) Hydrite R

Figure 4.54 Scanning electron micrographs of compacted kaolinites soaked in Acetic Acid.

4.3.2 Aniline

Visual inspection of the compacted kaolinites soaked in aniline revealed visible pores and cracks on the soil surface directly exposed to the organic base. The macrofabric change was more extensive in the lower half of both kaolin clay samples. Contaminated specimens examined by SEM at the end of the soaking tests show limited interaction between aniline and kaolinites of this research as indicated by Fig. 4.55. Apparently, aniline is too weak a base to cause significant dissolution of clay soil constituents upon exposure.

4.3.3 Ethanol

The same observation noticed after the leaching test was again noted at the end of the soaking test: Hydrite Flat-D and Hydrite R samples had both become dehydrated and had lost much of their plasticity. Visual observation of the soil after ethanol soaking showed some local shrinkage and cracking. Soil shrinkage is usually associated with dehydration, suggesting that ethanol had displaced water from clay particle surfaces. Examination of ethanol-treated soils by SEM revealed minor changes in the fabric of kaolinite as shown in Fig. 4.56. The lower relative permittivity (dielectric constant) of ethanol may have caused a decrease in spacing between the clay minerals present in the soils and, thereby, promoted those limited structural changes. While ethanol can displace water from clay surfaces by virtue of its comparable dipole moment to that of water, it probably cannot form as many adsorbed layers as water due to its lower dielectric constant and higher molecular weight.

4.3.4 Heptane

The water immiscible solvent heptane had no effect on the fabric of kaolinites soaked in the pure hydrocarbon. Such indication was exemplified by visual inspection after the test which showed that both samples preserved their as-compacted massive structure. SEM investigation also confirmed the visual observation. The micrographs shown in Fig. 4.57

(a) Hydrite Flat-D

(b) Hydrite R
Figure 4.55 Scanning electron micrographs of compacted kaolinites soaked in Aniline.
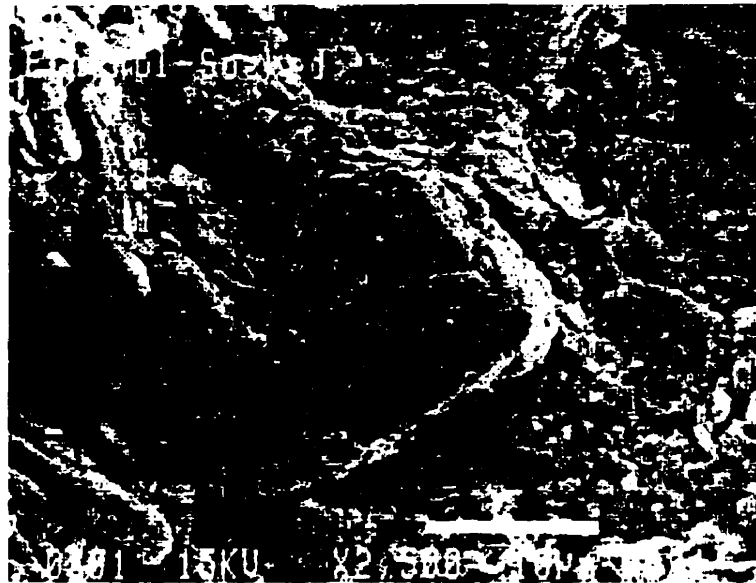
(a) Hydrite Flat-D

(b) Hydrite R

Figure 4.56 Scanning electron micrographs of compacted
kaolinites soaked in Ethanol.

(a) Hydrite Flat-D

(b) Hydrite R

Figure 4.57 Scanning electron micrographs of compacted kaolinites soaked in Heptane.

indicate that the particle arrangement of heptane-exposed kaolin clays was unaltered when compared with the fabric of the soils before treatment. Obviously, the limited ability of non-polar organic compounds to penetrate interlayer spaces of the clay minerals due to their hydrophobic nature is halting further interaction between clay particles and heptane.

4.4 Contaminant Transport Simulation

To simulate the one-dimensional transport problem of the present investigation, a steady-state seepage analysis had to be run first before solving the governing transport equation numerically. Modeling of the steady-state seepage flow was performed following the procedures outlined in chapter 3.

Results of numerical simulation conducted by finite element method using SEEP/W for the clays of this research are presented graphically on the finite element mesh as shown in Fig. 4.58. The total flux value in m^3/s across a defined section is computed and displayed for both kaolinites. Total head values in meters are also contoured and labeled in Fig. 4.58. SEEP/W computes the position of a specific contour line according to the values of total head at the nodes. Figure 4.58 displays the velocity vectors for each soil as determined from the finite element analysis. Velocity vectors are plotted with the tail of the vector at the center of the element; however, they cannot be drawn exactly to scale, since they would be too small to be visible.

Two cases of contaminant migration modeling are considered in this study. The first case is the analysis of the basic transport problem with diffusion and no adsorption. In other words, contaminant migration is only governed by the advection and dispersion processes. The modeling of this case is carried out by following the protocol discussed in chapter 3. The breakthrough of contaminant along the sample for different times is presented for both clays in Figs. 4.59(a) and 4.60(a).
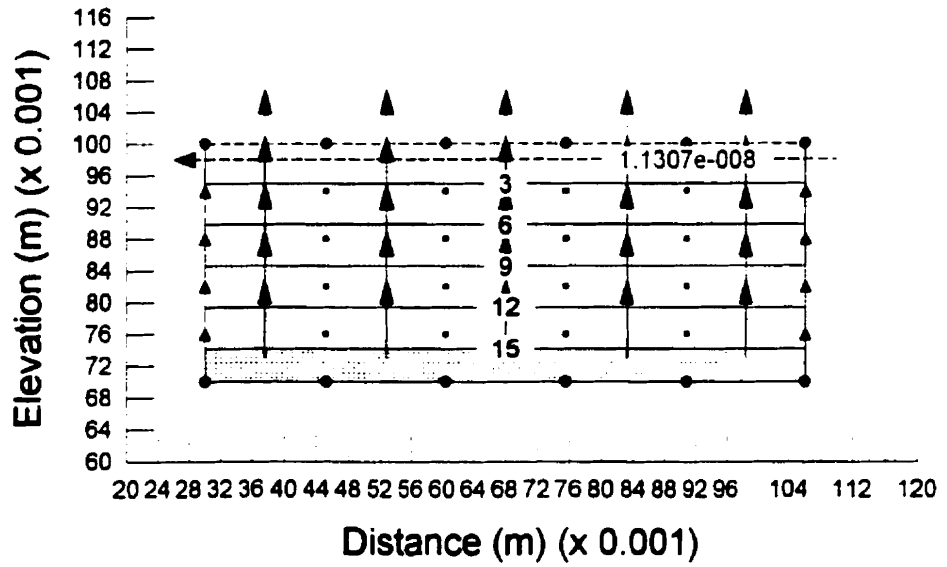
(a) Hydrite Flat-D
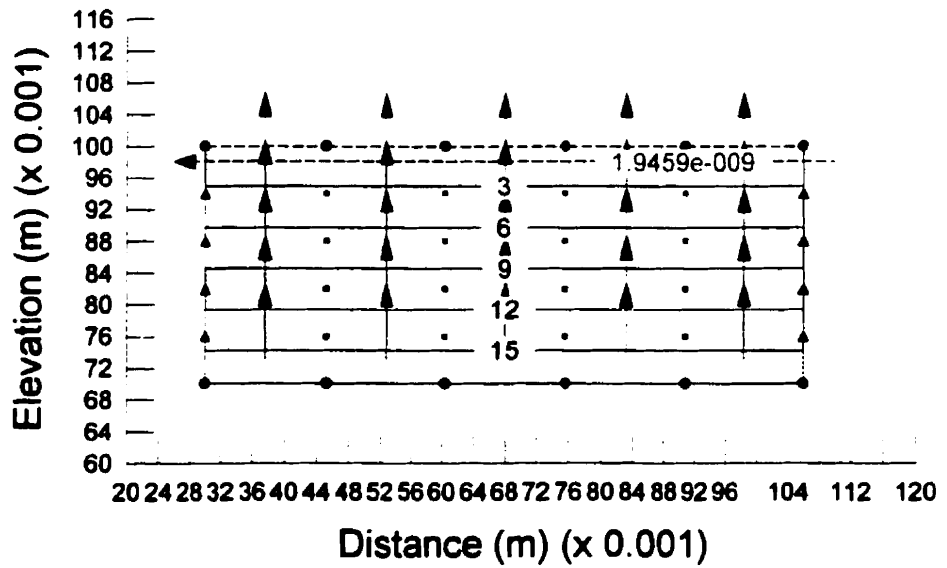
(b) Hydrite R

Figure 4.58 Numerical simulation results of SEEP/W.
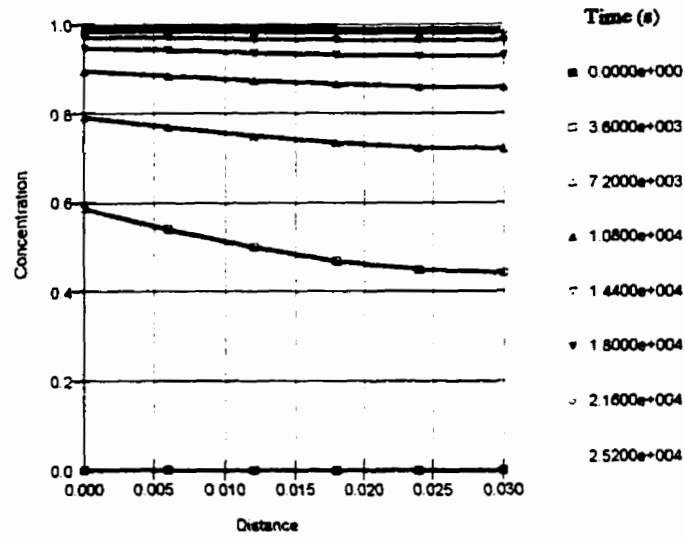
(a) with diffusion and no adsorption.
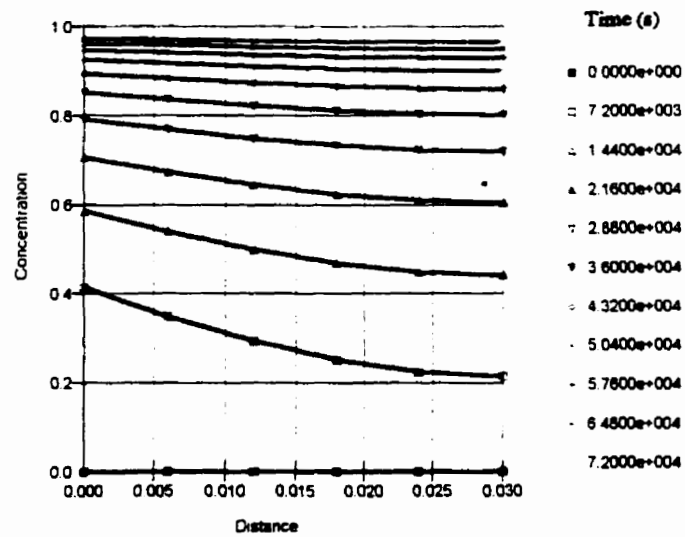
(b) with diffusion and adsorption

Figure 4.59 Numerical simulation results of CTRAN/W
for Hydrite Flat-D.
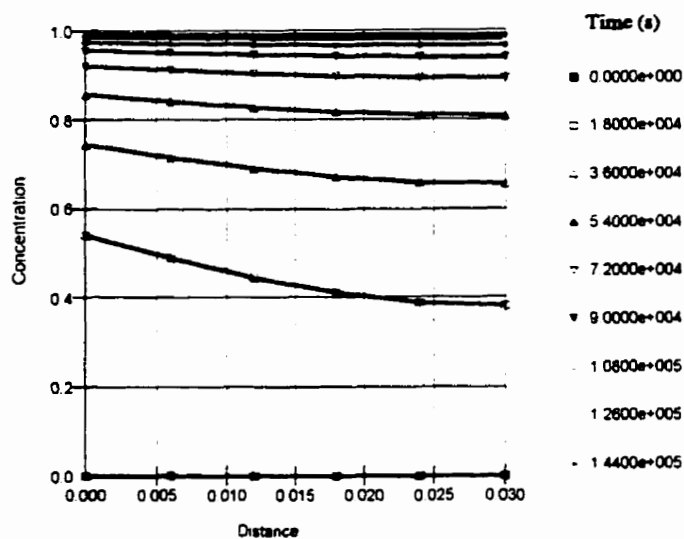
(a) with diffusion and no adsorption.
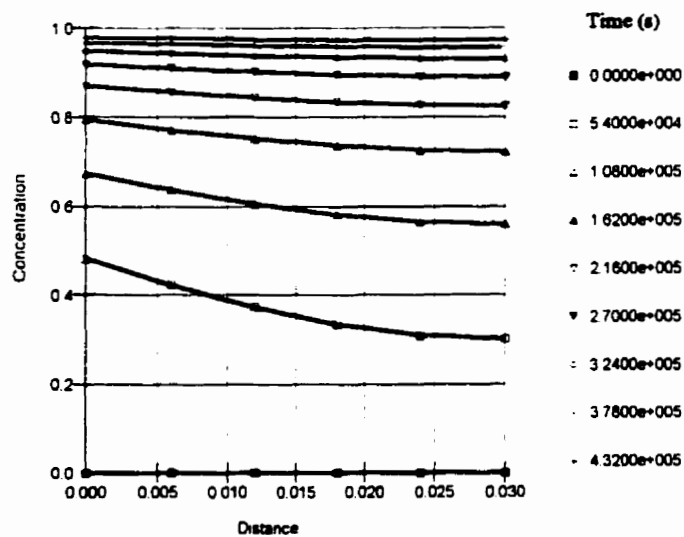
(b) with diffusion and adsorption

Figure 4.60 Numerical simulation results of CTRAN/W for Hydrite R.

The second scenario involves attenuation of the migrating contaminant. Adsorption in the transport process retards contaminant migration as the contaminant may be adsorbed to the soil particles. The effect of adsorption is expressed in a term generally referred to as the retardation factor R_d and is represented mathematically by Eq. 2.37. The simulation of this scenario is performed following the protocol described in the previous chapter. Numerical results of the contaminant transport considering both diffusion and adsorption processes are illustrated in Figs. 4.59(b) and 4.60(b) for *Hydrite Flat-D* and *Hydrite R*, respectively.

Contaminant breakthrough curves obtained analytically using the finite element method analysis and those resulted experimentally from the laboratory leaching tests are compared for the clays permeated with organic solvents and sodium chloride solution. Except for the first pore volume of flow, breakthrough curves of compacted kaolinites permeated with acetic acid are better simulated by the case where adsorption is considered with diffusion as shown in Fig. 4.61. On the other hand, soils leached with ethanol resulted in breakthrough curves which are closely simulated by the case of no adsorption, particularly for *Hydrite R*, as presented in Fig. 4.62 and excluding the result of first pore volume of flow.

Figure 4.63 shows the comparison between the experimental breakthrough curves of the clays contaminated by heptane and the numerical ones. No solid conclusion could be drawn from the trend illustrated by the heptane-treated *Hydrite Flat-D*, however, the results of *Hydrite R* confirm the belief that the breakthrough of hydrocarbon was triggered by sidewall leakage rather than genuine soil-contaminant interaction. Finally, the numerical simulation results obtained by taking into account the adsorption process are in perfect agreement with the breakthrough curves of chloride for both kaolin clays permeated with NaCl as shown in Fig. 4.64.

(a) Hydrite Flat-D

(b) Hydrite R
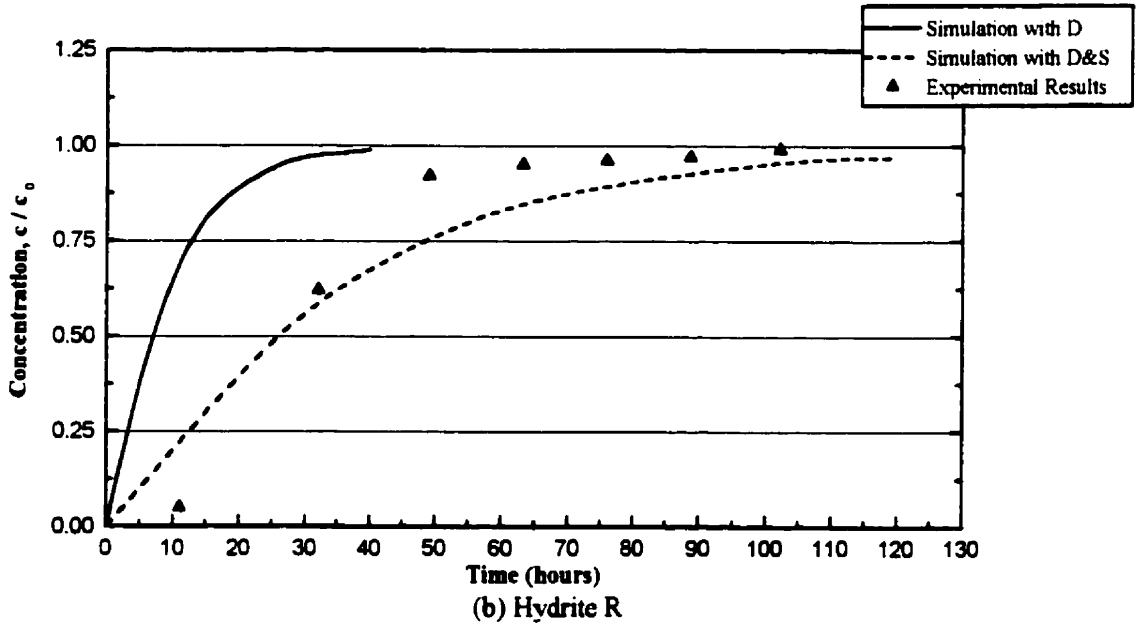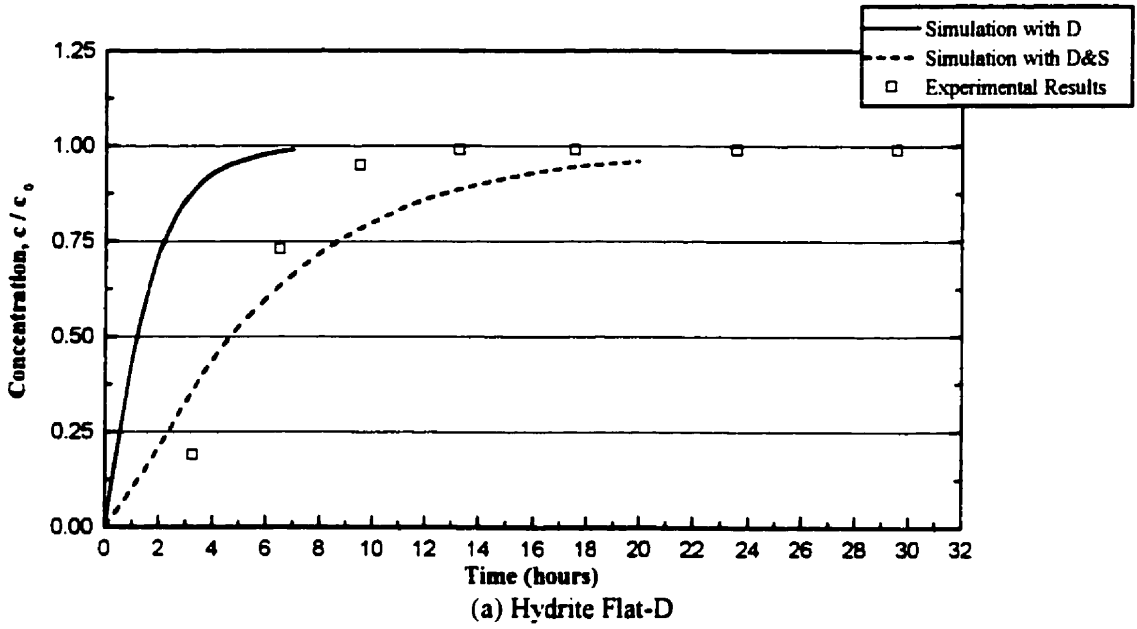
Figure 4.61 Comparison of breakthrough curves of compacted kaolinites permeated with Acetic Acid.

(a) Hydrite Flat-D

(b) Hydrite R
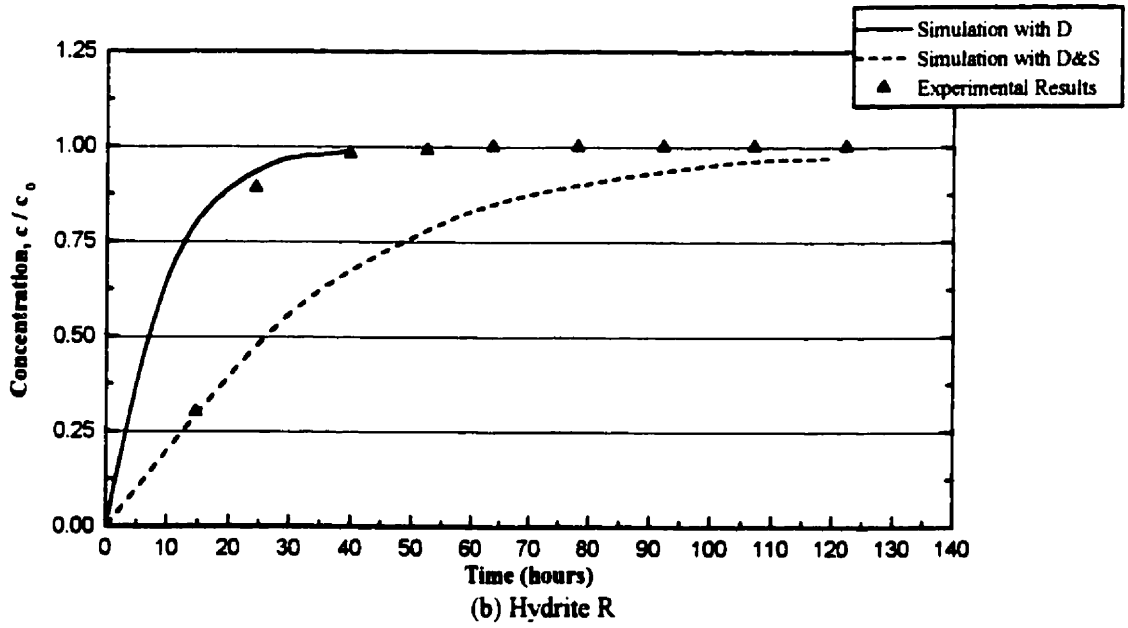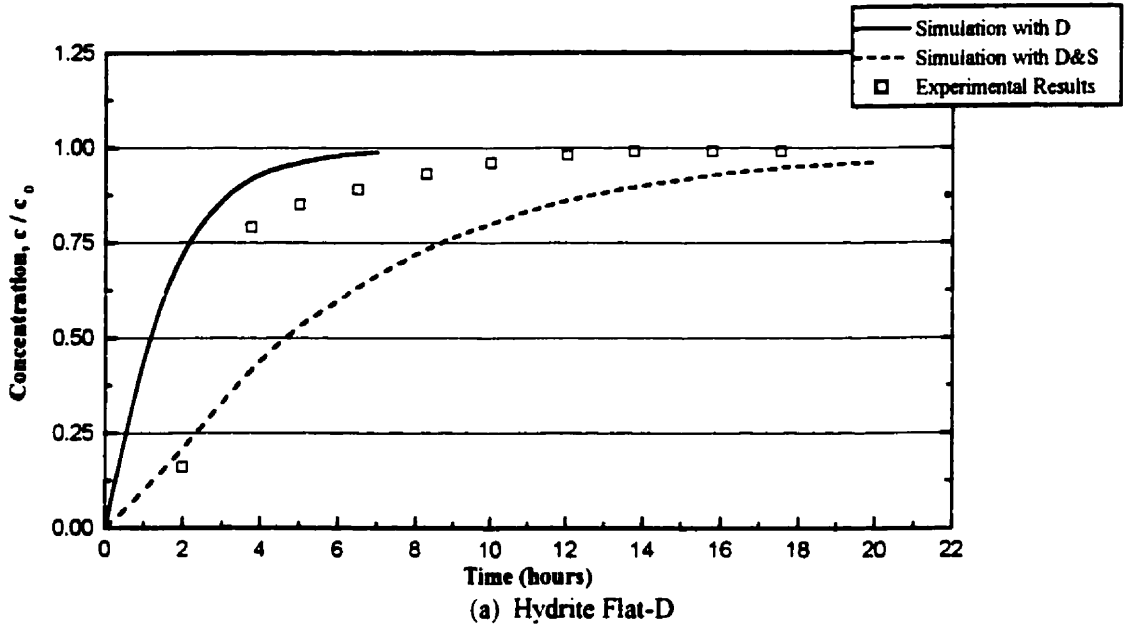
Figure 4.62 Comparison of breakthrough curves of compacted kaolinites permeated with Ethanol.
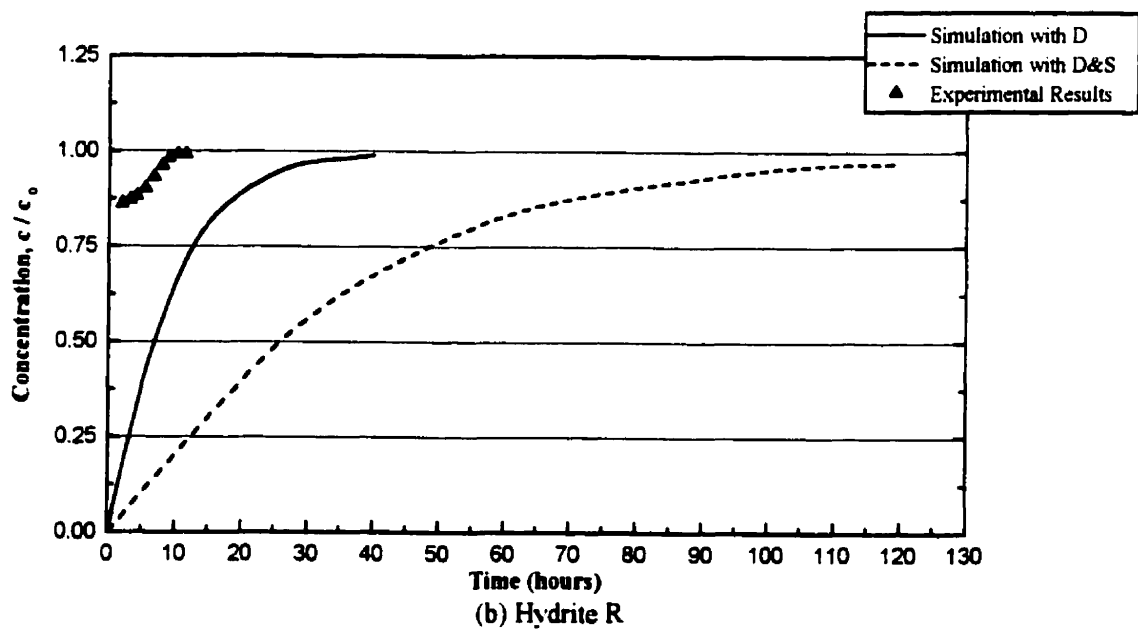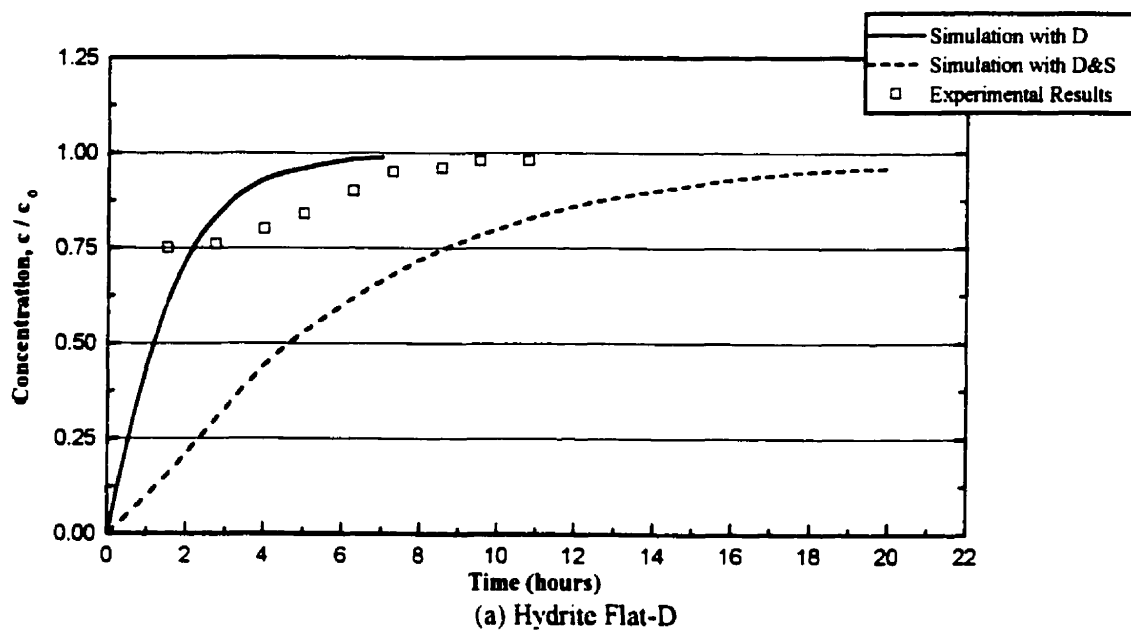
Figure 4.63 Comparison of breakthrough curves of compacted kaolinites permeated with Heptane.

(a) Hydrite Flat-D

(b) Hydrite R
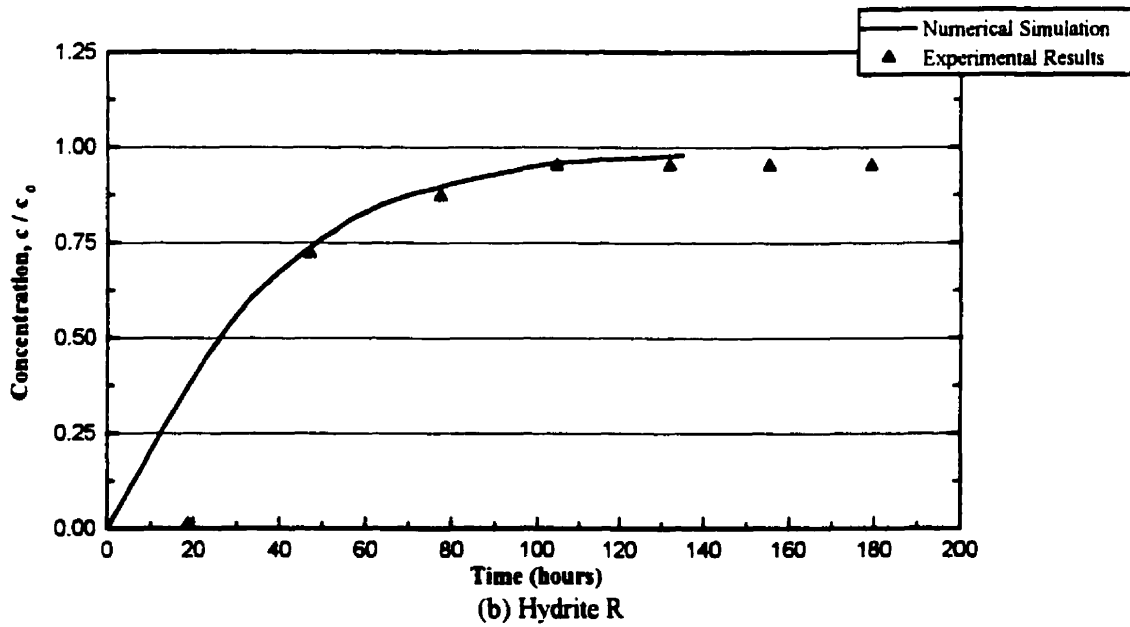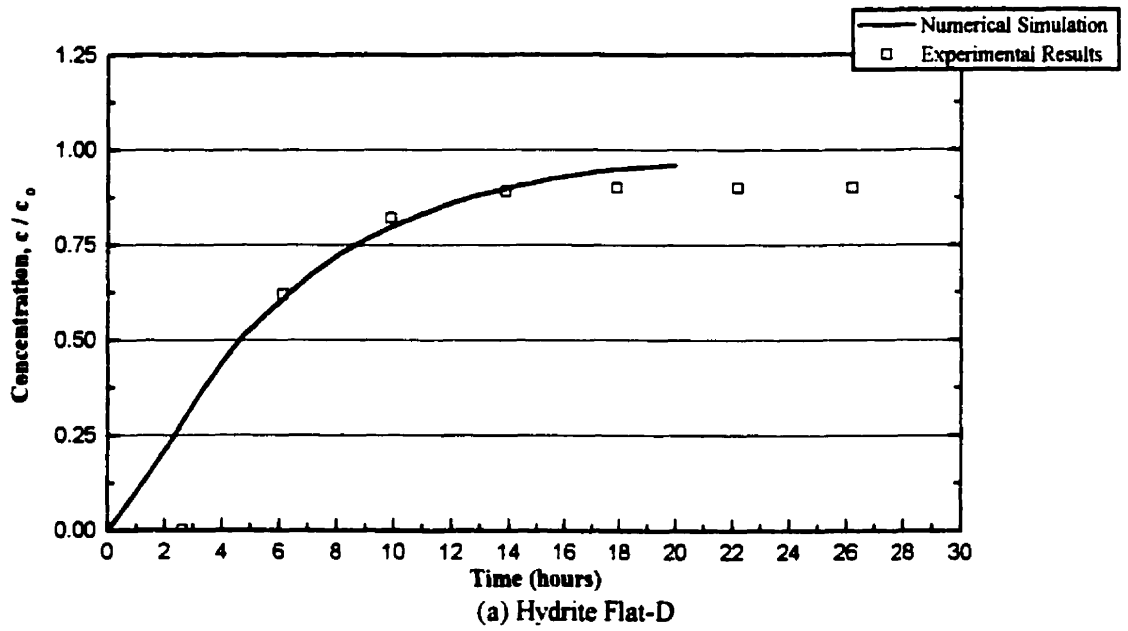
Figure 4.64 Comparison of breakthrough curves of compacted kaolinites permeated with 5M NaCl.

CHAPTER 5

CONCLUSIONS

Of the soil properties needed for solution of most geoenvironmental engineering problems, none varies over so wide a range or is so difficult to determine reliably as the hydraulic conductivity. The hydraulic conductivity and its susceptibility to changes with time or exposure to chemicals are the major factors in the selection of clay for use in waste containment barriers. A given soil, however, may exhibit large variations in hydraulic conductivity as a result of changes in fabric (particle arrangements), density, and water content. To understand how different chemicals can influence the hydraulic conductivity of fine-grained soils, and also, how variations of important magnitude in hydraulic conductivity can occur within small ranges of density and water content requires consideration of the importance of clay structure and the factors which affect it.

The present research performed on two different particle-size kaolin clays statically compacted at optimum moisture content and permeated with a spectrum of contaminants leads to the following conclusions with respect to soil structure and hydraulic conductivity:

❑ Despite the recently achieved advances in our knowledge concerning the field of soil-contaminant interactions and compatibility, the need is still persistent for the assessment of pollutants transport through soils and its impact on the soil structure; consequently, questioning the integrity of compacted clay barriers in waste disposal/containment facilities.

❑ An outstanding research is founded on a thorough, full characterization of the materials used in the research. The complete characterization of the clays and chemicals used as permeants in this study is accomplished. The different methods adopted to conduct the experimental program and numerical analysis are discussed and justified.

❑ Kaolinite compacted at optimum moisture content is characterized by an orderly arranged microfabric composed of flocculated aggregates and dispersed matrix. The matrix is formed by a dense stacking of domains in face-to-face contacts resulting in the so-called turbostratic structure. Maximum dry density is achieved by the matrix in clay compacted at

optimum water content. The aggregates are constructed of stepped face-to-face and edge-to-face arrangements of domains. The stair-stepped fabric provides strong resistance to compaction stress. The strong resistance of aggregates to compaction leads to the existence of large pores in clay compacted at optimum moisture content. Therefore, minimum values of hydraulic conductivity cannot be reached even though the soil possesses its maximum dry density, and thus the minimum void ratio.

❑ Pure organic contaminants are able to cause flocculation of clay particles by shrinking the diffuse double layer due to their relatively low permittivities. However, non-polar and hydrophobic compounds could not replace water in small pores, and thus has no effect on clay structure as revealed by scanning electron micrographs. Moreover, fabric changes observed in the soaked samples were restricted to local areas. The dissolution-precipitation phenomenon is confirmed by the attack of organic acid on both leached and soaked samples. Although a significant number of studies were carried out to evaluate the hydraulic conductivity of soils with organic fluids as permeants, it still is extremely difficult to select a single factor that can be identified as being responsible for the change in permeability when an organic fluid replaces water.

❑ Altered fabric and/or flocculated structure does not necessarily lead to an increase in hydraulic conductivity, especially if the clay has been properly compacted and is kept under confinement. Reductions in hydraulic conductivity were measured when the soil columns were permeated with the various chemicals. The value of this macroscopic property should be influenced by many other factors including: soil constituents and mineral composition, permeant properties, sample preparation procedures, stress conditions, hydraulic gradient range, and methods of hydraulic conductivity measurement.

❑ Permeation of a highly concentrated inorganic salt through compacted kaolinites did not result in a substantial change in intrinsic permeability. SEM investigations are consistent with the results of hydraulic conductivity measurements. Increase in electrolyte concentration does not alter the fabric of a properly compacted and confined clay.

❑ Inorganic acid and base with extremely low and high pHs have a slight effect on the structure of kaolin clays. Geochemical reactions, however, were detected. The buffer capacity

of clay particles might have played a more significant role in preventing the particles from being dissolved during leaching, as illustrated by SEM observations of the microfabric.

❏ Soaked samples in organic solvents for examining the impact of contaminant migration under pure diffusion on the structure of compacted clays confirmed the conclusions drawn upon the leaching tests. Except for the samples soaked in pure organic acid, no discernible differences in the clay fabric were observed with either *Hydrite Flat-D* or *Hydrite R*.

❏ Finite element method is employed to accomplish the analytical analysis of this research. The numerical simulation served as a bridge in evaluating the correlation between macroscopic and microscopic properties. It also shed more light on the extent of validity of simulating pollutant migration through soils by finite element method.

❏ Scanning electron microscopy has proved to be a powerful tool for revealing soil structure at the microscopic level. The SEM maintains high resolution under magnification and produces a depth field of the images. The shadows and perspective of the micrographs provide abundant topographical information invaluable to studying soil fabric. Smaller particles can be discerned from distant particles on the photo. Overlapping particles can also be identified. Nevertheless, the application of SEM to microfabric observation on compacted clays is challenging due to the complicated, and sometimes tedious, specimen preparation techniques and SEM operations.

Future Research:

Based on the findings of this study, the following recommendations could be concluded:

❏ Investigating the impact of contaminant migration, by direct observation using SEM, on the structure of more active clays, for instance, illite, would be the natural extent of this research. Furthermore, natural clays actually employed or potential to be acting as hydraulic barriers for engineered landfills and surface impoundments have to be scrutinized

by means of SEM analyses to assess their compatibility and integrity regarding hazardous waste storage.

❑ Geotechnical behavior of soils leached with hazardous contaminants has not attracted yet its due attention. A research concentrating on the mechanical behavior of clays after leaching with various contaminants would indeed add more insight into the problem of contaminant migration.

❑ Elevated hydraulic gradients ($i > 100$) typically are applied in laboratory hydraulic conductivity and contaminant compatibility tests to speed the testing times. A number of studies have investigated the effect of applied hydraulic gradient and the associated stress levels on the measurement of the hydraulic conductivity of soils. Most of these studies, however, pertain to the use of flexible-wall tests since the effective stress conditions in rigid-wall hydraulic conductivity tests are unknown. Further research examining the actual stress conditions in rigid-wall permeameters is certainly needed.

❑ Although it is generally accepted that rigid-wall tests tend to overestimate hydraulic conductivity values for various reasons, principally side-wall leakage, less information on the effects of hydraulic gradient exists for rigid-wall tests. More studies investigating the impact of different hydraulic gradients on the results of the rigid-wall tests are highly recommended.

REFERENCES

ACAR, Y.B. and SEALS, R.K. (1984). Clay Barrier Technology for Shallow Land Waste Disposal Facilities. *Hazardous Waste*, Vol. 1, No. 2, pp. 167-181.

ACAR, Y.B., HAMIDON, A., FIELD, S.D. and SCOTT, L. (1985a). The Effect of Organic Fluids on Hydraulic Conductivity of Compacted Kaolinite. *Hydraulic Barriers in Soil and Rock*, ASTM STP 874, A.I. Johnson et al., Eds., American Society for Testing and Materials, Philadelphia.

ACAR, Y.B., OLIVIERI, I. and FIELD, S.D. (1985b). The Effect of Organic Fluids on the Pore Size Distribution of Compacted Kaolinite. *Hydraulic Barriers in Soil and Rock*, ASTM STP 874, A.I. Johnson et al., Eds., American Society for Testing and Materials, Philadelphia.

ACAR, Y.B. and D'HOLLOSY, E. (1987). Assessment of Pore Fluid Effects using Flexible Wall and Consolidation Permeameters. *Geotechnical Practice for Waste Disposal '87*, ASCE GSP 13, R.D. Woods, Ed., American Society of Civil Engineers, New York.

ACAR, Y.B. and OLIVIERI, I. (1989). Pore Fluid Effects on the Fabric and Hydraulic Conductivity of Laboratory-Compacted Clay. *Geotechnical Engineering 1989, Transportation Research Record 1219*, Transportation Research Board, National Research Council, Washington, D.C., pp. 144-159.

AHMED, S., LOVELL, C.W. and DIAMOND, S. (1974). Pore Sizes and Strength of Compacted Clay. *Journal of the Geotechnical Engineering Division*, ASCE, Vol. 100, No. GT4, pp. 407-425.

AL-TABBAA, A. and WOOD, D.M. (1987). Some Measurements of the Permeability of Kaolin. *Géotechnique*, Vol. 37, No. 4, pp. 499-503.

ALTHER, G., EVANS, J.C., FANG, H.-Y. and WITMER, K. (1985). Influence of Inorganic Permeants upon the Permeability of Bentonite. *Hydraulic Barriers in Soil and Rock*, ASTM STP 874, A.I. Johnson et al., Eds., American Society for Testing and Materials, Philadelphia.

ANDERSON, D.C., BROWN, K.W. and THOMAS, J.C. (1985a). Conductivity of Compacted Clay Soils to Water and Organic Liquids. *Waste Management and Research*, Vol. 3, No. 4, pp. 339-349.

ANDERSON, D.C., CRAWLEY, W. and ZABCIK, J.D. (1985b). Effects of Various Liquids on Clay Soil: Bentonite Slurry Mixtures. *Hydraulic Barriers in Soil and Rock*, ASTM STP 874, A.I. Johnson et al., Eds., American Society for Testing and Materials, Philadelphia.

ANDERSON, M.P. (1984). Movement of Contaminants in Gorundwater: Groundwater Transport - Advection and Dispersion. In: *Groundwater Contamination*, Studies in Geophysics, National Academy Press, Washington, D.C.

ASTM (1995). *1995 Annual Book of ASTM Standards*. Section 4, Vol. 04.08, American Society for Testing and Materials, Philadelphia.

AYLMORE, L.A.G. and QUIRK, J.P. (1959). Swelling of Clay-Water Systems. *Nature*, Vol. 183, pp. 1752-53.

AYLMORE, L.A.G. and QUIRK, J.P. (1960). Domain or Turbostratic Structure of Clays. *Nature*, Vol. 187, pp. 1046-48.

AYLMORE, L.A.G. and QUIRK, J.P. (1962). The Structural Status of Clay Systems. *Proc. 9th National Conf. on Clays and Clay Minerals*, pp. 104-130.

BAILEY, S.W., BRINDLEY, G.W., JOHNS, W.D., MARTIN, R.D. and ROSS, M. (1971). Summary of National and International Recommendations on Clay Mineral Nomenclature and Report of Nomenclature Committee. *Clays and Clay Minerals*, Vol. 19, pp. 129-133.

BARBOUR, S.L. and YANG, N. (1993). A Review of the Influence of Clay-Brine Interactions on the Geotechnical Properties of Ca-Montmorillonitic Clayey Soils from Western Canada. *Canadian Geotechnical Journal*, Vol. 30, pp. 920-934.

BARDEN, L. (1972). The Influence of Structure on Deformation and Failure in Caly Soils. *Géotechnique*, Vol. 22, No. 2, pp. 159-163.

BARDEN, L. and SIDES, G.R. (1970). Engineering Behavior and Structure of Compacted Clay. *Journal of the Soil Mechanics and Foundations Division*, ASCE, Vol. 96, No. SM4, pp. 1171-1200.

BEAR, J. (1972). *Dynamics of Fluids in Porous Media*. American Elsevier Publishing, Inc., New York.

BEAR, J. (1979). *Hydraulics of Groundwater*. McGraw-Hill Book Co., New York.

BEAR, J. and VERRUIJT, A. (1987). *Theory and Applications of Transport in Porous Media*. D. Reidel Publ. Co., Dordrecht, Holland.

BENSON, C.H. and DANIEL, D.E. (1990). Influence of Clods on Hydraulic Conductivity of Compacted Clay. *Journal of Geotechnical Engineering*, ASCE, Vol. 116, No. 8, pp. 1231-48.

BERNAL, J.D. and FOWLER, R.H. (1933). A Theory of Water and Ionic Solution with Particular Reference to Hydrogen and Hydroxyl Ions. *J. Chem. Phys.*, 1:515-548.

BIGGAR, J.W. and NIELSON, D.R. (1960). Diffusion Effects in Miscible Displacement Occurring in Saturated and Unsaturated Porous Materials. *J. Geophys. Res.*, Vol. 65, No. 9, pp. 2887-95.

BNQ 2501-092 (1986). *Sols - Détermination de la Limite de Liquidité à l'aide du Pénétromètre à Cône Suédois et de la Limite de Plasticité*. Le Bureau de normalisation du Québec, Norme nationale du Canada.

BOHN, H.L., McNEAL, B.L. and O'CONNOR, G.A. (1969). *Soil Chemistry*. John Wiley & Sons, Inc., N.Y., 329 p.

BOLT, G.H. (1955). Analysis of the Validity of the Gouy-Chapman Theory of the Electric Double Layer. *J. Colloid Sci.*, Vol. 10, pp. 206-218.

BOWDERS, J.J., Jr., DANIEL, D.E., BRODERICK, G.P. and LILJESTRAND, H.M. (1986). Methods for Testing the Compatibility of Clay Liners with Landfill Leachate. *Hazardous and Industrial Solid Waste Testing: 4th Symposium*, ASTM STP 886, J.K. Petros et al., Eds., American Society for Testing and Materials, Philadelphia.

BOWDERS, J.J., Jr. and DANIEL, D.E. (1987). Hydraulic Conductivity of Compacted Clay to Dilute Organic Chemicals. *Journal of Geotechnical Engineering*, ASCE, Vol. 113, No. 12, pp. 1432-48.

BOWDERS, J.J., Jr. (1988). Discussion on: Termination Criteria for Clay Permeability Testing, by J.J. Peirce and K.A. Witter. *Journal of Geotechnical Engineering*, ASCE, Vol. 114, No. 8, pp. 947-950.

BOWLES, J.E. (1978). *Engineering Properties of Soils and their Measurement*. 2nd ed., Int'l. Student Edition, McGraw-Hill, Inc., 213 p.

BOWLES, J.E. (1979). *Physical and Geotechnical Properties of Soils*. Int'l. Student Edition, McGraw-Hill, Inc., 478 p.

BOYNTON, S.S. and DANIEL, D.E. (1985). Hydraulic Conductivity Tests on Compacted Clay. *Journal of Geotechnical Engineering*, ASCE, Vol. 111, No. 4, pp. 465-478.

BREWER, R. (1964). *Fabric and Mineral Analysis of Soils*. Wiley, New York.

BRODERICK, G.P. and DANIEL, D.E. (1990). Stabilizing Compacted Clay against Chemical Attack. *Journal of Geotechnical Engineering*, ASCE, Vol. 116, No. 10, pp. 1549-67.

BRONGNIART, A. (1807). *Traité élémentaire de minéralogie*. Vol. 1, Paris, p. 506.

BROWN, G. (1955). Report of the Clay Minerals Group Sub-Committee on Nomenclature of Clay Minerals. *Clay Minerals Bull.*, 2 (13), pp. 294-302.

BUDHU, M., GIESE, R.F., CAMPBELL, G. and BAUMGRASS, L. (1991). The Permeability of Soils with Organic Fluids. *Canadian Geotechnical Journal*, Vol. 28, pp. 140-147.

BUCKMAN, H.O. and BRADY, N.C. (1969). *The Nature and Properties of Soils*. 7th ed., The MacMillan Co., N.Y., 653 p.

CABRAL, A.R. (1992). *A Study of Clay Compatibility to Heavy Metal Transport in Permeability Testing*. Ph.D. Dissertation, Department of Civil Engineering and Applied Mechanics, McGill University, Montréal, Canada.

CARMAN, P.C. (1956). *Flow of Gases Through Porous Media*. Academic Press, New York.

CARPENTER, G.W. and STEPHENSON, R.W. (1985). Permeability Testing in the Triaxial Cell. *Geotechnical Testing Journal*, ASTM, Vol. 8, No. 1, pp. 3-10.

CARTER, D.L., MORTLAND, M.M. and KEMPER, W.D. (1986). Specific Surface. *Methods of Soil Analysis, Part 1. Physical and Mineralogical Methods.* 2nd ed., A. Klute, Ed., American Society of Agronomy & Soil Science Society of America, Madison, Wisconsin.

CASAGRANDE, A. (1932). The Structure of Clay and its Importance in Foundation Engineering. *Journal of the Boston Society of Civil Engineers,* BSCE, Vol. 19, No. 4, pp. 72-112.

CEDERGREN, H.R. (1989). *Seepage, Drainage, and Flow Nets.* 3rd ed., John Wiley & Sons, Inc., N.Y., 465 p.

CHAN, H.R. and KENNEY, T.C. (1973). Laboratory Investigation of the Permeability Ratio of New Liskeard Varved Soil. *Canadian Geotechnical Journal,* Vol. 10, pp. 453-472.

CHAPMAN, D. (1913). A Contribution to the Theory of Electrocapillarity. *Philosophical Magazine,* Vol. 25, No. 6, pp. 475-481.

CHAPMAN, H.D. (1965). Cation-Exchange Capacity. *Methods of Soil Analysis, Part 2. Chemical and Microbiological Properties.* C.A. Black et al., Eds., American Society of Agronomy & American Society for Testing and Materials, Madison, Wisconsin.

CHAPUIS, R.P. (1981). Permeability Testing of Soil-Bentonite Mixtures. *Proc. 10th Int'l. Conf. SMFE,* Stockholm.

CHAPUIS, R.P., BAASS, K. and DAVENNE, L. (1989). Granular Soils in Rigid-Wall Permeameters: Method for Determining the Degree of Saturation. *Canadian Geotechnical Journal,* Vol. 26, pp. 71-79.

CHAPUIS, R.P. (1990). Sand-Bentonite Liners: Predicting Permeability from Laboratory Tests. *Canadian Geotechnical Journal,* Vol. 27, pp. 47-57.

CHAPUIS, R.P. and MONTOUR, I. (1992). Évaluation de l'équation de Kozeny-Carman pour prédire la conductivité hydraulique. *Proc. 45th Canadian Geotechnical Conference,* Toronto.

CHAPUIS, R.P., CRESPO, R., CHENAF, D. and AUBERTIN, M. (1993). Evaluation of a Ground Water F.E.M. Software for Steady and Unsteady State Conditions. *Proc. 46th Canadian Geotechnical Conference,* Saskatoon.

CARTER, D.L., MORTLAND, M.M. and KEMPER, W.D. (1986). Specific Surface. *Methods of Soil Analysis, Part 1. Physical and Mineralogical Methods.* 2nd ed., A. Klute., Ed., American Society of Agronomy & Soil Science Society of America, Madison, Wisconsin.

COLLINS, K. and McGOWN, A. (1974). The Form and Function of Microfabric Features in a Variety of Natural Soils. *Géotechnique*, Vol. 24, pp. 223-254.

CRAIG, R.F. (1987). *Soil Mechanics.* 4th ed., Van Nostrand Reinhold Co. Ltd, UK, 410 p.

DANIEL, D.E. (1984). Predicting Hydraulic Conductivity of Clay Liners. *Journal of Geotechnical Engineering*, ASCE, Vol. 110, No. 2, pp. 285-300.

DANIEL, D.E., TRAUTWEIN, S.J., BOYNTON, S.S. and FOREMAN, D.E. (1984). Permeability Testing with Flexible-Wall Permeameters. *Geotechnical Testing Journal*, ASTM, Vol. 7, No. 3, pp. 113-122.

DANIEL, D.E., ANDERSON, D.C. and BOYNTON, S.S. (1985). Fixed-Wall Versus Flexible-Wall Permeameters. *Hydraulic Barriers in Soil and Rock*, ASTM STP 874, A.I. Johnson et al., Eds., American Society for Testing and Materials, Philadelphia.

DANIEL, D.E. (1987a). Earthen Liners for Land Disposal Facilities. *Geotechnical Practice for Waste Disposal '87*, ASCE GSP 13, Richard D. Woods, Ed., American Society of Civil Engineers, New York.

DANIEL, D.E. (1987b). Hydraulic Conductivity Tests for Clay Liners. *Geotechnical and Geohydrological Aspects of Waste Management*, D.J.A. van Zyl et al., Eds., Lewis Publishers, Inc., Michigan.

DANIEL, D.E. and BENSON, C.H. (1990). Water Content-Density Criteria for Compacted Soil Liners. *Journal of Geotechnical Engineering*, ASCE, Vol. 116, No. 12, pp. 1811-30.

DANIEL, D.E. (1993). Landfills and Impoundments. Chap. 5 in: *Geotechnical Practice for Waste Disposal*, David E. Daniel, Ed., Chapman & Hall, UK.

DANIEL, D.E. (1994). State-of-the-Art: Laboratory Hydraulic Conductivity Tests for Saturated Soils. *Hydraulic Conductivity and Waste Contaminant Transport in Soil*,

ASTM STP 1142, David E. Daniel and Stephen J. Trautwein, Eds., American Society for Testing and Materials, Philadelphia.

D'APPOLONIA, D.J. (1980). Soil-Bentonite Slurry Trench Cutoffs. *Journal of Geotechnical Engineering*, ASCE, Vol. 106, No. 4, pp. 399-417.

DARCY, H. (1856). *Les fontaines publiques de la ville de Dijon*. Victor Dalmont, Paris.

DAS, B.M. (1983). *Advanced Soil Mechanics*. Hemisphere Publishing Corporation, N.Y., 511 p.

DAS, B.M. (1994). *Principles of Geotechnical Engineering*. 3rd ed., PWS Pub. Co., Boston, Mass., 672 p.

De WEIST, R.J.M. (1965). *Geohydrology*. John Wiley and Sons, Inc., New York.

Des CLOIZEAUX, A. (1862). *Supplement to Manual of Mineralogy*. Vol. 1, Paris, pp. 548-549.

DIAMOND, S. (1970). Pore Size Distributions in Clays. *Clays and Clay Minerals*, Vol. 18, pp. 7-23.

DIAMOND, S. (1971). Microstructure and Pore Structure of Impact-Compacted Clays. *Clays and Clay Minerals*, Vol. 19, pp. 239-249.

DICK, A.B. (1908). Supplementary Note on the Mineral Kaolinite. *Mineral. Mag.*, 15:127.

DUNN, R.J. and MITCHELL, J.K. (1984). Fluid Conductivity Testing of Fine-Grained Soils. *Journal of Geotechnical Engineering*, ASCE, Vol. 110, No. 11, pp. 1648-65.

EDIL, T.B. and ERICKSON, A.E. (1985). Procedure and Equipment Factors Affecting Permeability Testing of a Bentonite-Sand Liner Material. *Hydraulic Barriers in Soil and Rock*, ASTM STP 874, A.I. Johnson et al., Eds., American Society for Testing and Materials, Philadelphia.

EISENBERG, D. and KAUZMAN, W. (1969). *The Structure and Properties of Water*. Oxford University Press, New York.

ELSBURY, B.R., DANIEL, D.E., SRADERS, G.A. and ANDERSON, D.C. (1990). Lessons Learned from Compacted Clay Liner. *Journal of Geotechnical Engineering*, ASCE, Vol. 116, No. 11, pp. 1641-60.

EVANS, J.C., FANG, H.-Y. and KUGELMAN, I.J. (1985). Organic Fluid Effects on the Permeability of Soil-Bentonite Slurry Walls. *Proc. Nat'l. Conf. Hazardous Wastes and Environmental Emergencies*, Cincinnati, OH.

FAHMY, Y. and SILVESTRI, V. (1999). Assessment of Fabric Changes of Clay due to Contaminant Transport. *Proc. 4th Int'l. Symp. on Environmental Geotechnology, Boston '98*, August 9-13, 1998, Boston (Danvers), MA.

FERNANDEZ, F. and QUIGLEY, R.M. (1985). Hydraulic Conductivity of Natural Clays Permeated with Simple Liquid Hydrocarbons. *Canadian Geotechnical Journal*, Vol. 22, pp. 205-214.

FERNANDEZ, F. and QUIGLEY, R.M. (1988). Viscosity and Dielectric Constant Controls on the Hydraulic Conductivity of Clayey Soils Permeated with Water-Soluble Organics. *Canadian Geotechnical Journal*, Vol. 25, pp. 582-589.

FITZPATRICK, E.A. (1993). *Soil Microscopy and Micromorphology*. John Wiley & Sons Ltd, U.K., 304 p.

FOREMAN, D.E. and DANIEL, D.E. (1986). Permeation of Compacted Clay with Organic Chemicals. *Journal of Geotechnical Engineering*, ASCE, Vol. 112, No. 7, pp. 669-681.

FREEZE, R.A. and CHERRY, J.A. (1979). *Groundwater*. Prentice-Hall, Inc., Englewood Cliffs, N.J., 604 p.

FRIED, J.J. (1975). *Groundwater Pollution*. Elsevier Scientific Publishers, Amsterdam.

FRIPIAT, J.J. (1964). Surface Properties of Alumino-Silicates. *Proc. 12th National Clay Conference*, Pergamon Press, N.Y., pp. 327-358.

GARCIA-BENGOCHEA, I., LOVELL, C.W. and ALTSCHAEFFL, A.G. (1979). Pore Distribution and Permeability of Silty Clays. *Journal of the Geotechnical Engineering Division*, ASCE, Vol. 105, No. GT7, pp. 839-856.

GARCIA-BENGOCHEA, I. and LOVELL, C.W. (1981). Correlative Measurements of Pore Size Distribution and Permeability in Soils. *Permeability and Groundwater Contaminant Transport*, ASTM STP 746, T.F. Zimmie and C.O. Riggs, Eds., American Society for Testing and Materials, Philadelphia.

GILLHAM, R.W., ROBIN, M.J.L., DYTYNYSHYN, D.J. and JOHNSTON, H.M. (1984). Diffusion of Nonreactive and Reactive Solutes Through Fine-Grained Barrier Materials. *Canadian Geotechnical Journal*, Vol. 21, pp. 541-550.

GOLDSCHMIDT, V.M. (1926). Undersokelser ved Lersedimenter. Nordisk Fordbrugsforskning, Kongress 3, Kobenhavn, pp. 434-445.

GORDON, B.B. and FORREST, M. (1981). Permeability of Soils Using Contaminated Permeant. *Permeability and Groundwater Contaminant Transport*, ASTM STP 746, T.F. Zimmie and C.O. Riggs, Eds., American Society for Testing and Materials, Philadelphia.

GOUY, G. (1910). Sur la constitution de la charge électrique à la surface d'un électrolyte. *Annale Physique*, Série 4, Vol. 9, pp. 457-468.

GRAY, D.H. and MITCHELL, J.K. (1967). Fundamental Aspects of Electro-Osmosis in Soils. *Journal of the Soil Mechanics and Foundations Division*, ASCE, Vol. 93, No. SM6, pp. 209-236, Closure Discussion: Vol. 95, No. SM3, pp. 875-879.

GRAY, D.H. and WEBER, W.J., Jr. (1984). Diffusional Transport of Hazardous Waste Leachate Across Clay Barriers. *Proc. 7th Ann. Madison Waste Conf.*, University of Wisconsin, Madison.

GREEN, W.J., LEE, G.F. and JONES, R.A. (1981). Clay-Soils Permeability and Hazardous Waste Storage. *J. Water Pollut. Control Fed.*, Water Pollution Control Federation, Washington, D.C., Vol. 53, No. 8, pp. 1347-54.

GREENBERG, J.A., MITCHELL, J.K. and WITHERSPOON, P.A. (1973). Coupled Salt and Water Flows in a Groundwater Basin. *J. Geophys. Res.*, Vol. 78, pp. 6341-53.

GRIFFIN, R.A. and ROY, W.R. (1985). *Interaction of Organic Solvents with Saturated Soil-Water Systems*. Environmental Institute for Waste Management Studies, University of Alabama, Tuscaloosa, Alabama.

GRIM, R.E. (1968). *Clay Mineralogy*. 2nd ed., McGraw-Hill, Inc., N.Y., 596 p.

GUPTA, R.P. and SWARTZENDRUBER, D. (1962). Flow-Associated Reduction in the Hydraulic Conductivity of Quartz Sand. *Soil Science Society of America Proc.*, pp. 6-10.

HANSBO, S. (1960). Consolidation of Clay with Special Reference to the Influence of Vertical Sand Drains. *Proceedings*, 18, Swedish Geotechnical Institute, Stockholm.

HANSBO, S. (1973). Influence of Mobile Particles in Soft Clay on Permeability. *Proc. Int'l. Symposium on Soil Structure*, Gothenburg, Sweden, pp. 132-135.

HESSE, P.R. (1971). *A Textbook of Soil Chemical Analysis*. John Murray Ltd., London, England.

HILLEL, D. (1980). *Fundamentals of Soil Physics*. Academic Press, Inc., New York.

HOLTZ, R.D. and KOVACS, W.D. (1981). *An Introduction to Geotechnical Engineering*. Prentice-Hall, Inc., Englewood Cliffs, N.J., 733 p.

HORTON, R., THOMPSON, M.L. and McBRIDE, J.F. (1985). Estimating Transit Times of Noninteracting Pollutants Through Compacted Soil Materials. *Proc. 11th Ann. Solid Waste Res. Symp.*, Cincinnati, Ohio.

INGLES, O.G. (1968). Soil Chemistry Relevant to the Engineering Behavior of Soils. Chapter I in *Soil Mechanics, Selected Topics*, I.K. Lee, Ed., Elsevier, New York.

IWATA, S., TABUCHI, T. and WARKENTIN, B.P. (1995). *Soil-Water Interactions: Mechanisms and Applications*. 2nd ed., Revised and Expanded, Marcel Dekker, New York.

JOHNSON, S.W. and BLAKE, J.M. (1867). On Kaolinite and Pholerite. *Am. J. Sci.*, ser. 2, 43, pp. 351-361.

KARICHOFF, S.W., BROWN, D.S. and SCOTT, T.A. (1979). Sorption of Hydrophobic Pollutants on Natural Sediments. *Water Research*, Vol. 13, pp. 241-248.

KING, K.S., QUIGLEY, R.M., FERNANDEZ, F., READES, D.W. and BACOPOULOS, A. (1993). Hydraulic Conductivity and Diffusion Monitoring of the Keele Valley Landfill Liner, Maple, Ontario. *Canadian Geotechnical Journal*, Vol. 30, pp. 124-134.

KIRKHAM, D. and POWERS, W.L. (1972). *Advanced Soil Physics*. John Wiley & Sons, Inc., New York.

KOZENY, J. (1927). Ueber Kapillare Leitung des Wassers im Boden. *Wien, Akad. Wiss.*, Vol. 136, Part 2a.

LAGALY, G. (1984). Clay-Organic Interactions. *Philosophical Transactions of the Royal Society of London*, Vol. A311, pp. 315-332.

LAMBE, T.W. (1953). The Structure of Inorganic Soil. *Proc. American Society of Civil Engineers*, ASCE, Vol. 79, Separate No. 315, pp. 1-49.

LAMBE, T.W. (1954). The Permeability of Fine-Grained Soils. *Permeability of Soils*, ASTM STP 163, American Society for Testing and Materials, Philadelphia.

LAMBE, T.W. (1956). The Storage of Oil in an Earth Reservoir. *Journal of the Boston Society of Civil Engineers*, BSCE, Vol. 43, No. 3, pp. 111-173.

LAMBE, T.W. (1958a). The Structure of Compacted Clay. *Journal of the Soil Mechanics and Foundations Division*, ASCE, Vol. 84, No. SM2, Paper 1655, pp. 1-35.

LAMBE, T.W. (1958b). The Engineering Behavior of Compacted Clay. *Journal of the Soil Mechanics and Foundations Division*, ASCE, Vol. 84, No. SM2, Paper 1654, pp. 1-34.

LAMBE, T.W. and WHITMAN, R.V. (1979). Soil Mechanics, SI Version. John Wiley & Sons, Inc., N.Y., 553 p.

LANGFELDER, L.J., CHEN, C.F. and JUSTICE, J.A. (1968). Air Permeability of Compacted Cohesive Soils. *Journal of the Soil Mechanics and Foundations Division*, ASCE, Vol. 94, No. SM4, Paper 6040, pp. 981-1001.

LENNARD-JONES, F.R.S. and POPLES, J.A. (1951). Molecular Association in Liquids I. Molecular Association due to Lone-Pair Electrons. *Proc. Royal Society*, London, A205, pp. 155-162.

LENTZ, R.W., HORST, W.D. and UPPOT, J.O. (1985). The Permeability of Clay to Acidic and Caustic Permeants. *Hydraulic Barriers in Soil and Rock*, ASTM STP 874, A.I. Johnson et al., Eds., American Society for Testing and Materials, Philadelphia.

LI, Y-H. and GREGORY, S. (1974). Diffusion of Ions in Sea Water and in Deep-Sea Sediments. *Geochimica et Cosmochimica Acta*, Vol. 38, pp. 703-714.

LIAO, W.P. and DANIEL, D.E. (1989). Time of Travel of Contaminants Through Soil Liners. *Proc. 12th Ann. Madison Waste Conf.*, University of Wisconsin, Madison.

LIDE, D.R. (1996). *CRC Handbook of Chemistry and Physics*. 76th ed., CRC Press, Inc.

LIU, C. and EVETT, J.B. (1984). *Soil Properties: Testing, Measurement, and Evaluation*. Prentice-Hall, Inc., Englewood Cliffs, New Jersey, 315 p.

LOW, P.F. (1961). Physical Chemistry of Clay-Water Interaction. *Advances in Agronomy*, Vol. 13, pp. 269-327.

LYMAN, W.J., REIDY, P.J. and LEVY, B. (1992). *Mobility and Degradation of Organic Contaminants in Subsurface Environments*. C.K. Smoley, Inc., Michigan.

MADSEN, F.T. and MITCHELL, J.K. (1987). *Chemical Effects on Clay Hydraulic Conductivity and their Determination*. Open File Report, Environmental Institute for Waste Management Studies, University of Alabama, Tuscaloosa, Alabama.

MADSEN, F.T. and MITCHELL, J.K. (1989). Chemical Effects on Clay Fabric and Hydraulic Conductivity. *Lecture Notes in Earth Sciences: The Landfill*, P. Baccini, Ed., Springer-Verlag Berlin Heidelberg, Germany.

MARSHALL, C.E. (1964). *The Physical Chemistry and Mineralogy of Soils*. Vol. 1: Soil Materials, Wiley, N.Y.

MELLOR, J.W. (1916). Do Fireclays Contain Halloysite or Clayite?. *Trans. Ceram. Soc. (Engl.)*, 16:83.

MELNYK, T.W. (1985). *Effects of Sorption Behavior on Contaminant Migration*. Atomic Energy of Canada Limited (AECL-8390), Whiteshell Nuclear Research Establishment, Pinawa, Manitoba.

MENZIES, B.K. (1988). A Computer Controlled Hydraulic Triaxial Testing System. *Advanced Triaxial Testing of Soil and Rock*, ASTM STP 977, R.T. Donaghe et al., Eds., American Society for Testing and Materials, Philadelphia.

MESRI, G. and OLSON, R.E. (1971). Mechanisms Controlling the Permeability of Clays. *Clays and Clay Minerals*, Vol. 19, pp. 151-158.

MICHAELS, A.S. and LIN, C.S. (1954). Permeability of Kaolinite. *Industrial and Engineering Chemistry*, American Chemical Society, Vol. 46, No. 6, pp. 1239-46.

MICHAELS, A.S. and LIN, C.S. (1955). Effects of Counterelectro-Osmosis and Sodium Ion Exchange on Permeability of Kaolinite. *Industrial and Engineering Chemistry*, American Chemical Society, Vol. 47, No. 6, pp. 1249-53.

MILLER, R.H., OVERMAN, A.R. and PEVERLY, J.H. (1969). The Absence of Threshold Gradients in Clay-Water Systems. *Soil Science Society of America Proc.*, SSSA, Vol. 33, No. 2, pp. 183-187.

MITCHELL, J.K. (1956). The Fabric of Natural Clays and its Relation to Engineering Properties. *Proc. 35th Highway Research Board*, NAS-NRC, pp. 693-713.

MITCHELL, J.K., HOOPER, D.R. and CAMPANELLA, R.G. (1965). Permeability of Compacted Clay. *Journal of the Soil Mechanics and Foundations Division*, ASCE, Vol. 91, No. SM4, pp. 41-65.

MITCHELL, J.K. and YOUNGER, J.S. (1967). Abnormalities in Hydraulic Flow Through Fine-Grained Soils. *Permeability and Capillarity of Soils*, ASTM STP 417, American Society for Testing and Materials, Philadelphia.

MITCHELL, J.K. and MADSEN, F.T. (1987). Chemical Effects on Clay Hydraulic Conductivity. *Geotechnical Practice for Waste Disposal '87*, ASCE GSP 13, R.D. Woods, Ed., American Society of Civil Engineers, New York.

MITCHELL, J.K. and JABER, M. (1990). Factors Controlling the Long-Term Properties of Clay Liners. *Waste Containment Systems: Construction, Regulation, and Performance*, ASCE GSP 26, R. Bonaparte, Ed., American Society of Civil Engineers, New York.

MITCHELL, J.K. and YEUNG, A.T. (1990). Electro-Kinetic Flow Barriers in Compacted Clay. *Geotechnical Engineering 1990, Transportation Research Record 1288*, Transportation Research Board, National Research Council, Washington, D.C., pp. 1-9.

MITCHELL, J.K. (1991). Conduction Phenomena: From Theory to Geotechnical Practice. *Géotechnique*, Vol. 41, pp. 299-340.

MITCHELL, J.K. (1993). *Fundamentals of Soil Behavior*. 2nd ed., John Wiley & Sons, Inc., N.Y., 437 p.

MOON, C.F. (1972). The Microstructure of Clay Sediments. *Earth-Science Reviews*, Vol. 8, No. 3, pp. 303-321.

OLSEN, H.W. (1962). Hydraulic Flow Through Saturated Clays. *Proc. 9th National Conf. on Clays and Clay Minerals*, pp. 131-161.

OLSEN, H.W. (1965). Deviations from Darcy's Law in Saturated Clays. *Soil Science Society of America Proc.*, SSSA, Vol. 29, No. 2, pp. 135-140.

OLSEN, H.W. (1966). Darcy's Law in Saturated Kaolinite. *Water Resources Research*, American Geophysical Union, Vol. 2, No. 2, pp. 287-295.

OLSEN, H.W. (1969). Simultaneous Fluxes of Liquid and Charge in Saturated Kaolinite. *Soil Science Society of America Proc.*, SSSA, Vol. 33, No. 3, pp. 338-344.

OLSEN, H.W. (1972). Liquid Movement Through Kaolinite under Hydraulic, Electric, and Osmotic Gradients. *The American Association of Petroleum Geologists Bulletin*, AAPG, Vol. 56, No. 10, pp. 2022-28.

OLSEN, H.W. (1985). Osmosis: A Cause of Apparent Deviations from Darcy's Law. Technical Note, *Canadian Geotechnical Journal*, Vol. 22, pp. 238-241.

OLSEN, H.W., NICHOLS, R.W. and RICE, T.L. (1985). Low Gradient Permeability Measurements in a Triaxial System. *Géotechnique*, Vol. 35, No. 2, pp. 145-157.

OLSEN, H.W., RICE, T.L. and NICHOLS, R.W. (1988a). Measuring Effects of Permeant Composition on Pore-Fluid Movement in Soil. *Ground-Water Contamination: Field Methods*, ASTM STP 963, A.G. Collins and A.I. Johnson, Eds., American Society for Testing and Materials, Philadelphia.

OLSEN, H.W., MORIN, R.H. and NICHOLS, R.W. (1988b). Flow Pump Applications in Triaxial Testing. *Advanced Triaxial Testing of Soil and Rock*, ASTM STP 977, R.T. Donaghe et al., Eds., American Society for Testing and Materials, Philadelphia.

OLSON, R.E. (1963). Effective Stress Theory of Soil Compaction. *Journal of the Soil Mechanics and Foundations Division*, ASCE, Vol. 89, No. SM2, Paper 3457, pp. 27-45.

OLSON, R.E. and DANIEL, D.E. (1981). Measurement of the Hydraulic Conductivity of Fine-Grained Soils. *Permeability and Groundwater Contaminant Transport*, ASTM STP 746, T.F. Zimmie and C.O. Riggs, Eds., American Society for Testing and Materials, Philadelphia.

PAULING, L. (1960). *The Nature of the Chemical Bond*. Cornell University Press, Ithaca, N.Y.

PEIRCE, J.J. and WITTER, K.A. (1986). Termination Criteria for Clay Permeability Testing. *Journal of Geotechnical Engineering*, ASCE, Vol. 112, No. 9, pp. 841-854.

PICKENS, J.F. and GRISAK, G.E. (1981). Scale-Dependent Dispersion in a Stratified Granular Aquifer. *Water Resources Res.*, Vol. 17, No. 4, pp. 1151-1211.

PUCSH, R. (1970). Microstructure Changes in Soft Quick Clay at Failure. *Canadian Geotechnical Journal*, Vol. 7, No. 1, pp. 1-7.

QUIGLEY, R.M. and ROWE, R.K. (1986). Leachate Migration Through Clay Below a Domestic Waste Landfill, Sarnia, Ontario, Canada: Chemical Interpretation and Modelling Philosophies. *Hazardous and Industrial Solid Waste Testing and Disposal*, ASTM STP 933, D. Lorenzen et al., Eds., American Society for Testing and Materials, Philadelphia.

QUIGLEY, R.M., FERNANDEZ, F., YANFUL, E., HELGASON, T., MARGARITIS, A. and WHITBY, J.L. (1987a). Hydraulic Conductivity of Contaminated Natural Clay Directly Below a Domestic Landfill. *Canadian Geotechnical Journal*, Vol. 24, pp. 377-383.

QUIGLEY, R.M., YANFUL, E. and FERNANDEZ, F. (1987b). Ion Transfer by Diffusion Through Clayey Barriers. *Geotechnical Practice for Waste Disposal '87*, ASCE GSP 13, R.D. Woods, Ed., American Society of Civil Engineers, New York.

QUIGLEY, R.M., FERNANDEZ, F. and ROWE, R.K. (1988). Clayey Barrier Assessment for Impoundment of Domestic Waste Leachate (Southern Ontario) Including Clay-Leachate Compatibility by Hydraulic Conductivity Testing. *Canadian Geotechnical Journal*, Vol. 25, pp. 574-581.

QUIGLEY, R.M. and FERNANDEZ, F. (1989). Clay/Organic Interactions and their Effect on the Hydraulic Conductivity of Barrier Clays. *Proc. Int'l. Symposium on Contaminant Transport in Groundwater*, Stuttgart, Germany.

QUIGLEY, R.M. and FERNANDEZ, F. (1994). Effect of Organic Liquids on the Hydraulic Conductivity of Natural Clays. *Landfilling of Waste: Barriers*, T.H. Christensen et al., Eds., E & FN Spon, UK.

QUIRK, J.P. and SCHOFIELD, R.K. (1955). The Effect of Electrolyte Concentration on Soil Permeability. *Journal of Soil Science*, Vol. 6, No. 2, pp. 163-178.

RAD, N.S. and ACAR, Y.B. (1984). A Study of Membrane-Permeant Compatibility. Technical Note, *Geotechnical Testing Journal*, ASTM, Vol. 7, No. 2, pp. 104-106.

RAND, B. and MELTON, I.E. (1977). Particle Interaction in Aqueous Kaolinite Suspensions: I. Effect of pH and Electrolyte upon the Mode of Particle Interaction in Homoionic Sodium Kaolinite Suspensions. *J. Colloid Interface Science*, Vol. 60, pp. 308-320.

RAUSSELL-COLOM, J.A. and SERRATOSA, J.M. (1987). Reactions of Clays with Organic Substances. Chap. 8. In: *Chemistry of Clays and Clay Minerals*, A.C.D. Newman, Ed., Mineralogical Society Monograph No. 6, London.

READES, D.W., LAHTI, L.R., QUIGLEY, R.M. and BACOPOULOS, A. (1990). Detailed Case History of Clay Liner Performance. *Waste Containment Systems: Construction, Regulation, and Performance*, ASCE GSP 26, R. Bonaparte, Ed., American Society of Civil Engineers, New York.

RHOADES, J.D. (1982a). Cation Exchange Capacity. *Methods of Soil Analysis, Part 2. Chemical and Microbiological Properties*. 2nd ed., A.L. Page et al., Eds., American Society of Agronomy & Soil Science Society of America, Madison, Wisconsin.

RHOADES, J.D. (1982b). Soluble Salts. *Methods of Soil Analysis, Part 2. Chemical and Microbiological Properties*. 2nd ed., A.L. Page et al., Eds., American Society of Agronomy & Soil Science Society of America, Madison, Wisconsin.

ROBINSON, R.A. and STOKES, R.H. (1959). *Electrolyte Solutions*. 2nd ed., Butterworths Scientific Publications, London, UK.

ROSENQVIST, I.Th. (1959). Physico-Chemical Properties of Soils: Soil-Water Systems. *Journal of the Soil Mechanics and Foundations Division*, ASCE, Vol. 85, No. SM2, pp. 31-53.

ROSS, C.S. and KERR, P.F. (1931). The Kaolin Minerals. *U.S. Geol. Surv.*, Profess. Paper 165E, pp. 151-175.

ROWE, P.W. and BARDEN, L. (1966). A New Consolidation Cell. *Géotechnique*, Vol. 16, No. 2, pp. 162-170.

ROWE, R.K. and BOOKER, J.R. (1985). 1-D Pollutant Migration in Soils of Finite Depth. *J. Geotech. Eng'g.*, ASCE, Vol. 111, No. 4, pp. 479-499.

ROWE, R.K. (1987). Pollutant Transport Through Barriers. *Geotechnical Practice for Waste Disposal '87*, ASCE GSP 13, Richard D. Woods, Ed., American Society of Civil Engineers, New York.

ROWE, R.K., CAERS, C.J. and BARONE, F. (1988). Laboratory Determination of Diffusion and Distribution Coefficients of Contaminants Using Undisturbed Clayey Soil. *Canadian Geotechnical Journal*, Vol. 25, pp. 108-118.

SAWHNEY, B.L. and BROWN, K., Eds. (1989). Reactions and Movement of Organic Chemicals in Soils. *SSSA & ASA Symposium Proc.*, SSSA Special Publication No. 22, Soil Science Society of America, Inc., American Society of Agronomy, Inc., Madison, Wisconsin.

SEED, H.B. and CHAN, C.K. (1959). Structure and Strength Characteristics of Compacted Clays. *Journal of the Soil Mechanics and Foundations Division*, ASCE, Vol. 85, No. SM5, pp. 87-128.

SEGAL, B.G. (1989). *Chemistry: Experiment and Theory*. 2nd ed., John Wiley & Sons, Inc., N.Y., 1008 p.

SHACKELFORD, C.D. (1988). Diffusion as a Transport Process in Fine-Grained Barrier Materials. *Geotechnical News*, Vol. 6, No. 2, pp. 24-27.

SHACKELFORD, C.D. (1989). Diffusion of Contaminants Through Waste Containment Barriers. *Geotechnical Engineering 1989, Transportation Research Record*

1219, Transportation Research Board, National Research Council, Washington, D.C., pp. 169-182.

SHACKELFORD, C.D. (1991). Laboratory Diffusion Testing for Waste Disposal-A Review. *Journal of Contaminant Hydrology*, Vol. 7, No. 3, pp. 177-217.

SHACKELFORD, C.D. and DANIEL, D.E. (1991). Diffusion in Saturated Soil: I. Background. *Journal of Geotechnical Engineering*, ASCE, Vol. 117, No. 3, pp. 467-484.

SHACKELFORD, C.D. (1993). Contaminant Transport. Chap. 3 in: *Geotechnical Practice for Waste Disposal*, David E. Daniel, Ed., Chapman & Hall, UK.

SHACKELFORD, C.D. (1994). Waste-Soil Interactions that Alter Hydraulic Conductivity. *Hydraulic Conductivity and Waste Contaminant Transport in Soil*, ASTM STP 1142, David E. Daniel and Stephen J. Trautwein, Eds., American Society for Testing and Materials, Philadelphia.

SHACKELFORD, C.D. and REDMOND, P.L. (1995). Solute Breakthrough Curves for Processed Kaolin at Low Flow Rates. *Journal of Geotechnical Engineering*, ASCE, Vol. 121, No. 1, pp. 17-32.

SILVESTRI, V., SIROIS, M. and CINCOU, A. (1990). Water Content-Suction Relationships in Intact Clays of Eastern Canada. *Proc. CSCE Annual Conf.*, Hamilton, Canadian Society for Civil Engineering.

SILVESTRI, V. and TABIB, C. (1991). Soil Water Content Variations Around Trees. *Proc. CSCE Annual Conf.*, Vancouver, Canadian Society for Civil Engineering.

SILVESTRI, V. and TABIB, C. (1992). Annual Water Content Variations Around Trees. *Proc. 45th Cdn. Geotech. Conf.*, Toronto, Canadian Geotechnical Society.

SILVESTRI, V., TABIB, C. and BEHIDJ, F. (1993). On the Modelling of Water Content Changes in Clay Deposits. *Proc. 46th Cdn. Geotech. Conf.*, Saskatoon, Canadian Geotechnical Society.

SILVESTRI, V. (1994). Water Content Relationships of a Sensitive Clay Subjected to Cycles of Capillary Pressures. *Geotechnical Testing Journal*, ASTM, Vol. 17, No. 1, pp. 57-64.

SILVESTRI, V. (1995). *Propriétés physico-chimiques des sols*. Graduate Course, Department of Civil Engineering, École Polytechnique de Montréal.

SINGH, U. and UEHARA, G. (1986). Electrochemistry of the Double Layer: Principles and Applications to Soils. Chapter 1 in *Soil Physical Chemistry*, D.L. Sparks, Ed., CRC Press, Fl.

SLOANE, R.C. and KELL, R.R. (1966). The Fabric of Mechanically Compacted Kaolin. *Clays and Clay Minerals, Proc. 14th National Clay Conf.*, pp. 289-296.

SMART, P. (1967). Particle Arrangements in Kaolin. *Clays and Clay Minerals, Proc. 15th National Clay Conf.*, pp. 241-254.

SMART, P. (1972). Discussion on: A Microstructure View of the Mechanical Properties of Saturated Clay, by C.R. Calladine. *Géotechnique*, Vol. 22, pp. 368-371.

SMART, P. and TOVEY, N.K. (1982). *Electron Microscopy of Soils and Sediments: Techniques*. Oxford University Press, UK.

SPOSITO, G. (1984). *The Surface Chemistry of Soils*. Oxford University Press, Inc., New York, N.Y., 234 p.

SPOSITO, G. (1989). *The Chemistry of Soils*. Oxford University Press, Inc., New York, N.Y., 277 p.

SRIDHARAN, A., ALTSCHAEFFL, A.G. and DIAMOND, S. (1971). Pore Size Distribution Studies. *Journal of the Soil Mechanics and Foundations Division*, ASCE, Vol. 97, No. SM5, Paper 8151, pp. 771-787.

STROMEYER, P. and HAUSMANN, J.F.L. (1816). *Göttingische Gelehrte Anziegen*, 2:125.

TAYLOR, D.W. (1948). *Fundamentals of Soil Mechanics*. John Wiley & Sons, Inc., New York.

TERZAGHI, K. (1925). *Erdbaumechanik auf Bodenphysikalischer Grundlage*. Leipzig und Wien, Franz Deuticke, Vienna, Austria.

TERZAGHI, K. (1943). *Theoretical Soil Mechanics*. John Wiley & Sons, Inc., New York.

TERZAGHI, K. (1960). *From Theory to Practice in Soil Mechanics*. John Wiley & Sons, Inc., New York.

TERZAGHI, K. and PECK, R. (1967). *Soil Mechanics in Engineering Practice*. 2nd ed., John Wiley & Sons, Inc., New York. The first edition was published in 1948.

THOMAS, G.W. (1982). Exchangeable Cations. *Methods of Soil Analysis, Part 2. Chemical and Microbiological Properties*. 2nd ed., A.L. Page et al., Eds., American Society of Agronomy & Soil Science Society of America, Madison, Wisconsin.

TODD, D.K. (1980). *Groundwater Hydrology*. 2nd ed., John Wiley & Sons, Inc., N.Y.

TOVEY, N.K. and WONG, K.Y. (1973). The Preparation of Soils and other Geological Materials for the S.E.M. *Proc. Int'l. Symposium on Soil Structure*, Gothenburg, Sweden, pp. 59-67.

U.S. EPA (1985). *Draft - Minimum Technology Guidance on Double Liner Systems for Landfills and Surface Impoundments: Design, Construction, and Operation*. 2nd ed., Report No. EPA/530/SW-85/014, U.S. EPA, Cincinnati, Ohio.

UPPOT, J.O. and STEPHENSON, R.W. (1989). Permeability of Clays under Organic Permeants. *Journal of Geotechnical Engineering*, ASCE, Vol. 115, No. 1, pp. 115-131.

Van OLPHEN, H. (1963). *An Introduction to Clay Colloid Chemistry*. Interscience, N.Y.

Van OLPHEN, H. (1977). *An Introduction to Clay Colloid Chemistry*. 2nd ed., Wiley Interscience, N.Y., 318 p.

VERWEY, E.J.W. and OVERBEEK, J.Th.G. (1948). *Theory of the Stability of Lyophobic Colloids*. Elsevier, Amsterdam.

WEBER, W.J., Jr. and SMITH, E.H. (1987). Simulation and Design Models for Adsorption Processes. *Environ. Sc. and Tech.*, Vol. 21, No. 11, pp. 1040-50.

WENTWORTH, C.K. (1922). A Scale of Grade and Class Terms for Clastic Sediments. *J. Geol.*, 30: 377-392.

WHITE, G.N. and ZELAZNY, L.W. (1988). Analysis and Implications of the Edge Structure of Dioctahedral Phyllosilicates. *Clays and Clay Minerals*, Vol. 36, pp. 141-146.

WONG, P. (1984). *Indirect Methods for the Quantification of Soil Fabric*. Master's thesis, Department of Civil Engineering and Applied Mechanics, McGill University, Montréal, Canada.

XU, J. (1994). *Compacted Kaolinite-Chemical Interactions: Microfabric and Hydraulic Conductivity Studies*. Ph.D. Dissertation, Department of Civil Engineering, Texas A&M University, College Station, Texas, U.S.A.

YANG, N. and BARBOUR, S.L. (1992). The Impact of Soil Structure and Confining Stress on the Hydraulic Conductivity of Clays in Brine Environments. *Canadian Geotechnical Journal*, Vol. 29, pp. 730-739.

YEUNG, A.T. (1992). Diffuse Double Layer Equations in SI Units. *Journal of Geotechnical Engineering*, ASCE, Vol. 118, No. 12, pp. 2000-2005.

YEUNG, A.T. and MITCHELL, J.K. (1993). Coupled Fluid, Electrical, and Chemical Flows in Soil. *Géotechnique*, Vol. 43, pp. 121-134.

YEUNG, A.T. (1994). Effects of Electro-Kinetic Coupling on the Measurement of Conductivity. *Hydraulic Conductivity and Waste Contaminant Transport in Soil*, ASTM STP 1142, David E. Daniel and Stephen J. Trautwein, Eds., American Society for Testing and Materials, Philadelphia.

YEUNG, A.T. and DATLA, S. (1995). Fundamental Formulation of Electrokinetic Extraction of Contaminants from Soil. *Canadian Geotechnical Journal*, Vol. 32, No. 4, pp. 569-583.

YEUNG, A.T. and JIANG, S. (1995). Appraisal of Ogata Solution for Solute Transport. *Journal of Geotechnical Engineering*, ASCE, Vol. 121, No. 2, pp. 111-118.

YONG, R.N. (1971). Soil Technology and Stabilization. *Proc. 4th Asian Regional Conf. S.M.F.E.*, Bangkok, Vol. 2, pp. 111-124.

YONG, R.N. and SHEERAN, D.E. (1973). Fabric Unit Interaction and Soil Behavior. *Proc. Int'l. Symposium on Soil Structure*, Gothenburg, Sweden, pp. 176-183.

YONG, R.N. and WARKENTIN, B.P. (1975). *Soil Properties and Behaviour*. Elsevier Scientific Publishing Co., Amsterdam, 449 p.

YONG, R.N., SETHI, A.J., LUDWIG, H.P. and JORGENSEN, M.A. (1979). Interparticle Action and Rheology of Dispersive Clays. *Journal of the Geotechnical Engineering Division*, ASCE, Vol. 105, No. GT10, pp. 1193-1209.

YONG, R.N., WARITH, M.A. and BOONSINSUK, P. (1986). Migration of Leachate Solution Through Clay Liner and Substrate. *Hazardous and Industrial Solid Waste Testing and Disposal*, ASTM STP 933, Douglas Lorenzen et al., Eds., American Society for Testing and Materials, Philadelphia.

YONG, R.N. and OHTSUBO, M. (1987). Interparticle Action and Rheology of Kaolinite-Amorphous Iron Hydroxide (Ferrihydrite) Complexes. *Applied Clay Science*, Vol. 2, pp. 63-81.

YONG, R.N. and SAMANI, H.M.V. (1987). Modelling of Contaminant Transport in Clays Via Irreversible Thermodynamics. *Geotechnical Practice for Waste Disposal '87*, ASCE GSP 13, Richard D. Woods, Ed., American Society of Civil Engineers, New York.

YONG, R.N. and WARKENTIN, B.P. (1987). Contaminant-Soil Interaction: Depletion of Soil Buffering Capacity. *Proc. CSCE Centennial Symposium on Management of Waste Contamination of Groundwater*, CSCE, Raymond N. Yong, Ed., pp. 225-237.

YONG, R.N. (1989). Waste Generation and Disposal. Keynote address, *Proc. 2nd Int'l. Symposium Environmental Geotechnology*, H.Y. Fang and S. Pamukcu, Eds., Vol. 1, pp. 1-24.

YONG, R.N. and WARITH, M.A. (1989). Leaching Effect of Organic Solutions on Geotechnical Properties of Three Clay Soils. *Proc. 2nd Int'l. Symposium Environmental Geotechnology*, H.Y. Fang and S. Pamukus, Eds., Vol. 1, pp. 99-110.

YONG, R.N. (1990). Contaminant Transport: Physical and Analytical Modelling Requirements and Problems. *Proc. CSCE Conf. Environmental Engineering*, CSCE, Vol. 1, pp. 627-630.

YONG, R.N. and MOURATO, D. (1990). Influence of Polysaccharides on Kaolinite Structure and Properties in a Kaolinite-Water System. *Canadian Geotechnical Journal*, Vol. 27, pp. 774-788.

YONG, R.N. and WARITH, M.A. (1990a). Contaminant Migration Effect on Dispersion Coefficients. *Physico-Chemical Aspects of Soil and Related Materials*, ASTM STP 1095, Keith B. Hoddinott and Robert O. Lamb, Eds., American Society for Testing and Materials, Philadelphia.

YONG, R.N. and WARITH, M.A. (1990b). Groundwater Contamination by Industrial and Domestic Wastes: A Case Study. *Proc. CSCE Conf. Environmental Engineering*, CSCE, Vol. 1, pp. 648-666.

YONG, R.N. (1991). Landfilling Waste Management Compliance with Regulatory Policy and Guidelines. Keynote address, *Proc. 1st Cdn. Conf. Environmental Geotechnics*, R.P. Chapuis and M. Aubertin, Eds., CGS, Montreal, pp. 3-8.

YONG, R.N. and DI PERNO, N. (1991). Sources and Characteristics of Waste -with Specific Reference to Canada. *Geo-Environmental Series 91-1*, Geotechnical Research Centre, McGill University.

YONG, R.N., CABRAL, A. and WEBER, L.M. (1991). Evaluation of Clay Compatibility to Heavy Metals Transport and Containment: Permeability and Retention. *Proc. 1st Cdn. Conf. Environmental Geotechnics*, R.P. Chapuis and M. Aubertin, Eds., CGS, Montreal, pp. 314-321.

YONG, R.N., MOHAMED, A.M.O. and WANG, B.W. (1992paper). Influence of Amorphous Silica and Iron Hydroxide on Interparticle Action and Soil Surface Properties. *Canadian Geotechnical Journal*, Vol. 29, pp. 803-818.

YONG, R.N., MOHAMED, A.M.O. and WARKENTIN, B.P. (1992). *Principles of Contaminant Transport in Soils*. Elsevier Science Publishers B.V., Amsterdam, The Netherlands, 327 p.

YONG, R.N., TAN, B.K. and MOHAMED, A.M.O. (1994). Evaluation of Attenuation Capability of a Micaceous Soil as Determined from Column Leaching Tests. *Hydraulic Conductivity and Waste Contaminant Transport in Soil*, ASTM STP 1142, David E. Daniel and Stephen J. Trautwein, Eds., American Society for Testing and Materials, Philadelphia.

APPENDIX A
BASIC PRINCIPLES

A.1 Clay Mineralogy

The term *soil* is likely to have a considerably different meaning when used by a geologist, by an agronomist, and by a civil engineer. Soil to a geologist is the weathered regolith at the earth's surface that supports vegetation. It is thought of generally as being loose, argillaceous, and with some organic content. To the agronomist, it is the loose regolith at the earth's surface. It need not be weathered nor contain any vegetation; it may be gravel, for example. Also according to agronomists, a soil is likely to be composed of a series of horizons and have properties quite independent of the underlying parent bedrock. The civil engineer tends to divide the material at the earth's crust into two categories: 1. rock, and 2. soils. Rock is defined as something that is hard and consolidated. Soil, according to Terzaghi and Peck (1948), "is a natural aggregate of mineral grains that can be separated by such gentle means as agitation in water." Substantially any loose material at the earth's crust, regardless of particle-size distribution, composition, or organic content, is soil to the engineer. It may or may not be weathered. Similarly, to the engineer, soil can extend to any depth below the surface so long as the material is not indurated substantially.

Clay is used as a rock term and also as a particle-size term in the mechanical analysis of sedimentary rocks, soils, etc. As a rock term, it is difficult to define precisely, because of the wide variety of materials that have been called clays. In general, the term clay implies a natural, earthy, fine-grained material which develops plasticity when mixed with a limited amount of water. By plasticity is meant the property of the moistened material to be deformed under the application of pressure, with the deformed shape being retained when the deforming pressure is removed. Chemical analyses of clays show them to be composed essentially of silica, alumina, and water, frequently with appreciable quantities of iron, alkalies, and alkaline earths. Moreover, the term clay has no genetic significance. It is used for material that is the product of weathering, has formed by hydrothermal action, or has been deposited as a sediment.

To the engineer, however, the term clay is primarily a particle-size term. As a particle-size term, the clay fraction is that size fraction composed of the smallest particles. The maximum size of particles in the clay size grade is defined differently in different disciplines. In geology, for instance, the tendency has been to follow the Wentworth (1922) scale and to define the clay grade as material finer than about 4 μm. On the other hand, in soil investigations, the tendency is to use 2 μm as the upper limit of the clay size grade. Although there is no sharp universal boundary between the particle size of the clay minerals and nonclay minerals in argillaceous materials, a large number of analyses have shown that there is a general tendency for the clay minerals to be concentrated in a size less than about 2 μm, or that naturally occurring larger clay- mineral particles break down easily to this size when the clay is slaked in water. Also such analyses have shown that the nonclay minerals usually are not present in particles much smaller than about 1 to 2 μm. There is, therefore, a fundamental reason for placing the upper limit of the clay size grade at 2 μm. Thus, the term *clay* is primarily a particle-size term.

A.1.1 Factors Controlling the Properties of Clay Materials

The factors which control the properties of clay materials or the attributes which must be known to completely characterize a clay material may be classified as follows:

A.1.1.1 Clay-Mineral Composition

This refers to the identity and relative abundance of all the clay-mineral components. Since certain clay minerals which may be present in very small amounts may exert a tremendous influence on the attributes of a clay material, it is not adequate to determine only the major clay-mineral components. Thus a small amount (5 %±) of smectite in a clay is likely to provide a material very different from another clay with the same composition in all ways except for the absence of smectite.

The perfection of crystallinity of the clay minerals is variable in clay materials. Therefore, kaolinite may be well organized or poorly organized in a given sample; illite may be degraded or well crystallized. It is known that certain properties, such as plasticity, vary with the crystalline character of the component clay minerals.

The morphology of the clay-mineral components may be a distinctive property of a particular clay. For instance, in some kaolins the flakes of kaolinite are large and thin, while in others they are thicker with less areal extent; in some bentonites the smectite particles are large and very thin, whereas in other bentonites the particles are more granular.

To characterize a clay material completely, and to provide adequate data to understand physical properties, therefore, clay-mineral analyses must be thorough and complete. In addition, the procedure must not alter the clay minerals. Frequently several lines of approach are necessary, e.g., diffraction, electron microscopy, and chemical methods. At times, however, even with a combination of methods, it is difficult to obtain complete data. For example, it is often difficult to establish the presence of allophane, and one can say only that the solubility data, diffraction data, etc., suggest the presence of very poorly organized material. Fortunately, clay-mineral analyses of samples composed entirely of kaolinite are relatively simple by any procedure.

A.1.1.2 Nonclay-Mineral Composition

This refers to the identity of the nonclay minerals, their relative abundance, and the particle-size distribution of the individual species. Calcite, dolomite, large flakes of mica, pyrite, feldspar, gibbsite, and other minerals are very abundant in some clay materials. Yet, the nonclay minerals in clay materials tend generally to be concentrated in particles coarser than about 2 μm. There are, however, materials in which they are much finer-grained.

Obviously, it is impossible or unjustifiably time-consuming to get all the data concerning the nonclay minerals in most investigations of clay materials. The lengths to which

one can and must go depend largely on the problem at hand and the purpose of the investigation. It is frequently adequate to determine the identity of only the more abundant nonclay minerals, and their sorting and particle-size distribution in a general way. As an example, the study of a soil from the point-of-view of soil mechanics demands that sorting within the silt-size range be studied in considerable detail, since the presence of some silt materials may yield a material with unique physical properties of great importance to the construction engineer.

The analysis of a clay material must be tailor-made to the material being studied and to the purpose of the investigation, and must provide comparable results from one sample to another. One cannot blindly use a set analytical procedure for all materials and all problems and still get adequate data without a tremendous waste of time and effort.

A.1.1.3 Organic Material

This refers to the kind and amount of organic material contained in a clay material. In general, the organic material occurs in clay materials in several ways: It may be present as discrete particles of wood, leaf matter, spores, etc.; it may be present as organic molecules adsorbed on the surface of the clay-mineral particles; or it may be intercalated between the silicate layers. The discrete particles may be present in any size, from large chunks easily visible to the naked eye to particles of colloidal size which act as a pigment in the clay-mineral materials.

The total amount of organic material can be determined simply by readily available standard analytical procedures. Determination of the kind of organic material is, however, a more difficult problem. The study of the organic content of clay materials is a problem worthy of intensive research for a variety of reasons. For instance, the organic content often is important in determining the properties of a clay material. Also, a knowledge of clay-mineral-organic relations might throw much light on some important geologic processes.

A.1.1.4 Exchangeable Ions and Soluble Salts

Some clay materials contain water-soluble salts which may have been entrained in the clay at the time of accumulation or may have developed subsequently as a consequence of weathering or alteration processes, as in the oxidation of pyrite to produce sulfates. Common water-soluble salts found in clay materials are chlorides, sulfates, and carbonates of alkalies, alkaline earths, aluminum, and iron.

The clay minerals and some of the organic material found in clay materials have significant ion-exchange capacity. The ion-exchange capacity of the clay minerals and the organic components, as well as the identity and relative abundance of the exchangeable ions which are present, are extremely important attributes of clay materials. To fully characterize a clay material, the relative abundance of both the exchangeable anions and cations should be determined. Nevertheless, it is difficult to distinguish sometimes between exchangeable ions and those present in a moderately soluble compound, and as a result the determinations of ion-exchange characteristics become a difficult task in a material containing appreciable water-soluble salts.

A.1.1.5 Texture

The textural factor refers to the particle-size distribution of the constituent particles, the shape of the particles, the orientation of the particles in space and with respect to each other, and the forces tending to bind the particles together.

Some knowledge of the particle-size distribution of the coarser grains can be obtained quickly by microscopic examinations, and detailed determinations can be made by sieving and/or wet sedimentation methods. Fine-grained particles require wet methods, and this applies to the clay-mineral fraction. It must be remembered that wet methods are likely to reflect only the degree to which clay-mineral units or aggregates have been cleaved or broken down in the process of making the analysis rather than any inherent attribute of the natural material.

The use of chemical dispersing agents almost certainly will alter the base-exchange composition of the material, and consequently such agents must not be used or at least used only with great caution, if exchangeable ions are to be determined. It is generally essential to determine the exchangeable ions on the "as received" material, since any mixing in water or washing is likely to cause a significant change.

It is obvious that the particle-size-grade analysis of clay materials is difficult, and care must be taken to devise a tailor-made procedure best suited to the material at hand and to the objectives of the investigation, if pertinent, reproducible, and comparable data are to be obtained.

The shape of the finest particles is best revealed by electron-microscope studies. Such investigations have shown the hexagonal outline of the flake-shaped units of kaolinite, the elongate tubular shape of the halloysite minerals, and the irregular flake shape of the illite, chlorite, vermiculite, and most smectite mineral particles. Information on the thickness, as well as areal dimensions, can frequently be obtained from electron micrographs; kaolinite particles that have been previously studied show a ratio of areal diameter to thickness of 2-25:1, whereas for smectite it is 100-300:1. However, in the application of the electron beam in electron microscopy, considerable heat is developed in the specimen so that some concern has been felt as to whether or not some of the observed results are due to this heat and the possible resulting dehydration rather than to the natural mineral.

Some information regarding the orientation of extremely fine particles can sometimes be obtained from the study of thin sections. Yet, thin-section studies appear to have distinct limitations. The thickness of the sections is many times that of the individual clay-mineral components, so that many individuals lie on top of each other. The presence of even small amounts of organic material or free ferric iron oxide or hydroxide will mask the individual components and distort the optical values. Also, the clay material must be dried in preparation for the cutting of the section, so that the texture observed may be not quite that of the original

material. Even with these deficiencies of thin-section study, it is usually worthwhile to cut sections and study them in any clay-material investigation.

Much remains to be done, and the texture of clay materials is an important and promising field for research that should attract ample investigators.

Moreover, so little is known in detail about the forces binding the particles together in clay materials that the possible types of binding forces can merely be enumerated:

1. Forces due to the attraction of the mass of one clay-mineral particle for the mass of another particle;

2. Intermolecular forces resulting from the nearness of one particle to another with the overlap of fields of force of molecules in the surface layers of adjacent particles;

3. Electrostatic forces due to charges on the lattice resulting from unbalanced substitution within the lattice, broken bonds on edges of the lattice, and the attractive force of certain ions adsorbed on clay-mineral surfaces; and

4. The bonding action of adsorbed polar molecules. For instance, oriented water molecules between two clay-mineral surfaces may form a bridge of considerable strength if only a few molecules thick, and of no strength if more than a few molecules thick. Similarly, adsorbed polar organic molecules could serve as a bond between clay-mineral particles.

In any given clay material all the bond forces probably are at work, and they are interrelated. Thus the nature of the adsorbed ion will itself influence bonding and also affect the development of oriented adsorbed water, which in turn is related to bonding.

Recent work by colloid chemists and others has begun to shed light on the interparticle forces in clay-mineral assemblages. Van Olphen (1963), for example, emphasized the probable difference and importance of the bonds found at the edges of clay-mineral particles as compared with those on the large flake surfaces. Fripiat (1964) considered in

detail the nature of the clay-mineral surfaces on structural grounds and the probable resulting bonding forces.

The matter of the bonding force in clay materials is of particular importance to soil-mechanics investigations and construction engineers, since it largely determines the sensitivity and strength of soil materials. Construction failures have occurred because the strength properties of a soil that developed during construction could not be predicted adequately from laboratory testing data. Without fundamental data on how and why clay materials are held together, it is impossible always to predict safely from any empirical data how a clay material will act when load is applied, when the water table is altered, or when it comes in contact with contaminants.

A.1.2 Interatomic Bonding

To better understand the interactions involved in the composition process of clay minerals, a brief review of the major types of interatomic bonds is in order.

Interatomic bonds form when electrons in adjacent atoms interact in such a way that their energy levels are lowered. If the energy reduction is large, then a strong, or primary, bond develops. The way in which the bonding electrons are localized in space determines whether or not the bonds are directional. The strength and directionality of interatomic bonds together with the relative sizes of the bonded atoms determine the type of crystal structure assumed by a given composition.

A.1.2.1 Primary Bonds

Only the outer shell or valence electrons participate in the formation of primary interatomic bonds. There are three limiting types: *covalent, ionic,* and *metallic* (Mitchell, 1993). They differ because of how the bonding electrons are localized in space. The energies of these bonds per mole of bonded atoms is from 60×10^3 to more than 400×10^3 joules (15-

100 kcal). As there are 6.023 x 10^{23} molecules per mole, it might be argued that such bonds are weak; however, relative to the weight of an atom they are very large.

A combination of ionic and covalent bonding is typical in most nonmetallic solids. Purely ionic and covalent bonding are limiting conditions that are the exception rather than the rule in most cases. For instance, the interatomic bond in silica (SiO_2) is about half covalent and half ionic; and silicate minerals are the most abundant constituents of most soils.

A.1.2.2 Secondary bonds

Secondary bonds that are weak relative to ionic and covalent bonds also form between units of matter. They may be strong enough to determine the final arrangements of atoms in solids, and they may be sources of attraction between very small particles and between liquids and solid particles. These includes:

i. The Hydrogen Bond:

If a hydrogen ion forms the positive end of a dipole, then its attraction to the negative end of an adjacent molecule is termed a *hydrogen bond*. Hydrogen bonds are formed only between strongly electronegative atoms, such as oxygen and fluorine, because these atoms produce the strongest dipoles. The formation of water (H_2O) is the most pronounced example of hydrogen bonds. The strength of the hydrogen bond is much greater than that of other secondary bonds because of the small size of the hydrogen ion. Hydrogen bonds are important in determining some of the characteristics of the clay minerals and in the interaction between soil particle surfaces and water.

ii. van der Waals Bonds:

Permanent dipole bonds, such as the hydrogen bond, are directional. Fluctuating dipole bonds, commonly termed *van der Waals bonds*, also exist because at any one time there may be more electrons on one side of the atomic nucleus than on the other. This creates weak instantaneous dipoles whose oppositely charged ends attract each other.

Although individual van der Waals bonds are weak, typically an order of magnitude weaker than a hydrogen bond, they are nondirectional and additive between atoms. Consequently, they decrease less rapidly with distance than primary valence and hydrogen bonds when large groups of atoms are considered. They are strong enough to determine the final arrangements of groups of atoms in some solids (e.g., many polymers), and they may be responsible for small cohesions in fine-grained soils (Mitchell, 1993).

A.1.3 Structure of the Kaolinite Minerals

The clay minerals in soils belong to the mineral family termed *phyllosilicates*, which also contains other layer silicates such as serpentine, pyrophyllite, talc, mica, and chlorite. The clay minerals occur in small particle sizes, and their unit cells ordinarily have a residual negative charge that is balanced by the adsorption of cations from solution. It is worth mentioning here that, in conformity with the nomenclature of the Clay Minerals Society (Bailey *et al.*, 1971), the following terms are used: a *plane* of atoms, a *sheet* of basic structural units, and a *layer* of unit cells composed of two, three, or four sheets.

A.1.3.1 Structural Units of the Layer Silicates

The structures of the common layer silicates are made up of combinations of two simple structural units, the *silicon tetrahedron* (Fig. A.1) and the *aluminum or magnesium octahedron* (Fig. A.2). The different clay mineral groups are characterized by the stacking arrangements of sheets of these units and the manner in which two successive two- or three-sheet layers are held together.

Differences among minerals within the clay mineral groups result primarily from differences in the type and amount of isomorphous substitution within the crystal structure. Because the possible substitutions are nearly endless in number and because the development of crystal structure may range from very poor to nearly perfect, it is not surprising that the

study of clay minerals is daunting to the beginner and provides an endless challenge to the expert.

i. Silica Sheet

In most clay mineral structures, the silica tetrahedra are interconnected in a sheet structure. Three of the four oxygens in each tetrahedron are shared to form a hexagonal net, as shown in Fig. A.1b. The bases of the tetrahedra are all in the same plane, and the tips all point in the same direction. The structure can repeat "indefinitely" and has the composition $(Si_4O_{10})^{4+}$. Electrical neutrality can be obtained by replacement of four oxygens by hydroxyls or by union with a sheet of different composition that is positively charged.

ii. Octahedral Sheet

This sheet structure is composed of magnesium or aluminum coordinated octahedrally with oxygens or hydroxyls. In some cases, other cations are present in place of Al^{3+} and Mg^{2+}, such as Fe^{2+}, and Fe^{3+}. Figure A.2b is a schematic diagram of such a sheet structure. If the cation is trivalent, then normally only two-thirds of the possible cationic spaces are filled, and the structure is termed *dioctahedral*. In the case of aluminum, the composition is $Al_2(OH)_6$. This composition and structure form the mineral gibbsite. When combined with silica sheets, as is the case in clay mineral structures, an aluminum octahedral sheet is referred to as a *gibbsite* sheet. On the other hand, if the octahedrally coordinated cation is divalent, then normally all possible cation sites are filled,, and the structure is *trioctahedral*. In the case of magnesium, the composition is $Mg_3(OH)_6$, giving the mineral brucite. In clay mineral structures, a sheet of magnesium octahedra is termed a *brucite* sheet.

A.1.3.2 Synthesis Pattern of the Clay Minerals

The manner in which atoms are assembled into tetrahedral and octahedral units, followed by the formation of sheets and their stacking to form layers that combine to produce the different clay mineral groups is illustrated in Fig. A.3. The basic structures shown in the

bottom row of Fig. A.3 comprise the great preponderance of the clay mineral types that are found in soils.

Grouping the clay minerals according to crystal structure and stacking sequence of the layers is convenient, since members of the same group have generally similar engineering properties. The minerals have unit cells consisting of two, three, or four sheets. The two-sheet minerals are made up of a silica sheet and an octahedral sheet. The unit layer of the three-sheet minerals is composed of either a dioctahedral or trioctahedral sheet sandwiched between two silica sheets. Unit layers may be stacked closely together or water layers may intervene. The four sheet structure of chlorite is composed of a 2:1 layer plus an interlayer hydroxide sheet.

Reference to the bottom row of Fig. A.3 shows that the 2:1 minerals differ from each other mainly in the type and amount of "glue" that holds the successive layers together. For example, the smectites have loosely held cations between the layers, the illites contain firmly fixed potassium ions, and the vermiculites have somewhat organized layers of water and cations. The chlorite group represents an end member that has 2:1 layers bonded by an organized hydroxide sheet. The charge per formula unit is variable both within and among groups, and this reflects the fact that the range of compositions is great owing to varying amounts of isomorphous substitution. Because of this, the boundaries between groups are somewhat arbitrary.

A.1.3.3 Intersheet and Interlayer Bonding

A single plane of atoms is common to both the tetrahedral and octahedral sheets in the formation of the clay mineral layers. Bonding between these sheets is of the primary valence type and is very strong. However, the bonds holding the unit layers together may be of several types, and they may be sufficiently weak that the physical and chemical behavior of the clay is influenced by the response of these bonds to changes in environmental conditions.

Isomorphous substitution in all of the clay minerals, with the possible exception of the kaolinites, gives clay particles a net negative charge. To preserve electrical neutrality, cations are attracted and held between the layers and on the surfaces and edges of the particles. Many of these cations are *exchangeable cations*, because they may be replaced by cations of another type. The quantity of exchangeable cations is termed the *cation exchange capacity* (CEC) and is usually expressed in milliequivalents (meq) per 100 grams of dry clay.

Five types of interlayer bonding are possible in the layer silicates (Marshall, 1964):

1. Neutral parallel layers are held by van der Waals forces. Bonding is weak; however, stable crystals of appreciable thickness such as pyrophyllite and talc may form. These minerals cleave parallel to the layers.

2. In some minerals, for instance, kaolinite, brucite, and gibbsite, there are opposing layers of oxygens and hydroxyls or hydroxyls and hydroxyls. Hydrogen bonding then develops between the layers, as well as van der Waals bonding. Hydrogen bonds remain stable in the presence of water.

3. Neutral silicate layers may be separated by layers of highly polar water molecules, which are held by hydrogen bonds.

4. Cations needed for electrical neutrality may be in positions that control interlayer bonding. Micas and chlorites are examples to this phenomenon. In micas, some of the silicon is replaced by aluminum in the silica sheets. The resulting charge deficiency is partly balanced by potassium ions between the unit cell layers. The size of the potassium ion is such that it just fits into the holes formed by the bases of the silica tetrahedra. As a result, it generates a strong bond between the layers. In chlorites, on the other hand, the charge deficiencies from substitutions in the octahedral sheet of the 2:1 sandwich are balanced by a charge excess on the one sheet layer interleaved between the three sheet layers. This provides a strongly bonded structure that, while exhibiting cleavage, will not separate in the presence of water or other polar liquids.

5. When the surface charge density is moderate, as for smectites and vermiculites, the silicate layers readily adsorb polar molecules, and also, the adsorbed cations may

hydrate, resulting in layer separation and expansion. The strength of the interlayer bond is low and is strongly function of charge distribution, ion hydration energy, surface ion configuration, and structure of the polar molecule.

In addition, according to van Olphen, 1977, there are two possible reasons for the smectite and vermiculite particles to swell; whereas, particles of pyrophyllite and talc do not. These two possible reasons are:

1. The interlayer cations in the smectites hydrate, and the hydration energy overcomes the attractive forces between the unite layers. There are no interlayer cations in pyrophyllite; hence, no swelling.

2. Water does not hydrate the cations but is adsorbed on oxygen surfaces by hydrogen bonds. There is no swelling in pyrophyllites and talc because the surface hydration energy is too small to overcome the van der Waals forces between layers, which are greater in these minerals because of a smaller interlayer distance.

A.1.3.4 The 1:1 Minerals

The *kaolinite-serpentine* minerals are composed of alternating silica and octahedral sheets as shown schematically in Fig. A.4. The tips of the silica tetrahedra and one of the planes of atoms in the octahedral sheet are common. The tips of the tetrahedra all point in the same direction, towards the center of the unit layer. In the plane of atoms common to both sheets, two-thirds of the atoms are oxygens and are shared by both silicon and the octahedral cations. The remaining atoms in this plane are (OH) located so that each is directly below the hole in the hexagonal net formed by the bases of the silica tetrahedra. If the octahedral layer is brucite, then a mineral of the serpentine subgroup results; whereas, dioctahedral gibbsite layers give clay minerals in the kaolinite subgroup. Trioctahedral 1:1 minerals are relatively rare, usually occur mixed with kaolinite or illite, and are hard to identify. A diagrammatic sketch of the kaolinite structure is shown in Fig. A.5. The structural formula of which is $(OH)_8Si_4Al_4O_{10}$.

Mineral particles of the kaolinite subgroup consist of the basic units stacked in the vertical direction. The bonding between successive layers is by both van der Waals forces and hydrogen bonds. The bonding is sufficiently strong that there is no interlayer swelling.

Variations among members of the kaolinite subgroup include variations in the manner layers are stacked above each other and possibly in the position of aluminum ions within the available sites in the octahedral sheet. The dickite unit cell is made up of two unit layers, and the nacrite unit cell contains six. Both appear to be formed by hydrothermal processes. Dickite is fairly common as a secondary clay in the pores of sandstone and in coal beds. Neither dickite nor nacrite is common in soils; whereas kaolinite is the most abundant member of the subgroup and a common soil mineral.

i. Isomorphous Substitution and Exchange Capacity

The concept of isomorphous substitution is an important factor in the structure and properties of the clay minerals. In an ideal gibbsite sheet, only two-thirds of the octahedral positions are filled, and all of the cations are aluminum. In an ideal brucite sheet, all the octahedral spaces are filled by magnesium. In an ideal silica sheet, all the tetrahedral spaces are filled by silicons. In the clay minerals, however, some of the tetrahedral and octahedral spaces are occupied by cations other than those in the ideal structure. Common examples are aluminum in place of silicon, magnesium instead of aluminum, and ferrous iron (Fe^{2+}) for magnesium. This presence in an octahedral or tetrahedral position of a cation other than that normally found, without change in crystal structure, is isomorphous substitution. The actual tetrahedral and octahedral cation distributions may develop during initial formation or subsequent alteration of the mineral.

Whether or not measurable isomorphous substitution exists within the structure of the kaolinites is uncertain (Mitchell, 1993). Nevertheless, values of cation exchange capacity for kaolinite in the range of 3 to 15 meq/100 g have been reported. Thus, particles possess a net negative charge. Possible sources are:

1. Substitution of Al^{3+} for Si^{4+} in the silica sheet, or a divalent ion for Al^{3+} in the octahedral sheet. Replacement of only 1 Si in every 400 would be adequate to account for the exchange capacity of many kaolinites.

2. The hydrogen of exposed hydroxyls may be replaced by exchangeable cations. According to Grim, 1968, however, this mechanism is not likely, because the hydrogen would probably not be replaceable under the conditions of most exchange reactions.

3. Broken bonds around particle edges may give unsatisfied charges that are balanced by adsorbed cations.

Kaolinite particles are charged positively on their edges when in a low pH (acid) environment, but negatively charged in a high pH (basic) environment. Low exchange capacities are measured under low pH conditions, whereas high exchange capacities are obtained for determinations at high pH. This suggests that broken bonds are at least a partial source of exchange capacity. That a positive cation exchange capacity is measured under low pH conditions when edges are positively charged indicates that some isomorphous substitution must exist also.

Interlayer separation does not occur in kaolinite; therefore, balancing cations must be adsorbed on the exterior surfaces and edges of the particles.

ii. Morphology and Surface Area

Well-crystallized particles of kaolinite, nacrite, and dickite occur as well-formed six-sided plates. The lateral dimensions of these plates range from about 0.1 to 4 μm, and their thicknesses are from about 0.05 to 2 μm. Poorly crystallized kaolinite generally occurs as less distinct hexagonal plates, and the particle size is usually smaller than for the well-crystallizes varieties.

Finally, the specific surface area of kaolinite is about 10 to 20 m^2/g of dry clay.

A.1.4 Surface Functional Groups

All clay particles demonstrate strong surface reactivity derived from the chemical behavior of the surface functional groups (SFGs). A SFG is a chemically reactive molecular unit bound into the structure of a solid at its periphery such that the reactive components of the unit can be bathed by a fluid (Sposito, 1984). When a SFG reacts with a molecule dissolved in a surrounding fluid to form a stable unit, a surface complex is produced and the reaction process is called surface complexation. There are two principle types of surface functional groups in clay minerals.

The *siloxane ditrigonal cavity* is associated with the basal plane (called the siloxane surface) of oxygen ions bound into a silica tetrahedral sheet in a mineral structure. The hexagonal cavity is distorted into a trigonal one when the apexes (tips) of the tetrahedrons fit into the vertices of the octahedral sheet to form a layer, resulting in a corrugated basal plane. Electric charge distribution in the phyllosilicate structure caused mainly by isomorphic cation substitution will determine the reactivity of the siloxane ditrigonal cavity. If there is no substitution to create an excess negative charge in the structure, the cavity will function as a very soft Lewis base (weak electron donor), and is able to form complexes only with neutral dipolar molecules (i.e., H_2O). However, if Al^{3+} is replaced by Fe^{2+} or Mg^{2+} in the octahedral sheet, the resultant excess negative charge will be distributed mainly over the ten surface oxygen ions of four tetrahedrons that are associated through their tips with a single octahedron in the layer. As a result, the Lewis base character of the ditrigonal cavity will be enhanced, making it possible to form complexes with cations as well as dipolar molecules. The siloxane ditrigonal cavity will behave as a much stronger electron donor if isomorphic substitution of Si^{4+} by Al^{3+} occurs in the silica tetrahedron because the excess negative charge can be distributed primarily over just the three oxygen ions of one tetrahedron. Much stronger complexes with cations and dipolar molecules become possible due to the localization of electric charges.

The second surface functional group is the *inorganic hydroxyl group* exposed on the outer peripheries of a clay particle. It is the most abundant and reactive SFG in clay minerals (Sposito, 1984). There are three types of surface OH group on a kaolinite crystallite. On the basal plane, the structural OH groups are exposed on the surface, showing rather different reactivity from the bulk structural OH groups. Singly coordinated OH groups are exposed on the edge surface when clay crystallites are broken apart. At the edge of an octahedral sheet where $Al(III) \cdot H_2O$ is found, the coordinated OH groups are called aluminols. They can form complexes with a H^- at low pH values or with an OH^- at high pH values. The water molecule bound to an Al^{3+} cation can also be replaced by an OH^- at higher pH values. At the edge of a tetrahedral sheet, OH groups singly coordinated to Si^{4+} cations are called silanols. They tend to complex with OH^- only because of the greater valence of the silica. The metal cations exposed due to the breaking of crystallite such as $Al(III) \cdot H_2O$ and Si^{4+}, act as Lewis acid sites: molecular units that use an empty electron orbital in initiating a reaction.

Most of the surface functional groups in soil clays carry electric charges. The sign and magnitude depend on the structure of the clay and composition of the soil solution. The siloxane ditrigonal cavity often carries a more or less localized negative charge produced by isomorphic substitution, whereas the surface hydroxyl group can carry either a positive or negative charge depending on the pH of the soil (Sposito, 1984). The effects of pH on the charge properties of edge sites for two types of dioctahedral phyllosilicates were predicted by crystal growth theory (White and Zelazny, 1988). The charge on the aluminol is more sensitive to pH than that on the silanol, as the latter keeps a zero charge within the pH range of 3 to .5. It appears that the 1:1 phyllosilicate would become negatively charged at pH values above 6.5.

The dominant organic surface functional groups in soil humus include: (a) carboxyl (-COOH), (b) hydroxyl (-OH) {phenolic and alcoholic}, (c) carbonyl (C=O), (d) amino (-NH_2), and (e) sulfhydryl (-SH). These functional groups contribute most to the cation

exchange capacity of soil organic materials, and allow these materials to act as proton donors or acceptors.

A.2 Clay-Water System

Water is the most prevalent substance on earth, covering more than two-thirds of its surface in oceans, seas, and lakes. The continental areas are themselves frequently charged with and shaped by water. In vapor form, water is always present in the atmosphere. Finally, water is the principal constituent of all living organisms, plants and animals alike. Water and its ionization products, hydrogen and hydroxyl ions, are important factors determining the structure and biological properties of proteins and other cell and tissue components. The basic processes of life are intrinsically dependent upon water's unique attributes. Far from being a bland, inert liquid, water is, in fact, a highly reactive substance and an exceedingly effective solvent and transporter of numerous substances.

Air and water comprise a large part of the soil. It is estimated that for an average soil, air and water take up 50 percent of the space. Organic matter and mineral matter take up the other 50 percent. A saturated soil with a void ratio greater than 1.0 contains a greater volume of water than of solids, and void ratios greater than 1.0 are more the rule than the exception in the case of fine-grained soils.

Since water is the transporting agency for contaminants, it is important to obtain an understanding of soil-water interaction and the relationships established. The processes involved during the transport of contaminants through soil will control: (1) the amount of contaminants transported at any one time through a particular region, (2) the attenuation of contaminant concentration through adsorption and desorption processes, (3) the rate and extent of propagation or advance of a contaminant plume. Many of the controlling processes are similar to those involved in soil-water relations. In reality, however, the situation is not so simple because neither water nor soil surfaces are inert chemically, and water and soil

particles interact with each other because water molecules are strongly attracted to and adsorbed on soil particle surfaces. These interactions influence the physical and physicochemical behavior of the material. Although details of these interactions and their consequences cannot always be stated with certainty, some things are known, and these considerations form the subject of this division.

A.2.1 Molecular Structure of Water

Notwithstanding its ubiquity, water remains something of an enigma, possessing unusual and anomalous attributes still not entirely understood. Perhaps the first anomaly is that water, despite its low molecular weight, is a liquid and not a gas at normal temperatures (its sister compound, H_2S, has its boiling point at $-60.7°C$). Compared with other common liquids, furthermore, water has unusually high melting and boiling points, heats of fusion and vaporization, specific heat, dielectric constant, viscosity, and surface tension. These properties suggest that there must be some particularly strong force of attraction between molecules in liquid water to impart to this of all liquids such a high internal cohesion. The secret is in the *molecular structure* and *intermolecular bonding* of the peculiar substance called water (Hillel, 1980).

To understand the physical behavior of water in soil, one needs a mental picture of the water molecule. The water molecule (Fig. A.6) is composed of two hydrogen atoms and one oxygen atom. The water molecule is positively charged on one side and negatively on the other, and is thus a dipole. The accepted molecular structure of this dipole was first proposed by Bernal and Fowler in 1933. From spectral and x-ray data, they concluded that two hydrogen atoms share a pair of electrons with a single oxygen atom. The two hydrogen atoms of the water molecule are separated at an angle of $103-106°$, measured with the oxygen atom as the apex of the angle and with the two hydrogen protons as points on the angle sides. In Fig. A.6, the electron pairs shared between the oxygen nucleus and the two hydrogen protons

only partially screen (neutralize) the positive charge of the protons. The result is that the proton side of the molecule becomes the positive side of the water molecule.

In addition to the shared pairs of electrons, Bernal and Fowler (1933) found two concentrations of negative electricity, one concentration above and one concentration below a plane defined by the two hydrogen protons and the oxygen atom. Lennard-Jones and Pople (1951) describe the concentration of negative electricity as "lone-pair electrons." One pair is above the plane, and one pair is below (Fig. A.6). These two lone pairs of electrons do not take part directly in bond formation as do the electrons shared between the hydrogen and oxygen atoms of the water molecule.

The electric charge structure of the water molecule resembles a tetrahedron with the oxygen near the center, two of its corners positively charged due to the partially screened protons of the hydrogen, and the remaining two corners of the tetrahedron negatively charged due to the two pairs of lone-pair electrons. This arrangement makes the water molecule a *dipole*, that is, one end of the molecule tends to be positive while the other tends to be negative. Bond energy considerations (Pauling, 1960) indicate that the H-O bond is about 40 percent ionic and 60 percent covalent, thereby accounting both for the directionality of the bond and for producing a permanent dipole.

In water and ice, the positive corner of one molecule attracts the negative corner of another. The proton is shared by the two oxygens, which results in hydrogen bonding and a tendency for each molecule to bond to four neighboring molecules, which surround it tetrahedrally. In ice-I, the stable crystalline state of water at temperatures less than 0°C and atmospheric pressure, a hexagonal network structure is formed. As the melting point is approached, the number of broken or distorted hydrogen bonds increases. This accounts for the lower strength and higher creep rates in ice as the temperature increases. At temperatures above 0°C (under atmospheric pressure conditions), enough hydrogen bonds are ruptured or bent that ice loses its rigidity, and water exists in the liquid state.

Though the structure of ice is known, the structure of liquid water is not definitely known, except that some hydrogen bonding and structure remain. The high melting point, boiling point, heat of fusion, heat of vaporization, specific heat, dielectric constant, and viscosity of water are ascribed to the energy needed to break hydrogen bonds. Evidently, bond rupture and distortion predominate at temperatures less than 4°C; whereas, increased intermolecular distances (as a result of the increased thermal agitation) prevail above, thus giving maximum density at 4°C.

Various models have been proposed for the structure of water in the light of available physical and chemical evidence (Eisenberg and Kauzman, 1969). These can be gathered under the following: *Mixture models, Interstitial models, Distorted Hydrogen Bond model,* and *Random Network model.* Eisenberg and Kauzman (1969) concluded that mixture models are not supported by the data, but that the distorted H-bond models (including random networks) seem to accord with most of what is known about water from experiment.

A.2.2 Clay-Water Interaction

Ample evidence shows that water is attracted to soil minerals, particularly to clays. Dried clays adsorbed water from the atmosphere at low relative humidities, many soils swell when given access to water, and temperatures above 100°C are needed to remove "all" the water from a soil. In fact, it is not always evident just what is meant by a dry soil.

Possible mechanisms for clay-water interaction include the following (Low, 1961) and are shown schematically in Fig. A.7.

(a) Hydrogen Bonding

Because the surface of the soil minerals are usually composed of a layer of either oxygens or hydroxyls, hydrogen bonding can develop easily, with oxygens attracting the positive corners and hydroxyls attracting the negative corners of water molecules (Fig. A.7a).

Early concepts of the structure of adsorbed water suggested an icelike character because of the similarity between the hexagonal symmetry of the oxygens and hydroxyls in clay surfaces and the structure of ice. Subsequent work has shown, however, that the structure cannot be that of ice (Mitchell, 1993).

The formation of H bonds with particle surfaces would alter the electron distribution from that in normal water, thus making it easier for bonded molecules to form additional bonds with molecules in the same and next layer. The directional properties of the bonds would induce a tetrahedral arrangement of water molecules, which would become less rigid with distance from the surface due to a decrease in the surface force fields and an increase in the force fields of normal water structure.

(b) Hydration of Exchangeable Cations

Because cations are attracted to negatively charged clay surfaces, so is their water of hydration (Fig. A.7b). This mechanism should be most important at low water contents.

(c) Attraction by Osmosis

The concentration of cations increases as negatively charged clay surfaces are approached (Fig. A.7c). Because of this increased concentration and the restriction on diffusion of ions from the vicinity of the surface, as a result of electrostatic attraction, water molecules tend to diffuse toward the surface in an attempt to equalize concentrations.

(d) Charged Surface-Dipole Attraction

Clay particles can be viewed as negative condenser plates. Water dipoles would then orient with their positive poles directed toward the negative surfaces and with the degree of orientation decreasing with increasing distance from the surface. However, at the midplane between parallel plates there would be structural disorder, because like poles would be adjacent to each other. Ingles (1968) suggests that because of the high hydration number and energy of aluminum in the clay structure, water is strongly attracted to the surfaces and

interposes itself between the surfaces and the counterions, with the counterions removed as far as possible from the surface, that is, to the midplane between opposing parallel sheets. With this model, the structure shown in Fig. A.7d can be conceived.

The same type of arrangement could result simply from ion hydration. In a dry clay, adsorbed cations occupy positions in holes on the clay surfaces. On hydration, they surround themselves with water and move to the central region between clay layers.

(e) Attraction by London Dispersion Forces

Van der Waals attractive forces could bond water molecules to clay surfaces. In-phase fluctuations of electron clouds form temporary dipoles and induce displacements in neighboring molecules so that dipole-dipole attraction occurs. Because such bonds would be nondirectional, the water structure would be close packed and more fluid than the H-bonded structure.

A.2.3 Clay-Water-Electrolyte System

Interactions between small soil particles, dissolved ions, and water are caused by unbalanced force fields at the interfaces between soil and water. When two particles are in close proximity, their respective force fields overlap and influence the behavior of the system if the magnitudes of these forces are large relative to the weights of the particles themselves. Clay particles, because of their very small size and platy shapes, have large surface areas and are especially influenced by these forces. The effects of surface force interactions and small particle size are manifested by a variety of interparticle attractive and repulsive forces, which, in turn, influence the flocculation-deflocculation behavior of clays in suspension.

Colloid chemistry provides a means for description of many of the interactions in the clay-water-electrolyte system, because most clay particles are small enough to behave as colloids. Clays are considered to be lyophobic (liquid hating) or hydrophobic (water hating)

colloids rather than as lyophilic or hydrophilic colloids, even though water wets clays and is adsorbed on particle surfaces. This designation has resulted from the need, historically, to distinguish colloids such as clay from colloids already termed hydrophilic, such as gums, which exhibit such an affinity for water that they spontaneously form a colloidal solution (van Olphen, 1977). Hydrophobic colloids are liquid dispersions of small, solid particles that are (1) two-phase systems with a large interfacial surface area, (2) have a behavior dominated by surface forces, and (3) can flocculate in the presence of small amounts of salt. Clay-water-electrolyte systems satisfy all of these criteria. In this section, emphasis is on the development of an understanding and appreciation for interactions in systems of interest in engineering rather than on rigor in the treatment of colloid chemistry.

A.2.3.1 Ion Distributions in Clay-Water Systems

In a dry clay, adsorbed cations are tightly held by the negatively charged clay particles. Cations in excess of those needed to neutralize the electronegativity of the clay particles and associated anions are present as salt precipitates. When the clay is placed in water, the precipitated salts go into solution. Because the adsorbed cations produce a much higher concentration near the surfaces of particles, they try to diffuse away in order to equalize concentrations throughout. Their freedom to do so, however, is restricted by the negative electrical field originating in the particle surfaces. The escaping tendency due to diffusion and the opposing electrostatic attraction lead to ion distributions adjacent to a clay particle in suspension as shown in Fig. A.8. The distribution of cations is analogous to that of air molecules in the atmosphere, where the escaping tendency of the gas is countered by the gravitational attraction of the earth. Anions, however, are excluded from the negative force fields of the particles, as shown in Fig. A.8.

The charged surface and the distributed charge in the adjacent phase are together termed the *diffuse double layer*. It has to be mentioned that in some clay minerals, e.g., kaolinite, and under certain conditions, broken bonds at particle edges create a positive edge charge. This is balanced by a negative diffuse layer.

A.2.3.2 Diffuse Double Layer Models

The negative surface charges associated with the clay particles present an electrified interface. Since soil-water contains dissolved solutes with positive charges, e.g., cations such as earth and heavy metals, the interaction between a negatively charged soil particle surface and the cations in the soil-water will generate an electric double layer (EDL), i.e., the arrangement of positive and negative charges at the electrified interface. The separation distance between the positive charges and the negatively charged surface, the distribution of the positive charges, and whether the first layer of positively charged ions, molecules or solutes will satisfy the negative surface density, are some of the many important items considered in the development of what is generally identified as *diffuse double layer models* (DDL models).

The schematic diagram in Fig. A.9 shows a simplified picture of the net negatively charged clay particle in soil water containing cations and anions. The electric double layer, EDL, commonly referred to as the double layer, consists of the row of negative charges shown in the side view of the clay particle in Fig. A.9, and the first row of positive charges (cations). Convenience in model representation permits one to indicate the negative charges of the clay particle in a nicely arranged vertical row next to the clay particle surface, even though this is not physically correct. Depending on how accurate one wishes to be in representation of the physico-chemical system, and depending on the use to which the model is applied, several levels of sophistication in DDL models representation and calculations exist. This is not to say that the more sophisticated DDL model is necessarily more accurate or correct (Yong *et al.*, 1992).

Beginning with the work done by Helmholtz and Perrin, where the double layer model was represented by the parallel-plate condenser, the double layer is considered to consist of the two equal magnitude negatively and positively charged sheets. No diffuse ion-layer (DL) is considered necessary in this model, since this model is assumed to function as a parallel-

plate capacitor. Because the ions (both cations and anions) in solution are free to move, the parallel-plate condenser model is seen to be severely constrained and too simplistic.

The DDL model which was developed independently by Gouy (1910) and Chapman (1913) has received the greatest attention. Although this theory has been shown to accurately describe the actual distribution of ions only for smectite particles suspended in monovalent electrolyte solutions at low (less than 100 mole/m³) concentration (Sposito, 1989), it provides a very useful basis for the understanding of flocculation and deflocculation and the relationships of these processes to formation of soil structure. It also provides the recognition necessary to account for the mobility of the ions in solution. Whereas it does not fully answer the questions pertaining to the nature and distribution of the ions immediately adjacent to the surface of the charged particle, the Gouy-Chapman model nevertheless provides researchers with the capability to compute the average electrical potential, Ψ, as a function of distance, x, from the charged particle surface.

For the mathematical development of the Gouy-Chapman theory of the diffuse double layer, the following idealizing assumptions are made:

1. Ions in the double layer are point charges and there are no interactions between them. They are assumed to be distributed according to the Boltzmann distribution.

2. Charge on the particle surface is uniformly distributed.

3. The particle surface is a plate that is large relative to the thickness of the double layer (i.e., one-dimensional condition).

4. The permittivity of the medium is independent of position; or in other words, the solvent is assumed to influence the double layer only through its dielectric constant, which is assumed to have the same value throughout the diffuse part.

The illustration given in Fig. A.10 shows the cations and anions as positive and negative space charges, along with the variation of the average electrical potential with distance from a clay particle surface.

The Coulombic interaction between the charges and the charged particle surfaces in relation to distance x away from the particle surface is described by the Poisson equation. As a matter of fact, the Poisson equation relates potential, charge, and distance. This equation is given as:

$$\frac{d^2\Psi}{dx^2} = \frac{-4\pi\rho}{\epsilon} \qquad \text{(A.1)}$$

where Ψ is the electrical potential at the point (V), x is the distance from the surface (m), ρ is the charge density (C/m^3), and ϵ is the static permittivity of the medium (C^{2}J^{-1}m^{-1}).

The space charge density, ρ, can be obtained in terms of the Boltzmann distribution as:

$$\rho = e \sum v_i\, n_{i0} \exp\left(\frac{-v_i e\Psi}{kT}\right) \qquad \text{(A.2)}$$

where e is the electronic charge (1.602 x 10^{-19} Coulomb), v_i is the ionic valence of the ith species, n_{i0} is the concentration of the ith species of ion in the bulk solution (ions/m^3), k is the Boltzmann constant (1.38 x 10^{-23} J$^\circ$K^{-1}), and T is the temperature ($^\circ$K).

By substituting Eq. A.2 in Eq. A.1, we obtain the Poisson-Boltzmann equation:

$$\frac{d^2\Psi}{dx^2} = \frac{-4\pi e}{\epsilon} \sum v_i\, n_{i0} \exp\left(\frac{-v_i e\Psi}{kT}\right) \qquad \text{(A.3)}$$

Equation A.3 is the differential equation for the electric double layer adjacent to a charged planar surface. Its solution provides a basis for computation of electrical potential and ion concentrations as a function of distance from the surface. The detailed techniques for the solution of Eq. A.3 can be found in many reference textbooks, e.g., Yong and Warkentin (1975), van Olphen (1977), Mitchell (1993), and Iwata *et al.* (1995).

For a single diffuse double layer, solutions are given in terms of the dimensionless quantities:

$$y = \frac{ve\Psi}{kT}$$
$$z = \frac{ve\Psi_0}{kT}$$

Potential functions (A.4)

and

$$\xi = K x \qquad \textit{Distance function} \qquad \textbf{(A.5)}$$

where

$$\frac{1}{K} = \left(\frac{\epsilon_0 D kT}{2n_0 e^2 v^2} \right)^{1/2} \qquad \textbf{(A.6)}$$

with ϵ_0 as the permittivity of vacuum $(8.854 \times 10^{-12} \, C^2 J^{-1} m^{-1})$, D as the dielectric constant (dimensionless). The quantity $(1 K)$ is a measure of the "thickness" of the double layer. Equation A.6 shows that the value of $1 K$ depends only on the characteristics of the dissolved salts and the fluid phase. However, the actual values of concentration and potential at any distance from the surface depend on the particle surface charge and surface potential, and these depend on the type of clay and conditions in the pore solution.

It can be seen readily from Eq. A.6 that the thickness of the double layer varies inversely with the valence and the square root of the concentration, and directly with the square root of the dielectric constant and temperature, other factors remaining constant. It is worth pointing here that not only does the increase in electrolyte concentration reduce the surface potential for the condition of constant surface charge, but also the decay of potential with distance is much more rapid.

The electrical potential and charge distributions for the case of interacting double layers from parallel flat plates, separated at distance $2d$ are shown in Fig. A.11. The development of the resultant potential is shown in Fig. A.11a, while Fig. A.11b illustrates the charge distributions for the interacting double layers.

To account for the limitation in Gouy-Chapman theory, Bolt (1955) has introduced the following corrections: the effect of ion size, dielectric saturation, polarization energies of the ion, Coulombic interaction of the ions, and the short-range repulsion between the ions. With these modifications, Bolt successfully described the distribution of Na^- and Ca^{2-} around an "illite" particle without having to invoke any specific adsorption mechanism. Bolt's extension of Gouy theory further enabled distinction of ions with the same valence.

However, dielectric saturation and ionic polarization seem to offset each other almost completely if the charge density on the colloids is ≤ 0.2 C/m^2 (Bolt, 1955). For larger values, the polarization term increases very rapidly, leading to an overestimation of ionic concentrations by the Gouy-Chapman equation. Generally, the Coulombic interaction exceeds the influence of the short-range repulsion up to concentrations of 1 to 2 M. Thus, in colloids with charge density of 0.2 C/m^2 or less, the Coulombic interaction of the ions will be the main correction factor. In short, the simple Gouy-Chapman model gives fairly reliable results, for colloids with a charge density > 0.2 to 0.3 C/m^2 and especially if the colloid under consideration has constant charge density.

In his theory, Stern (1924) has divided the region near the surface into two parts: the first consisting of a layer of ions adsorbed at the surface forming a compact double-layer (the Stern layer), and the second consisting of the diffuse ion-layer (the Gouy layer) (Fig. A.10). He has accounted for the finite size of ions and the possibility of their specific adsorption.

The Stern theory of the electrical double layer then assumes that the surface charge is balanced by the charge in solution which is distributed between the Stern layer at a distance

(d) from the surface and a diffuse layer which has a Boltzmann distribution. The total surface charge in this model is therefore due to the charge in the two layers.

There have been a number of further modifications to the double layer theory, primarily to explain experimental observations. Grahame (1947) suggested through what is called in the literature (e.g., Singh and Uehara, 1986) the Gouy-Chapman-Stern-Grahame model that specifically adsorbed ions can approach the inner Helmholtz plane or IHP (i.e., adsorbed into the Stern layer) when they lose their water of hydration, whereas the hydrated cations are only electrostatically attracted to the surface (outer Helmholtz plane, or OHP).

Two types of arrangement are illustrated in Fig. A.12. The first arrangement (A-arrangement) shows hydrated ions interacting with the electrified surface through a layer of water molecules, while the B-arrangement presents ions in direct contact with the surface, resulting thereby in partial hydration of the ions.

A.2.3.3 Net Energy of Interaction

Relationships for diffuse layer energies of repulsion have been combined with those for van der Waals attraction to give curves of *net energy of interaction* as a function of distance of the type shown in Fig. A.13 (Verwey and Overbeek, 1948). The energy of repulsion is sensitive to changes in electrolyte concentration, cation valence, dielectric constant, and pH; whereas, the attractive energy is sensitive only to changes in the dielectric constant and temperature.

In systems where the net curve of interaction exhibits a high repulsive energy barrier, particles in suspension are prevented from close approach, and the suspension is stable. In cases where the repulsive energy barrier does not exist, particles can easily come into close proximity, and flocculation results, represented by the minima in the energy curves (Fig. A.13). In these systems, flocs or aggregates of several particles settle together from suspension.

The character of the net curve of interaction also has a major influence on particle arrangement and stability in sedimented, consolidated, or compacted deposits of clay. Changes in system chemistry, which in turn causes changes in the net curve of interaction, may have important consequences in terms of the behavior of the soil when disturbed or subjected to the action of flowing water.

A.3 Soil Fabric

The term *fabric* refers to the arrangement of particles, particle groups, and pore spaces in a soil. The term *structure* is sometimes used interchangeably with fabric. It is preferable, however, to use structure to refer to the combined effects of fabric, composition, and interparticle forces.

The particle arrangements in soils remained largely unknown until development of suitable optical, x-ray diffraction, and electron microscope techniques made direct observations possible starting in the mid-1950s. Interest then centered mainly on clay particle arrangements and their relationships to mechanical properties. It was not until the late 1960s that knowledge expanded rapidly, sparked by improved techniques of sample preparation and the development of the scanning electron microscope.

In the early 1970s attention was directed also at particle arrangements in cohesionless soils. From this work came a realization that characterization of the properties of sands and gravels cannot be done in terms of density or relative density alone, as had previously been thought. In fact, particle arrangements and stress history should be considered in these materials as well.

In this division, methods for determination of fine-grained soils fabric are illustrated and examples of different fabric types are described. The importance of soil fabric as a factor

determining clay properties and behavior relevant to compaction and hydraulic conductivity is discussed in the next divisions.

A.3.1 Definitions of Fabrics and Fabric Elements

There has been a proliferation of terms for the description of fabrics and fabric features. The number of special terms will be kept to a minimum; however, it is necessary to consider the size, the form, and the function of different fabric units. It is also necessary to keep in mind the scale at which the fabric is of interest. For instance, a carefully compacted clay liner for an impoundment may have uniformly and closely spaced particle groups within it, thus giving a material with very low hydraulic conductivity. If, however, the liner becomes broken into sections measuring a meter or so in each direction as a result of shrinkage cracking, then leakage through it will be dominated totally by flow through the cracks, and the small-scale fabric becomes unimportant.

A.3.1.1 Particle Associations in Clay Suspensions

Particle associations in clay suspensions can be described as follows and as illustrated in Fig. A.14 (van Olphen, 1977):

1. *Dispersed*: no face-to-face association of clay particles;

2. *Aggregated*: face-to-face association (FF) of several clay particles;

3. *Flocculated*: edge-to-edge (EE) or edge-to-face (EF) association of aggregates;

4. *Deflocculated*: no association between aggregates.

Thicker and larger particles result from FF association. EF and EE associations can produce cardhouse structures that are quite voluminous until compressed. Referring to Fig. A.14, the terminology of the various modes is as following:

(a) Dispersed and deflocculated, (b) Aggregated but deflocculated (FF association, or parallel or oriented aggregation), (c) EF flocculated but dispersed, (d) EE flocculated but dispersed,

(e) EF flocculated and aggregated, (f) EE flocculated and aggregated, and (g) EF and EE flocculated and aggregated.

Although the above terminology is specified, the terms flocculated and aggregated are often used synonymously in a generic sense to refer to multiparticle assemblages, and deflocculated and dispersed are used synonymously in a generic sense to refer to single particles or particle groups acting independently.

A.3.1.2 Particle Associations in Soils

Particle associations in sediments, residual soils, and compacted clays assume a variety of forms; however, most of them are related to the combinations of the configurations shown in Fig. A.14, and reflect the difference in water content between a suspension and a denser soil mass. Whereas single grain fabrics are found in cohesionless soils, fine-grained soils are almost always composed of multiparticle aggregates. Overall, three main groupings of fabric elements may be identified (Collins and McGown, 1974):

1. *Elementary particle arrangements*: single forms of particle interaction at the level of individual clay, silt, or sand particles.

2. *Particle assemblages*: units of particle organization having definable physical boundaries and a specific mechanical function, and which consist of one or more forms of the elementary particle arrangements.

3. *Pore spaces*.

Schematic illustrations of each of the fabric features in these three classes are shown in Figs. A.15 through A.17. The features shown in Figs. A.14 through A.17 are sufficient to describe most fabrics. A number of additional terms, however, have also been used in the literature to describe the same or similar features.

Cardhouse is an edge-to-face arrangement forming an open fabric similar to the edge-to-face flocculated but dispersed arrangement of Fig. A.14c (Goldschmidt, 1926). A *domain*

(Aylmore and Quirk, 1960, 1962) or *packet* or *book* (Sloane and Kell, 1966) is an aggregate of parallel clay plates. An array of such fabrics is termed a *turbostratic fabric* and is similar to the interweaving bunches of Fig. A.16h. An edge-to-face association of packets or books is termed a *bookhouse* and is similar to the arrangement of Fig. A.14e. A *cluster* is a grouping of particles or aggregates into larger fabric units (Olsen, 1962; Yong and Sheeran, 1973). In a fabric composed of groupings of clusters, it is many times useful to refer to intracluster and intercluster pore space and to cluster and total void ratios. The term *ped* (Brewer, 1964) has a similar meaning to cluster.

A.3.1.3 Fabric Scale

The fabric of a soil may be considered relative to three levels of scale. From smallest to largest they are:

1. *Microfabric*: the microfabric consists of the regular aggregations of particles and the very small pores between them, perhaps with sizes up to about 1 μm, through which very little fluid will flow. Typical fabric units are up to a few tens of micrometers across.

2. *Minifabric*: the minifabric contains the aggregations of the microfabric and the interassemblage pores between them. The interassemblage pores may be up to several tens of micrometers in diameter. Flow through these pores will be much greater than through the intra-aggregate pores. Minifabric units may be a few hundred micrometers in size.

3. *Macrofabric*: the macrofabric may contain cracks, fissures, laminations, or root holes, corresponding to the transassemblage pores (Fig. A.17), through which the flow rate is so great as to totally obscure that through the other pore space types.

The mechanical and flow properties of soil depend on details of these three levels of fabric to varying degrees. For example, the hydraulic conductivity of a fine-grained soil will be almost totally dominated by the macro- and minifabrics, whereas time-dependent

deformations such as creep and secondary compression will be controlled most strongly by the mini- and microfabrics.

A.3.2 Fabric Determination of Fine-Grained Soils

Both direct and indirect methods are used to study the fabric and fabric features of fine-grained soils. An illustrative schematic diagram prepared by Professor R.N. Yong that summarizes methods for analysis of soil composition and fabric using various parts of the electromagnetic spectrum is shown in Fig. A.18.

Of the methods used to study the fabric of fine-grained soils, optical and electron microscopy, x-ray diffraction, and pore size distribution offer the advantage of providing direct, and usually, unambiguous information about specific fabric features, provided the samples are representative and the sample preparation procedures have not destroyed the original fabric. On the other hand, these techniques are limited to small samples, and they are destructive of the samples studied.

Other available techniques, such as wave propagation, thermal conductivity, magnetic susceptibility, dielectric dispersion and electrical conductivity, are nondestructive, at least in principle, and can be used for the study of soil fabric *in situ* and for study of changes in fabric that accompany compression, shear, and fluid flow. However, with most of these methods interpretation is seldom straightforward or unambiguous. In some cases, the use of several methods of fabric analysis may be appropriate in order to obtain information of more than one type or level of detail.

A.3.3 Fabric of Fine-Grained Soils

The study of clay structure involves three aspects: (1) the fabric; (2) the composition; and (3) the interparticle forces (physico-chemical interactions). The fabric of a clayey soil

refers to the spatial distribution, orientation, and particle-to-particle relation of the clay particles and particle domains. Understanding clay structure is fundamental to many soil-related disciplines including geology, soil science, ceramics engineering, as well as civil engineering, in general, and geoenvironmental engineering, in particular. Terzaghi (1925) discussed the arrangement of particles and bonding of fine-grained soils. He postulated that clay minerals stick together at points of contact with forces strong enough to construct a honeycomb structure. This open structure allows large amounts of fluid to be stored in large pores. Casagrande (1932) also proposed a honeycomb model of sensitive soil, which is very similar to the Terzaghi's structure. This type of clay fabric is named the "Terzaghi-Casagrande honeycomb structure."

By the same time, Goldschmidt (1926) suggested a cardhouse structure, where flaky clay particles orient in edge-to-face contacts. He thought that it was the adsorbed water molecules around the clay particle that adhere the minerals together by their dipolar moment. Nearly thirty years later, Lambe (1953) presented a more complicated concept of soil fabric. His proposed fabric of undisturbed marine clays is similar to what Goldschmidt proposed. In an environment of high electrolyte concentration, clay particles flocculate under the dominant electrostatic attractive forces between the negatively charged faces and positively charged edges, resulting in a random orientation of particles. The fabric of soil with low ionic strength pore water was thought to be denser due to parallel arrangement of particles as repulsive forces between particles become dominant, resulting in a dispersed structure. In a remolded clay, particles become even more preferentially oriented due to the breakage of particle-to-particle bonds and the tendency of the particles to establish their most stable arrangement. Clearly, the Goldschmidt-Lambe concept of a cardhouse structure is very different from the Terzaghi-Casagrande honeycomb concept.

The only technology available for most of the earliest direct observations of microfabric was the optical microscope. Mitchell (1956) conducted some of the pioneering experiments on natural sediments in both undisturbed and remolded states. He determined the

degree of clay particle orientation in parallel arrangements indirectly by the intensity of illumination as the microscope stage was rotated. Mitchell's observations basically confirmed the fabric proposed by Lambe (1953) on marine and fresh water clays, yet with some modifications and expansions. He attributed the significantly preferred orientation in undisturbed marine clays mainly to one-dimensional compression in nature, and stated that the formation of a deposit in fresh water does not necessarily insure a dispersed and oriented clay fabric due to impurities in the environment. He also emphasized the effects of remolding on the preferred orientation of clay particles, and consequently on the engineering properties of soils.

Application of electron microscope made the direct observation of single clay particles arrangement possible. Carbon replica transmission electron microscopy (TEM) on marine sediments confirmed the validity of the cardhouse model. Clay particles were found to arrange dominantly by contacts between edges and planes (Rosenqvist, 1959). There was increasing evidence that groups of particles in suspension, referred to as clay clusters, behave as single units (Terzaghi, 1960). Intensive observation on soil microfabric led to a revolutionary concept: the domain. A domain is defined as a parallel arrangement of clay crystals (Aylmore and Quirk, 1959, 1960). By comparing the behavior of illite domains with those of montmorillonite, it was concluded that a domain structure in some respects resembles a montmorillonite crystal. Clay mass was considered to be composed of pores and matrix, within which domains of one micrometer diameter are randomly placed with respect to each other (Aylmore and Quirk, 1959). Turbostratic arrangement was proposed for the fabric composed of domains (Aylmore and Quirk, 1960). Domain structure is so common in compacted soil that Sloane and Kell (1966) suggested that the cardhouse model be replaced by a bookhouse fabric model when they investigated the carbon replica of compacted kaolinite. They called the domains paralleled packets.

During the 1970s, the use of scanning electron microscopy (SEM) increased due to the relative simplicity of specimen preparation and larger scope of view which reveals the

important role of aggregates in constituting soil fabric (Pucsh, 1970; Yong, 1971; Barden, 1972; Moon, 1972; Smart, 1972; Collins and McGown, 1974). Multiplate particles have been recognized as a significant aspect of clay fabric in various sediment types ever since. Pucsh (1970) proposed that the natural microstructure pattern of soft quick clay is a very porous network of dense aggregates connected by links of clay particles. When such soil is sheared, the aggregates behave like rigid bodies, up to certain stress levels, and move as integral units. On the other hand, the movement of the aggregates induces large deformations in the connecting links leading to the development of domains of oriented particles. Barden (1972) stated that both natural and artificial clay soils are made up of plates aggregated into peds, crumbs, or domains. There is no such thing as single plate cardhouse structure, but a general occurrence of plates aggregated in a face-to-face association. The turbostratic structure is thus formed by dispersed association, while bookhouse structure is formed by flocculated association. He argued that the single plate theory is relevant only to dilute colloidal suspensions, and that naturally consolidated clay requires consideration of multiplate units. Yong (1971) concluded that crumbs (aggregates), which showed finite particle shape and structural integrity, tended to re-arrange and re-orient under small stress without internal single-particle distortion. Crumbs distortion and single particle reorientation occur only at high loads and accompanying soil volume change. To confirm the tendency toward face-to-face attraction of clay platelets into groups, Collins and McGown (1974) presented a much more complex diagram of microfabric of natural sediment based on SEM observations. Multilevel particle assemblages consisting of clay groups, silt, and sand of many forms and functions were suggested. Particle assemblages are defined as units of particle organization (association) having definable physical boundaries and a specific mechanical function. An assemblage consists of elementary particle arrangements or smaller particle assemblages. Aggregations are assemblages acting effectively as individual units within the fabric and varying in size, shape, and internal structure. Clay particle matrices are assemblages forming the background of microfabric and may act as a binder within the overall fabric in certain cases. As a result of their arrangement of clay particles in different levels, multilevel pore spaces were proposed (Fig. A.17).

Optical microscopy is suitable for macrofabric study, but cannot provide detailed information on the microfabric at particle level due to its low magnification and thickness of the specimen. The most serious drawback of SEM is that observations are restricted to rough surfaces casually formed by breaking a soil block. It is impossible to investigate the detailed internal structure. Even at the highest possible magnification, it is hard to differentiate different structures (Barden and Sides, 1970). Carbon replica TEM is also limited to the observation made on broken surfaces. Therefore, the results obtained could be grossly misleading (Smart, 1967).

THE END
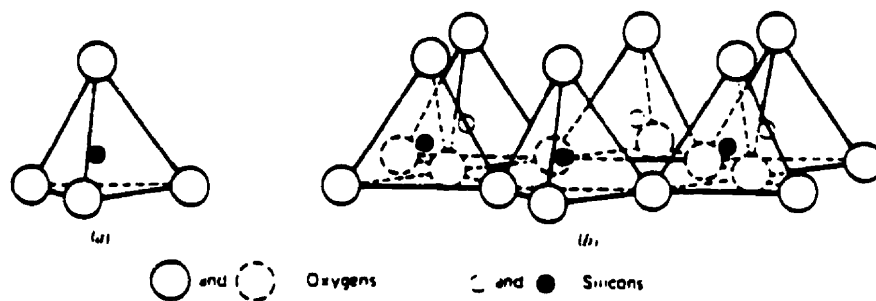
Figure A.1 Silicon tetrahedron and silica tetrahedra arranged in a hexagonal network (Mitchell, 1993).
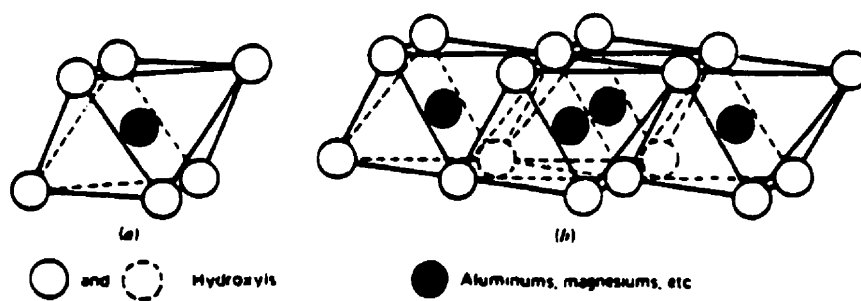
Figure A.2 Octahedral unit and sheet structure of octahedral units (Mitchell, 1993).
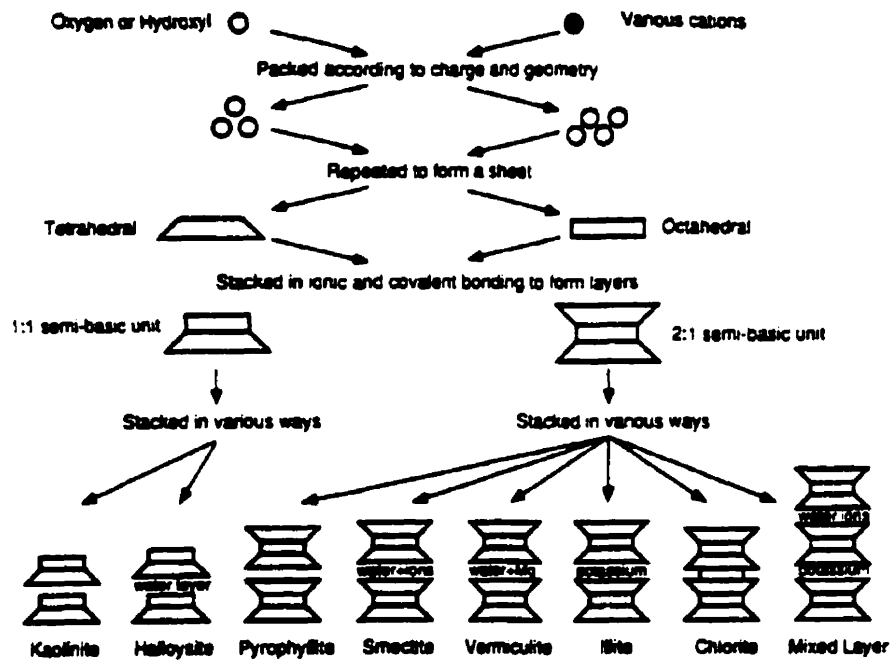
Figure A.3 Synthesis pattern for the clay minerals (Mitchell, 1993).
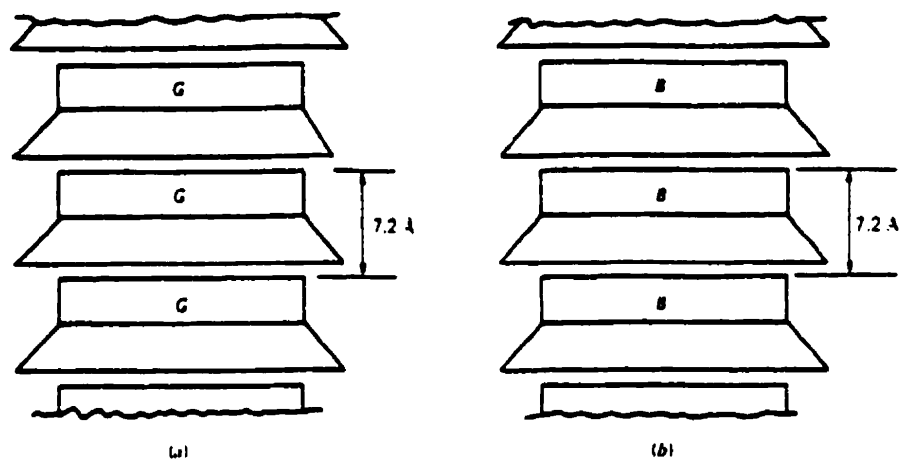
Figure A.4 Schematic diagrams of the structures of (a) kaolinite and (b) serpentine (Mitchell, 1993).
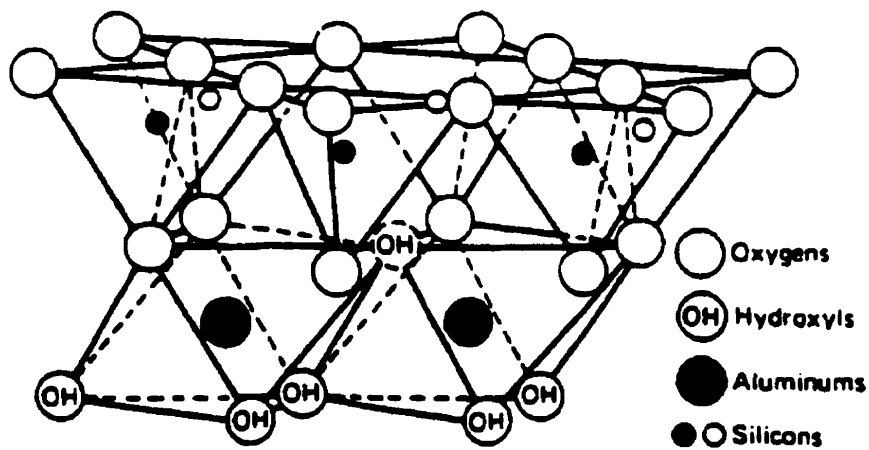
Figure A.5 Diagrammatic sketch of the kaolinite structure (Mitchell, 1993).
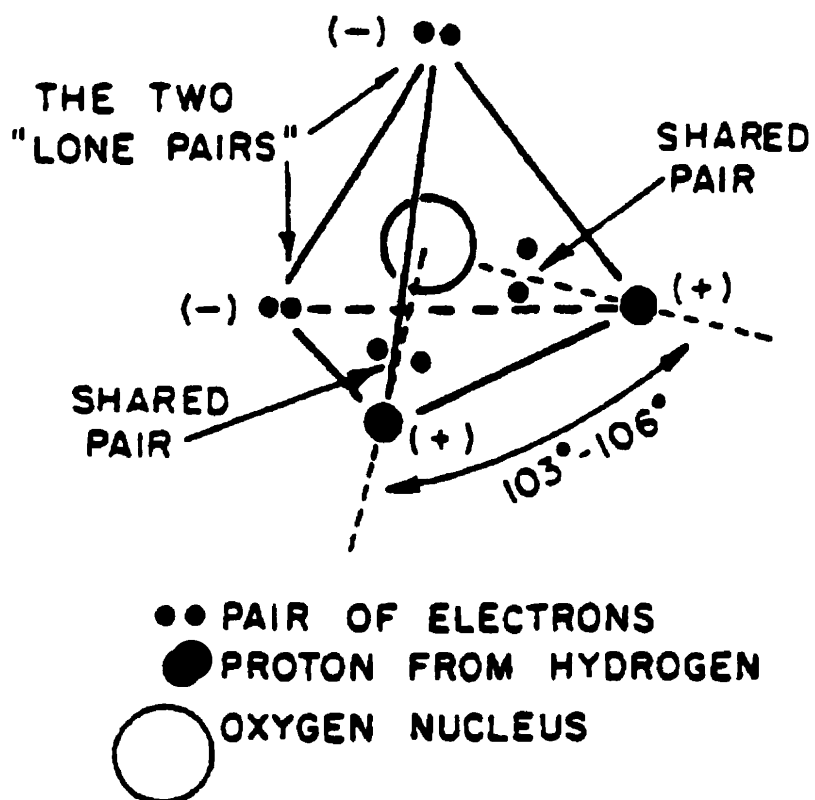
Figure A.6 Tetrahedral charge structure of a water molecule (Kirkham and Powers, 1972).
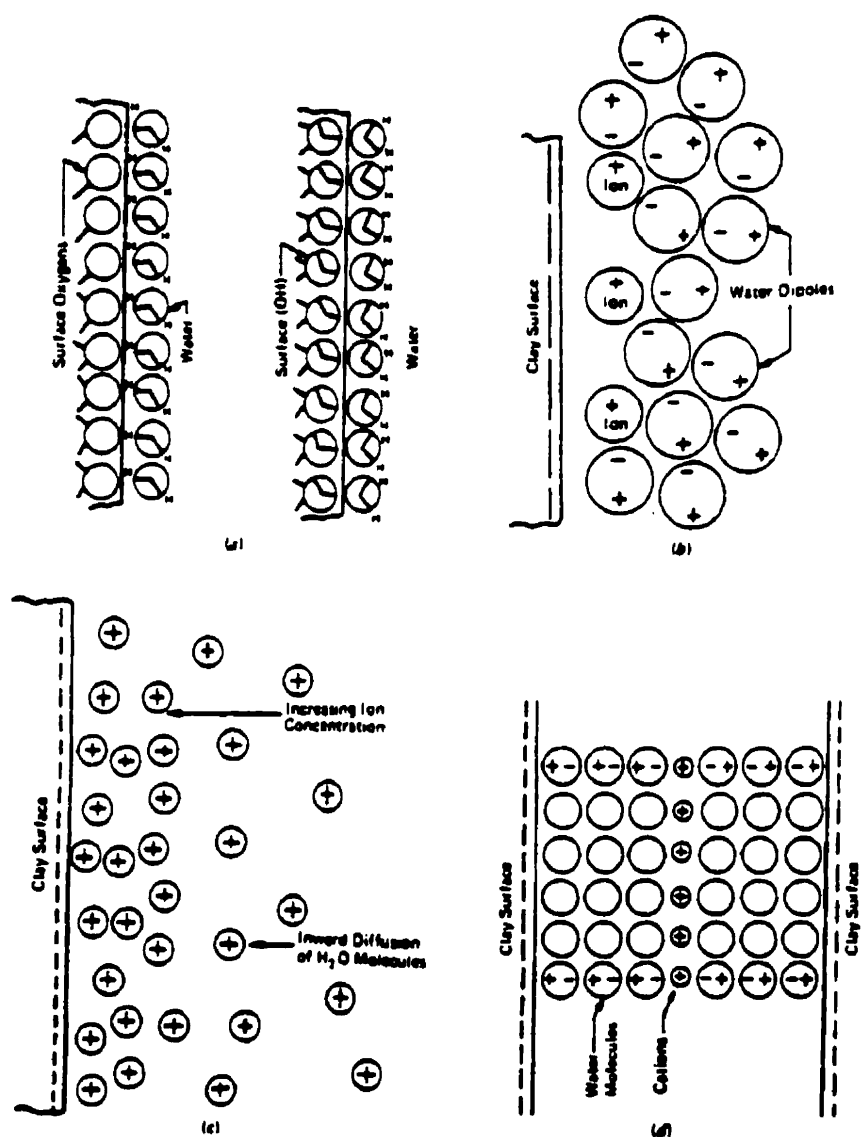
Figure A.7 Possible mechanisms of water adsorption by clay surfaces (Mitchell, 1993). (a) Hydrogen bonding. (b) Ion hydration. (c) Attraction by osmosis. (d) Dipole attraction.
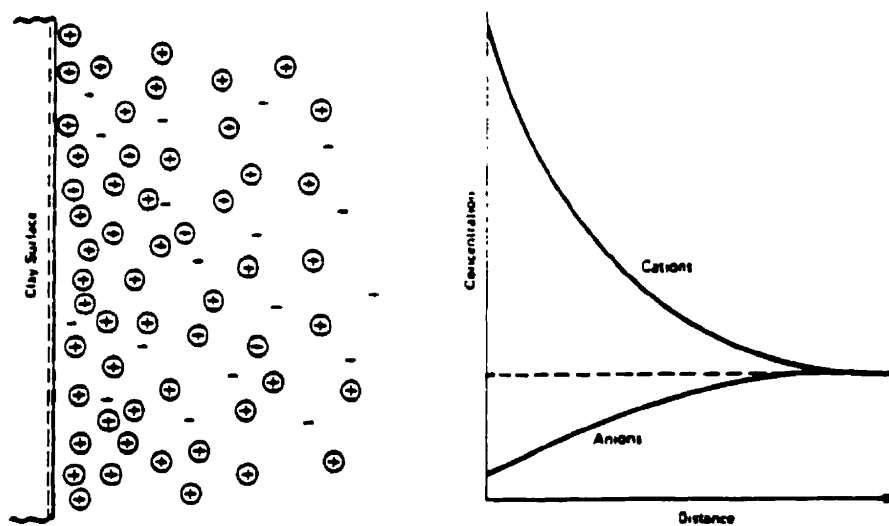
Figure A.8 Distribution of ions adjacent to a clay surface according to the concept of the diffuse double layer (Mitchell, 1993).
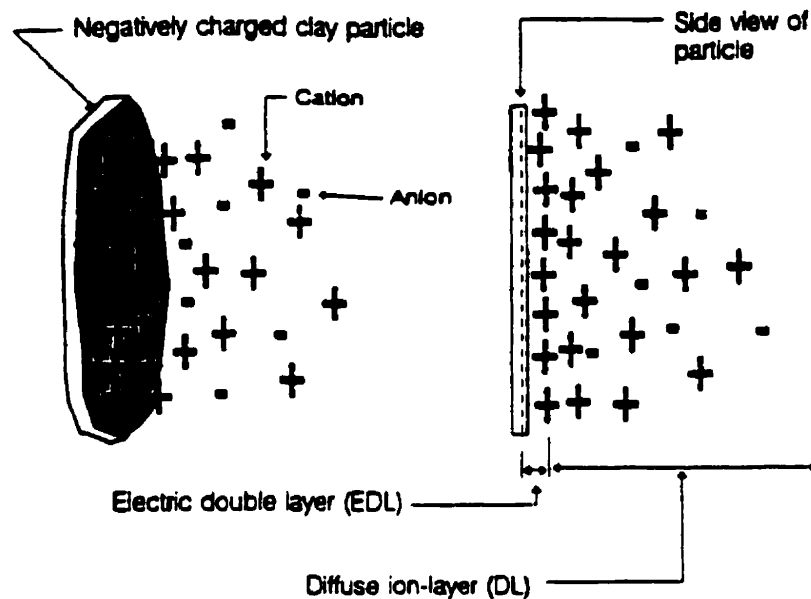
Figure A.9 Development of electric double layer (EDL) and diffuse ion-layer (DL) (Yong *et al.*, 1992).
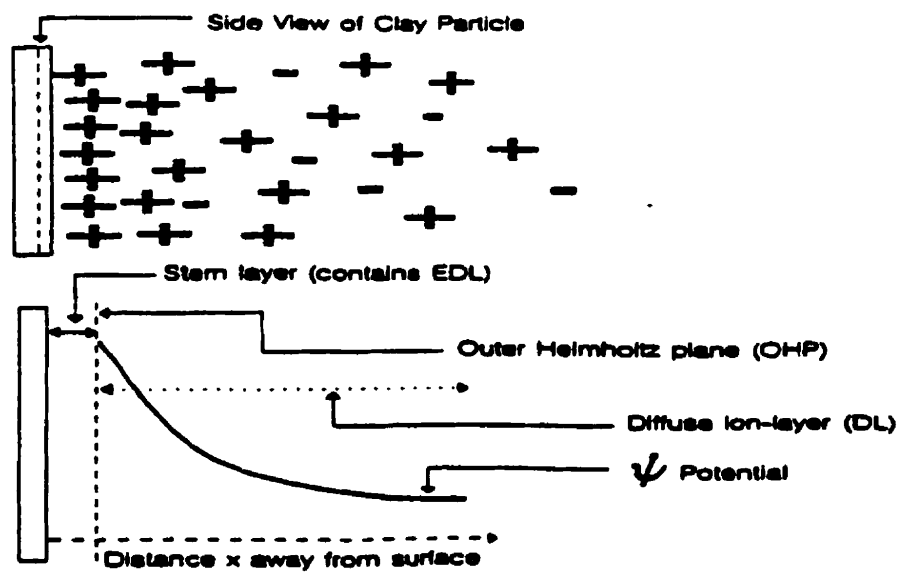
Figure A.10 Average electric potential as a function of distance x away from clay particle surface (Yong *et al.*, 1992).
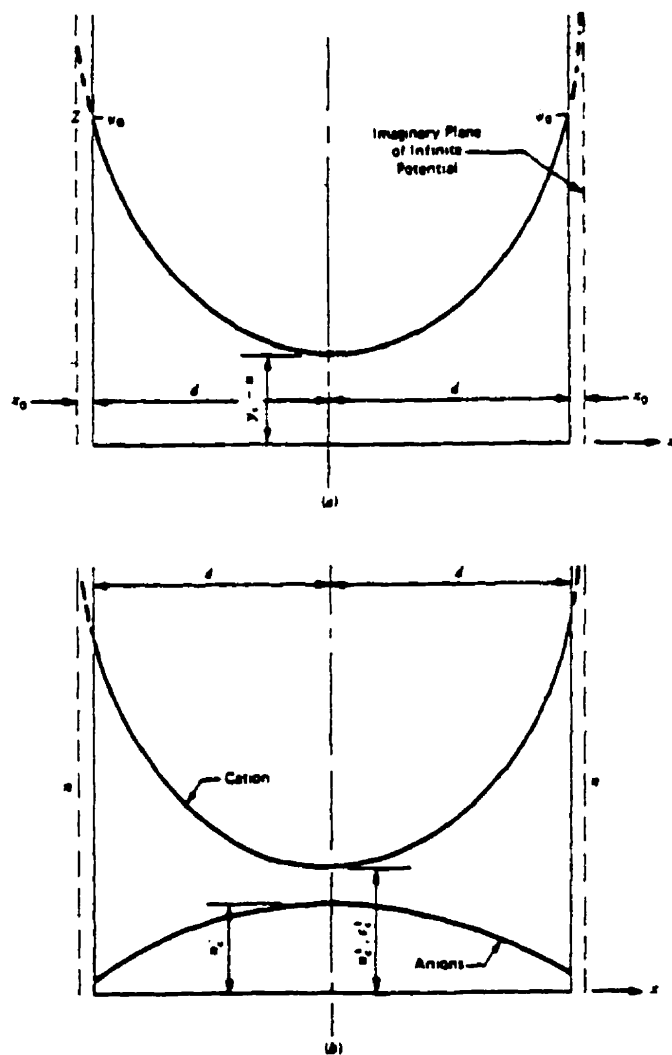
Figure A.11 (a) Potential and (b) charge distributions for interacting double
layers from parallel flat plates (Mitchell, 1993).
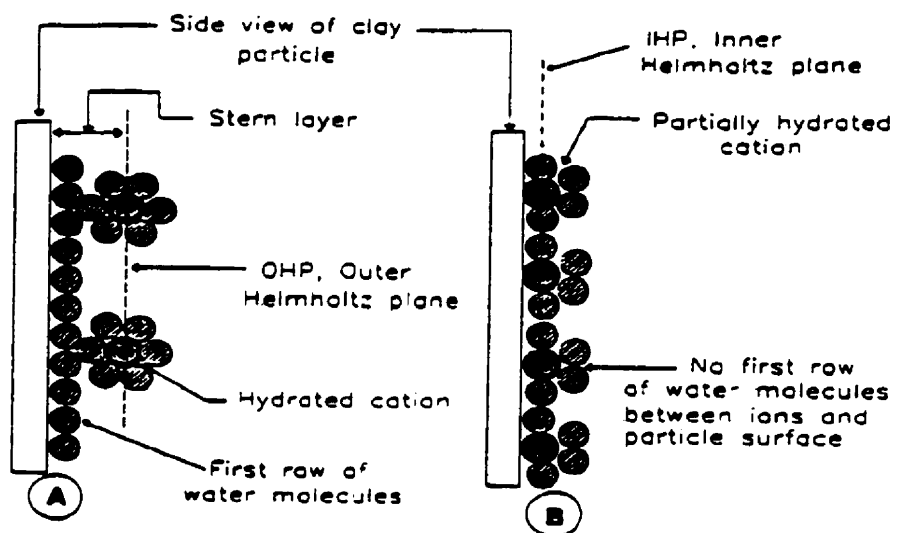
Figure A.12 Two types of ions arrangement at the particle surface-water interface (Yong *et al.*, 1992).
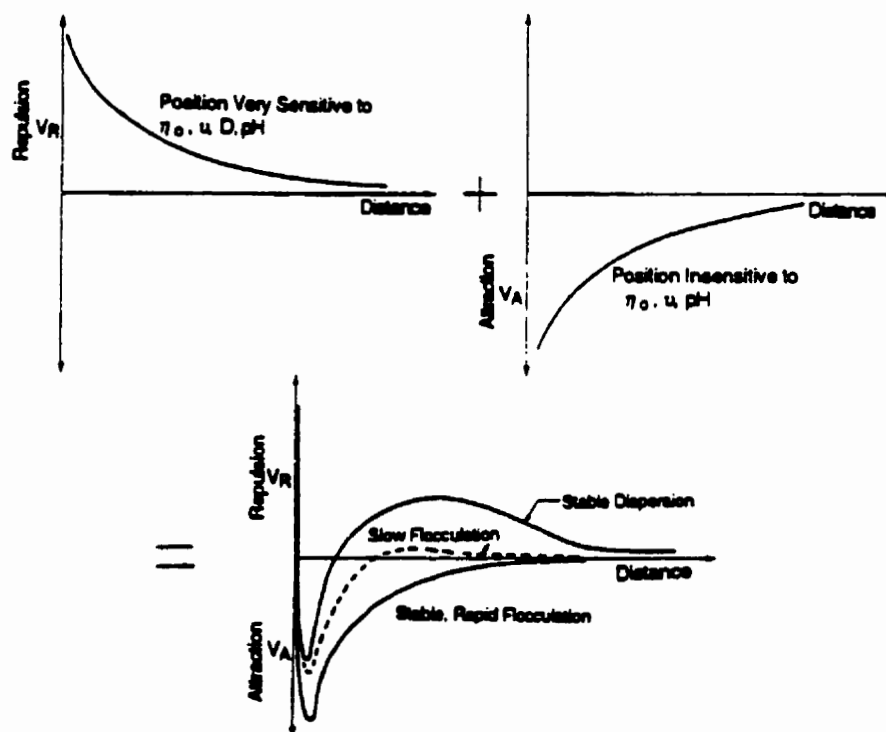
Figure A.13 Energies of repulsion, attraction, and net curves of interaction for parallel flat plates (Mitchell, 1993).
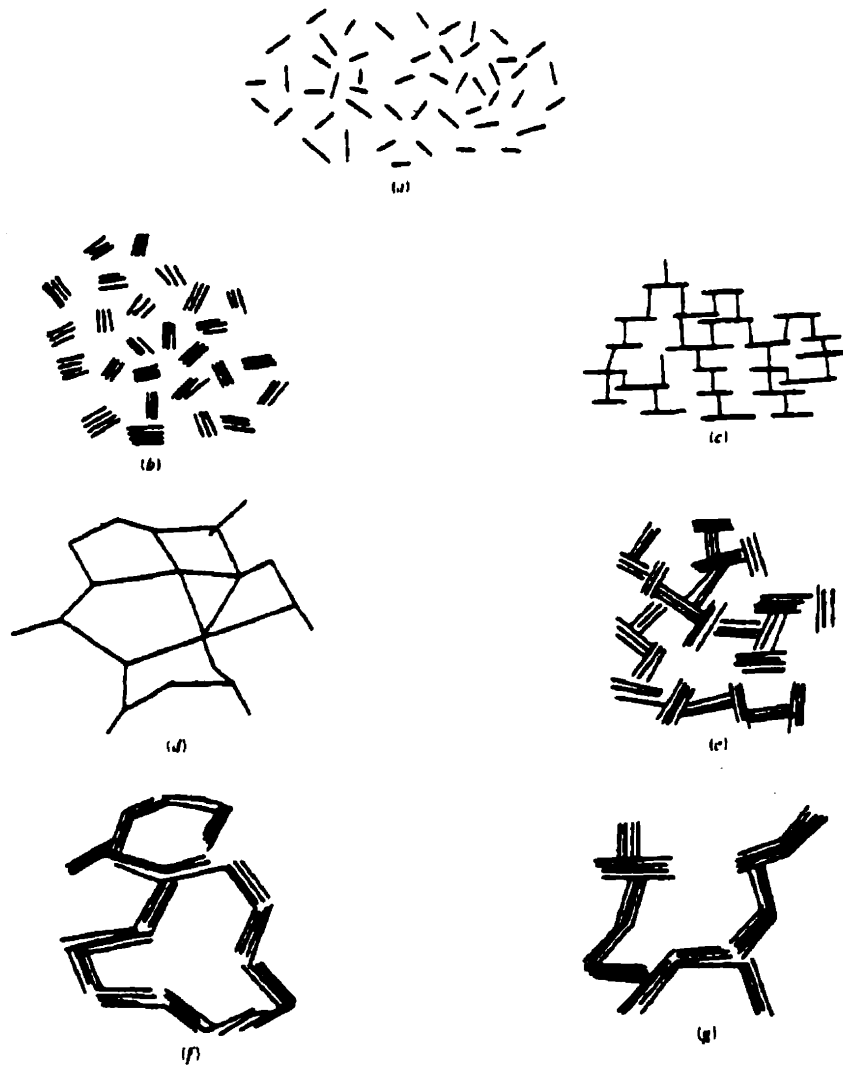
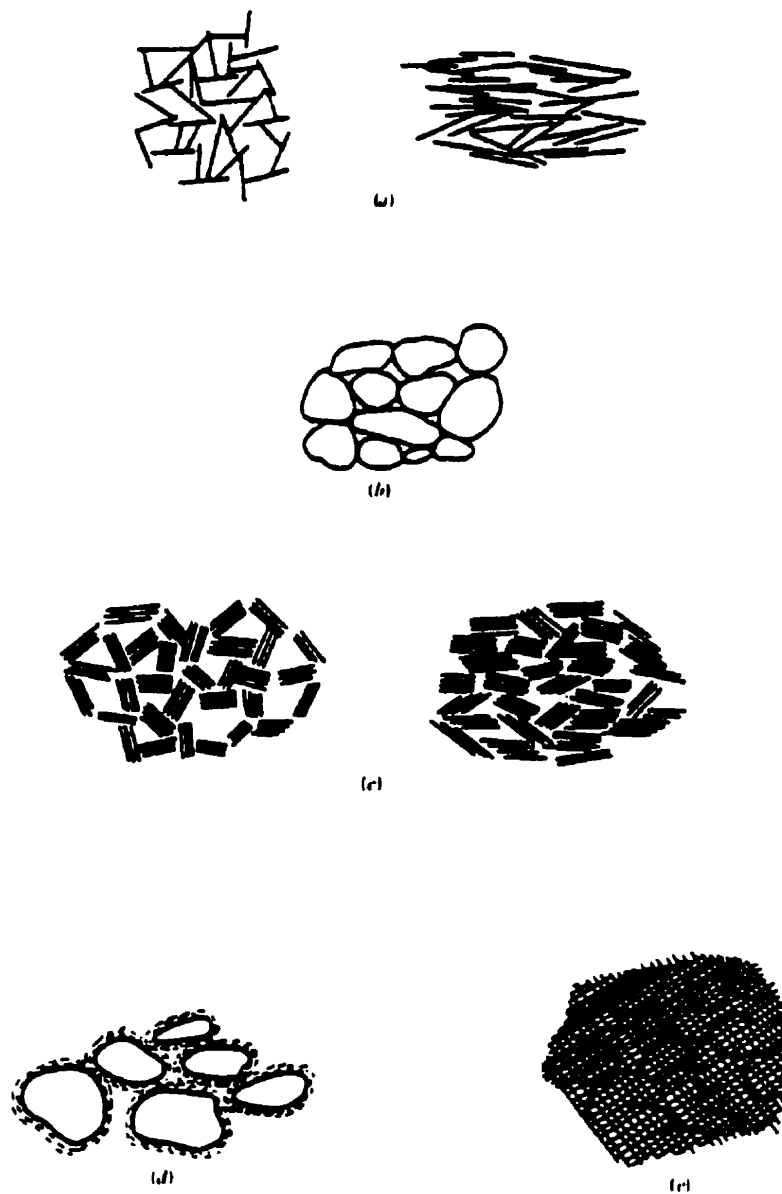Figure A.14 Modes of particle associations in clay suspensions (after van Olphen, 1977).

Figure A.15 Schematic representation of elementary particle arrangements (after Collins and McGown, 1974). (a) Individual clay platelet interaction. (b) Individual silt or sand particle interaction. (c) Clay platelet group interaction. (d) Clothed silt or sand particle interaction. (e) Partly discernible particle interaction.
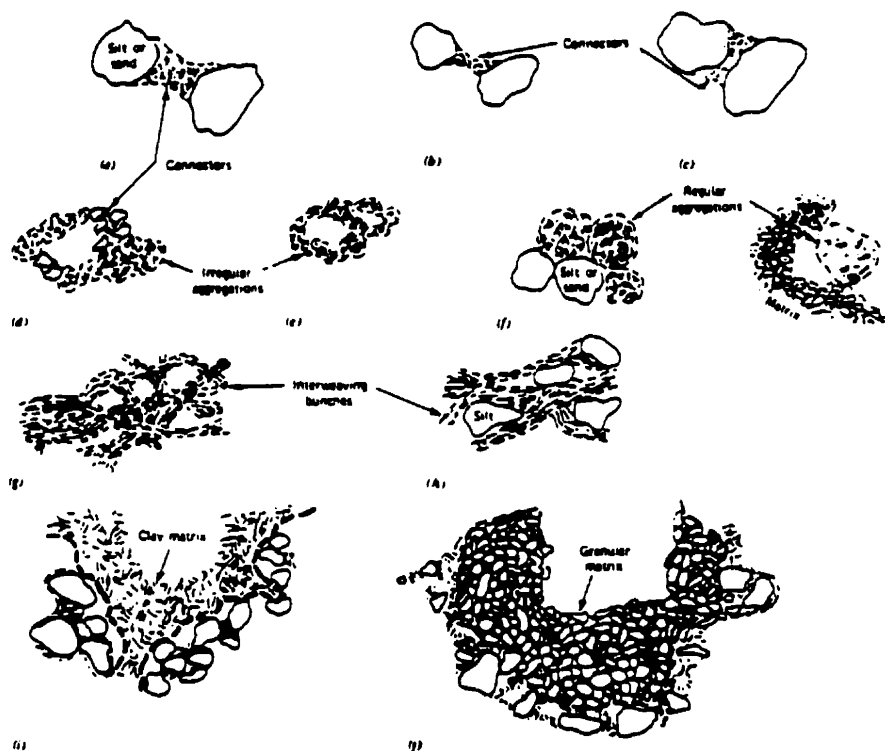
Figure A.16 Schematic representation of particle assemblages (after Collins and McGown, 1974). (a), (b), and (c) Connectors. (d) Irregular aggregations by connector assemblages. (e) Irregular aggregations in a honeycomb. (f) Regular aggregations interacting with particle matrix. (g) Interweaving bunches of clay. (h) Interweaving bunches of clay with silt inclusions. (i) Clay particle matrix. (j) Granular particle matrix.
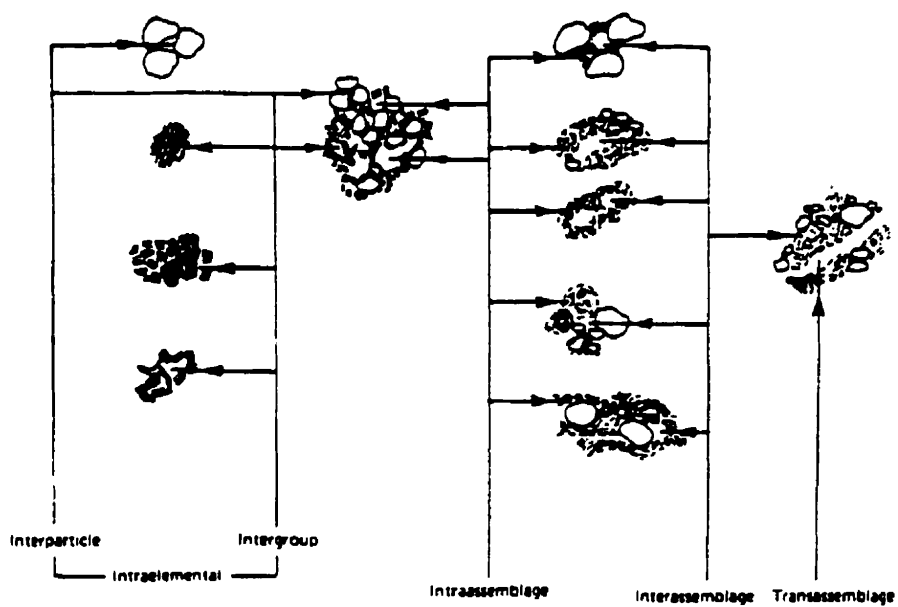
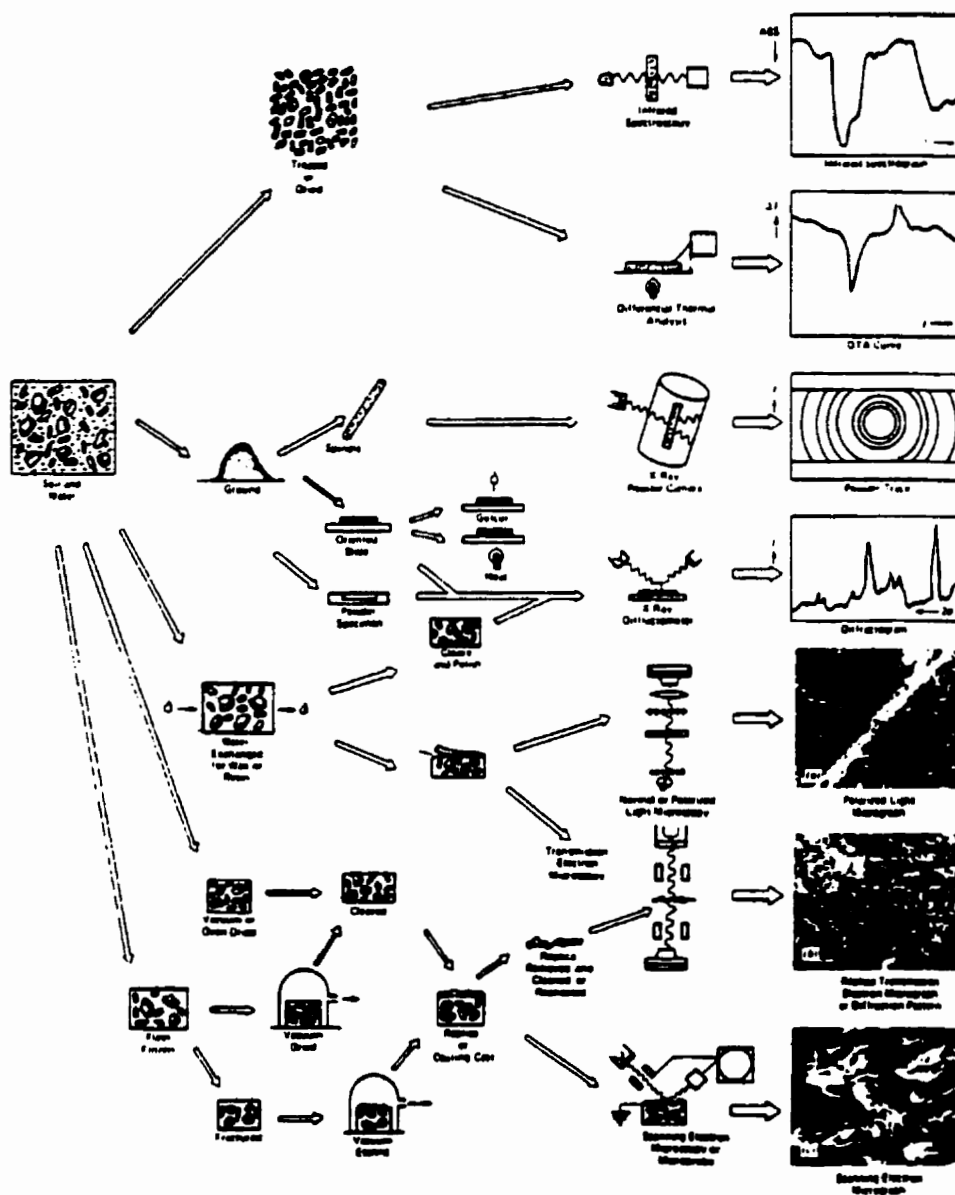Figure A.17 Schematic representation of pore space types (after Collins and McGown, 1974).

Figure A.18 Methods for examining mineralogy, fabric, and structure of soils using parts of the electromagnetic spectrum (prepared by R.N. Yong, Geotechnical Research Centre, McGill University).